



THE UNIVERSITY OF QUEENSLAND
AUSTRALIA

**Examining the Impact of Genetic Variation on the Structure and
Function of the Brain**

Lachlan Thomas Strike

Bachelor of Psychological Science (Honours)

A thesis submitted for the degree of Doctor of Philosophy at

The University of Queensland in 2018

Queensland Brain Institute

Abstract

This thesis aimed to examine genetic and non-genetic (i.e. environmental) contributions to normal variation in the structure of the human brain. Disentangling and quantifying these sources of variance (genetic and environmental) may be crucial to our understanding of the genetic architecture of the brain and how it relates to normal function and mental health disorders.

Studies show genetic and environmental factors, some of which overlap across the brain, contribute to individual differences in brain structure. Whether this genetic and environmental framework is similar across different samples is unknown. Further, some brain structures are difficult to delineate accurately and consistently; however, the reliability of imaging measures is also often overlooked. To provide a normative reference of healthy brain structure for future studies of neurological and psychiatric disorders, a reliable and robust map of genetic and environmental influences on the brain is required. We investigate this using two large, genetically informative samples of healthy adults with retest datasets: (*QTIM* Queensland Twin IMaging study, $N = 1028$; *HCP* Human Connectome Project, $N = 1105$).

In the first empirical study, we estimated region-specific genetic and environmental influence (i.e. independent of global effects – whole brain total surface area/average cortical thickness) on surface area and thickness of 34 neuroanatomical regions (Chapter 4). As expected, we found significant genetic influence for both surface area and thickness, and showed there is a wide range of heritability, which is generally independent of measurement reliability. Further, for several regions we found that a substantial amount of the variance was due to unique (non-shared) environmental factors rather than measurement error. Bivariate analyses revealed generally weak associations between the surface area of different regions, except within the occipital lobe. In contrast, cortical thickness was positively correlated within lobar divisions and negatively correlated across lobes. Further this covariation was mostly due to genetic factors. These results indicate that, independent of global effects, there is a complex pattern of region-specific, genetically mediated associations across the cortex, strongest for cortical thickness, and more limited for surface area.

In Chapter 5, we estimated mean-standardised genetic and environmental variance in cortical and subcortical structure volumes, as well as total brain volume and bodyweight.

Mean-standardised measures reflect the amount of absolute genetic or environmental variance that exists in the trait – not relative to other variance components (as for heritability; Chapter 4), and may elucidate differences in the genetic architecture or developmental constraints of individual brain structures. Estimates of mean-standardised genetic variance ranged across the brain structures examined, and there was no association between mean-standardised and relative estimates of genetic variance. Differences in mean-standardised genetic variance across the brain were not explained by straightforward factors (e.g. measurement error, spatial topography), and further research is required to understand the implications of differences in mean-standardised measures of variance in the human brain.

We then investigated bivariate associations between vertex-wise (i.e. continuous) measures of the cortical surface, using a clustering technique to identify a genetic parcellation of the cortex (Chapter 6). We found genetic divisions which were bilaterally symmetrical, and matched boundaries of structure and function. There was a consistent pattern of genetic parcellations across three large, twin datasets, indicating that genetic parcellations of cortical surface area are robust across sample and methodology.

In the last empirical study, we investigated genetic and environmental covariation between cortical brain structure and a behavioural measure (reading ability; Chapter 7). In the HCP dataset, we found significant associations between reading ability and the surface area of several cortical regions in the reading network. This association is influenced by a common genetic factor; however, this genetic factor is not region-specific (i.e. effects are shared with whole brain total surface area). These findings were not replicated in the QTIM dataset, perhaps due to the relatively longer delay between reading assessments and image acquisition in this cohort. These results suggest that patterns of covariation between cortical structure and reading ability are not robust, and may be sensitive to sample-specific methodology.

Together these findings illustrate a complex and somewhat unexpected pattern of genetic and environmental influences on human brain morphology. Encouragingly, these patterns of genetic and environmental influence were largely similar between two independent datasets of healthy young adults, and further, differences in measurement error are unlikely to underlie these complexities. Future work should focus on high-level MRI data making use of more advanced analysis techniques (e.g. machine learning), and collect dense genetic and environmental variables (e.g. whole genome sequencing, early life

events) to facilitate the next wave of studies investigating the aetiology of variation in brain morphology.

Declaration by author

This thesis **is composed of my original work, and contains** no material previously published or written by another person except where due reference has been made in the text. I have clearly stated the contribution by others to jointly-authored works that I have included in my thesis.

I have clearly stated the contribution of others to my thesis as a whole, including statistical assistance, survey design, data analysis, significant technical procedures, professional editorial advice, financial support and any other original research work used or reported in my thesis. The content of my thesis is the result of work I have carried out since the commencement of my higher degree by research candidature and does not include a substantial part of work that has been submitted **to qualify for the award of any** other degree or diploma in any university or other tertiary institution. I have clearly stated which parts of my thesis, if any, have been submitted to qualify for another award.

I acknowledge that an electronic copy of my thesis must be lodged with the University Library and, subject to the policy and procedures of The University of Queensland, the thesis be made available for research and study in accordance with the Copyright Act 1968 unless a period of embargo has been approved by the Dean of the Graduate School.

I acknowledge that copyright of all material contained in my thesis resides with the copyright holder(s) of that material. Where appropriate I have obtained copyright permission from the copyright holder to reproduce material in this thesis and have sought permission from co-authors for any jointly authored works included in the thesis.

Publications during candidature

First-author peer-reviewed papers

Strike, L.T., Couvy-Duchesne, B., Hansell, N.K., Cuellar-Partida, G., Medland, S.E., Wright, M.J. (2015) Genetics and brain morphology. *Neuropsychol. Rev.*, 25:63-96.

Strike, L. T., Hansell, N. K., Couvy-Duchesne, B., Thompson, P. M., de Zubicaray, G. I., McMahon, K. L., & Wright, M. J. (2018). Genetic Complexity of Cortical Structure: Differences in Genetic and Environmental Factors Influencing Cortical Surface Area and Thickness. *Cereb Cortex*. doi:10.1093/cercor/bhy002

Peer-reviewed papers

Lupton, M. K., **Strike, L.T**, Hansell, N. K., Wen, W., Mather, K. A., Armstrong, N. J., . . . Wright, M. J. (2016). The effect of increased genetic risk for Alzheimer's disease on hippocampal and amygdala volume. *Neurobiology of Aging*, 40, 68-77. doi:10.1016/j.neurobiolaging.2015.12.023

Couvy-Duchesne, B., **Strike, L. T.**, de Zubicaray, G. I., McMahon, K. L., Thompson, P. M., Hickie, I. B., . . . Wright, M. J. (2018). Lingual Gyrus Surface Area Is Associated with Anxiety-Depression Severity in Young Adults: A Genetic Clustering Approach. *eneuro*, 5(1). doi:10.1523/ENEURO.0153-17.2017

Consortia peer-reviewed papers

Adams, H. H., Hibar, D. P., Chouraki, V., Stein, J. L., Nyquist, P. A., Renteria, M. E., . . . Thompson, P. M. (2016). Novel genetic loci underlying human intracranial volume identified through genome-wide association. *Nature Neuroscience*, 19(12), 1569-1582. doi:10.1038/nn.4398

Brouwer, R. M., Panizzon, M. S., Glahn, D. C., Hibar, D. P., Hua, X., Jahanshad, N., . . . Hulshoff Pol, H. E. (2017). Genetic influences on individual differences in longitudinal changes in global and subcortical brain volumes: Results of the

ENIGMA plasticity working group. *Human Brain Mapping*, 38(9), 4444-4458.
doi:10.1002/hbm.23672

Guadalupe, T., Mathias, S. R., vanErp, T. G. M., Whelan, C. D., Zwiers, M. P., Abe, Y., . . .
Francks, C. (2017). Human subcortical brain asymmetries in 15,847 people
worldwide reveal effects of age and sex. *Brain Imaging and Behavior*, 11(5), 1497-
1514. doi:10.1007/s11682-016-9629-z

Hibar, D. P., Adams, H. H., Jahanshad, N., Chauhan, G., Stein, J. L., Hofer, E., . . . Ikram,
M. A. (2017). Novel genetic loci associated with hippocampal volume. *Nat
Commun*, 8, 13624. doi:10.1038/ncomms13624

Hibar, D. P., Stein, J. L., Renteria, M. E., Arias-Vasquez, A., Desrivieres, S., Jahanshad,
N., . . . Medland, S. E. (2015). Common genetic variants influence human
subcortical brain structures. *Nature*, 520(7546), 224-229. doi:10.1038/nature14101

Renteria, M. E., Hansell, N. K., Strike, L. T., McMahon, K. L., de Zubicaray, G. I., Hickie, I.
B., . . . Wright, M. J. (2014). Genetic architecture of subcortical brain regions:
common and region-specific genetic contributions. *Genes Brain Behav*, 13(8), 821-
830. doi:10.1111/gbb.12177

Schmaal, L., Hibar, D. P., Samann, P. G., Hall, G. B., Baune, B. T., Jahanshad, N., . . .
Veltman, D. J. (2017). Cortical abnormalities in adults and adolescents with major
depression based on brain scans from 20 cohorts worldwide in the ENIGMA Major
Depressive Disorder Working Group. *Molecular Psychiatry*, 22(6), 900-909.
doi:10.1038/mp.2016.60

Schmaal, L., Veltman, D. J., van Erp, T. G., Samann, P. G., Frodl, T., Jahanshad, N., . . .
Hibar, D. P. (2016). Subcortical brain alterations in major depressive disorder:
findings from the ENIGMA Major Depressive Disorder working group. *Molecular
Psychiatry*, 21(6), 806-812. doi:10.1038/mp.2015.69

Thompson, P. M., Stein, J. L., Medland, S. E., Hibar, D. P., Vasquez, A. A., Renteria, M.
E., . . . Alzheimer's Disease Neuroimaging Initiative, E. C. I. C. S. Y. S. G. (2014).
The ENIGMA Consortium: large-scale collaborative analyses of neuroimaging and
genetic data. *Brain Imaging and Behavior*, 8(2), 153-182. doi:10.1007/s11682-013-
9269-5

Oral presentations/posters

Strike, L. T., Couvy-Duchesne, B., McMahon, K. L., de Zubicaray, G. I., Thompson, P. M., Martin, N. G., & Wright, M. J. (2015). *Genetic contributions to cortical thickness patterning in young adults*. Oral presentation at the Behavior Genetics Association Annual General Meeting. San Diego, USA, 2015.

Strike, L. T., Hansell, N. K., McMahon, K. L., Luciano, M., Bates, T. C., Martin, N. G., Thompson, P. T., Wright, M. J., de Zubicaray, G. I. *Genetic and Environmental Covariation between Cortical Brain Structure (Thickness, Surface Area) and Written Language Ability*. Poster presented at the Seventh Annual Meeting of the Society for the Neurobiology of Language, Chicago, 2015.

Strike, L. T., Hansell, N. K., Couvy-Duchesne, B., Thompson, P. M., Martin, N. G. I, de Zubicaray, G., McMahon, K. L., Wright, M. J. *Genetic influences on the cerebral cortex*. Poster presented at the 22nd Annual Meeting of the Organization for Human Brain Mapping. Geneva, Switzerland, 2016.

Strike, L. T., Zietsch, B. P., Wright, M. J. *Comparing absolute and relative variance components of brain structure*. Poster presented at the IEEE International Symposium on Biomedical Imaging. Melbourne, Australia, 2017.

Strike, L.T., Hansell, N.K., Couvy-Duchesne, B., Thompson, P.M., Zietsch, B.P, de Zubicaray, G.I., McMahon, K.L., Wright, M.J. *Using imaging and genetics to unravel the complexity of the human brain*. Oral presentation at the SBMS 8th International Postgraduate Symposium. Brisbane, Australia, 2017.

Publications included in this thesis

Strike, L.T., Couvy-Duchesne, B., Hansell, N.K., Cuellar-Partida, G., Medland, S.E., Wright, M.J. (2015) Genetics and brain morphology. *Neuropsychol. Rev.*, 25:63-96.

LS, BCD, and NH contributed equally to the published work. Only the section written by LS is incorporated as Chapter 2.

Contributor	Statement of contribution
Lachlan T. Strike (Candidate)	Conception and design (30%) Analysis and interpretation (30%) Drafting and production (25%)
Baptiste Couvy-Duchesne	Conception and design (30%) Analysis and interpretation (30%) Drafting and production (25%)
Narelle K. Hansell	Conception and design (30%) Analysis and interpretation (30%) Drafting and production (25%)
Gabriel Cuellar-Partida	Conception and design (10%) Analysis and interpretation (10%)
Sarah E. Medland	Drafting and production (5%)
Margaret J. Wright	Drafting and production (20%)

Strike, L. T., Hansell, N. K., Couvy-Duchesne, B., Thompson, P. M., de Zubicaray, G. I., McMahon, K. L., & Wright, M. J. (2018). Genetic Complexity of Cortical Structure: Differences in Genetic and Environmental Factors Influencing Cortical Surface Area and Thickness. *Cereb Cortex*. doi:10.1093/cercor/bhy002

Incorporated as Chapter 4.

Contributor	Statement of contribution
Lachlan T. Strike (Candidate)	Conception and design (70%) Analysis and interpretation (100%) Drafting and production (70%)
Narelle K. Hansell	Drafting and production (2.5%)
Baptiste Couvy-Duchesne	Drafting and production (2.5%)
Paul M. Thompson	Drafting and production (2.5%)
Greig I. de Zubicaray	Conception and design (5%) Drafting and production (2.5%)
Katie L. McMahon	Conception and design (5%) Drafting and production (2.5%)
Margaret J. Wright	Conception and design (20%) Drafting and production (17.5%)

Contributions by others to the thesis

Imaging data collected as part of the Queensland Twin IMaging (QTIM) study. Margie (Margaret) Wright, Nick (Nicholas) Martin, Paul Thompson, Greig de Zubicaray and Katie McMahon were responsible for the conception and design of QTIM. Cognitive data for QTIM participants was collected as part of the Brisbane Adolescent Twin Study (BATS). Margaret Wright and Nick Martin were responsible for the conception and design of BATS. Marlene Grace and Ann Eldridge were responsible for participant recruitment, and Kerrie McAloney co-ordinated the studies. Kori Johnson, Aaron Quiggle, Natalie Garden, Matthew Meredith, Peter Hobden, Kate Borg, Aiman Al Najjar and Anita Burns contributed to imaging data acquisition, and David Butler and Daniel Park provided IT support.

Data were provided [in part] by the Human Connectome Project, WU-Minn Consortium (Principal Investigators: David Van Essen and Kamil Ugurbil; 1U54MH091657) funded by the 16 NIH Institutes and Centers that support the NIH Blueprint for Neuroscience Research; and by the McDonnell Center for Systems Neuroscience at Washington University.

Chapter 2: As stated in the “publications included in this thesis” section.

Chapter 4: As stated in the “publications included in this thesis” section.

Chapter 5: Narelle K. Hansell, Brendan P. Zietsch, and Margaret J. Wright edited the chapter.

Chapter 6: Katie L. McMahon and Margaret J. Wright edited the chapter.

Chapter 7: Narelle K. Hansell, Katie L. McMahon, Michelle Luciano, Timothy C. Bates, Nicholas G. Martin, Paul M. Thompson, Margaret J. Wright, and Greig I. de Zubicaray edited the chapter.

Statement of parts of the thesis submitted to qualify for the award of another degree

None.

Research Involving Human or Animal Subjects

Project Title: Genetics of Brain Structure and Function

Approval Number: 2004000185

Name of responsible Committee: Medical Research Ethics Committee

Project Title: Genes for Cognition

Approval Number: 2008001873

Name of responsible Committee: Medical Research Ethics Committee

Project Title: Data Sharing using the Human Connectome Project (HCP) Databases:
Replication and Meta/Mega-analyses

Approval Number: 2017000229

Name of responsible Committee: University of Queensland Human Research Ethics
Committee B

Acknowledgements

First and foremost, I would like to thank Margie Wright for her support and guidance before and throughout my PhD. Many thanks as well to my associate supervisors Katie McMahon and Greig de Zubicaray (and unofficial fourth supervisor Narelle Hansell) for all their help over the past four years.

I would also like to thank my colleagues in the Wright group, as well as those from QIMR Berghofer, for many good times inside and outside of the lab. Thank you also to the support staff at QBI and QIMR Berghofer for their assistance with scholarships, computing, and candidature milestones.

Thank you to my friends and family - in terms of genetic and environmental influences, I have a lot better than I deserve.

Lastly, thank you to the participants who volunteered their time to undergo brain scans, blood draws, and cognitive testing. Only through your generosity is this research possible.

Financial support

This research was supported by an Australian Government Research Training Program Scholarship, as well as a Queensland Brain Institute (QBI) Top-Up Scholarship. Additional financial support provided by the National Institute of Biomedical Imaging and Bioengineering (NIH Award 1U54EB020403-01, subaward no. 56929223).

The QTIM study was supported by the National Institute of Child Health and Human Development (R01 HD050735), and the National Health and Medical Research Council (NHMRC 486682, 1009064). The collection of cognition data was supported by the Australian Research Council (A79600334, A79906588, A79801419, DP0212016, DP0343921, and DP1093900).

Data were provided [in part] by the Human Connectome Project, WU-Minn Consortium (Principal Investigators: David Van Essen and Kamil Ugurbil; 1U54MH091657) funded by the 16 NIH Institutes and Centers that support the NIH Blueprint for Neuroscience Research; and by the McDonnell Center for Systems Neuroscience at Washington University.

Keywords

imaging genetics, magnetic resonance imaging, twin study, heritability, brain

Australian and New Zealand Standard Research Classifications (ANZSRC)

ANZSRC code: 060410, Neurogenetics, 30%

ANZSRC code: 060412, Quantitative Genetics (incl. Disease and Trait Mapping Genetics), 30%

ANZSRC code: 110999, Neurosciences not elsewhere classified 40%

Fields of Research (FoR) Classification

FoR code: 0604, Genetics, 40%

FoR code: 1109, Neurosciences, 40%

FoR code: 1702, Cognitive Sciences, 20%

Table of Contents

Abstract	ii
List of Figures	xxi
List of Tables	xxii
List of Abbreviations	xxiii
1 Introduction	28
1.1 General Introduction	28
1.2 Aims and Thesis Outline	28
1.3 Chapter Overview	29
2 Genetics and Brain Morphology	33
Abstract	33
2.1 General Introduction	33
2.2 Twin and Family Imaging Studies	34
2.3 Estimating Heritability and Multivariate Genetic Analysis	35
2.4 Heritability of Brain Structure	38
2.5 Issues in Estimating Heritability for Imaging Phenotypes	42
2.6 Overlapping or Distinct Genetic Factors?	44
2.7 Shared Genetic Influences Across Brain Structure and Cognitive Ability	45
2.8 Conclusions	50
3 Imaging Phenotypes/Contributions to the ENIGMA Consortium	52
3.1 Datasets	52
3.2 Imaging Phenotypes	52
3.2.1 Quality Checking	53
3.2.2 Acquisition Artefacts	53
3.2.3 Segmentation/Reconstruction/Delineation Errors.....	60
3.3 Contributions to the ENIGMA Consortium	62
4 Genetic Complexity of Cortical Structure: Differences in Genetic and Environmental Factors Influencing Cortical Surface Area and Thickness	66
Abstract	66
4.1 Introduction	67
4.2 Materials and Methods	68
4.2.1 Participants.....	68
4.2.2 Image Acquisition and Processing.....	70

4.2.3	Heritabilities of Cortical Surface Area and Thickness.....	70
4.2.4	Test-Retest Reliability.....	72
4.2.5	Associations Between Left/Right Homologous ROIs and Across Regions.....	72
4.2.6	Replication in an Independent Sample.....	75
4.3	Results.....	76
4.3.1	Preliminary Analyses.....	76
4.3.2	Heritability of Cortical Surface Area and Thickness.....	76
4.3.3	ROI Correlations Between Hemispheres.....	77
4.3.4	ROI Correlations Across the Cortex.....	80
4.3.5	ROI Correlations Between Surface Area and Cortical Thickness.....	80
4.3.6	Replication Using the HCP sample.....	81
4.4	Discussion.....	82
4.5	Conclusions.....	88
5	Absolute and Relative Estimates of Genetic and Environmental Influence on Brain Structure Volume.....	90
	Abstract.....	90
5.1	Introduction.....	91
5.2	Method.....	94
5.2.1	Participants.....	94
5.2.2	Image Acquisition and Processing.....	94
5.2.3	Estimation of Variance Components.....	95
5.2.4	Mean-Standardised Variance.....	96
5.2.5	Replication in an Independent Sample.....	97
5.3	Results.....	97
5.3.1	Replication Using the HCP Sample.....	101
5.4	Discussion.....	104
6	A Consistent Pattern of Genetic Parcellations of Cortical Surface Area Across Three Large Twin Datasets.....	111
	Abstract.....	111
6.1	Introduction.....	112
6.2	Methods.....	113
6.2.1	Study Participants and Imaging Protocols.....	113
6.2.2	Vertex-Wise Surface Area.....	114
6.2.3	Statistical Analysis.....	115
6.2.4	Fuzzy Clustering.....	116
6.3	Results.....	118

6.3.1	Genetic Parcellations for the QTIM and HCP Datasets.....	118
6.3.2	Pairwise Cluster Comparisons.....	118
6.3.3	Similarity Across all Three Datasets.....	119
6.4	Discussion.....	121
6.5	Conclusion.....	124
7	Genetic and Environmental Covariation Between Cortical Brain Structure (Surface Area, Thickness) and Reading Ability.....	126
	Abstract.....	126
7.1	Introduction.....	127
7.2	Materials and Methods.....	129
7.2.1	Participants.....	129
7.2.2	Reading Measure.....	130
7.2.3	Cortical Surface Area and Thickness Measures.....	130
7.2.4	Heritability of Reading Ability.....	131
7.2.5	Associations Between Brain Structure and Reading Ability.....	132
7.2.6	Replication in an Independent Sample (QTIM).....	133
7.3	Results.....	135
7.3.1	Demographics, Heritability, Covariate Effects, and Reliability of Reading Ability.....	135
7.3.2	Associations Between Cortical Structure and Reading Ability.....	135
7.3.3	The Influence of Global Effects.....	136
7.3.4	Replication of Associations in QTIM.....	137
7.4	Discussion.....	138
7.5	Conclusion.....	141
8	Discussion and Conclusion.....	143
8.1	Overview.....	143
8.2	Genetic Variance.....	146
8.3	Environmental Variance.....	147
8.4	Robustness of Findings Across Datasets.....	149
8.5	Test-Retest Reliability.....	149
8.6	Genes, Brain, and Behaviour.....	151
8.7	The Continuing Importance of Twin Imaging Studies.....	151
8.8	Potential Limitations.....	153
8.9	Future Directions.....	154
8.10	Conclusion.....	155
9	Bibliography.....	156
	Appendix 1 Ethics Approval for QTIM and HCP Datasets.....	185

Appendix 2 The Desikan-Killiany Atlas, with Total Surface Area and Mean Cortical Thickness Estimates in the QTIM Dataset.....	188
Appendix 3 Descriptive Statistics for Surface Area and Cortical Thickness in the QTIM Dataset	190
Appendix 4 The Classic Twin Design and the AE Bivariate Twin Design	193
Appendix 5 Regression Coefficients and q values for Surface Area Covariates in the QTIM Dataset	196
Appendix 6 Regression Coefficients and q values for Cortical Thickness Covariates in the QTIM Dataset.....	198
Appendix 7 Variance Component Estimates for QTIM Surface Area and Cortical Thickness.....	200
Appendix 8 Test-Retest Correlations for QTIM Surface Area and Cortical Thickness	204
Appendix 9 Twin and Test-Retest Correlations for QTIM Surface Area and Cortical	205
Appendix 10 Heatmaps of Genetic Correlations Across ROIs for QTIM Surface Area and Cortical Thickness	206
Appendix 11 Phenotypic Correlations with Genetic and Environmental Contributions, between QTIM Surface Area and Cortical Thickness.....	207
Appendix 12 Descriptive Statistics for Surface Area and Cortical Thickness in the HCP Dataset.....	208
Appendix 13 Covariate Effects for Surface Area Measures in the HCP Dataset.....	210
Appendix 14 Covariate Effects for Cortical Thickness Measures in the HCP Dataset	212
Appendix 15 Variance Component Estimates for HCP Surface Area and Cortical Thickness.....	214
Appendix 16 Twin and Test-Retest Correlations for HCP Surface Area and Cortical Thickness.....	218
Appendix 17 Surface Area and Cortical Thickness ACE Estimates and Test-Retest Correlations in the HCP Dataset	219

Appendix 18 Phenotypic Correlations, with Genetic and Environmental Contributions, for HCP Surface Area and Cortical Thickness	220
Appendix 19 Phenotypic Correlations with Genetic and Environmental Contributions, between HCP Surface Area and Cortical Thickness	221
Appendix 20 Means and Variances for Brain Structure Volumes and Body Weight in the QTIM Dataset	222
Appendix 21 Mean-Standardised and Relative Variances Estimates, and Test-Retest Correlations for Brain Structure Volume and Body Weight in the QTIM Dataset	223
Appendix 22 Associations with Mean-Standardised Variance Estimates in the QTIM Dataset	225
Appendix 23 Mean-Standardised and Relative Variances Estimates for HCP Brain Structure Volume	226
Appendix 24 Mean-Standardised and Relative Genetic and Environmental Variance Estimates for HCP Cortical Structure Volumes	229
Appendix 25 Mean-Standardised and Relative Genetic and Environmental Variance Estimates for HCP Subcortical and Ventricular Structure Volumes	230
Appendix 26 Associations with Mean-Standardised Variance Estimates in the HCP Dataset	231
Appendix 27 Associations Between HCP Cortical Structure and Reading Ability ..	232
Appendix 28 Associations Between QTIM Cortical Structure and Reading Ability.	233

List of Figures

Figure 2.1 Correlated factors bivariate twin model.	37
Figure 2.2 Heritability estimates with 95% confidence intervals for brain structure	39
Figure 2.3 Variance component estimates for brain structure (meta-analysis)	40
Figure 3.1 Head motion artefact	54
Figure 3.2 Metal induced artefact	55
Figure 3.3 Non-uniform (bias) intensity artefact.....	56
Figure 3.4 Susceptibility artefact.....	57
Figure 3.5 Flow/pulstation artefact.....	58
Figure 3.6 Radio frequency artefact.....	59
Figure 3.7 Incorrect subcortical segmentation.....	60
Figure 3.8 Incorrect cortical delineation	61
Figure 3.9 Incorrect cortical reconstruction	61
Figure 4.1 Variance component estimates for surface area and cortical thickness	78
Figure 4.2 Phenotypic correlations, with genetic and environmental contributions, between corresponding left/right ROIs for surface area and cortical thickness in the QTIM and HCP samples.....	79
Figure 4.3 Phenotypic correlations, with genetic and environmental contributions, for surface area and cortical thickness across regions in the QTIM sample.....	82
Figure 5.1 Average of mean-standardised variance component estimates in the QTIM and HCP datasets.....	98
Figure 5.2 Mean-standardised and relative genetic and environmental variances for cortical structures in the QITM dataset.....	100
Figure 5.3 Mean-standardised and relative genetic and environmental variances for subcortical and ventricular structures in the QITM dataset.....	101
Figure 5.4 Mean-standardised genetic variance estimates for cortical, subcortical, and ventricular structres in the QTIM and HCP datasets.....	103
Figure 6.1 Plot of silhouette coefficients for clustering solutions in QTIM and HCP datasets.....	117
Figure 6.2 12-cluster, genetic parcellations across three datasets	119
Figure 6.3 Similarity of neruoanaotmical and genetic parcellations in the QTIM and HCP datasets .	120
Figure 6.4 Similarity of vertex-membership across datasets.....	121
Figure 7.1 Regions of interest involved in the written language network investigated in the present study.	131
Figure 7.2 Phenotypic correlations, with genetic and environmental contributions, between surface area of reading network ROIs and TORRT score in the HCP dataset.....	137

List of Tables

Table 2.1 Twin and family cohorts with imaging data	36
Table 2.2 Shared genetic influence across brain structures.....	47
Table 2.3 Shared genetic influence between brain structure and cognitive ability.....	49
Table 3.1 Contributions of the QTIM dataset to ENIGMA publications.....	63
Table 4.1 Demographic characteristics (mean \pm SD) of the QTIM sample.....	69
Table 5.1 Published estimates of mean-standardised phenotypic variance in brain structure volume	93
Table 6.1 Demographic and imaging information for the three datasets used in this study.....	115
Table 7.1 Descriptive statistics for the HCP and QTIM datasets.....	136
Table 8.1 Aims and findings of empirical thesis chapters	144

List of Abbreviations

A	latent additive genetic influences/factor
a	path coefficient for additive genetic influences
A1, A2	First, second latent additive genetic factors
a²	variance explained by additive genetic influences
3rd V	third ventricle
AMYG	amygdala
bilat	bilateral
BSTS	banks of the superior temporal sulcus
C	latent common environmental influences/factor
c	path coefficient for common environmental influences
C1, C2	First, second latent common environmental factors
c²	variance explained by common environmental influences
CACING	caudal anterior cingulate
CAUD	caudate
CB	cerebellum
CC	corpus callosum
cGM	cerebral grey matter
CING_G	cingulum gyrus
CLDRC	Colorado Learning Disabilities Research Centre
CMFR	caudal middle frontal gyrus
CR	corona radiate
CST	corticospinal tract
CT	cortical thickness
CUN	cuneus cortex
CV	cerebral volume
CV_A	coefficient of additive genetic variance
CV_P	coefficient of phenotypic variance
cWM	cerebral white matter
DZ	dizygotic
E	latent unique environment influences/factor
e	path coefficient for unique environmental influences
E1, E2	First, second latent unique environmental factors
e²	variance explained by unique environmental influences
EC	external capsule
ENT	entorhinal cortex
FA	fractional anisotropy
FHS	Framingham Heart Study
FNTR	Finnish National Twin Registry
FR	frontal
FRP	frontal pole
FUS	fusiform gyrus
FX	fornix

GI	gyrification index
GM	grey matter
GOBS	Genetics of Brain Structure and Function
GP	globus pallidus
h^2	heritability
HIP	hippocampus
I	index of the opportunity for selection
I_A	mean-standardised additive genetic variance
IC	internal capsule
ICV	intracranial volume
IFO	inferior fronto-occipital fasciculus
I_E	mean-standardised unique environment variance
inf	inferior
INFPAR	inferior parietal cortex
INFTEMP	inferior temporal gyrus
INS	insular cortex
I_P	mean-standardised phenotypic variance
IQ	intelligence quotient
ISTHMCING	isthmus cingulate
JPL	juxtaparacentral lobule
L	left
$L_{ }$	axial diffusivity
L_{\perp}	radial diffusivity
lat	lateral
LATOCC	lateral occipital cortex
LATORB	lateral orbitofrontal cortex
LH	left hemisphere
LING	lingual gyrus
LV	lateral ventricle
MDD-NSS	major depressive disorder with no suicidal symptoms
MDD-SS	major depressive disorder with suicidal symptoms
MEDORB	medial orbitofrontal cortex
MIDTEMP	middle temporal gyrus
msa	midsagittal area
MZ	monozygotic
NA	nucleus accumbens
NHLBI	National Heart, Lung, and Blood Institute
NIMH	National Institute of Mental Health
NTR	Netherlands Twin Registry
OATS	Older Adult Twins Study
OCC	occipital
OP	occipital pole
PAR	parietal
PARAC	paracentral lobule

PARAH	parahippocampal gyrus
PARSOPE	pars opercularis
PARSORB	pars orbitalis
PARSTR	pars triangularis
PCAL	pericalcarine cortex
PCC	posterior cingulate cortex
PCN	precuneus
PCUN	precuneus
POSTC	postcentral gyrus
POSTCING	posterior cingulate
PREC	precentral gyrus
PRECUN	precuneus cortex
PTR	posterior thalamic radiation
PTS	Pediatric Twin Study
PUT	putamen
QNTS	Quebec Newborn Twin Study
QTIM	Queensland Twin IMaging
R	right
RACING	rostral anterior cingulate
r_e	environmental correlation
r_g	genetic correlation
RH	right hemisphere
RMFR	rostral middle frontal gyrus
ROI	region of interest
r_{ph}	phenotypic correlation
r_{ph-a}	genetic contribution to the phenotypic correlation
r_{ph-e}	environmental contribution to the phenotypic correlation
SA	surface area
SAFHS	San Antonio Family Heart Study
SFO	superior fronto-occipital fasciculus
SGa	supramarginal gyrus, anterior
SLF	superior longitudinal fasciculus
SMG	supramarginal cortex
SS	sagittal stratum
sup	superior
SUPFR	superior frontal gyrus
SUPPAR	superior parietal cortex
SUPTEMP	superior temporal gyrus
T1/T2	time one/time two
T2a	middle temporal gyrus, anterior
TBV	total brain volume
TCV	total cerebral volume
TEDS	Twins Early Development Study
TEMP	temporal

TEMPP	temporal pole
THAL	thalamus
TTEMP	transverse temporal cortex.
TWIN-E	The Twin study in Wellbeing using Integrative Neuroscience of Emotion
UMCU	University Medical Centre Utrecht
UNC	University of North Carolina
\bar{x}	sample mean
V_A	additive genetic variance
V_E	unique environmental variance
VETSA	Vietnam Era Twin Study of Aging
V_P	total phenotypic variance
WM	white matter
WMHI	white matter hyperintensities
Δ	change

1

Introduction

1 Introduction

1.1 General Introduction

The human brain is the most complex structure in the known universe. It generates the higher consciousness associated with human creativity, but also the debilitating effects of mental illness. Due to differences in genetic and environmental influences during neurodevelopment, there is substantial variation in brain morphology among individuals. Disentangling and quantifying these sources of variance may be crucial to our understanding of the genetic architecture of the brain and how it relates to normal function and mental health disorders. As noted by Insel and Wang (2010), “the genetics of mental illness may really be the genetics of brain development”.

Magnetic resonance imaging (MRI) allows for non-invasive, *in vivo* study of structural brain differences between individuals. This technology, combined with genetic modelling, has shown high heritability (the proportion of phenotypic variance in a trait due to genetic differences among individuals within a population) for global brain structure (e.g. total brain volume) (Blokland, de Zubicaray, McMahon, & Wright, 2012; Gu & Kanai, 2014; Jansen, Mous, White, Posthuma, & Polderman, 2015). However, quantifying the source of genetic and non-genetic (i.e. environmental) contributions to differences in individual brain structures, particularly for the cerebral cortex, as well as identifying how these factors contribute to associations across the brain, are continuing challenges.

Further, some brain structures are difficult to delineate accurately and reliably, suggesting heterogeneity in measurement error across the brain. This is critical, as measurement error typically sets the upper limit for heritability (Dohm, 2002). The effect of measurement error on heritability estimates for a trait can be estimated by contrasting test-retest correlations with correlations between monozygotic (i.e. identical) twin pairs. However, such data is not widely available for prior research.

1.2 Aims and Thesis Outline

The goal of this thesis is to examine genetic and non-genetic contributions to normal brain variation in humans. To study this, a combination of *in vivo* imaging and twin studies was used. Twin studies assess not only the genetic and environmental variance of brain structure, but importantly, the genetic and environmental covariance between different

brain structure phenotypes (e.g. brain regions). In this thesis, we use two of the world's largest, genetically informative samples of healthy adults (*QTIM* Queensland Twin IMaging study; *HCP* Human Connectome Project). Specifically, we aimed to:

- quantify the variance components of region-specific variation in cortical surface area and thickness, and assess the genetic and non-genetic contributions to associations between cortical surface area and/or cortical thickness
- compare amounts of mean-standardised genetic and non-genetic variance for individual brain structures
- investigate whether patterns of genetic covariance are robust across sample and methodology
- examine covariance between cortical structure and reading ability, and assess the genetic and non-genetic contributions to these associations

In addressing these aims, we consider estimates of test-retest reliability for imaging phenotypes in both datasets to, importantly, consider the role of measurement error when examining genetic and environmental influences on brain morphology. Further, the use of two large independent datasets, consisting of participants of a similar age, facilitates the investigation of similarities in patterns of genetic and environmental variance across samples and imaging methodology.

1.3 Chapter Overview

In Chapter 2, we review the imaging genetics field. This provides a brief introduction to the techniques of twin imaging studies, as well as a meta-analysis of heritability estimates (the proportion of phenotypic variance attributed to genetic differences among individuals within a population) for structural brain phenotypes. Further, we discuss several issues with current estimates of heritability for brain structure.

Chapter 3 details the image processing and quality checking undertaken to produce the imaging phenotypes used in this thesis. In addition, we discuss how these phenotypes are used more widely by the Enhancing NeuroIMaging Genetics through Meta-Analysis (ENIGMA) consortium.

In the first empirical study (Chapter 4), we focus on variation in the cerebral cortex: the home of higher order cognition in humans. We examine patterns of region-specific (i.e. not shared throughout the whole brain) genetic and environmental influence on cortical surface area and thickness. In addition, we consider estimates of test-retest reliability to better evaluate differences in heritability across the cortex. We then investigate bivariate associations across the surface area and/or cortical thickness of cortical ROIs, and quantify the genetic and environmental contributions to these phenotypic associations. Lastly, we examine whether these patterns are replicable in an independent sample of twins and singletons.

In Chapter 5, we investigate mean-standardised measures of genetic and environmental variance, an ancillary method of comparing variance components. Unlike proportional measures of variance (i.e. heritability, Chapter 4), mean-standardised estimates reflect the strength of factors which maintain or deplete variability in a trait, which in turn may provide insights into the development or genetic architecture of a trait. Estimates of mean-standardised variance are typically neglected in imaging genetics, so in Chapter 5 we report estimates of mean-standardised genetic and environmental variance in the size of cortical, subcortical, and ventricular structures.

Chapter 6 extends the work of Chapter 4, examining genetic covariance between vertex-wise measures of the cortical surface (i.e. continuous as opposed to predefined regions). Using a clustering technique, we identify a genetic parcellation of the cortex in the QTIM and HCP datasets. We compare the similarity of the genetic divisions in our newly created parcellations to those previously defined in a sample of middle-aged males (Chen et al., 2012) to assess whether a genetically identified parcellation of the cerebral cortex is robust across samples and acquisition methodology.

In the last empirical chapter (Chapter 7), we investigate genetic and environmental covariation between cortical brain structure and a behavioural measure (reading ability). This chapter investigates whether cortical structures provide insights into the neurobiology underlying cognition. While several studies have investigated associations with general cognitive ability (Bohlken et al., 2014; Bohlken et al., 2016; Chiang et al., 2009; Vuoksimaa et al., 2016), studies of other cognitive processes are more limited. Here we were focused on reading ability to improve the literature surrounding genetic influences on brain structure and cognition, and to study whether associations are robust across sample and

methodology. Lastly, we summarise the main findings from the above chapters, and discuss their implications within the broader context of this thesis (Chapter 8).

2

Genetics and Brain Morphology

This chapter is published as:

Strike, L. T., Couvy-Duchesne, B., Hansell, N. K., Cuellar-Partida, G., Medland, S. E., & Wright, M. J. (2015). Genetics and brain morphology. *Neuropsychology Review*, 25(1), 63-96. doi:10.1007/s11065-015-9281-1

LS, BCD and NH contributed equally to the published work. Only the section written by LS is included here.

2 Genetics and Brain Morphology

Lachlan T. Strike^{1,2,3}, Baptiste Couvy-Duchesne^{1,2,3}, Narelle K. Hansell¹, Gabriel Cuellar-Partida⁴, Sarah E. Medland⁵, Margaret J. Wright^{1,2}

¹Neuroimaging Genetics, QIMR Berghofer Medical Research Institute, Brisbane QLD 4006, Australia.

²School of Psychology, University of Queensland, Brisbane QLD 4072, Australia. ³Centre for Advanced Imaging, University of Queensland, Brisbane QLD 4072, Australia. ⁴Statistical Genetics, QIMR Berghofer Medical Research Institute, Brisbane QLD 4006, Australia. ⁵Quantitative Genetics, QIMR Berghofer Medical Research Institute, Brisbane QLD 4006, Australia.

Abstract

A wealth of empirical evidence is accumulating on the genetic mediation of brain structure phenotypes. This comes from twin studies that assess heritability and genetic covariance between traits, candidate gene associations, and genome-wide association studies (GWAS) that can identify specific genetic variants. Here we review the major findings from twin studies and consider how they inform on the genetic architecture of brain structure. The findings from twin studies show there is a strong genetic influence (heritability) on brain structure, and overlap of genetic effects (pleiotropy) between structures, and between structure and cognition. Though there is also evidence for genetic specificity, with distinct genetic effects across some brain regions. Together these studies are revealing new insights into the genetic architecture of brain morphology. As the scope of inquiry broadens, including measures that capture the complexity of the brain, along with larger samples and new analyses, such as genome-wide common trait analysis (GCTA) and polygenic scores, which combine variant effects for a phenotype, as well as whole-genome sequencing, more genetic variants for brain structure will be identified. Increasingly, large-scale multi-site studies will facilitate this next wave of studies, and promise to enhance our understanding of the etiology of variation in brain morphology, as well as brain disorders.

2.1 General Introduction

Imaging genetics is a rapidly emerging field integrating imaging and genetic approaches to better understand the aetiology of normal brain variation and especially, mental illness. As magnetic resonance imaging (MRI) measures of brain morphology are thought to be closer

to the biology of genetic function than a behavioural phenotype or a disease syndrome itself, they are often used as endophenotypes to provide an objective tool to search for genetic variability in the brain (Glahn, Thompson, & Blangero, 2007; Gottesman & Gould, 2003). To be the most useful, endophenotypes must meet certain criteria (Gottesman & Gould, 2003; Gottesman & Shields, 1967), including that the endophenotype is heritable. Endophenotypes have been hypothesised to have a simpler genetic architecture (Gottesman & Gould, 2003), or reduced genetic complexity (de Geus, 2010) than other complex traits and have higher penetrance for genetic variants because they are biologically closer to the genes. However, there is a shift in current perspective such that the importance of endophenotypes is not in gene discovery itself, but rather, in the critical insights they will likely provide into the neurobiology underlying neurodegenerative, developmental, and neuropsychiatric conditions (Iacono, Vaidyanathan, Vrieze, & Malone, 2014).

Here we review imaging genetic studies focussing on brain morphology, including twin studies that assess not only the heritability of brain structure, but, importantly, the genetic covariance between different brain structure phenotypes (e.g. brain regions). We review the major findings from each of these approaches, and consider how they inform on the genetic architecture of brain structure. We also provide a brief overview of the methodology, highlighting important design considerations and central themes that emerge from the work, which are relevant to future research.

2.2 Twin and Family Imaging Studies

Twin and family studies provide a powerful method to establish the heritability of brain imaging phenotypes (see below for a brief overview of how twin studies estimate heritability). The very first study examined total brain volume and included ten identical (monozygotic (MZ)) and nine non-identical (dizygotic (DZ)) twin pairs (Bartley, Jones, & Weinberger, 1997). Today there are several large imaging cohorts for which structural scans have been acquired in over 100 pairs of twins (200 individuals) or multiple members from the one family. These studies include imaging cohorts from North America (CLDRC, GOBS/SAFHS, FHS, NIMH/PTS, NHLBI, QNTS, UNC, VETSA), Europe and the UK (FNTR, TEDS, NTR/UMCU) and Australia (OATS, QTIM, TWIN-E) (Table 2.1). Together, the cohorts cover a wide age range. Some cohorts themselves cover much of the lifespan

(FHS, GOBS/SAFHS, NTR/UMCU, TWIN-E), whereas others are more restricted with respect to age, focussing on either neonates and children (NIMH/PTS, QNTS, TEDS, UNC), adolescents and young adults (CLDRC, QTIM), middle-aged adults (FNTR, VETSA) or the elderly (NHLBI, OATS). Encouragingly, for a number of the cohorts (NIMH/PTS, NHLBI, NTR/UMCU, OATS, QTIM) imaging data are being acquired at more than one time point using the same imaging protocol. Longitudinal studies in genetically informative samples are vital to characterise the extent that changes in brain structure during the life course are due to genes and/or the environment. As can be seen in Table 2.1, for almost all cohorts global and regional brain volumes have been extracted, with more recent efforts examining cortical topography and white matter integrity. For many cohorts, there is also extensive phenotyping on a wide range of measures, including cognition, as well as resting state and/or task based functional magnetic resonance imaging (fMRI) (Blokland et al., 2011; Koten et al., 2009).

2.3 Estimating Heritability and Multivariate Genetic Analysis

The pattern of MZ and DZ twin correlations provides a first indication of whether there is a genetic contribution to brain morphology. Increased similarity between MZ twins compared to DZ suggests that variation in brain structure is influenced by additive genetic factors, while increased similarity between DZ twins (DZ twin correlation is more than half the MZ twin correlation) suggests an effect of common (i.e. shared) environment. Non-additive genetic effects will further increase the degree of similarity between MZ twins compared to DZ, though large samples are required to detect non-additive genetic effects (Martin, Eaves, Kearsley, & Davies, 1978). As well as examining twin correlations most studies use standard ACE model fitting analysis in *Mx* (Neale & Cardon, 1992) to partition the variance in a structure into additive genetic (A), common environmental (C) and unique or non-shared environmental (E) sources. Variation due to dominant genetic (D) effects can also be partitioned; though not simultaneously with C in samples where twins are reared together (C and D are confounded in this instance). See D. M. Evans, Gillespie, and Martin (2002), (Neale & Cardon, 1992) and Verweij, Mosing, Zietsch, and Medland (2012) for excellent reviews of the twin method and genetic analyses.

Table 2.1 Twin and family cohorts with imaging data

Cohort*	Reference	<i>n</i> pairs MZ/DZ†	Age range (years)	Structural Imaging Phenotypes	Cognitive phenotypes
<i>Twin</i>					
Colorado Learning Disabilities Research Centre (CLDRC)	Betjemann et al. (2010)	41/30	12-24	Global, regional	General cognitive ability, reading
Finnish National Twin Registry (FNTR)	Thompson et al. (2001)	10/10	Mean=48±3	Voxel-wise morphometry	General cognitive ability
National Heart, Lung, and Blood Institute (NHLBI)	Pfefferbaum, Sullivan, Swan, and Carmelli (2000)	72/70	69-80	Global, regional, subcortical, white matter hyperintensities	General cognitive ability
National Institute of Mental Health (NIMH) / Paediatric Twin Study (PTS)	Schmitt et al. (2007)	127/36	6-19	Global, regional, subcortical, cortical thickness	General cognitive ability
Netherlands Twin Registry (NTR)/ University Medical Centre Utrecht (UMCU)	Brans et al. (2010)	102/131	9-69	Global, regional, subcortical, cortical thickness & surface area, white matter integrity, voxel-wise morphometry.	General cognitive ability, working memory
Older Adult Twins Study (OATS)	Sachdev et al. (2009)	77/41	65-88	Global, regional, subcortical	General cognitive ability, memory, language
Quebec Newborn Twin Study (QNTS)	Yoon, Fahim, Perusse, and Evans (2010)	57/35	Mean=8	Global, regional, subcortical, cortical thickness, voxel-wise morphometry	General cognitive ability
Queensland Twin IMaging (QTIM) study	(Blokland et al., 2014)	148/202	12-30	Global, regional, subcortical, cortical thickness & surface area, white matter integrity, voxel-wise morphometry	General cognitive ability, reading
Twins Early Development Study (TEDS)	Rijsdijk et al. (2010)	31/35	Mean=9	Voxel-wise morphometry	General cognitive ability, reading, mathematics
The Twin study in Wellbeing using Integrative Neuroscience of Emotion (TWIN-E)‡	Gatt et al. (2012)	122 pairs	18-65	Global, regional, cortical thickness & surface area, white matter integrity	General cognitive ability
University of North Carolina (UNC)	Gilmore et al. (2010)	41/50	0 – 1 week	Global, regional, subcortical, white matter integrity	
Vietnam Era Twin Study of Aging (VETSA)	Kremen, Franz, and Lyons (2013)	110/92	51 - 59	Global, regional, cortical thickness & surface area, voxel-wise morphometry	General cognitive ability, working memory
<i>Family/pedigree</i>					
Framingham Heart Study (FHS)	DeStefano et al. (2009)	1538 subjects	34-97	Global, regional, subcortical	Verbal memory, visuospatial memory
Genetics of Brain Structure and Function (GOBS) / San Antonio Family Heart Study (SAFHS)	Kochunov et al. (2011)	1129 subjects	19 - 85	Global, regional, subcortical, cortical thickness & surface area, white matter integrity, voxel-wise morphometry	General cognitive ability, working and declarative memory, language and emotional processing

DZ dizygotic; *MZ* monozygotic.

*Several cohorts function as combinations (NIMH/PTS, NTR/UMCU) or subsamples (GOBS/SAFHS). Cohorts with small sample sizes (<20 pairs) are not included.

† Largest published complete pairs.

‡ Sample size and age range are projected figures.

The twin design can be extended to include additional family members such as siblings, estimate the effects of covariates such as age to improve the fit of the model, allow multiple phenotypes to be studied simultaneously or to analyse more complex genetic and environmental influences (e.g. interaction terms such as gene-environment correlation). By including multiple phenotypes, as shown in Figure 2.1, it is possible to decompose the variance both within and between variables into genetic and environmental components. From this, genetic, environmental, and phenotypic correlations can be calculated, with the genetic correlation indicating the extent to which two different structural measures share genetic influence. For example, a genetic correlation of 1 indicates two traits are influenced completely by the same latent genetic factor(s). Several studies have examined the genetic overlap among different brain measures, and a few have investigated whether there is any genetic overlap across brain structure and cognition. We review these studies in the sections below.

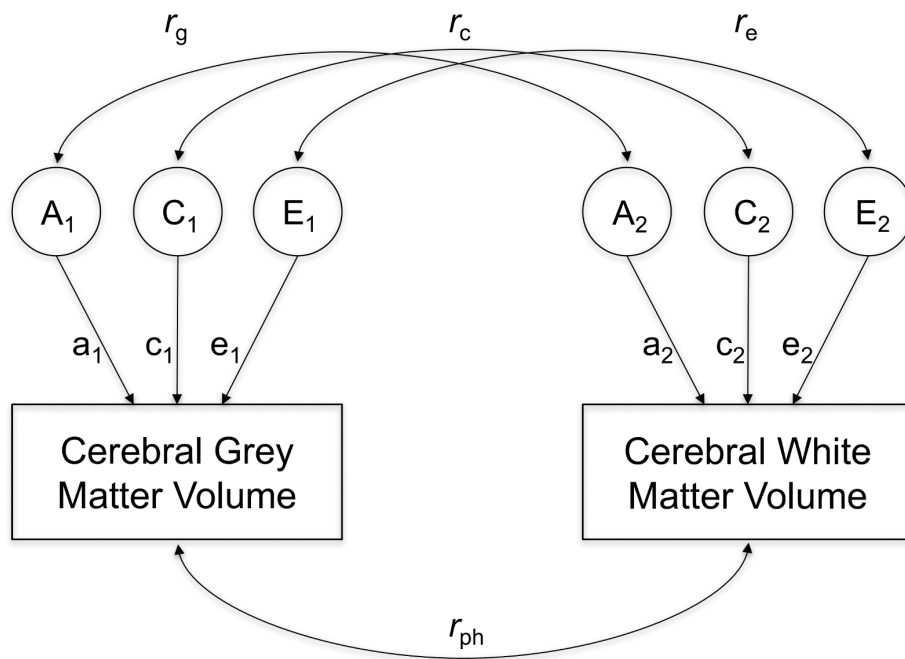


Figure 2.1 Correlated factors bivariate twin model.

A, C, and E are the latent additive genetic, common environment and unique environment factors respectively, which influence cerebral grey and white matter volume. r_g , r_c and r_e are the genetic, common environmental and unique environmental correlations respectively, with r_{ph} the phenotypic correlation between the two observed traits. a , c and e represent parameter estimates, conceptualised as the strength of the latent factor on the phenotype.

Besides twin studies, heritability can also be estimated from family pedigrees (Kochunov et al., 2009). More recently it has become possible to estimate heritability directly from DNA (Yang, Lee, Goddard, & Visscher, 2011). This method, often called GCTA (Genome-wide Complex Trait Analysis), estimates the genetic influence (heritability) using genome-wide genotypes from very large samples (i.e. thousands) of unrelated individuals, rather than comparing MZ and DZ twins. GCTA detects only the genetic effects that are tagged by common single nucleotide polymorphisms (SNPs) (allele frequencies greater than 1%) available on a DNA array used in GWAS. Thus, GCTA heritability (or SNP heritability) is not expected to be as large as the heritability estimated from twin studies that can detect genetic influences due to DNA variants of any kind (Vinkhuyzen, Wray, Yang, Goddard, & Visscher, 2013). GCTA can also be extended to multivariate analysis to estimate the SNP heritability of each phenotype and the SNP-correlation between phenotypes (Wray et al., 2014). To date only a few studies have estimated SNP heritability of brain imaging phenotypes (Adib-Samii et al., 2015; Bryant et al., 2013), mainly because very large samples are necessary, requiring genotypes and phenotypes to be shared among several research groups (which is not always possible). We discuss these results later.

2.4 Heritability of Brain Structure

The growing number of imaging studies in twins and families provides strong evidence that individual differences in brain structure are due to both genetic factors and the environment. Figure 2.2 shows heritability estimates for a range of measures, including global and regional brain volumes, subcortical volumes, cortical thickness and white matter integrity. These results are from a recent meta- and mega-analysis (Blokland et al., 2012; Kochunov et al., 2014), or a new meta-analysis, including data that has accumulated since 2012. Heritability estimates range from moderate to high i.e. 40% to >80%. As noted previously (Blokland et al., 2012), lower heritability estimates are generally found for smaller brain structures relative to larger global or lobar structures. However, whether one structure has a higher heritability than the other needs to be interpreted with care. As seen in Figure 2.2, confidence intervals for heritability estimates overlap for many structures.

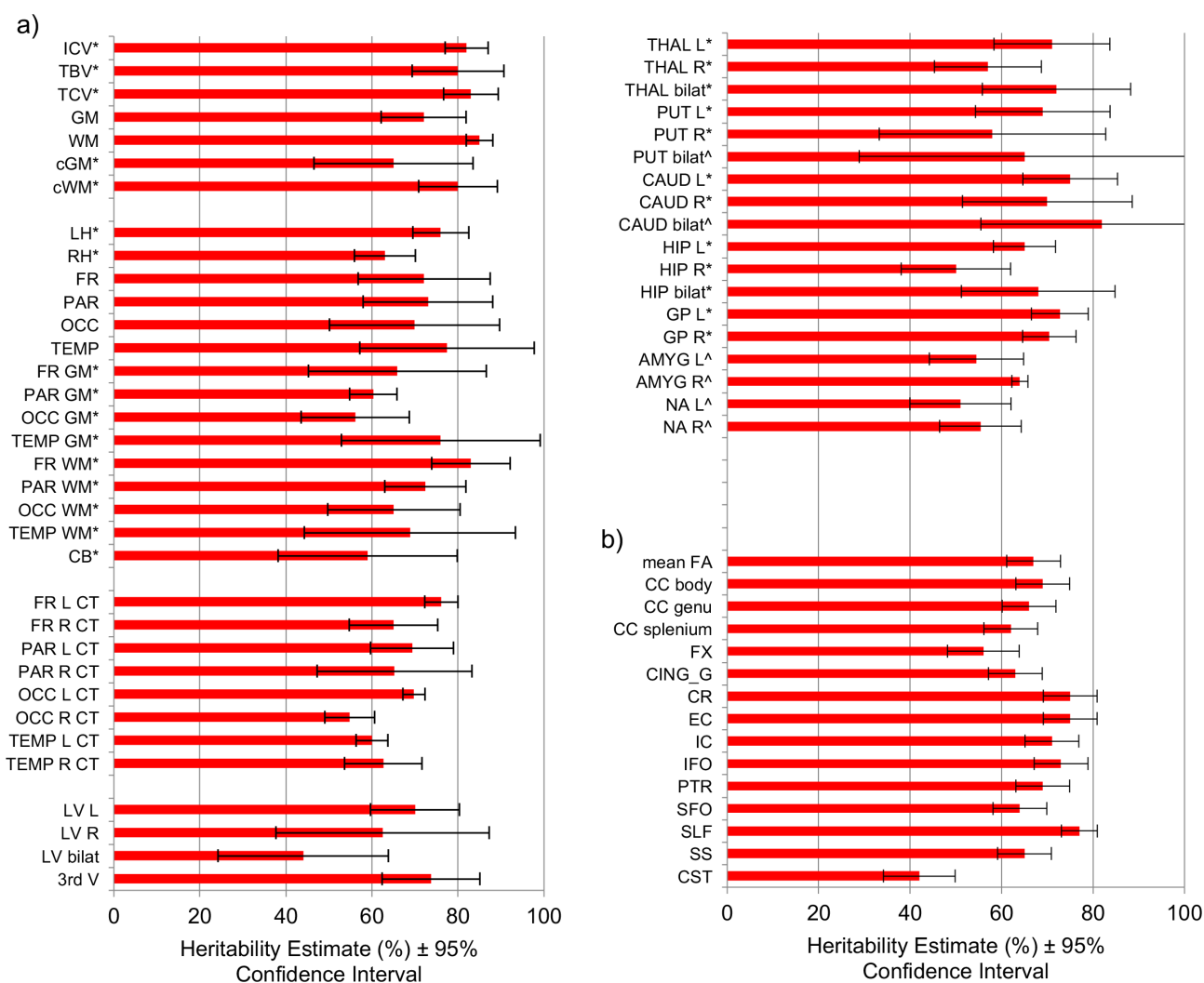


Figure 2.2 Heritability estimates with 95% confidence intervals for brain structure

Additive genetic estimates and 95% confidence intervals for (a) volumetric and cortical thickness and (b) fractional anisotropy (FA) white matter integrity. a) Meta-analysis combining estimates from Blokland et al. (2012) and 3 additional studies, some of which include new imaging phenotypes not included in Blokland et al. 2012; * denotes revised heritability estimate, and ^ denotes new phenotype. The meta-analyses including the additional studies (Batouli et al., 2014; den Braber et al., 2013; Renteria et al., 2014) used the same methodology as Blokland et al. (2012). Full ACE estimates available in Figure 2.3. b) FA white matter mega-analysis estimates (Kochunov et al., 2014) publicly available from http://enigma.ini.usc.edu/ongoing/dti-working-group/2014_nimg/. A harmonisation protocol combined DTI for 2248 participants from five cohorts followed by a mega-analysis to estimate heritability.

3rd V third ventricle; *AMYG* amygdala; *bilat* bilateral; *CB* cerebellum; *CAUD* caudate; *CC* corpus callosum; *CING_G* cingulum gyrus; *cGM* cerebral grey matter; *CST* corticospinal tract; *CR* corona radiata; *cortical thickness* cortical thickness; *cWM* cerebral white matter; *EC* external capsule; *FA* fractional anisotropy; *FR* frontal; *FX* fornix; *GM* grey matter; *GP* globus pallidus; *HIP* hippocampus; *IC* internal capsule; *ICV* intracranial volume; *IFO* inferior fronto-occipital fasciculus; *L* left; *LH* left hemisphere; *LV* lateral ventricle; *NA* nucleus accumbens; *OCC* occipital; *PAR* parietal; *PTR* posterior thalamic radiation; *PUT* putamen; *R* right; *RH* right hemisphere; *SFO* superior fronto-occipital fasciculus; *SLF* superior longitudinal fasciculus; *SS* sagittal stratum; *TBV* total brain volume; *TCV* total cerebral volume; *TEMP* temporal; *THAL* thalamus; *WM* white matter.

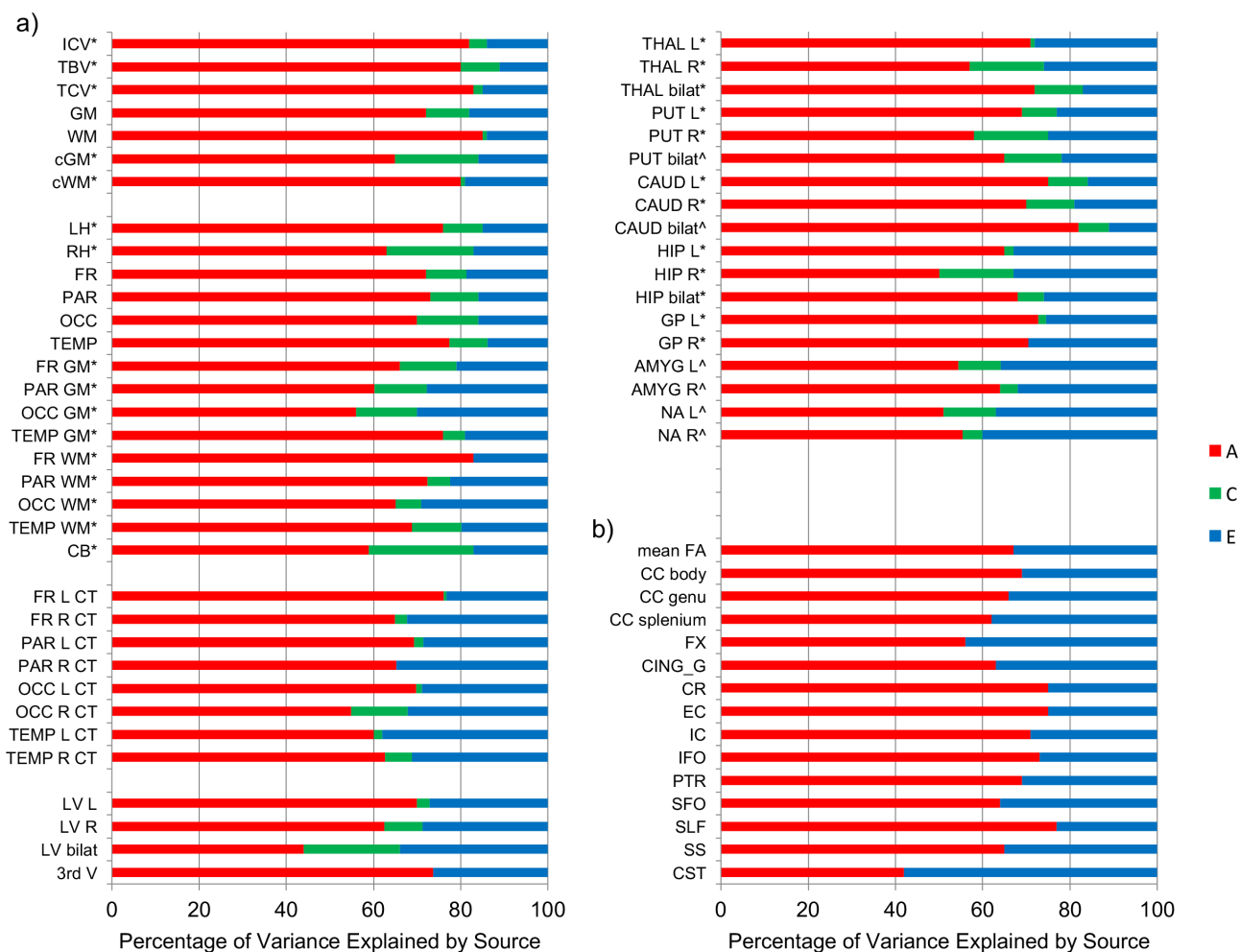


Figure 2.3 Variance component estimates for brain structure (meta-analysis)

Proportion of variance explained by additive genetic ('A'), common or shared environment ('C'), and unique or non-shared environment ('E') sources for (a) volumetric and cortical thickness and (b) fractional anisotropy (FA) white matter integrity brain phenotypes. 'C' effects were not estimated for FA measures; hence all non-genetic variance is attributed to 'E'.

Notably, few studies have examined whether the heritability of imaging phenotypes is a function of gender (Chiang et al., 2011). By dividing twin pairs into five groups (MZ male, MZ female, DZ male, DZ female, DZ opposite sex pairs), sex limitation modelling can estimate both qualitative and quantitative differences between males and females (. i.e. is heritability larger in one sex than in the other (same genetic source, different magnitude), or whether a factor (genetic or environmental) effects one sex but not the other). As different neurodevelopmental trajectories for males and females have been reported (Dennison et al., 2013; Koolschijn & Crone, 2013; Lenroot & Giedd, 2010), and as the majority of the cohorts include both opposite and same sex pairs, these studies will be well placed to examine sex-dependent effects as their samples increase. Additionally, throughout development into old age, the structure of the brain changes over the life

course. While cross sectional studies have demonstrated heritability changes associated with age (Lenroot et al., 2009; Wallace et al., 2006), longitudinal twin studies (Schmitt et al., 2014; van Soelen et al., 2012) that are well powered (large samples) are needed to detect changes in heritability for different brain structures as a function of age. Recently, some progress was made when several groups with longitudinal imaging data on twins worked together as part of the ENIGMA Consortium to estimate the heritability of subcortical brain plasticity (Brouwer et al., 2015).

Though heritability tells us nothing about the underlying genes or the number of genes involved or their effect size, the magnitude of the heritability estimate does provide some indication of the statistical power for discovering the causal genes of a trait (Bochud, 2012). For example, if the heritability estimates of several brain structures are available, the structure with the highest heritability estimate can be chosen for genome-wide association studies (e.g. Stein et al. (2012) selected hippocampus and intracranial volume on this basis). A general benchmark is to consider heritability estimates below 20% as low, those between 20% and 50% as moderate, and estimates above 50% as high. Of the 67 brain structure phenotypes in Figure 2.2 and Figure 2.3, two structures (bilateral lateral ventricles, corticospinal tract) are moderately heritable, with all others highly heritable. Nonetheless a high heritability estimate does not imply that genetic variants associated with the brain structure will have a large effect on the phenotype (Visscher, Hill, & Wray, 2008). Limitations of heritability estimation include a lack of information on the mode of inheritance of the trait, and the possibility that heritability estimates may vary across populations or with time. This may be especially relevant to child and adolescent samples, with Schmitt et al. (2014) reporting increases in cortical thickness heritability estimates during the first two decades of life. The finding of a similar genetic architecture behind subcortical structures in young (Renteria et al. (2014) and middle-aged (Eyler et al., 2011) adults possibly suggests greater stability in heritability estimates following adolescence. In samples with a wide age range there may be cohort effects, which may confound the “equal environment” within the sample population (Bochud, 2012).

The pervasiveness of a genetic contribution to brain structural measures does not mean that environmental influences are not important. Both genetic and environmental (non-genetic) factors contribute to the variance in brain structure. Non-genetic factors include identifiable environmental factors and measurement error, though both are not well assessed. However, most recently imaging studies such as IMAGEMEND (Frangou, 2014)

have begun collecting both genetic and environmental data. This will facilitate considerations of the interplay between genes and the environment in the development of the brain, brain ageing, as well as psychiatric disorders.

2.5 Issues in Estimating Heritability for Imaging Phenotypes

Sample size, namely whether it is large enough to provide sufficient power to detect genetic variance (heritability) is an important consideration. Generally, the global brain measures in Figure 2.2 and Figure 2.3 are available on large samples; the smaller confidence intervals for the heritability estimates reflect this increased power. Many of the early imaging studies in twins were restricted by small sample size (Bartley et al., 1997; Pennington et al., 2000; I. C. Wright, Sham, Murray, Weinberger, & Bullmore, 2002) so the degree to which the results can be generalised to larger populations is somewhat limited. The high cost of brain imaging and twin recruitment are ever present factors impacting sample size for imaging genetics studies. The mega-analysis approach undertaken by Kochunov et al. (2014) is an engaging future research direction for addressing such concerns. In this method, imaging data from multiple sites are pooled together and analysed as one data set, ensuring homogeneity of processing. Though the sharing of data across research groups is not always possible, this technique allows for large sample sizes to be amassed and removes one level in which error variance may be introduced (measurement variability).

Another issue is that some brain structures are more easily measured than others. In assessing or ranking heritability estimates, any differences in measurement error need to be considered. For example, the lower heritability estimates for smaller brain structures (e.g. nucleus accumbens) may be due to increased measurement error, as reflected in lower test-retest reliability (Morey et al., 2010; Nugent et al., 2013; Renteria et al., 2014). Measurement error artificially reduces the similarity between MZ twins and thereby reduces heritability estimates (i.e. reliability sets the upper limit for heritability by constraining the maximum possible correlation between MZ twins). How well a brain region or white matter tract can be reliably measured is often overlooked, but in the absence of test-retest reliability statistics it is difficult to determine if low heritability estimates are valid or simply reflect measurement error (Kuntsi et al., 2006). If test-retest statistics were provided alongside heritability estimates (e.g. as per Renteria et al. (2014)),

any differences in the genetic contribution across measures could be better evaluated. For example, as the intra-class correlation (ICC) is conceptually analogous to the r^2 obtained in regression analysis (Rousson, Gasser, & Seifert, 2002), it is possible to make a direct comparison between the portion of variability not explained between the repeats ($1 - r^2$ test-retest or $1 - \text{ICC test-retest}$) and e^2 (variance due to non-shared environment and measurement error). Where e^2 exceeds unreliability ($1 - r^2$ test-retest), non-shared environmental influences are greater than measurement error. Conversely, measurement error is greater than non-shared environment when unreliability ($1 - r^2$ test-retest) is greater than e^2 . Further, the accuracy of the heritability estimate can be increased by modelling unreliability (Kuntsi et al., 2006; Luciano et al., 2001), though this can result in an overestimation of the genetic effects (Luciano et al., 2001). Thus it is better to improve measurement of a phenotype rather than statistically adjust for measurement error (Kuntsi et al., 2006). For genetic association studies to build upon the findings of heritability estimates, imaging phenotypes, and the resulting heritability estimates, should be as reliable as possible.

A further consideration, especially when comparing or meta-analysing heritability estimates, is the use of different software to segment and measure the brain (Gronenschild et al., 2012; Morey et al., 2009), as well as the MRI platform or field strength used for scanning (Han et al., 2006; Jovicich et al., 2009). Variation in measurement can arise through differences in software methodologies (FreeSurfer, FSL, SPM), but also differences within the same analysis package (i.e. different versions of the same software). For instance, Renteria et al. (2014) reported test-retest Pearson's correlations of 0.51 and 0.52 for mean nucleus accumbens and amygdala volume respectively, extracted through FreeSurfer 5.1. Correlations from the same sample extracted through FreeSurfer 5.3, and with improved intensity inhomogeneity correction, increased to 0.68 and 0.77 respectively. Recently, standardised imaging and analysis protocols have been adopted for multi-site analyses (e.g. as implemented by the ENIGMA consortium) to address this issue and enhance phenotypic heritability.

2.6 *Overlapping or Distinct Genetic Factors?*

While the brain can be segmented into many regions and quantified in different ways, several brain structure phenotypes are highly correlated. For instance, individuals with a large grey matter volume also have a large white matter volume (Baare et al., 2001). Several twin studies have investigated whether different brain structure phenotypes are genetically correlated (Table 2.2). A number of these show high genetic correlations, such as between intracranial and thalamus volume (Renteria et al., 2014), cortical grey and white matter volume (Baare et al., 2001), grey matter volume and surface area (Winkler et al., 2010) and longitudinal change in total cerebral and cerebellum volume (van Soelen et al., 2013). The average phenotypic correlation for these studies is .60. The genetic correlations are slightly higher, ranging from 0.68 to 0.88, indicating an overlapping set of genes are responsible for the heritability of these brain structure phenotypes. Genetic correlations estimate the extent that genetic effects on one phenotype are correlated with the genetic effects on another phenotype, independent of their heritability. Overlapping genetic effects provide evidence for pleiotropy (each gene affects many traits) across the brain, and this has mostly been demonstrated between regional brain volumes and/or global measures.

Examining cortical thickness in 54 cortical sub-regions, Schmitt et al. (2008) identified a single factor accounting for over 60% of the genetic variability in cortical thickness measurements. Using the same sample, they also reported a strong genetic factor influencing variation between lobar volumes (Schmitt et al., 2010). Interestingly, in both studies, after correcting for mean cortical thickness or total brain volume, regionally specific patterns of genetic influence emerged, showing that there is genetic specificity, with distinct genetic effects across brain regions. Examining cortical thickness, Chen et al. (2013) reported distinct clusters of genetic influence throughout the cortex, i.e. different sets of genes influenced cortical thickness in different areas of the cortex. The structuring of these clusters appeared to reflect differences in maturation timing, and also the division between primary and association cortex. However, in an older sample, genetic effects on lobar volumes tended to be general rather than specific (Batouli et al., 2014). Differences in sample age and methodology across studies may account for these findings.

The low phenotypic and genetic correlations found for some of the studies shown in Table 2.2 also suggest that a common genetic influence does not extend to all areas of the brain, or two measures of the same structure. For example, (Panizzon et al., 2009) and Winkler

et al. (2010) found that two standard measures of grey matter (cortical thickness and surface area), shared little genetic overlap. Further, Renteria et al. (2014) identified region specific genetic factors explaining over 50% of the heritability in hippocampus, caudate nucleus, amygdala, and nucleus accumbens volumetric measures. These findings confirmed those of a prior study (Eyler et al., 2011), and demonstrate a similar genetic framework for subcortical structures across young and older adults.

Clearly, further work is needed to determine the pattern of genetic effects on brain structure phenotypes. A limited range of brain structure phenotypes have been examined and we have little understanding of whether the genetic covariance across brain structure phenotypes changes throughout the lifespan, or how such genetic organization reflects brain function.

2.7 Shared Genetic Influences Across Brain Structure and Cognitive Ability

Both brain structure (Blokland et al., 2012; Kremen et al., 2010) and cognitive ability (Deary, Penke, & Johnson, 2010; van Soelen et al., 2011) show substantial individual variability, much of which appears to be influenced by genetic factors. Multivariate studies have revealed that, to some degree, these genetic factors overlap. Table 2.3 displays phenotypic, genetic, and environmental correlations between measures of brain morphology and intelligence. Notably, the phenotypic correlations peak at approximately $\pm .30$, thus brain structure is at best moderately associated with cognitive ability. However, genetic and environmental influences can sometimes have opposing effects that cancel each other out (Brans et al., 2010). Alternatively, both genetic and environmental factors can have the same direction of influence and thus enhance the phenotypic correlation (Brouwer, van Soelen, et al., 2014), and in some cases, the association is largely due to a common genetic source (Brans et al., 2010). The majority of studies to-date have focused on total measures of grey and white matter tissue (Betjemann et al., 2010; Posthuma et al., 2003; Posthuma et al., 2002; van Leeuwen et al., 2009). Interesting, Vuoksimaa et al. (2015) recently demonstrated genetic associations between cortical volume and cognitive ability to be the result of variation in cortical surface area, but not cortical thickness. White matter tracts have also shown phenotypic and genetic overlap with cognition (Chiang et al., 2009; Karlsgodt et al., 2010), possibly illustrating biological networks underpinning intelligence. Overall, the low phenotypic correlations reported by studies signify that while

there does appear to be pleiotropy across brain structure and function, overlapping genes have only a small association with intelligence. Future studies focusing on the neural circuitry associated with cognitive ability (as opposed to global or anatomical brain divisions) may be able to tap into a greater phenotypic relationship between brain morphology and function, thereby identifying genetic factors with stronger genetic influences on cognition. Further, the relative importance of genetic and environmental factors may vary across the lifespan, with periods such as adolescence being of particular interest (Lenroot & Giedd, 2008) and a potential target for future work.

Examining associations between brain development trajectories and whether this predicts cognitive performance, and whether shared genetic factors underlie such an association (and if this represents causality) are important future research questions. Additionally, as studies have shown environmental factors can influence intelligence (Bates, Lewis, & Weiss, 2013; Tucker-Drob, Rhemtulla, Harden, Turkheimer, & Fask, 2011; Turkheimer, Haley, Waldron, D'Onofrio, & Gottesman, 2003), determining if gene by environment interactions modify genetic associations between structure and cognition could prove crucial to our understanding of brain development. Also worth exploration is the gene-environment correlation (Plomin, DeFries, & Loehlin, 1977), which denotes the possibility that differential environmental effects can occur as a function of genetics (active gene-environment correlation). For example, individuals may choose to undertake mentally challenging activities (due to genetic influences) which may then influence cognitive ability or brain morphology. Furthermore, examining if the magnitude of genetic overlap between brain morphology and cognitive ability differs by brain regions and structural phenotype (cortical thickness, volume, white matter integrity) will aid in identifying "higher order" brain structures especially sensitive to genetic or environmental influences. Multivariate twin studies provide unparalleled insights into the genetic relationships between brain structures and behavioural traits, and offer basic insights into the genetic mechanisms behind the human brain, which genetic association studies can build upon.

Table 2.2 Shared genetic influence across brain structures.

Reference	Cohort	<i>n</i> pairs MZ/DZ (age in years)	Phenotypes*	r_{ph}	r_g	r_e
Posthuma et al. (2000)	NTR / UMCU	53/58 (19-69)	ICV & CB	-	0.57	0.44
Pfefferbaum et al. (2000)	NHLBI	45/40 (68-78)	CC msa height & LV bilat	0.66	0.68	0.58
Baare et al. (2001)	NTR / UMCU	54/58 (19-69)	cGM & cWM	0.59	0.68	0.03
			ICV & cWM	0.81	0.83	0.66
			ICV & cGM	0.84	0.90	0.49
			ICV & TBV	0.93	0.95	0.79
Schmitt et al. (2007)	NIMH	127/36 (5-18)	(Lowest r_g) LV bilat & THAL bilat	-	0	-0.22
			(Highest r_g) TCV & THAL bilat	-	0.97	0.35
DeStefano et al. (2009)	FHS	1538 subjects (34-97)	(Lowest r_g) OCC lobe & LV bilat	-0.01	0.01	0.01
			(Highest r_g) TEMP lobe & HIP bilat	0.38	0.76	-0.11
(Panizzon et al., 2009)	VETSA	110/92 (51-59)	cGM cortical thickness & surface area	0.01	0.08	-0.13
			(Lowest r_g) PCC R cortical thickness & surface area	-0.06	0.01	-0.03
			(Highest r_g) lat OCC R cortical thickness & surface area	-0.03	0.88	-0.11
Kochunov et al. (2009)	SAFHS	459 subjects (19/85)	Subcortical WMHI & ependymal WMHI	-	0.46	0.07
Kochunov et al. (2010)	SAFHS	467 subjects (19-85)	FA mean & L_{\perp} mean	-	-0.68	-
			FA mean & L_{\parallel} mean	-	-0.70	-
			L_{\perp} mean & L_{\parallel} mean	-	0.95	-
Rogers et al. (2010)	GOBS	242 subjects (19-85)	surface area mean & GI mean	-	-0.60	-
			CV mean & GI mean	-	-0.73	-
Schmitt et al. (2010)	NIMH	127/36 (5-18)	(Lowest r_g) PAR GM & TEMP WM	-	0.56	-0.10
			(Highest r_g) FR GM & TEMP GM	-	0.94	0.86
Winkler et al. (2010)	GOBS	486 subjects (26-85)	(Lowest r_g) PCUN GM & PCUN cortical thickness	0.10	0.03	0.16
			cGM & surface area	0.85	0.85	0.85
			(Highest r_g) TEMP pole GM & TEMP pole surface area	0.81	1	0.76
Eyler et al. (2011)	VETSA	110/92 (51-59)	(Lowest r_g) THAL L & LV L	-	0	-
			THAL L & HIP R	-	0.51	-
			(Highest r_g) CAUD L & CAUD R	-	1	-
Panizzon et al. (2012)	VETSA	130/97 (51-60)	(Lowest r_g) PCUN L WM/GM contrast & PCUN L cortical thickness	0.15	-0.01	0.33
			(Highest r_g) PCAL R WM/GM contrast & PCAL R cortical thickness	-0.54	-0.89	-0.34
van Soelen et al. (2012)	NTR / UMCU	23/28 (T1 Mean=9) (T2 Mean=12)	(Lowest r_g) Δ in FR R cortical thickness & Δ in sup TEMP L cortical thickness over 3 years	0	-0.01	-
			(Highest r_g) Δ in inf PAR L cortical thickness & Δ in inf FR L cortical thickness Δ over 3 yrs	0.30	1	-
van Soelen et al. (2013)	NTR / UMCU	23/28 (T1 Mean=9) (T2 Mean=12)	Δ in TCV & Δ in height over 3 yrs	0.09	0.39	-0.13
			Δ in CB & Δ in height over 3 yrs	0.24	0.48	-0.05
			Δ in TCV & Δ in CB over 3 yrs	0.49	0.88	0.34
Batouli et al. (2014)	OATS	77/41 (65-88)	(Lowest r_g) cGM & cWM	-	0.17	0.56
			(Highest r_g) TEMP & TCV	-	0.95	0.90
Renteria et al. (2014)	QTIMS	148/202 (16-29)	(Lowest r_g) CAUD mean & AMYG mean	0.10	0.13	-
			(Highest r_g) ICV & THAL mean	0.76	0.86	-

Note. Multivariate studies were identified through a PubMed search of the following terms: *twin - brain - imaging - MRI - genetic*. With a cut-off date of 1 July 2014, 27 studies were identified, with an additional 18 studies identified manually through references. Those that could be quantified are summarised in Table 2.2 and Table 2.3, with those that could not be quantified (Chen et al., 2013; Chen et al., 2012; Chen et al., 2011; Chiang et al., 2012; Chiang et al., 2009; Eyler et al., 2011;

Giedd, Schmitt, & Neale, 2007; Jahanshad et al., 2013; Rimol et al., 2010; Schmitt et al., 2009; Schmitt et al., 2008; Wallace et al., 2010; I. C. Wright et al., 2002) consistent with tabled findings.

AMYG amygdala; *bilat* bilateral; *CAUD* caudate; *CB* cerebellum; *CC* corpus callosum; *cGM* cerebral grey matter; *CV* cerebral volume; *cWM* cerebral white matter; *cortical thickness* cortical thickness; *FA* fractional anisotropy; *FR* frontal; *GI* gyrification index; *GM* grey matter; *HIP* hippocampus; *inf* inferior; *ICV* intracranial volume; *L* left; *lat* lateral; $L_{||}$ axial diffusivity; L_{\perp} radial diffusivity; *LV* lateral ventricle; *msa* midsagittal area; *OCC* occipital; *PAR* parietal; *PCAL* pericalcarine cortex; *PCC* posterior cingulate cortex; *PCUN* precuneus; *R* right; r_e environmental correlation; r_g genetic correlation; r_{ph} phenotypic correlation; *surface area* surface area; *sup* superior; *T1/T2* time one/time two; *TBV* total brain volume; *TCV* total cerebral volume; *TEMP* temporal; *THAL* thalamus; *WM* white matter; *WMHI* white matter hyperintensities; Δ change.

*These phenotypes are volumes unless otherwise stated. Where results for many structures are reported, the regions with lowest and highest genetic correlations are shown.

Table 2.3 Shared genetic influence between brain structure and cognitive ability.

Reference	Cohort	<i>n</i> pairs MZ/DZ (age in years)	Phenotypes*	r_{ph}	r_g	r_e
Pennington et al. (2000)	CLDRC	25/23 (>12)	TCV & FSIQ	-	0.48	-
Carmelli, Reed, and DeCarli (2002)	NHLBI	72/70 (69-80)	WMHI & EF	-0.20	-0.24	-0.22
Carmelli, Swan, DeCarli, and Reed (2002)	NHLBI	72/67 (69-80)	WMHI & MMSE	-0.20	-0.36	0
			LV L & EF	-0.25	-0.57	-
			LV R & EF	-0.26	-0.25	-
			cGM & <i>g</i>	0.25	0.29	-
Posthuma et al. (2002)	NTR/UMCU	24/31 (19-69)	cGM & WMem	0.29	0.38	-
			cWM & <i>g</i>	0.24	0.24	-
			cWM & Wmem	0.29	0.35	-
Posthuma et al. (2003)	NTR/UMCU	102/131 (19-69)	(Lowest r_g) CB & VC	-	0.03	-0.23
			(Highest r_g) cGM & WMem	-	0.40	-0.13
Hulshoff Pol et al. (2006)	NTR/UMCU	54/58 (19-69)	(Lowest r_g) CC WM & VIQ	0.14	0.15	-
			(Highest r_g) PH GM & PIQ	0.23	0.40	-
van Leeuwen et al. (2009)	NTR	48/64 (Mean=9)	(Lowest r_g) cGM & PS	0.06	0.09	0.05
			(Highest r_g) cGM & Raven	0.22	0.36	-0.16
Betjemann et al. (2010)	CLDRC	41/30 (12-24)	(Lowest r_g) cGM & reading ability	0.15	0.14	-
			(Highest r_g) cWM & PS	0.28	0.89	-
Brans et al. (2010)	NTR/UMCU	77/84 (T1 Mean=30)	(Lowest r_g) Δ in MF L cortical thickness over 5 yrs & FSIQ	0.08	0.56	-0.66
			(Highest r_g) Δ in OP R cortical thickness over 5 yrs & FSIQ	0.34	1	0.22
Karlsgodt et al. (2010)	GOBS	467 subjects (19-85)	(Lowest r_g) CING FA & DB	-	0.02	0.01
			(Highest r_g) SLF FA & SDRT	-	0.59	0.25
Glahn et al. (2013)	GOBS	1129 subjects (18-83)	(Lowest r_g) EC FA & FMD	0.06	0	0.11
			(Highest r_g) CING_G FA & SDRT	-0.08	-0.47	0.11
Brouwer, Hedman, et al. (2014)	NTR/UMCU	11/21 (T1 19-56)	(Lowest r_g) Δ in whole brain L over 5 yrs & FSIQ	0.27	0.50	-0.17
			(Highest r_g) Δ in cWM L over 5 yrs & VIQ	0.29	1	-0.41
Brouwer, van Soelen, et al. (2014)	NTR/UMCU	23/28 (Mean=12)	(Lowest r_g) PCL L cortical thickness & FSIQ	-0.29	-0.32	-0.24
			(Highest r_g) CUN L cortical thickness & VIQ	-0.28	-1	0.39
Bohken et al. (2014)	NTR/UMCU	50/56 (19-55)	(Lowest r_g) PUT bilat & FSIQ	0.01	0	0.08
			(Highest r_g) THAL bilat & FSIQ	0.26	0.29	0.08
Vuoksima et al. (2015)	VETSA	131/96 (51-60)	cGM cortical thickness & general cognitive ability	0.08	0.09	0.10
			cGM surface area & general cognitive ability	0.21	0.24	0.21

bilat bilateral; *CB* cerebellum; *CC* corpus callosum; *cGM* cerebral grey matter; *CING* cingulum; *CING_G* cingulum gyrus; *cortical thickness* cortical thickness; *CUN* cuneus; *cWM* cerebral white matter; *DB* digits backwards; *EC* external capsule; *EF* executive function; *FA* fractional anisotropy; *FMD* facial memory display; *FSIQ* full scale intelligence; *g* general intelligence; *GM* grey matter; *L* left; *LV* lateral ventricle; *MF* medial frontal; *MMSE* Mini-mental state examination; *OP* occipital pole; *PCL* paracentral lobule; *PIQ* performance intelligence; *PH* parahippocampal; *PS* processing speed; *PUT* putamen; *R* right; *RAVEN* Raven standard progressive matrices; r_e environmental correlation; r_g genetic correlation; r_{ph} phenotypic correlation; *surface area* surface area; *SDRT* spatial delayed response task; *SLF* superior longitudinal fasciculus; *TCV* total cerebral volume; *THAL* thalamus; *VC* verbal comprehension; *VIQ* verbal intelligence; *WM* white matter; *WMem* working memory; *WMHI* white matter hyperintensities; Δ change.

*These phenotypes are volumes unless otherwise stated. Where results for many structures are reported, the regions with lowest and highest genetic correlations are shown. Refer to Table 2.2 for details regarding how studies were identified.

2.8 Conclusions

The findings emerging from the work reviewed here show that the genetic architecture of the brain is indeed complex. However, sample sizes are increasing in parallel with deep phenotyping and measures that capture the complexity of the brain. Large scale multi-site studies of brain structure phenotypes will enable well powered GWAS to discover more loci, which may be tied in with other information to further our understanding of the function of a particular genetic variant, and link to the neurobiology. The next stage of multi-site studies will also enable us to gain a more complete picture by examining the effect of rare variants, environmental risk factors, and gene by environment interactions, incorporating whole genome sequencing data, as well as the impact of epigenetic factors on brain structure.

3

Imaging Phenotypes/Contributions to the ENGIMA Consortium

3 Imaging Phenotypes/Contributions to the ENIGMA Consortium

3.1 Datasets

Two datasets were used in this thesis: the Queensland Twin Imaging study (QTIM) and the Human Connectome Project (HCP). The QTIM dataset consisted of brain imaging collected in a large ($N > 1000$), genetically informative sample of young adult monozygotic and dizygotic twin pairs and their non-twin singleton siblings (demographic and acquisition parameters are detailed in each empirical chapter). Participants were recruited from a program at the QIMR Berghofer Medical Research Institute (formally Queensland Institute of Medical Research), having previously participated in behavioural studies such as the Brisbane Adolescent Twin Study (M. J. Wright & Martin, 2004).

Data from the HCP (S1200 release) (Glasser et al., 2016; Van Essen et al., 2012) was used as a secondary analysis sample (demographic and acquisition parameters are discussed in each empirical chapter). The S1200 release contains imaging data from a large ($N > 1100$), genetically informative sample of young adult monozygotic and dizygotic twin pairs and their non-twin siblings, as well as participants from entirely singleton families. In addition to imaging data, the HCP young adult dataset includes a wide range of behavioural phenotypes, including measures of cognitive, emotional, motor and sensory processes.

3.2 Imaging Phenotypes

For all empirical analyses in this thesis, measures of the cortex (volume, surface area, thickness) and subcortical/ventricular structures (volume) were derived using the FreeSurfer software suite (v5.3 for QTIM, v5.3-HCP for HCP; <http://surfer.nmr.mgh.harvard.edu>) and used as phenotypes. Imaging phenotypes in the QTIM dataset were wholly processed by myself, while HCP imaging phenotypes were processed by the HCP consortium (Glasser et al., 2013). In the QTIM dataset, subcortical structure and intracranial volume phenotypes were also extracted using FSL (v4.1.9;

<https://fsl.fmrib.ox.ac.uk/fsl/fslwiki/>). However, due to difficulties in FSL amygdala and hippocampal segmentations in the QTIM dataset, and to facilitate comparisons with the HCP dataset, only FreeSurfer phenotypes were included in analyses.

3.2.1 Quality Checking

The quality of QTIM imaging phenotypes was assessed in a two-step procedure. Firstly, raw brain scans were checked for acquisition artefacts. Secondly, the outputs of FreeSurfer processing (e.g. delineation of cortical regions of interest, segmentation of subcortical structures) were checked for errors. HCP imaging phenotypes were quality checked by the HCP consortium (Glasser et al., 2013).

3.2.2 Acquisition Artefacts

Acquisition artefacts occur due to issues with the MRI scanner itself or interactions between the participant and MRI scanner. In the QTIM dataset, there were a variety of imaging artefacts present, including head motion (Figure 3.1), metal induced (Figure 3.2), non-uniform (bias) intensity (Figure 3.3), susceptibility (Figure 3.4), flow/pulsation (Figure 3.5), and radio frequency interference (Figure 3.6).

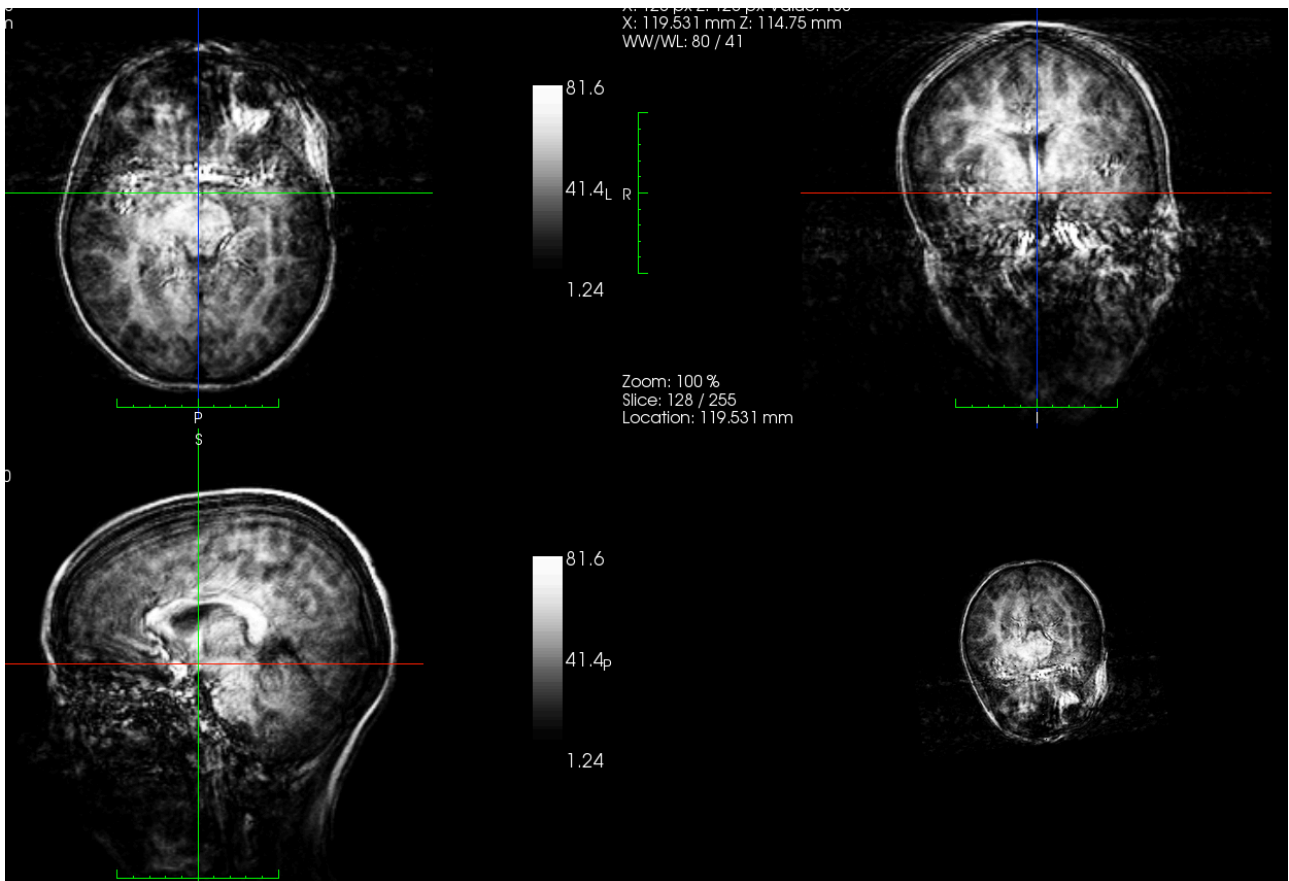


Figure 3.1 Head motion artefact
Head movement during scanning.

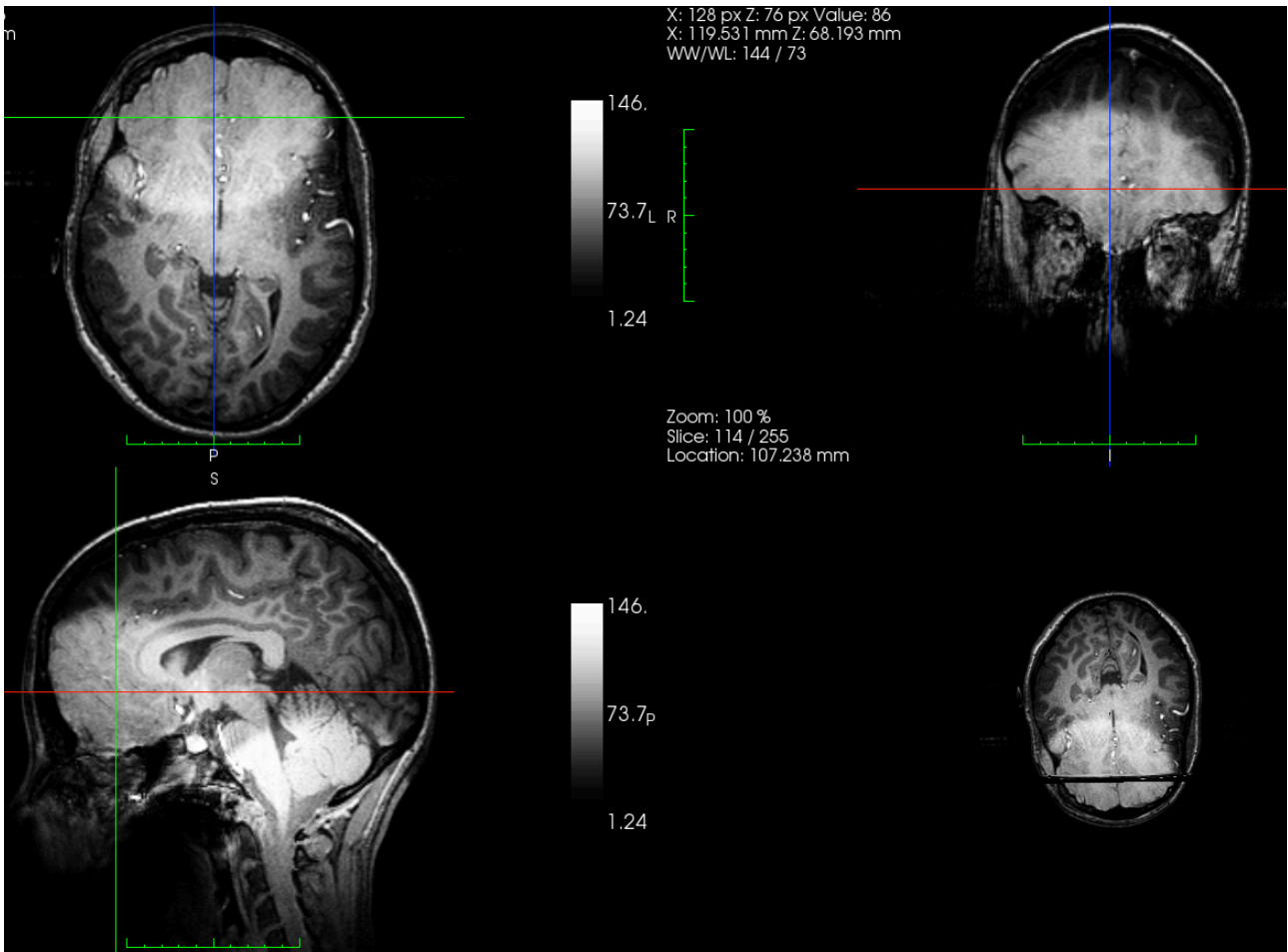


Figure 3.2 Metal induced artefact

In this example, the participant had dental braces.

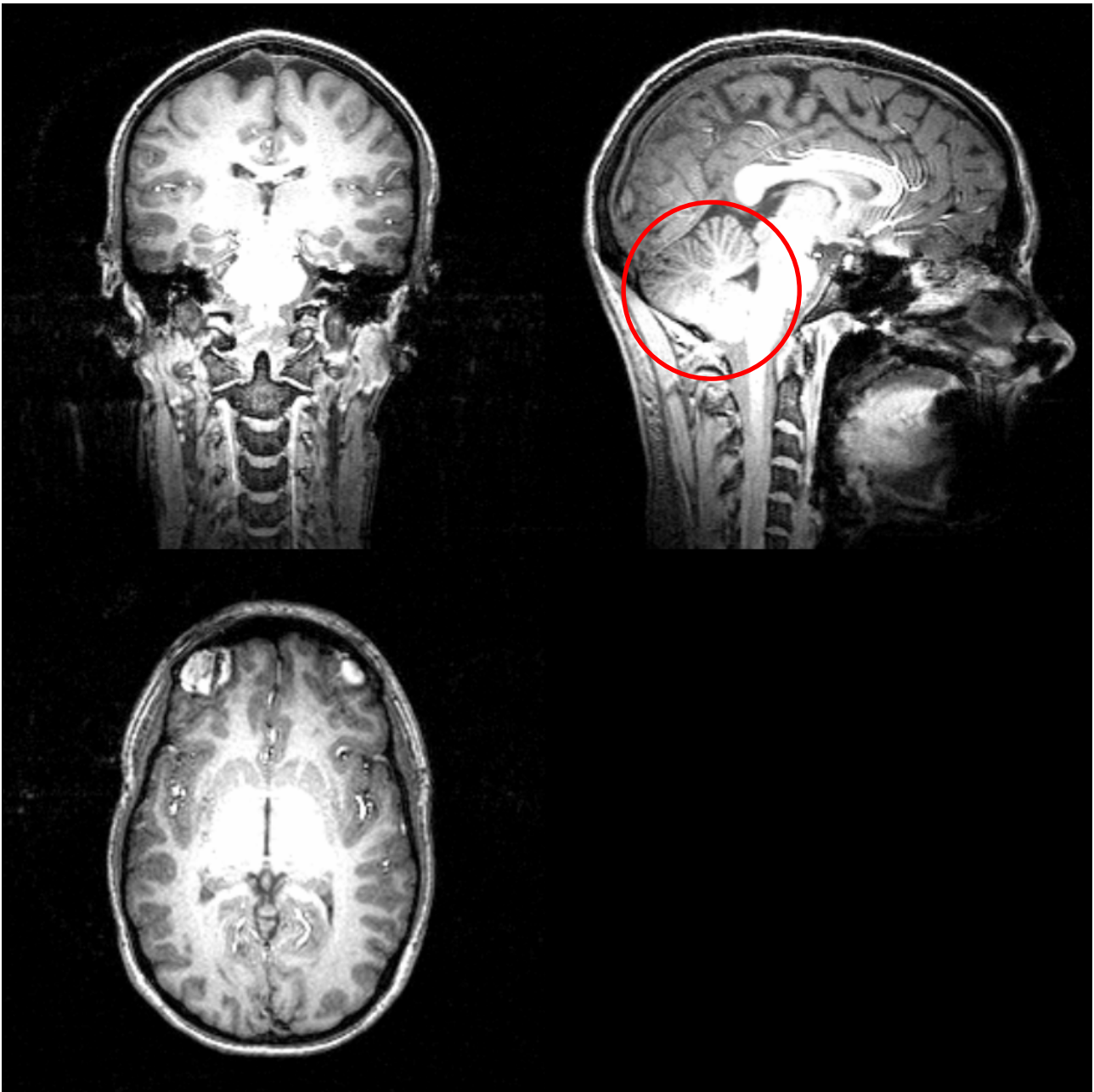


Figure 3.3 Non-uniform (bias) intensity artefact

In this example, the lower section of cerebellum (red circle) has greater signal intensity (much brighter) than rest of cerebellum. Some degree of intensity bias can be corrected; though the bias is likely too severe in the example scan below & as a result, parts of the cerebellum would not be recognised as brain.

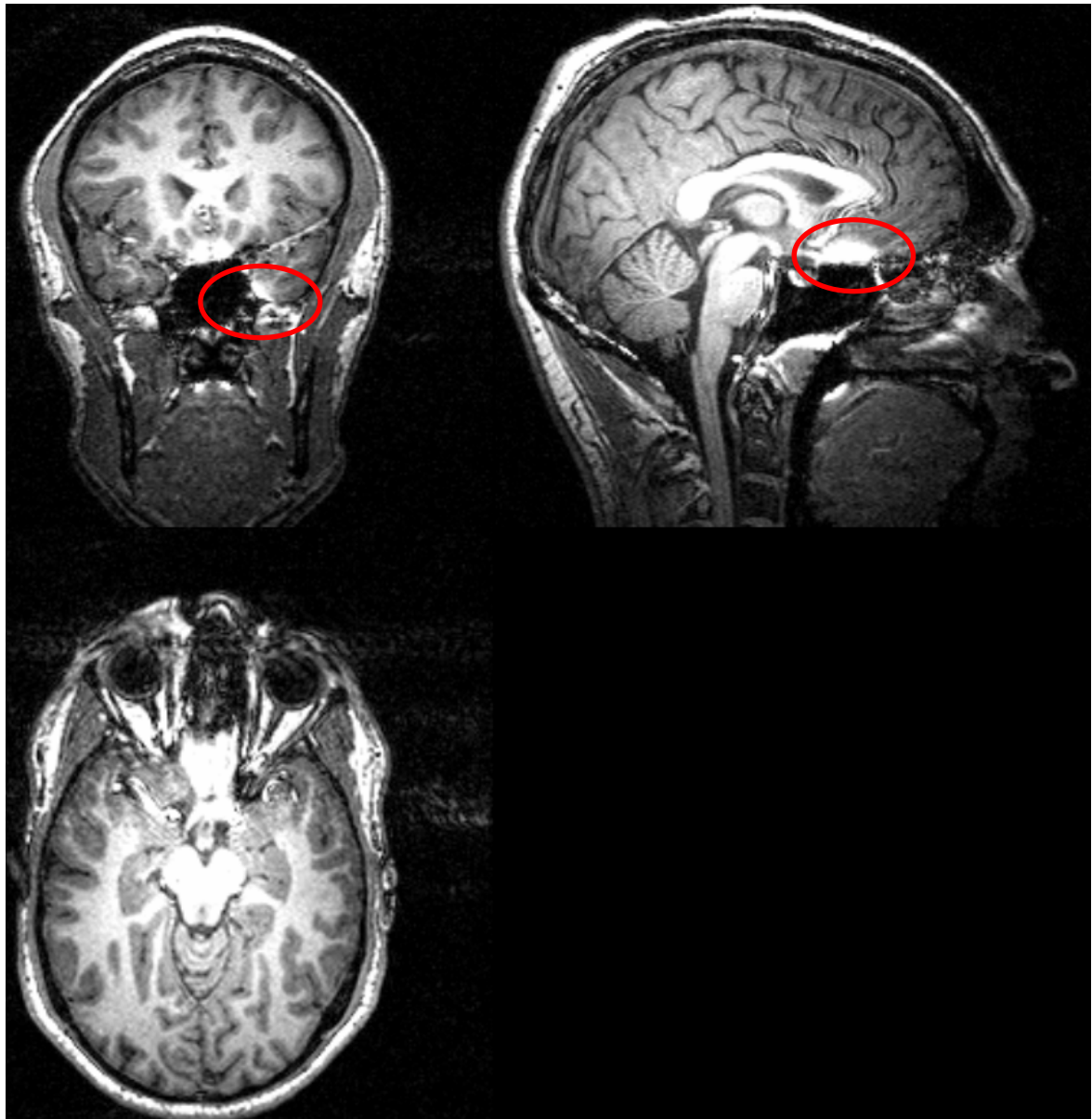
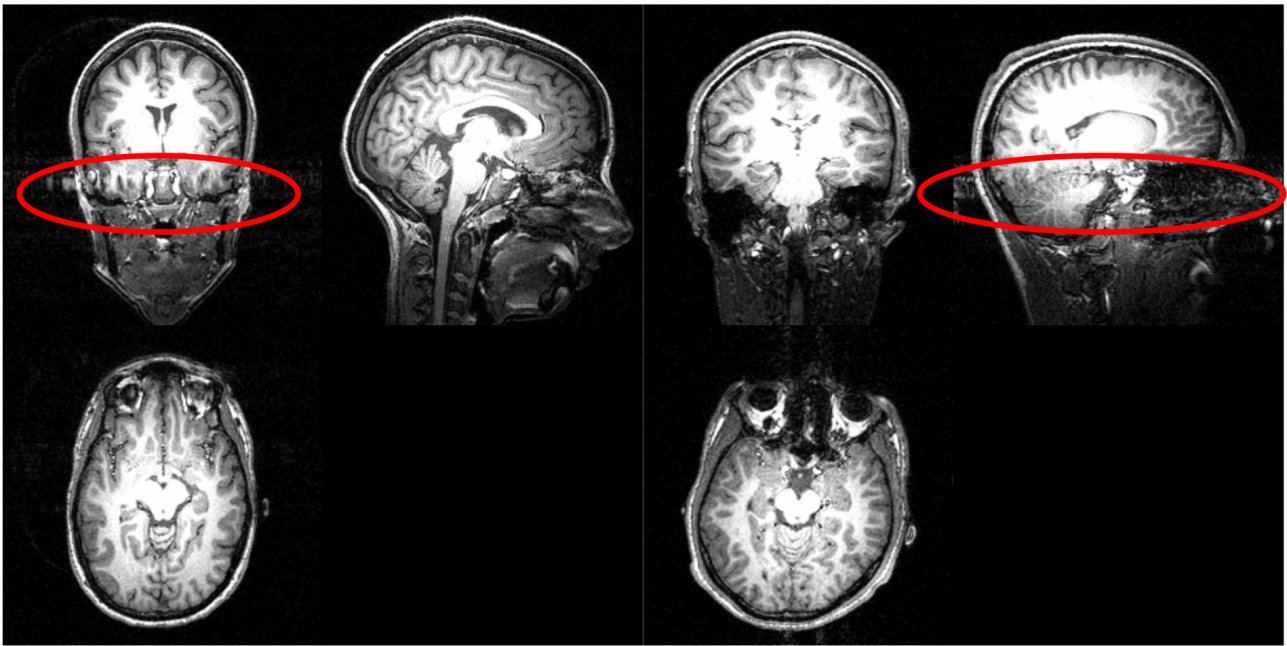


Figure 3.4 Susceptibility artefact

Often due to large sinuses. Typically, not a major issue, though automated image processing pipelines (e.g. FreeSurfer) can fail to recognise the affected area (red circle) as brain.



Coronal Acquisition

Sagittal Acquisition

Figure 3.5 Flow/pulstataion artefact

Strong blood or cerebrospinal fluid flow causes ghost images of blood vessels to be seen in acquisition orientation; appears differently between coronal and sagittal acquisitions. In this thesis, I used a covariate to control for acquisition differences (Chapters 4,6,7) or excluded participants with a sagittal acquisition (Chapter 5).

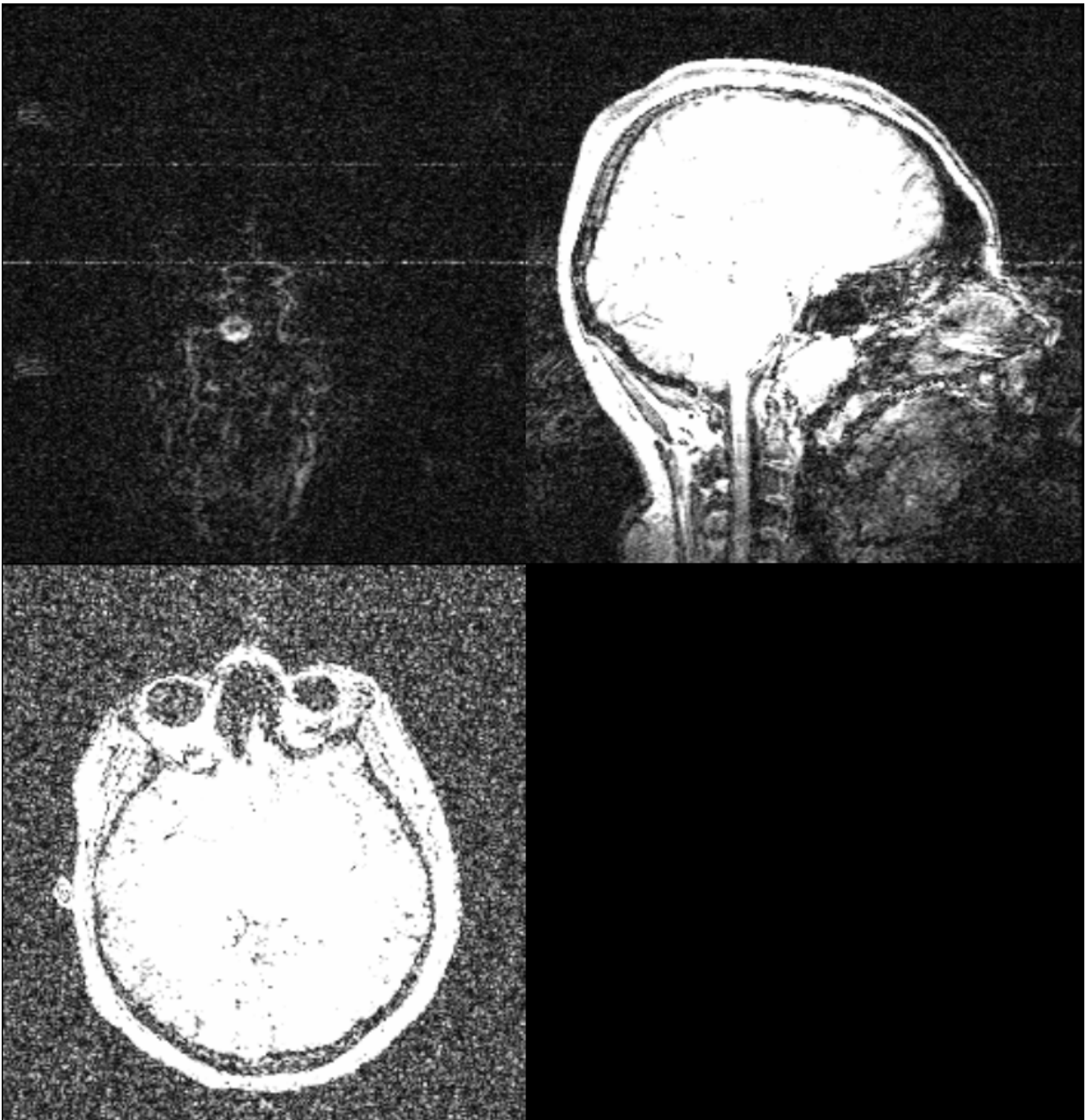


Figure 3.6 Radio frequency artefact

Radio frequency interference from within the MRI room appears as straight vertical lines, and is more noticeable after adjusting brightness levels (windowing).

3.2.3 Segmentation/Reconstruction/Delineation Errors

Following image processing, subcortical/ventricular segmentations and cortical reconstructions/delineations were visually inspected following the procedures of the ENIGMA consortium (<http://www.enigma.ini.usc.edu/>). The ENIGMA quality checking procedure uses a combination of FreeSurfer output visual inspection, as well as statistical checks (i.e. distribution, outliers). Outputs were generally free of error, though some errors were present in the automated processing outputs (detailed below). Incorrectly delineated/segmented structures were excluded from analysis (number of incorrectly delineated cortical and subcortical structures are listed in Chapters 4 and 5). The percentage of individual subcortical and cortical structures excluded ranged from no exclusions to 1.68% (thalamus) and 2.28% (supramarginal gyrus) respectively in the QTIM dataset.

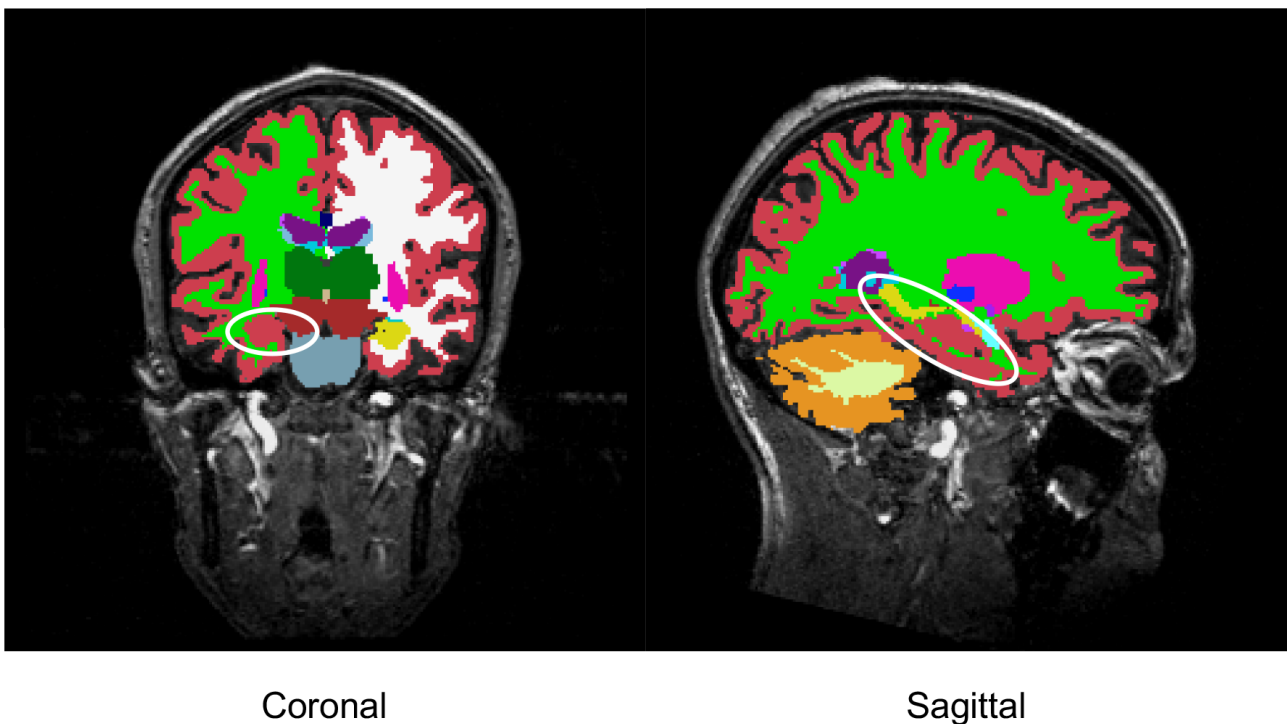
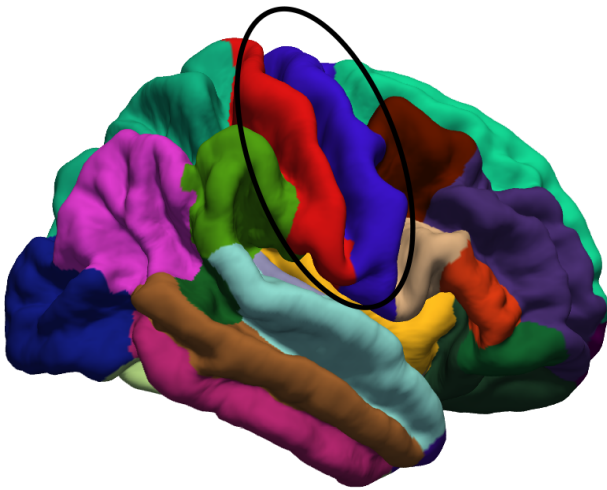
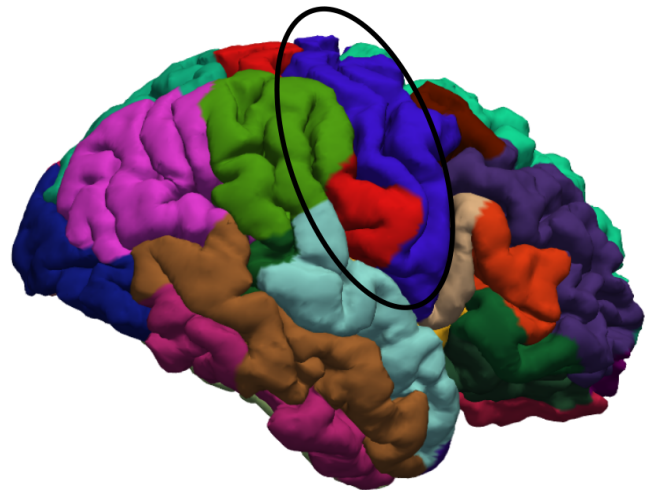


Figure 3.7 Incorrect subcortical segmentation

Here, the right hippocampus has been incorrectly segmented as cortical grey matter.



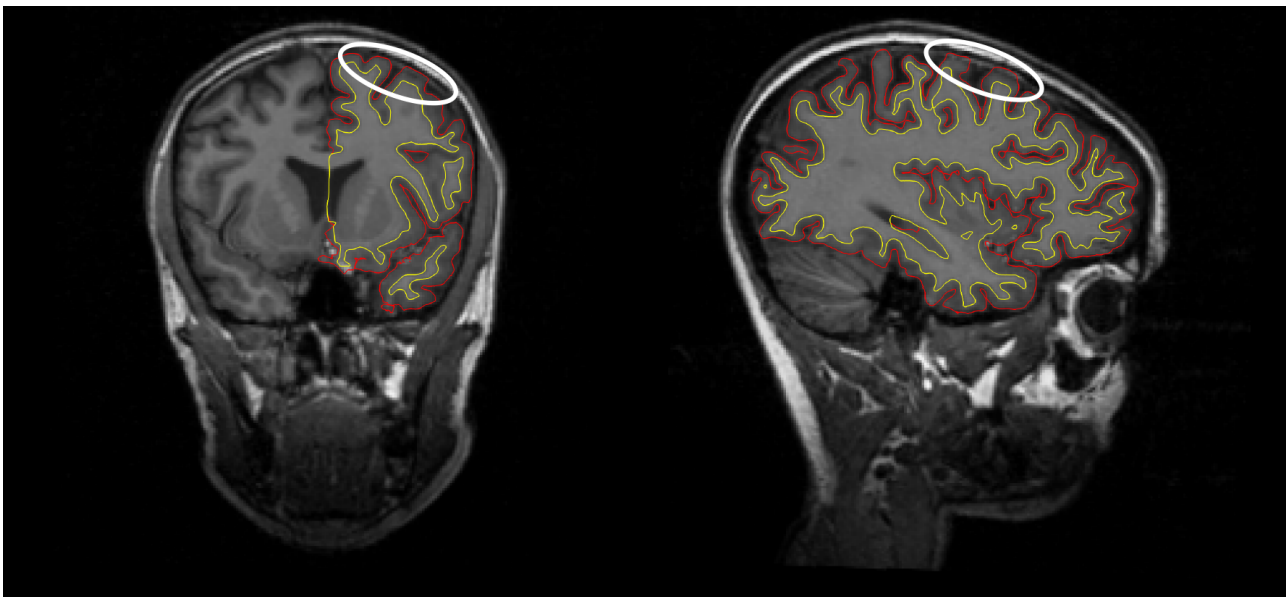
Template Brain



Incorrect Delineation

Figure 3.8 Incorrect cortical delineation

As seen in the comparison of the template brain (left) and the participant brain (right), the pre- and post-central gyri are incorrectly delineated.



Coronal

Sagittal

Figure 3.9 Incorrect cortical reconstruction

Incorrect cortical delineation. Here, the pial surface (red line) has been incorrectly extended into the dura matter of the brain.

3.3 Contributions to the ENIGMA Consortium

Enhancing NeuroImaging Genetics through Meta-Analysis (ENIGMA) is a worldwide consortium of brain scientists working on a range of large-scale neuroscience studies (Thompson et al., 2014). Through the consortium approach, ENIGMA can address questions that individual studies do not have the statistical power to address. ENIGMA studies are organised into working groups, and cover a variety of neuroimaging genetics topics, from genome-wide association studies (GWAS) and psychiatric disorders, to secondary projects such as brain plasticity, lateralization, and data harmonisation (Thompson et al., 2017).

The imaging phenotypes produced as part of my candidature overlapped with the phenotypes examined by several ENIGMA working groups. Consequently, I contributed data to a number of ENIGMA working groups over the course of my thesis (Table 3.1). Furthermore, I contributed toward beta-testing of quality control scripts of ENIGMA protocols, as well as providing test-retest reliability estimates for imaging phenotypes based on the QTIM test-retest sample.

By sharing data, the ENIGMA consortium can investigate questions of genetics and neuroscience that individual studies cannot. Importantly, the number of studies contributing data to ENIGMA projects continues to increase, as does the extent of ENIGMA working groups. Current ENIGMA studies (not yet published), to which I have contributed data on behalf of the QTIM study include a GWAS meta-analysis of cortical surface area and thickness, as well as a study of associations between copy number variants and brain structure. These projects, as well as many more to come, will likely offer great insights into the phenotypic implications of variations within the genome.

Table 3.1 Contributions of the QTIM dataset to ENIGMA publications

Reference	QTIM Contribution	Phenotypes	Findings
(Adams et al., 2016) Novel genetic loci underlying human intracranial volume identified through genome-wide association, <i>Nature Neuroscience</i>	845 participants	ICV	7 genome-wide significant loci associated with ICV
Brouwer et al. (2017) Genetic influences on individual differences in longitudinal changes in global and subcortical brain volumes: Results of the ENIGMA plasticity working group, <i>Human Brain Mapping</i>	49 longitudinal participants (two scans each, at 16 and 20 years of age)	Volume of seven subcortical structures, global structures	Change in brain volume over time significantly heritable for all global and most subcortical structures
Guadalupe et al. (2017) Human subcortical brain asymmetries in 15,847 people worldwide reveal effects of age and sex, <i>Brain Imaging and Behaviour</i>	591 participants	Volume of seven subcortical structures	Significant heritability of asymmetric index for volume of globus pallidus, hippocampus, thalamus, putamen
Hibar et al. (2015) Common genetic variants influence human subcortical brain structures, <i>Nature</i>	364 participants	Volume of seven subcortical structures, ICV	8 genome-wide significant loci associated with putamen, hippocampus, caudate nucleus, ICV
(Hibar et al., 2017) Novel genetic loci associated with hippocampal volume, <i>Nature Communications</i>	845 participants	Hippocampal volume	6 genome-wide significant loci associated with hippocampal volume
Renteria et al. (2017) Subcortical brain structure and suicidal behaviour in major depressive disorder: a meta-analysis from the ENIGMA-MDD	331 controls, 27 MDD-NSS, 27 MDD-SS	Volume of seven subcortical structures, lateral ventricles, ICV	Smaller ICV for MDD-SS than controls

working group, *Translational Psychiatry*

Schmaal et al. (2016) Subcortical brain alterations in major depressive disorder: findings from the ENIGMA Major Depressive Disorder working group, <i>Molecular Psychiatry</i>	38 cases, 262 controls	Volume of seven subcortical structures, lateral ventricles, ICV	Significantly lower hippocampal volume for cases compared to controls
Schmaal et al. (2017) Cortical abnormalities in adults and adolescents with major depression based on brain scans from 20 cohorts worldwide in the ENIGMA Major Depressive Disorder Working Group, <i>Molecular Psychiatry</i>	54 cases, 304 controls	Cortical surface area and thickness for 68 (34 per hemisphere) regions	Adolescent cases had lower total surface area than controls. Adults cases with MDD had less cortical thickness than controls in several regions (orbitofrontal cortex, anterior and posterior cingulate, insula and temporal lobes).

ICV intracranial volume; MDD major depressive disorder; MDD-NSS major depressive disorder with no suicidal symptoms; MDD-SS major depressive disorder with suicidal symptoms

4

Genetic Complexity of Cortical Structure: Differences in Genetic and Environmental Factors Influencing Cortical Surface Area and Thickness

This chapter is published as:

Strike, L. T., Hansell, N. K., Couvy-Duchesne, B., Thompson, P. M., de Zubicaray, G. I., McMahon, K. L., & Wright, M. J. (2018). Genetic Complexity of Cortical Structure: Differences in Genetic and Environmental Factors Influencing Cortical Surface Area and Thickness. *Cereb Cortex*. doi:10.1093/cercor/bhy002

4 Genetic Complexity of Cortical Structure: Differences in Genetic and Environmental Factors Influencing Cortical Surface Area and Thickness

Lachlan T. Strike¹, Narelle K. Hansell¹, Baptiste Couvy-Duchesne¹, Paul M. Thompson², Greig I. de Zubicaray³, Katie L. McMahon⁴, Margaret J. Wright^{1,4}

¹Queensland Brain Institute, University of Queensland, Brisbane QLD 4072, Australia. ²Imaging Genetics Center, University of Southern California, Marina del Rey, CA 90292, USA. ³Faculty of Health and Institute of Health and Biomedical Innovation, Queensland University of Technology (QUT), Brisbane QLD 4059, Australia. ⁴Centre for Advanced Imaging, University of Queensland, Brisbane QLD 4072, Australia.

Abstract

Quantifying the genetic architecture of the cerebral cortex is necessary for understanding disease and changes to the brain across the lifespan. Prior work shows that both surface area and cortical thickness are heritable. However, we do not yet understand the extent to which region-specific genetic factors (i.e. independent of global effects) play a dominant role in the regional patterning or inter-regional associations across the cortex. Using a population sample of young adult twins (N = 923), we show that the heritability of surface area and cortical thickness varies widely across regions, generally independent of measurement error. When global effects are controlled for, we detected a complex pattern of genetically mediated clusters of inter-regional associations, which varied between hemispheres. There were generally weak associations between the surface area of different regions, except within the occipital lobe, whereas cortical thickness was positively correlated within lobar divisions and negatively correlated across lobes, mostly due to genetic covariation. These findings were replicated in an independent sample of twins and siblings (N = 698) from the Human Connectome Project. The different genetic contributions to surface area and cortical thickness across regions reveal the value of quantifying sources of covariation to appreciate the genetic complexity of cortical structures.

4.1 Introduction

Individual variation within the cerebral cortex can be related to both normal and abnormal behaviour (Bakken et al., 2012; Geschwind & Rakic, 2013; Schnack et al., 2015). This variation arises due to environmental or genetic factors and the interplay between the two, and their relative contributions may be crucial to elucidating the aetiology of mental illness and neurodegenerative diseases (Kendler, 2013; Zhao & Castellanos, 2016). Twin and family studies can partition the variance in a phenotype among individuals into genetic and environmental sources; they show that the proportion of variance attributed to genetic factors (heritability) for cortical structure (surface area and cortical thickness) varies substantially across different cortical regions (Eyer et al., 2012; Schmitt et al., 2008; Winkler et al., 2010).

Several studies have investigated the degree to which genetic effects on different cortical structures/parcellations are correlated. Generally high genetic correlations have been reported between corresponding left/right hemisphere regions (Docherty et al., 2015; Eyer et al., 2014; Schmitt et al., 2008). Examining cortical thickness in 54 neuroanatomical regions of interest (ROIs), Schmitt et al. (2008) demonstrated strong and positive genetic correlations across the cortex. However, when whole brain mean cortical thickness was included as a covariate, regionally specific patterns of genetic influence emerged, showing there is genetic specificity, with distinct genetic effects across brain regions. Genetic covariance across surface area measures of neuroanatomical ROIs has not been examined, though a wide range of genetic correlations across genetically-identified cortical regions (corrected for total surface area) has been reported (Peng et al., 2016). Perhaps surprisingly, the genetic factors that affect surface area and cortical thickness are largely independent (Panizzon et al., 2009; Winkler et al., 2010), and this may be due to differences in the cellular processes that influence each measure during corticogenesis (Rakic, 2009).

For all the evidence of a strong genetic influence on surface area and cortical thickness, the question remains whether genetic factors are the dominant force behind regional patterning or inter-regional associations across the cortex. Significant estimates of environmental variance (Kremen et al., 2010; Schmitt et al., 2008) and evidence of cortical variation associated with activity and behaviour (Erickson, Leckie, & Weinstein, 2014; Kuhn, Gleich, Lorenz, Lindenberger, & Gallinat, 2014; McEwen & Morrison, 2013) suggest

that neuroplasticity may underlie some aspects of cortical organization. Even so, it can be hard to differentiate environmental variance from measurement error - the two are attributed to the same factor in twin models as they are unrelated to twin similarity. However, by calculating the reliability of surface area/cortical thickness measures, estimates of the variance attributed to measurement unreliability can be considered in conjunction with estimates of genetic and environmental variance to better evaluate differences between variance components. Past studies of cortical variation have not examined the role of measurement reliability, nor the contribution of environmental factors to phenotypic associations across different cortical regions.

In this study, we use the QTIM dataset (one of the largest in neuroimaging genetics, including brain scans from 157 monozygotic (MZ) and 194 dizygotic (DZ) twin pairs) to estimate region-specific genetic and environmental influence (i.e. independent of global effects) on surface area and cortical thickness in 34 ROIs. We then examine associations between regions, and the strength of genetic and environmental contributions to these associations. Using this large dataset, we seek to determine (1) whether regional differences in estimates of variance components across the cortex primarily reflect differences in measurement reliability, and (2), whether genetic factors contribute predominantly to phenotypic associations across different cortical neuroanatomical regions. For generalizability, we undertake the same analyses using an independent sample (237 twin pairs) from the Human Connectome Project (HCP).

4.2 *Materials and Methods*

4.2.1 *Participants*

Participants were from the Queensland Twin IMaging (QTIM) study of brain structure and function (for example (Blokland et al., 2014; Chiang et al., 2009; de Zubicaray et al., 2008; Joshi et al., 2011; Whelan et al., 2016)). Here we included 923 healthy, right-handed young adults (597 female, 326 male, mean age 22.27 ± 3.37 years, age range 15.40 to 30.11 years), consisting of 157 MZ pairs (106 female, 51 male), 194 DZ pairs (88 female, 30 male, 76 opposite sex), and 221 unpaired twins (75 MZ, 146 DZ; 133 female, 88 male). In addition, 53 participants were scanned a second time (mean duration between first and

second scan was 113.36 ± 52.25 days) to assess the test-retest reliability of imaging measures. Sample demographics are described in Table 4.1. Prior to scanning, participants were screened for neurological and psychiatric conditions, including loss of consciousness for more than 5 minutes, and general MRI contraindications. Zygosity of same-sex twin pairs was determined using a commercial kit (AmpFISTR Profiler Plus Amplification Kit, ABI) and later confirmed by genome-wide single nucleotide polymorphism genotyping (Illumina 610K chip). The study was approved by the Human Research Ethics Committees of the University of Queensland, QIMR Berghofer Medical Research Institute, and UnitingCare Health. Written informed consent was obtained from all participants, including a parent or guardian for those aged under 18 years. Participants received an honorarium for their time and to cover any transport expenses.

Table 4.1 Demographic characteristics (mean \pm SD) of the QTIM sample

	Females	Males	Total
<i>Full Sample*</i>	(<i>n</i> = 597 individuals)	(<i>n</i> = 326 individuals)	(<i>n</i> = 923 individuals)
Age (years)	22.20 \pm 3.32	22.39 \pm 3.46	22.27 \pm 3.37
FIQ [†]	111.76 \pm 12.14	116.79 \pm 13.11	113.55 \pm 12.72
Gestational age (weeks) [‡]	36.94 \pm 2.69	37.21 \pm 2.62	37.04 \pm 2.66
Birth weight (kg)	2.43 \pm 0.50	2.64 \pm 0.58	2.51 \pm 0.54
Socioeconomic index	61.06 \pm 23.73	63.77 \pm 24.40	62.03 \pm 23.99
Total surface area (mm ²)	164049.03 \pm 13046.33	184379.82 \pm 14713.69	171229.79 \pm 16759.10
Mean cortical thickness (mm)	2.51 \pm 0.09	2.51 \pm 0.09	2.51 \pm 0.09
<i>Retest sub-sample</i>	(<i>n</i> = 31 individuals)	(<i>n</i> = 22 individuals)	(<i>n</i> = 53 individuals)
Age (years)	24.15 \pm 2.09	23.19 \pm 2.33	23.75 \pm 2.22
FIQ	111.94 \pm 11.88	120.91 \pm 11.52	115.66 \pm 12.45
Gestational age (weeks)	37.92 \pm 2.02	37.88 \pm 2.43	37.90 \pm 2.23
Birth weight (kg)	2.60 \pm 0.30	3.13 \pm 0.51	2.80 \pm 0.46
Socioeconomic index	52.59 \pm 24.04	72.48 \pm 25.94	61.17 \pm 26.56
Total surface area (mm ²)	160742.11 \pm 10684.84	188993.09 \pm 12223.13	172468.93 \pm 17991.77
Mean cortical thickness (mm)	2.52 \pm 0.08	2.47 \pm 0.11	2.50 \pm 0.10

*The QTIM sample (N=923 individuals) consisted of 157 MZ pairs, 194 DZ pairs, 75 unpaired MZ twins, and 146 unpaired DZ twins. Unpaired twins were included to improve estimates of means and variances. The retest sample (i.e. participants scanned twice) consisted of a sub-sample of 53 participants, including 11 MZ pairs, 12 DZ pairs, and 7 unpaired twins.

[†]Full-scale intelligence quotient (FIQ) measured using the Multidimensional Aptitude Battery (Jackson, 1984) as close as possible to participants' 16th birthday.

[‡]Gestational age, birth weight and socioeconomic status (McMillan, Beavis, & Jones, 2009) were obtained from parental reports when participants were 12 or 16 years of age.

4.2.2 Image Acquisition and Processing

Imaging was conducted on a 4T Bruker Medspec (Bruker, Germany) whole-body MRI system paired with a transverse electromagnetic (TEM) head coil. Structural T1-weighted 3D images were acquired (TR=1500 ms, TE=3.35 ms, TI=700 ms, 230 mm FOV, 0.9 mm slice thickness, 256 or 240 slices depending on acquisition orientation (86% coronal (256 slices), 14% sagittal (240 slices))). Surface area and cortical thickness were measured using FreeSurfer (v5.3; <http://surfer.nmr.mgh.harvard.edu/>) previously reported in depth (Fischl & Dale, 2000). Prior to FreeSurfer analysis, the raw T1-weighted images were corrected for intensity inhomogeneity with SPM12 (Wellcome Trust Centre for Neuroimaging, London, UK; <http://www.fil.ion.ucl.ac.uk/spm>). Total surface area and mean cortical thickness were extracted for 34 regions of interest (ROI) per hemisphere from the Desikan-Killiany atlas (Desikan et al., 2006) (Appendix 2) contained within FreeSurfer. Measures for whole brain, global variables (total surface area, mean cortical thickness) were also extracted. Cortical reconstructions and ROI labelling were checked using the procedures of the ENIGMA consortium (enigma.ini.usc.edu), with incorrectly delineated cortical structures excluded from the analysis. Prior to analysis, raw scores were standardised (i.e. converted to z-scores) and outliers at ± 3.29 SD from the mean were replaced by the relevant threshold value (± 3.29 ; see Appendix 3 for the number of excluded and replaced values).

4.2.3 Heritabilities of Cortical Surface Area and Thickness

Genetic and environmental influences on cortical surface area and thickness were examined through twin analyses using the maximum-likelihood structural equation modelling package OpenMx 2.7.11 (Neale et al., 2016) in R 3.2.2 (R Core Team, 2015). Correlations between pairs of monozygotic and dizygotic twins were estimated for each ROI through saturated models in which the means and variances of twin 1 and twin 2 are equated. Next, the heritabilities of surface area and cortical thickness were estimated for each ROI in a series of univariate ACE models. Briefly, the classic twin model partitions the variance within a phenotype into additive genetic (A), common or shared environment (C) and unique or non-shared environment (E) sources (Neale & Cardon, 1992) (Appendix 4). Correlations between additive genetic factors (A) are fixed to 1 for MZ and 0.5 for DZ

twins as MZ and DZ twins share 100% and (on average) 50% of their genetic material respectively. For common environment factors (C), correlations are fixed at 1 for both MZ and DZ twins (the model assumes MZ and DZ twins raised together experience similar environments), and the unique environment factors (E) are uncorrelated between twin pairs as this represents environmental influence affecting one twin only. Estimates of unique environment also include measurement error, as it is random and unrelated to twin similarity.

To determine the most parsimonious model, nested models containing AE, CE, or E sources of variance were compared to the ACE decomposition. We assessed the fit of the constrained models by examining the -2 log likelihood difference between the ACE model and the reduced model (AE, CE or E). The difference in the maximum likelihood (assessed through the -2 log likelihood difference) is distributed as a chi-squared statistic for a given number of degrees of freedom (equal to the difference in the number of free parameters estimated), which denotes whether the parameter is significant. If a reduced model is significant, this indicates that the parameter removed from the model accounted for a significant proportion of the phenotypic variance. If a reduced model is not significant, this indicates that the fit of the nested model is not significantly worse than the unconstrained ACE model, and that the simpler model should be used as it provides a more parsimonious explanation of the fitted model (Neale & Cardon, 1992; Sham, 1998).

Saturated and univariate models included a simultaneous means regression to adjust for effects of whole brain total surface area/mean cortical thickness, sex, linear and non-linear age effects (modelled through normal splines with three degrees of freedom), interactions between age and sex, and MRI acquisition orientation. The significance of covariate effects was tested by fitting reduced ACE models in which the covariate of interest was dropped from the model (i.e. the regression coefficient was set to zero), but all other covariates remained, and comparing the model fit with the full (i.e. all covariates included) ACE model. Maximum-likelihood 95% confidence-intervals were estimated for all model parameters.

4.2.4 Test-Retest Reliability

Test-retest reliability was estimated by calculating the Pearson correlation coefficient between surface area/cortical thickness measures from time one and time two scans (covariate effects were removed by using regression residuals; same covariates as for heritability estimates). The square of the Pearson correlation coefficient (r^2) can be used to make direct comparisons between the portion of variability not explained by the repeats ($1 - r^2$ test-retest) and e^2 (variance due to non-shared environment and measurement error). Where e^2 exceeds unreliability ($1 - r^2$ test-retest), non-shared environmental influences are greater than measurement error. Conversely, measurement error is greater than non-shared environment when unreliability ($1 - r^2$ test-retest) is greater than e^2 . While unreliability can be modelled to disassociate the unique environmental variance component ('E') from measurement error (see Luciano et al. (2001) for an example), the size of our retest sample is too small to provide an accurate estimate of measurement unreliability (i.e. the retest sample of 53 individuals is substantially smaller than the twin sample of 351 pairs; hence, estimates of measurement error will be much rougher, and have wider confidence intervals than estimates of genetic/environmental variance).

4.2.5 Associations Between Left/Right Homologous ROIs and Across Regions

Prior studies (McKay et al., 2014; Winkler et al., 2010) have combined left and right hemisphere ROIs to form 34 bilateral brain phenotypes, reducing the number of statistical tests and possibly increasing power. Here, before combining measures from left and right regions, we estimated correlations between corresponding left/right ROIs, and then tested whether the genetic variance to left and right regions was the same. Bivariate analyses extended the univariate design to decompose the variance in a trait, and also the covariance between two traits, into genetic and unique environmental sources (Appendix 4). As estimates of common environment (C) were small and could be dropped from all univariate models without a significant reduction in model fit (discussed later in 4.3.2), models specifying only additive genetic and unique environment sources of variance (i.e. AE) were tested. From the covariance decompositions, we further estimated genetic, unique or non-shared environmental (from this point forward referred to as environmental)

and phenotypic correlations. Genetic (environmental) correlations indicate the extent to which two phenotypes share genetic (environmental) variance. Both genetic and unique environmental correlations underlie the phenotypic correlation. As a high genetic correlation between two traits can be observed, even if the traits themselves have low heritability, a high genetic correlation can be misleading when genes explain only a small portion of the phenotypic variance. Hence, we examined shared genetic influence between ROIs by calculating the genetic contribution to the phenotypic correlation (r_{ph-a}):

$$\sqrt{(ROI\ 1\ heritability)} \times \text{genetic correlation} \times \sqrt{(ROI\ 2\ heritability)}$$

r_{ph-a} is easily conceptualised as the phenotypic correlation (r_{ph}) between two traits based only on the shared genetic variance. We similarly calculated the environmental contribution to the phenotypic correlation (r_{ph-e}). Both r_{ph-a} and r_{ph-e} were computed using variance estimates from the bivariate model in which the genetic (environmental) correlations were estimated. The significance of the genetic or environmental contribution to the phenotypic correlation was assessed by fitting a reduced model in which the genetic or environmental covariance between ROIs was set to zero and assessing model fit. The significance of the phenotypic correlation was assessed by setting both the genetic and environmental covariances between ROIs to zero.

We then fitted nested sub-models in which the second genetic variable was dropped from the bivariate AE model (Appendix 4) to test if the genetic variance in corresponding left/right regions could be attributed to one genetic source without a significant reduction in model fit. Variables were entered into the bivariate Cholesky first in a left-right ordering, and as a second check, the variable order was reversed and the Cholesky decomposition was refitted. There were two brain regions for surface area (parahippocampal gyrus, superior temporal gyrus) and four for cortical thickness (superior frontal gyrus, pars opercularis, supramarginal gyrus and lateral occipital cortex) in which removal of the second genetic variance source resulted in a significantly worse fit (i.e., the same, or one, genetic source did not explain the genetic variance for both left and right brain regions as well as a model specifying two genetic variables). For all subsequent analyses, unilateral left/right ROIs were retained for these brain regions, with bilateral (mean of left and right) measures used for all other ROIs. In total, for surface area we derived 32 bilateral (mean

of left and right) and 4 unilateral regional measures (total of 36) and for cortical thickness 30 bilateral and 8 unilateral measures (total of 38).

Next, bivariate analyses were used to estimate phenotypic correlations, and the genetic and environmental contributions to the phenotypic correlations, for all possible pairs of surface area and cortical thickness ROI measures (74 in total; 36 surface area and 38 cortical thickness). These 2,701 pairwise AE models populated a 74 by 74 correlation matrix (one each for phenotypic correlations, genetic & environmental contributions). The R package *corrplot* (Wei & Simko, 2016) was used to illustrate the correlation matrices. To further examine patterns of genetic covariance, and compare results with a previous examination of genetic covariance (Schmitt et al., 2009), we applied hierarchical clustering using Euclidian distances to the genetic association matrix using the R package *gplots* (Warnes et al., 2016).

We used the Benjamini–Hochberg procedure to control the false discovery rate (FDR) for the multiple comparisons (Benjamini & Hochberg, 1995). Here, p values obtained from model fit likelihood ratio tests are ordered and ranked from smallest to largest (e.g. the smallest p value is ranked $i=1$, the next smallest is ranked $i=2$, and so on). The adjusted p value (or q value) is calculated by multiplying the individual p value ($p_{(i)}$) by the total number of multiple comparisons (m) divided by the rank number (i): $p_{(i)}*(m/i)$. A q value less than 0.05 was considered significant. The procedure was applied separately to surface area and cortical thickness results for 1) covariate effects ($m = 612$; significance of 9 covariates tested for 68 ROIs), 2) heritability estimates ($m = 204$; significance of three model fits (AE, CE, E) tested for 68 ROIs), 3) bivariate analyses of corresponding left/right regions ($m = 102$; significance of three covariances (phenotypic, genetic, environmental) tested between 34 left/right ROIs), 4) bivariate analyses of specific left/right genetic influence ($m = 34$; significance of dropping second genetic variance source for 34 ROIs), and 5) bivariate analyses of the 74 ROIs across the cortex ($m = 630$ for pairwise surface area, $m = 703$ for pairwise cortical thickness, $m = 1368$ for pairwise surface area and cortical thickness). All bivariate analyses included simultaneous means regressions to adjust for covariate effects (same covariates as for heritability estimates).

4.2.6 Replication in an Independent Sample

Data from the Human Connectome Project (S1200 release) (Glasser et al., 2016; Van Essen et al., 2012) was used as a secondary analysis sample. The S1200 release contains imaging data for 1113 individuals from families; here, we included only participants classified as a twin (by genotype or self-report), as well as the non-twin siblings of these participants (i.e. families consisting purely of singletons were not examined). The final sample of 698 adults (399 female, 299 male, mean age 29.30 ± 3.60 years, age range 22 to 36 years) consisted of 152 MZ pairs (93 female, 59 male), 85 DZ pairs (52 female, 33 male), 203 singleton siblings of twins (1-2 per family; 96 female, 107 male), 10 members of singleton families (2 per family; 7 females, 3 males), and 11 unpaired twins (6 female, 5 male). MZ and DZ twin zygosity was determined through genotyping, if available (215 of 237 pairs), otherwise by self-report (22 of 237 pairs). A subset of twins ($n = 45$ individuals) were scanned a second time (mean duration between first and second scan was 139.30 ± 68.99 days). Details relating to participant selection and MRI acquisition have been reported (Van Essen et al., 2012). Pre-processed FreeSurfer surface area and cortical thickness measures (Glasser et al., 2013) were used. We used bilateral composite measures (mean of left and right hemispheres) for all ROIs, with the exception of parahippocampal surface area, pericalcarine surface area, superior temporal surface area, transverse temporal surface area, and rostral anterior cingulate cortical thickness, where the genetic influence for left and right regions could not be constrained to one factor. All univariate and bivariate genetic analyses completed on the QTIM sample were undertaken on the HCP data, with simultaneous means regressions to control for covariate effects (same covariates as QTIM data, apart from acquisition orientation, which did not vary in the HCP dataset). Univariate and bivariate models were extended to include non-twin siblings in order to increase statistical power (Posthuma & Boomsma, 2000).

4.3 Results

4.3.1 Preliminary Analyses

The global effect of surface area/cortical thickness (i.e. total surface area and whole brain average cortical thickness) on each ROI was highly significant; standardised regression coefficients ranged from 0.26 (entorhinal cortex right) to 0.86 (superior frontal gyrus right) for surface area and 0.16 (entorhinal cortex right) to 0.81 (inferior parietal cortex right) for cortical thickness (regression coefficients and associated q values of all covariates are presented in Appendix 5 and Appendix 6). Test-retest correlations varied across ROIs, ranging from 0.30 to 0.97, and were generally high for surface area (test-retest correlation > 0.70 for 55/68 ROIs) and more moderate for cortical thickness (test-retest correlation > 0.70 for 39/68 ROIs), with the mean reliability estimate (weighted by ROI size) being higher for surface area (0.84) than cortical thickness (0.72). Test-retest reliability estimates are shown in Figure 4.1a (also provided in Appendix 7 and Appendix 8).

4.3.2 Heritability of Cortical Surface Area and Thickness

For almost all ROIs, for both surface area (65/68) and cortical thickness (65/68) the MZ twin correlations were higher than the DZ correlations, suggesting individual variation in surface area and cortical thickness is genetically influenced (Appendix 7 and Appendix 9). ACE modelling indicated a range of heritability estimates across ROIs for both surface area and cortical thickness (Appendix 7; Figure 4.1a/b), from not heritable up to 0.65 for surface area and 0.55 for cortical thickness. Low heritability estimates were found for regions of poor reliability (e.g. insular cortex right (INS R) surface area; heritability = 0.33, test-retest correlation = 0.32), but also for regions of high reliability (e.g. postcentral gyrus left (POSTC L) surface area; heritability = 0.16, test-retest correlation = 0.97). Common environmental effects were small (c^2 range 0 – 0.30) and non-significant for all ROIs ($q = 0.05$). Unique or non-shared environmental variance was greater than measurement error (i.e. e^2 greater than unreliability ($1 - r^2$ test-retest)) for the majority of surface area (62/68) and cortical thickness (54/68) ROIs, suggesting that non-genetic variance was largely due to unique environmental factors rather than measurement error. Heritability estimates for total surface area and whole brain average cortical thickness were 0.91 and 0.58

respectively (corrected for all covariates excluding total surface area/mean cortical thickness).

In Figure 4.1c, using bilateral measures (mean of left & right ROIs, for regions in which this was suitable), we map both the genetic and environmental variance using an AE model. As with unilateral measures, heritability estimates varied across the cortex, ranging from 0.19 (frontal pole) to 0.75 (pericalcarine cortex) for surface area and 0.28 (banks of the superior temporal sulcus) to 0.68 (pericalcarine cortex) for cortical thickness.

4.3.3 ROI Correlations Between Hemispheres

Phenotypic correlations between corresponding left/right ROIs, though varying widely in magnitude (r_{ph} -0.06 to 0.65; Figure 4.2), were all significant. Phenotypic correlations greater than 0.40 were largely due to strong genetic covariation between left and right hemispheres. In contrast, phenotypic correlations less than 0.20 were due to weak genetic and environmental covariance, except for surface area of the caudal anterior cingulate where the low phenotypic correlation between left and right hemispheres (r_{ph} -0.06) was due to genetic and environmental contributions of opposing directions (r_{ph-a} 0.17, r_{ph-e} -0.23).

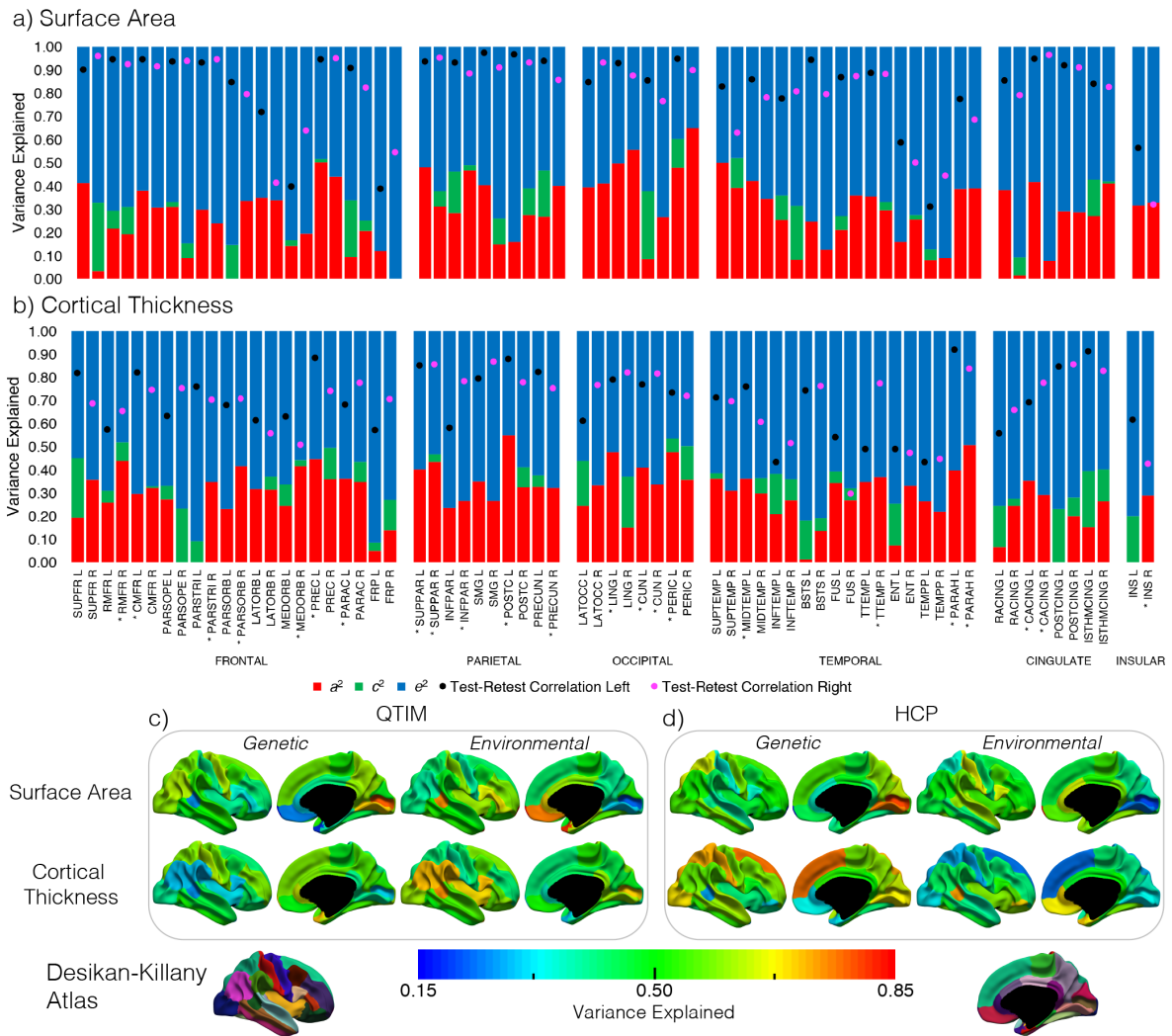


Figure 4.1 Variance component estimates for surface area and cortical thickness

Variance component estimates for surface area (a) and cortical thickness (b) for 68 ROIs (34 in each of the left (L) and right (R) hemisphere). a^2 = additive genetic (red), c^2 = common environment (green), e^2 = unique environment (blue). * preceding x-axis labels denotes ROIs with heritability estimates (a^2) significantly different from zero. ROIs are grouped in lobar divisions (Frontal, Parietal, Occipital, Temporal, Cingulate, Insular cortex). Reliability of left and right ROIs are denoted by black and pink dots respectively. Heritability estimates for lobar divisions (mean of ROIs, weighted by size) were: frontal 0.27, parietal 0.33 occipital 0.43, temporal 0.31, cingulate 0.27, insular cortex 0.32 for surface area and frontal 0.31, parietal 0.35, occipital 0.32, temporal 0.29, cingulate 0.18, insular cortex 0.15. The lower panel maps the genetic and environmental variance for surface area (top row) and cortical thickness (bottom row) for up to 34 bilateral cortical regions in the QTIM (c) and HCP (d) samples. Heritability estimates range: 0.19 to 0.75 (QTIM surface area), 0.27 to 0.68 (QTIM cortical thickness), 0.15 to 0.81 (HCP surface area), 0.27 to 0.76 (HCP cortical thickness). For regions where genetic variance of left and right ROIs did not completely overlap (i.e. QTIM: surface area of the superior temporal and parahippocampal gyrus, and cortical thickness of the superior frontal gyrus, pars opercularis, supramarginal gyri and lateral occipital, HCP: surface area of the superior temporal, parahippocampal, and transverse temporal gyri, pericalcarine cortex, and cortical

thickness of the rostral anterior cingulate), the mean genetic (and environmental) variance of the left and right ROI is shown. $N = 157/194$ MZ/DZ pairs and 221 unpaired twins (QTIM), 152/85 MZ/DZ pairs and 224 siblings/unpaired twins (HCP). ROI abbreviations listed in Appendix 2.

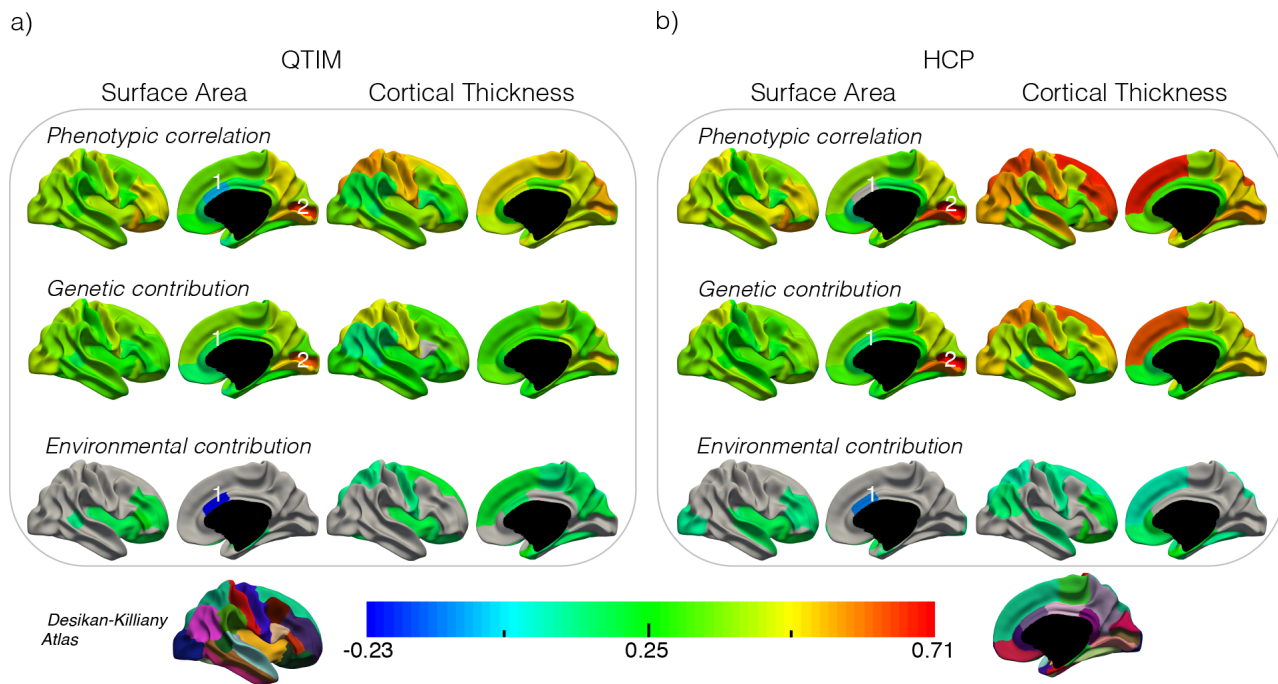


Figure 4.2 Phenotypic correlations, with genetic and environmental contributions, between corresponding left/right ROIs for surface area and cortical thickness in the QTIM and HCP samples.

Phenotypic correlations, with genetic and environmental contributions, between corresponding left/right ROIs for surface area and cortical thickness in the QTIM (a) and HCP (b) samples. Phenotypic correlations between corresponding left/right ROIs ranged from -0.05 to 0.65 (all significant) for QTIM and from 0.01 to 0.71 (all significant except caudal anterior cingulate surface area) for HCP. Genetic covariance accounted primarily for phenotypic correlations between hemispheres, but this was not always the case (e.g. genetic and environmental influence of a similar magnitude contributed to the phenotypic correlation left and right cortical thickness of the superior frontal gyrus in the QTIM sample). While low phenotypic correlations were typically due to very weak genetic and environmental contributions, they were also found to mask somewhat larger opposing genetic and environmental influences in the caudal anterior cingulate surface area (see footnote 1 below). Regions with correlations not significantly different from zero are in grey.

¹ For one region there was significant opposing genetic and environmental influence (caudal anterior cingulate surface area: QTIM - $r_{ph} -0.06$, $r_{ph-a} 0.17$, $r_{ph-e} -0.23$, HCP - $r_{ph} 0.01$ (estimate not significant, $q = 0.051$), $r_{ph-a} 0.13$, $r_{ph-e} -0.11$).

² In both samples, the highest phenotypic correlation was for pericalcarine surface area ($r_{ph} 0.65$ (QTIM) and 0.71 (HCP)), with associations due almost entirely to genetic contributions.

4.3.4 ROI Correlations Across the Cortex

There was a complex pattern of associations across cortical regions. For surface area, strong correlations were found between occipital lobe ROIs (r_{ph} 0.23 to 0.63), with weaker and mainly negative associations across lobar divisions (Figure 4.3a). Phenotypic associations (r_{ph} -0.30 to 0.63) were predominantly due to genetic contributions (r_{ph-a} -0.26 to 0.54; Figure 4.3b lower) with very little environmental covariance (r_{ph-e} -0.20 to 0.19; Figure 4.3b upper). A much stronger pattern of positive correlations between regions within a lobar division was found for cortical thickness (Figure 4.3c). Moderate negative correlations were found between regions not sharing spatial proximity. Some regions (e.g. rostral middle frontal gyrus (RMFR), rostral anterior cingulate (RACING)) were associated with the majority of ROIs. The posterior (POSTCING) and isthmus (ISTHMCING) divisions of the cingulate were generally not associated with other regions across the cortex. Genetic contributions (r_{ph-a} -0.36 to 0.37; Figure 4.3d lower) largely accounted for phenotypic correlations (r_{ph} -0.42 to 0.59; Figure 4.3c), though some sparse patterns of environmental covariance (r_{ph-e} -0.22 to 0.27; Figure 4.3d upper) were present between prefrontal and temporal ROIs. The application of hierarchical cluster analysis to the genetic association matrices generally resulted in patterns following lobar organisation for cortical thickness, whereas for surface area, outside of occipital ROIs, there was a greater clustering of regions from different lobes (Appendix 10).

4.3.5 ROI Correlations Between Surface Area and Cortical Thickness

While we found that whole brain total surface area and mean cortical thickness were inversely associated (r_{ph} -0.26, r_{ph-a} = -0.21, r_{ph-e} = -0.05; measures corrected for all covariates excluding total surface area/mean cortical thickness), at the regional level associations between surface area and cortical thickness were sparse and while some were negative, others were positive (range: r_{ph} -0.34 to 0.25, r_{ph-a} -0.25 to 0.21, r_{ph-e} -0.31 to 0.15; Appendix 11). These associations were weak, due to low genetic and environmental covariation, with the exception of pericalcarine surface area and cortical thickness in which a positive genetic and negative environmental contribution resulted in a weak phenotypic correlation (r_{ph} 0.04, r_{ph-a} 0.13, r_{ph-e} -0.09).

4.3.6 Replication Using the HCP sample

Patterns of genetic and environmental (co)variance were similar across the QTIM and HCP datasets (Figure 4.1d, Figure 4.2b, Appendices 12-19). Evidence of separate genetic influence on left and right regions for parahippocampal and superior temporal gyri surface area was replicated. Further, the pattern of strong associations between surface area measures for occipital lobe ROIs, as well as the same pattern of positive associations within, and negative associations between, cortical thickness ROIs, was found. These associations were predominantly due to genetic factors, with some thinly dispersed environmental influence contributing to several cortical thickness associations.

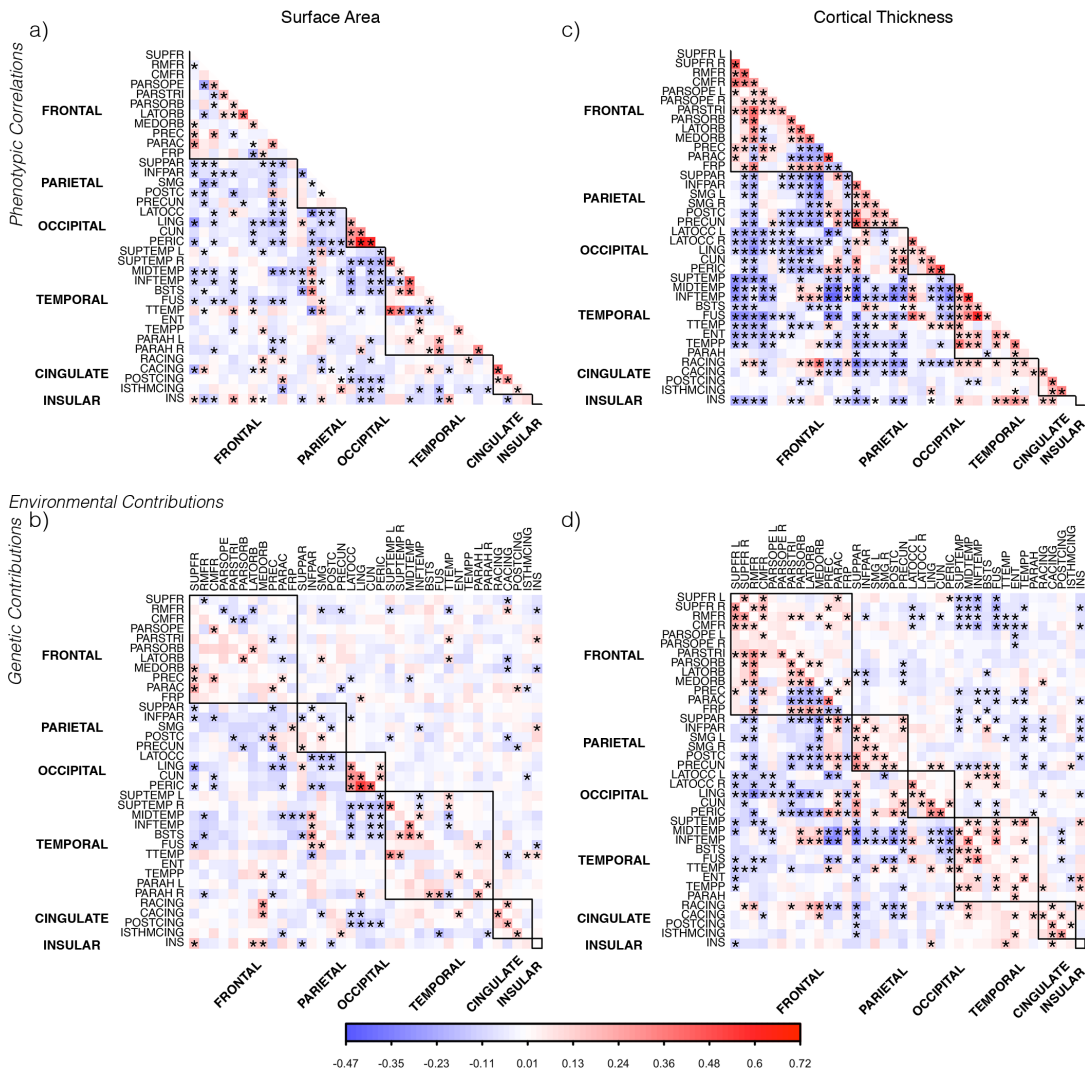


Figure 4.3 Phenotypic correlations, with genetic and environmental contributions, for surface area and cortical thickness across regions in the QTIM sample.

Phenotypic correlations, with genetic and environmental contributions, for surface area and cortical thickness across regions in the QTIM sample. Surface area (a) was mainly associated within rather than across lobar divisions, particularly for the occipital lobe. Phenotypic associations were predominantly due to genetic associations (c; lower triangle), with very few environmental associations (c; upper triangle). For cortical thickness (b) there is a much stronger pattern of associations. Correlations are positive within-lobe and negative between-lobes. These phenotypic associations are due largely to genetic covariance (d; lower triangle), however, some associations are due to environmental covariance (d; upper diagonal). * denotes a significant correlation (q value < 0.05). ROI abbreviations listed in Appendix 2.

4.4 Discussion

Here we extend prior work, showing there is a strong, region-specific genetic influence on the area and thickness of the human cerebral cortex (surface area up to 65%; cortical thickness up to 55%). A wide range of heritabilities, for both surface area and cortical thickness, is evident across the cortex, largely independent of measurement error. We

also show that there is substantial environmental variance, which is not due to measurement error, but find little evidence for any strong common (shared) environmental factors. In addition, we show that associations across regions are surprisingly complex. While for most regions genetic covariance accounts for phenotypic correlations between hemispheres, this was not always the case. For some ROIs the same genetic factor did not explain the genetic variance for both left and right hemisphere measures. Further, when we covaried for total surface area, with the exception of the occipital lobe, regional surface area was only weakly associated, suggesting that there are limited region-specific interrelationships for surface area. In contrast, cortical thickness of neighbouring regions was associated after controlling for mean cortical thickness; positively within lobar divisions and negatively across regions, mainly due to genetic covariance. Lastly, correlations between surface area and cortical thickness at the regional level did not follow the inverse relationship observed at the global level, rather there was a complex pattern of negative and positive regional associations.

We report several novel results. Firstly, the striking finding that surface area/cortical thickness heritability estimates vary widely, largely independent of test-retest reliability, i.e. while high reliability was required to detect high heritability, a high reliability estimate did not guarantee a substantial genetic effect. Notably, across ROIs with high reliability (85 (QTIM) and 114 (HCP) out of 136 ROIs with test-retest correlation > 0.75) heritability estimates ranged from zero to 0.65 (QTIM) and 0.79 (HCP). Also, while in general heritability estimates for QTIM and HCP were in line with those reported previously, particularly for ROIs with high test-retest reliability, there were some notable exceptions. For example, heritability for cortical thickness of the right parahippocampal gyrus (reliability ~ 0.85 in QTIM and HCP) ranged from 6 to 55% across five datasets: QTIM, HCP, National Institute of Mental Health (Schmitt et al., 2008), Genetics of Brain Structure and Function Study (Winkler et al., 2010), Vietnam Era Twin Study of Ageing (Eyler et al., 2012). In addition to differences across the samples, differences in imaging and/or genetic analyses may, in part, underlie these contrasting results.

The wide range of heritability estimates we report here may relate to cortical neuroplasticity; an intrinsic characteristic of the cortex (Jancke, 2009; Pascual-Leone, Amedi, Fregni, & Merabet, 2005). Underlying differences in tissue organization and microstructure permit neural circuit plasticity (Zatorre, Fields, & Johansen-Berg, 2012),

allowing neural circuitry to be formed/altered due to sensory experience and learning (Lendvai, Stern, Chen, & Svoboda, 2000; Pantev, Engelien, Candia, & Elbert, 2001; Trachtenberg et al., 2002). Indeed, we found a substantial environmental influence ($e^2 > 0.60$), which was not due to measurement error (test-retest correlation > 0.75), on both surface area and cortical thickness for several association areas in both the QTIM and HCP datasets (surface area: rostral/caudal middle frontal gyrus left and right, pars opercularis left and right, cortical thickness: posterior cingulate left and right). Greater environmental variation may be indicative of functional cortical areas adapting to environmental stimuli for development/function. This notion is consistent with a comparative study of non-human primates, (Gomez-Robles, Hopkins, Schapiro, & Sherwood, 2015), where human cortical morphology was shown to be substantially less heritable than in chimpanzees (lobe and sulcal dimension heritability estimates up to 0.65 in humans and 0.77 in chimpanzees), with the lower heritability of human cortical organisation attributed to greater plasticity in humans. Though speculative, this capacity for greater plasticity in humans may also contribute to gene by environment interaction effects. Further, while plasticity is often discussed in terms of positive effects (e.g. learning), there are likely adverse effects associated with increased plasticity (e.g. a greater possibility of maladaptive brain circuits).

Interestingly, the broad range of cortical heritability estimates we report here contrasts with that found for subcortical brain structures in the same sample (Renteria et al., 2014). For subcortical structure volumes, environmental variance was smaller and genetic variance substantially larger, even though test-retest reliability estimates for subcortical and cortical measures are comparable. The supposition that cortical variation is more environmentally mediated than subcortical variation is reasonable, given the cortex's role in social interaction and learning, characteristics essential for human cognitive function and development (Boyd, Richerson, & Henrich, 2011). Conversely, the evolutionarily older subcortical system, responsible for behaviour regulation, emotion and memory, may require and/or be less malleable to interaction with the environment. This is not to say that subcortical structures are incapable of plasticity; an increasing body of work provides evidence for hippocampal and amygdala plasticity (Jhaveri et al., 2018; Kuhn et al., 2014; Leuner & Gould, 2010; Rabl et al., 2014; Sahay et al., 2011). Rather, we speculate that it is the uniquely human abilities afforded by the cerebral cortex (and their dependency upon

environmental influence) that is responsible for the higher levels of environmental variance found in the cortex.

In addition to the wide range in heritability estimates, a second major finding was the complex patterning of genetic and environmental covariation, which had not been investigated previously. When we directly examined whether different genetic factors influence left/right cortical regions we found a specific (different) genetic influence between hemispheres for two regions - superior temporal gyrus surface area, parahippocampal gyrus surface area; findings replicated in the HCP sample. This specific left/right genetic influence has not been previously found (Eyler et al., 2014), likely due to the larger sample size of the present study. Further complexity was evident from the vastly different covariance patterns found for surface area compared to cortical thickness. surface area measures for neuroanatomical regions did not correlate highly (outside of the occipital lobe), suggesting that when covaried for total surface area, there are limited, and generally weak, region-specific genetic and environmental contributions to covariance across the area of cortical regions. Intriguingly, the occipital lobe appears as an anomaly. Structural covariation between occipital regions, occurring not as a function of overall brain size, has previously been shown in *ex vivo* measurements (Andrews, Halpern, & Purves, 1997). The authors related the importance of coordinated occipital variation to visual ability, though whether the degree of structural covariation relates to individual differences in visual ability is currently unknown. In the present study, structural interdependence between occipital regions appears mainly due to genetic factors, with some environmental influence, possibly in the form of experience-expectant plasticity (Greenough, Black, & Wallace, 1987).

The finding of generally weak genetic associations across the cortex for surface area appear to contrast with the work of Chen et al. (2012), in which 12, maximally genetically correlated divisions of the cortical surface were identified based on vertex-wise (i.e. continuous) surface area measures (corrected for total surface area). How could genetic covariance in surface area be best explained by 12 divisions, when the present study found generally weak associations (outside of the occipital lobe) between regional surface area? Firstly, vertex-based approaches to surface area measurement are more heritable than ROI-based surface area measures, possibly due to the degree of spatial averaging in vertex-based approaches (Eyler et al., 2012), which could result in higher genetic

correlations. Secondly, it is important to reiterate that the findings of Chen et al. (2012) and those of the present study are based on different metrics. Chen et al. (2012) examined genetic covariance through genetic correlations (i.e. the extent to which two ROIs share genetic variance, regardless of their contribution to phenotypic covariance), whereas we examined genetic correlations weighted by heritability to standardize genetic covariance in terms of its contribution to phenotypic covariance. Thus, these two metrics answer different questions regarding the role of genetics in cortical organisation.

In contrast to surface area, we found cortical thickness covaried weakly to strongly across regions, and as effects of mean cortical thickness were removed, these associations were not due to a global factor. Highly correlated cortical regions share maturational trajectories (Alexander-Bloch, Raznahan, Bullmore, & Giedd, 2013; Fjell et al., 2015; Mechelli, Friston, Frackowiak, & Price, 2005) and form systems underlying perception, behaviour and cognition (Alexander-Bloch, Giedd, & Bullmore, 2013; A. C. Evans, 2013; Richmond, Johnson, Seal, Allen, & Whittle, 2016; Vertes & Bullmore, 2015). With genetic factors largely accounting for structural associations, these results suggest genes play an important role in the organisational principles of the cortex. Only Schmitt et al. (2008) has examined genetic covariance between cortical thickness measures of neuroanatomical regions. Using hierarchical cluster analysis, they identified two major blocks: a temporo-occipital cluster and a fronto-parietal cluster. We did not find the same divisions, rather in QTIM we found a parietal/occipital cluster and a fronto-temporo-cingulate cluster, and in HCP we found a frontal cluster and temporo-occipital-cingulate-parietal cluster. These results suggest that patterns of genetic covariance in cortical thickness may not be stable from childhood to adulthood.

Our finding that surface area and cortical thickness are only weakly associated (both negatively and positively) over a number of neuroanatomical regions, replicates and extends prior work showing regional surface area and cortical thickness to be distinct characteristics of the cortex (Panizzon et al., 2009; Winkler et al., 2010). As noted previously (Panizzon et al., 2009), these differences likely correspond to the cellular architecture of the cortex; neurons within the cerebral cortex are organized into ontogenetic columns (Mountcastle, 1997), with the size, number and density of cells within columns hypothesized to determine thickness, and the number of cortical columns responsible for surface area (Rakic, 1988). Thus, it is entirely rational that the genetic and

environmental factors that influence variation in surface area are separate from those responsible for cortical thickness variation. The unique contributions of surface area and cortical thickness variation to cortical morphometry and function should not be undervalued.

In examining variation within the cerebral cortex, it is important not to disregard the effects of age and sex, as well as global factors. Very strong relationships between regional and global measures were found for surface area and to a lesser extent, cortical thickness. Prior studies have reported a degree of genetic overlap between global and regional measures, stronger for surface area than cortical thickness (Eyler et al., 2012; Winkler et al., 2010). Without adjustment for global effects, it is likely that genetic associations across cortical regions would be substantially higher, particularly for surface area. Whether regions with a greater degree of region-specific genetic variance provide better phenotypes for genome association studies is an intriguing future research direction. Subtle but complex age and sex effects were found in the current sample. Age and sex effects are well documented for cortical thickness (Salat et al., 2004; Sowell et al., 2007; Tamnes et al., 2010; van Soelen et al., 2012), but effects for surface area have been difficult to establish as studies have focused on cortical volume rather than area. Based on the present results, we posit that after controlling for total cortical area, small and sparse regional sex differences in cortical surface area are present. Studies of sexual dimorphisms within the cortex may provide insights into disorders with sex specific risk factors.

A limitation of the present study is that surface area and cortical thickness measures were estimated for cortical regions based on macroanatomical landmarks (gyri and sulci), with such regions not completely representing cytoarchitectural variation within the cortex. Measures of genetic covariation on a continuous basis throughout the cortical ribbon (Chen et al., 2013; Cui et al., 2016; Eyler et al., 2012; Schmitt et al., 2009) may provide an elegant means to circumvent this limitation. Also, cortical parcellations based on structural, functional, and connectional imaging data (Fan et al., 2016; Glasser et al., 2016) provide an enticing basis for ROI measures with increased neuroanatomical precision. Nevertheless, the Desikan-Killiany atlas has been, and will continue to be, one of the main cortical parcellations used in studying surface area and cortical thickness. An understanding of genetically and environmentally mediated variance within these regions

will aid interpretation of past and future studies using this cortical parcellation. We additionally note that the Cholesky decomposition used to test the similarity of sources of genetic variance in left/right brain regions does not explicitly model common and specific factors (Loehlin, 1996), and future research should examine alternate methods to assess common and specific sources of variance in corresponding left/right brain structures (Wen et al., 2016).

4.5 Conclusions

A complex pattern of genetic and environmental influences underlie the surface area and cortical thickness of the cerebral cortex. When controlling for global effects, region-specific genetic factors account for much of the structural variation within anatomically distinct cortical regions, but environmental sources are clearly involved. Identifying cellular and molecular level changes within the brain which intercede between genetically and environmentally mediated variation is a challenging next step, but one that will likely go far in advancing our understanding of the origins of normal and abnormal brain circuitry.

5

Absolute and Relative Estimates of Genetic and Environmental Influence on Brain Structure Volume

This chapter is based on:

Strike, L. T., Hansell, N. K., Thompson, P. M., de Zubicaray, G. I., McMahon, K. L., Zietsch, B. P., & Wright, M. J. (2017). Mean-standardised and relative estimates of genetic and environmental influence on brain structure. *Manuscript in preparation.*

5 Absolute and Relative Estimates of Genetic and Environmental Influence on Brain Structure Volume

Lachlan T. Strike¹, Narelle K. Hansell¹, Paul M. Thompson², Greig I. de Zubicaray³, Katie L. McMahon⁴, Brendan P. Zietsch^{5†}, Margaret J. Wright^{1†}

¹Queensland Brain Institute, University of Queensland, Brisbane QLD 4072, Australia. ²Imaging Genetics Center, University of Southern California, Marina del Rey, CA 90032, USA. ³Faculty of Health and Institute of Health and Biomedical Innovation, Queensland University of Technology, Brisbane QLD 4059, Australia.

⁴Centre for Advanced Imaging, University of Queensland, Brisbane QLD 4072, Australia. ⁵School of Psychology, University of Queensland, Brisbane QLD 4072, Australia.

† BPZ and MJW contributed to this work equally

Abstract

Comparing estimates of the amount of genetic and environmental variance for different brain structures may elucidate differences in the genetic architecture or developmental constraints of individual brain structures. However, most studies compare estimates of relative genetic (heritability) and environmental variance in brain structure, which do not reflect differences in absolute variance between brain regions. Here we used a population sample of young adult twins and singleton siblings of twins ($n = 831$; $M = 23$ years) to estimate the absolute genetic and environmental variance, standardised by the phenotypic mean, in the size of cortical, subcortical, and ventricular brain structures. Mean-standardised genetic variance differed widely across structures (17-fold range: 0.77% (hippocampus) to 13.08% (lateral ventricles)), but the range of estimates within cortical, subcortical, or ventricular structures was more moderate (2 to 4-fold range). There was no association between mean-standardised and relative measures of genetic variance in brain structure. We found similar results in an independent sample ($n = 1105$, $M = 29$ years, Human Connectome Project). These findings open important new lines of enquiry: namely, understanding the bases of these variance patterns, and their implications regarding the genetic architecture, evolution, and development of the human brain.

5.1 Introduction

Despite broad similarities (e.g. in lobar divisions, primary gyri and sulci), the anatomy of the human brain varies substantially across individuals. The majority of this variation is likely normal and has both genetic and non-genetic (i.e. environmental) causes (Gu & Kanai, 2014; Jansen et al., 2015). Estimates of raw or non-standardised genetic or environmental variance can be compared (Kremen et al., 2012), but this is problematic because variance may, in part, be determined by structure size, making it difficult to interpret variance differences between structures of different size. Hence, genetic and non-genetic variance components need to be standardised to facilitate comparisons across different brain regions.

Additive genetic variance is normally standardised by dividing the genetic variance by the total phenotypic variance, giving heritability (h^2 ; the proportion of phenotypic variance attributed to additive genetic differences among individuals within a population). Studies show high heritability for global brain traits (e.g. intracranial volume, 0.90, or 90% (Renteria et al., 2014)), whereas estimates for specific structures across the brain vary widely (Joshi et al., 2011; Kremen et al., 2010; Renteria et al., 2014; Schmitt et al., 2014; Winkler et al., 2010). However, a problem with comparing heritability across brain regions is that higher heritability could reflect higher genetic variance, or lower environmental variance, or both; it is therefore uninformative with respect to patterns of actual variation across structures. A solution is to standardize genetic and environmental variance by the phenotypic mean; then variance estimates are independent of measurement units and can be compared across traits. For genetic variance, this statistic equals the additive genetic variance divided by the square of the phenotypic mean (Charlesworth, 1984, 1987; Hansen, Pélabon, & Houle, 2011; Houle, 1992) (I_A ; henceforth referred to as mean-standardised genetic variance) and provides absolute estimates of genetic variance that are robust to other sources of variance.

Several studies comparing mean-standardised phenotypic variance in brain structures provide an intriguing first look at the strength and patterns of variability in the brain. In these studies, estimates of phenotypic variance in the volume of individual brain components differed substantially across the brain (Allen, Damasio, & Grabowski, 2002; Kennedy et al., 1998; Lange, Giedd, Castellanos, Vaituzis, & Rapoport, 1997) (Table 5.1). These differences were found not only between structural divisions (e.g. cortical,

subcortical), but also within divisions (e.g. mean-standardised phenotypic variance for amygdala volume was substantially greater than for hippocampal volume (Lange et al., 1997)). Only one study has examined mean-standardised genetic variance in the human brain. Miller and Penke (2007) calculated the mean-standardised genetic variance for total brain-volume ($I_A = 0.61\%$), based on a meta-analysis of 19 studies, and also found this was substantially smaller than for other human organs or life-history traits (e.g. body weight in females $I_A = 2.46\%$, heart ventricle volume $I_A = 7.08\%$).

Here, we use a population sample of young adult twins and singleton siblings of twins from the Queensland Twin IMaging (QTIM) study ($n = 831$) to compare, for the first time, mean-standardised estimates of additive genetic, environmental, and phenotypic variance across brain structures. In addition, we assess the association between mean-standardised and relative (i.e. heritability) measures of genetic variance. Comparisons with traits of different dimensionality (e.g. length, area) are difficult, as variation increases with the number of dimensions (Garcia-Gonzalez, Simmons, Tomkins, Kotiaho, & Evans, 2012; Hansen et al., 2011; Houle, 1992). Hence, we examined only volumetric measures of the brain (45 cortical, subcortical, and ventricular structures), as well as total brain volume, and a comparable volumetric, non-brain phenotype (body weight). We include estimates of test-retest reliability to assess the contribution of measurement error towards trait variance. To assess the generalizability of our findings, we perform the same analyses in an independent sample of twins and singletons ($n = 1105$) from the Human Connectome Project (HCP).

Table 5.1 Published estimates of mean-standardised phenotypic variance in brain structure volume

Reference	Sample Size	Age	Structure	CV _P *	I _P
Lange et al. (1997)	115	4 to 20 years	Total cerebrum	11.30%	1.28%
			Superior temporal gyrus	11.50%	1.32%
			Putamen	9.40%	0.88%
			Caudate	12.70%	1.61%
			Lateral ventricles	63.50%	40.32%
			Hippocampus	10.30%	1.06%
			Amygdala	19.30%	3.72%
			Globus pallidus	15.40%	2.37%
			Cerebellum	10.70%	1.14%
			Corpus callosum	14.70%	2.16%
Kennedy et al. (1998) †	20	Mean age 20 years	Total cerebrum	9.50%	0.90%
			Frontal lobe (<i>mean</i>)	9.50%	0.90%
			F1 (<i>min</i>)	11.70%	1.37%
			JPL (<i>max</i>)	30.00%	9.00%
			Parietal lobe (<i>mean</i>)	14.40%	2.07%
			PCN (<i>min</i>)	14.40%	2.07%
			SGa (<i>max</i>)	33.70%	11.36%
			Temporal lobe (<i>mean</i>)	13.40%	1.80%
			INS (<i>min</i>)	11.10%	1.23%
			T2a (<i>max</i>)	34.70%	12.04%
			Occipital lobe (<i>mean</i>)	11.60%	1.35%
			LING (<i>min</i>)	17.60%	3.10%
			OP (<i>max</i>)	49.00%	24.01%
Allen et al. (2002)	46	22 to 49 years	Left hem	8.80%	0.77%
			Right hem	9.40%	0.88%
			Left frontal	12.60%	1.59%
			Right frontal	11.50%	1.32%
			Left temporal	12.40%	1.54%
			Right temporal	13.20%	1.74%
			Left parietal	9.20%	0.85%
			Right parietal	11.20%	1.25%
			Left occipital	13.60%	1.85%
			Right occipital	13.80%	1.90%
			Left cingulate	17.90%	3.20%
			Right cingulate	17.30%	2.99%
			Left insula	14.40%	2.07%
			Right insula	14.30%	2.04%
			Left cerebellum	9.80%	0.96%
			Right cerebellum	9.60%	0.92%
			Left lateral ventricle	66.20%	43.82%
			Right lateral ventricle	69.10%	47.75%

F1 superior frontal gyrus; *JPL* juxtaparacentral lobule; *INS* insula; *LING* lingual gyrus; *OP* occipital pole; *PCN* precuneus; *SGa* supramarginal gyrus, anterior; *T2a* middle temporal gyrus, anterior.

*Mean-standardised phenotypic variance was reported as the coefficient of variation (CV_P; phenotypic variance divided by the phenotypic mean); estimates are displayed here as the opportunity for selection (I_P; the square of the coefficient of variation).

†For Kennedy et al. (1998), the mean of estimates for each lobar division is presented, as well as the minimum and maximum estimate.

5.2 Method

5.2.1 Participants

Participants were from the Queensland Twin IMaging (QTIM) study of brain structure and function (Blokland et al., 2014; Chiang et al., 2011; de Zubicaray et al., 2008; Strike et al., 2018; Whelan et al., 2016). For the present study, we included twins and singleton siblings of twins, scanned between age 15 and 30 years, for whom T1-weighted images were available. The sample consisted of 831 healthy, right-handed young adults (63% female, $M = 23.04$ years, $SD = 3.33$ years), including 127 monozygotic (MZ) and 161 dizygotic (DZ) twin pairs, 3 triplet trios (all DZ), 164 unpaired twins, and 82 siblings of twins (0-2 per family). In addition, 45 participants were scanned a second time (mean duration between first and second scan was 113.15 ± 56.30 days) to assess the test-retest reliability of imaging measures. Prior to scanning, participants were screened for neurological and psychiatric conditions, including loss of consciousness for more than 5 minutes, and general MRI contraindications. Zygosity of same-sex twin pairs was determined using a commercial kit (AmpFISTR Profiler Plus Amplification Kit, ABI) and later confirmed by genome-wide single nucleotide polymorphism genotyping (Illumina 610K chip). The study was approved by the Human Research Ethics Committees at the University of Queensland, QIMR Berghofer Medical Research Institute, and UnitingCare Health. Written informed consent was obtained from all participants, including a parent or guardian for those aged under 18 years. Participants received an honorarium for their time and to cover any transport expenses.

5.2.2 Image Acquisition and Processing

Imaging was conducted on a 4T Bruker Medspec (Bruker, Germany) whole-body MRI system paired with a transverse electromagnetic (TEM) head coil. Structural T1-weighted 3D images were acquired (TR=1500 ms, TE=3.35 ms, TI=700 ms, 230 mm FOV, 0.9 mm slice thickness, 256 slices). Scans were corrected for intensity inhomogeneity with SPM12 (Wellcome Trust Centre for Neuroimaging, London, UK; <http://www.fil.ion.ucl.ac.uk/spm>) prior to extracting cortical, subcortical, and ventricular volumes (mm^3) using FreeSurfer (v5.3; <http://surfer.nmr.mgh.harvard.edu/>) previously reported in depth (Fischl and Dale

2000). These included volumes for 34 cortical (regions of interest (ROI) from the Desikan-Killiany atlas (Desikan et al., 2006)) and 7 subcortical (hippocampus, amygdala, putamen, caudate, thalamus, nucleus accumbens, globus pallidus) structures per hemisphere, as well as the lateral ventricle and choroid plexus from each hemisphere, and the 3rd and 4th ventricles. In addition, total brain volume (FreeSurfer variable *BrainSegVolNotVent*) was extracted. Structure segmentation and labelling were checked using the procedures of the ENIGMA consortium (enigma.ini.usc.edu), with incorrectly delineated structures excluded from the analysis (number of excluded structures listed in Appendix 20). For each bilateral structure, we then computed a mean volume using the left and right hemisphere volumes. Test-retest reliability was estimated using Pearson correlations for a subset of participants scanned twice ($n = 45$, approximately three months apart). The centroid of each cortical ROI was calculated (FreeSurfer command *mri_surfcluster*; centroids for right hemisphere regions used) to allow for comparisons with spatial topography (i.e. anterior-posterior, superior-inferior, medial-lateral).

5.2.3 Estimation of Variance Components

Raw/non-standardised additive genetic (V_A), environmental (V_E), and phenotypic (V_P) variances in ventricular, subcortical, and cortical volumes were estimated in a series of univariate models using structural equation modelling using the *OpenMx 2.7.12* package (Neale et al., 2016) in R 3.3.3 (R Core Team, 2017), which provides maximum-likelihood estimates for model parameters. Briefly, the variance within a phenotype is partitioned into additive genetic (A) and unique/non-shared environment (E) sources by contrasting phenotypic covariance between MZ and DZ twins (Neale & Cardon, 1992). Estimates of unique environment also include measurement error, as it is random and unrelated to twin similarity. Variance due to common/shared environment was also estimated, but estimates were small and could be dropped from all models without significantly worsening fit. Hence, a model specifying only A and E sources of variance was used. 95% maximum-likelihood confidence intervals were estimated for all mean-standardised and relative variance measures through *OpenMx*.

5.2.4 Mean-Standardised Variance

Estimates of raw/non-standardised additive genetic and environmental variance (detailed in the previous section) for each phenotype were then standardised by the phenotypic mean. Mean-standardised genetic variance (I_A) equals the additive genetic variance (V_A) divided by the phenotypic mean of the trait squared:

$$I_A = \frac{V_A}{\bar{x}^2}$$

Here, I_A is an extension of the index of opportunity for natural selection (I ; the extent to which variation in a population could be subject to selection (larger values indicate a greater opportunity for selection (Crow, 1958))). Similar to I_A , I (denoted here as I_P) is the phenotypic variance (V_P) divided by the phenotypic mean of the trait squared:

$$I_P = \frac{V_P}{\bar{x}^2}$$

Mean-standardised genetic variance is also commonly expressed as the coefficient of additive genetic variance (CV_A) (Hansen et al., 2011; Houle, 1992), which is intrinsically related to the measure of mean-standardised genetic variance used in the present study ($I_A = CV_A^2$). I_A is favoured in studies of evolvability or artificial selection, since it is interpreted as the expected percentage change per generation under a unit of selection (Garcia-Gonzalez et al., 2012; Hansen, Pelabon, Armbruster, & Carlson, 2003; Hansen et al., 2011). In addition to mean-standardised additive genetic (I_A) and phenotypic (I_P) variance, we estimated mean-standardised unique environmental variance (I_E ; unique environmental variance divided by the phenotypic mean of the trait squared) for all brain measures.

We further calculated relative estimates of genetic (a^2 or h^2) and environmental (e^2) variance by dividing raw/non-standardised additive genetic variance (V_A) or unique environmental variance (V_E) by total phenotypic variance (V_P). Both mean-standardised and relative variance estimates are dimensionless units, which can be expressed as a percentage.

For comparison with a volumetric, non-brain phenotype, we also estimated mean-standardised variance components of body weight (kilograms). Comparisons with traits of

different dimensionality (e.g. length, area) are difficult, as variation increases with the number of dimensions (Garcia-Gonzalez et al., 2012; Hansen et al., 2011; Houle, 1992). Downscaling estimates based on dimensionality is sometimes used to facilitate comparison in these situations (Houle, 1992; Lande, 1977), but this is only appropriate for perfectly geometrically proportioned objects (Garcia-Gonzalez et al., 2012). Further, the mean-standardised variance can only be estimated for traits measured on a true ratio scale, with an absolute zero (Garcia-Gonzalez et al., 2012). Hence, we are unable to compare mean-standardised variance in brain structures with traits of different dimensionality (e.g. height), or traits without true ratio measurement scales (e.g. intelligence or personality).

5.2.5 Replication in an Independent Sample

Data from the Human Connectome Project (HCP: S1200 release) (Glasser et al., 2016; Van Essen et al., 2012) was used as a secondary analysis sample. Here we included 1105 adults (604 females, $M = 28.80$ years, $SD = 3.70$ years), consisting of 152 monozygotic (MZ) and 85 dizygotic (DZ) twin pairs, 16 unpaired twins, 208 siblings of twins (0-2 per family), and 407 members of singleton families (1-4 per family). MZ and DZ twin zygosity was determined through genotyping, if available (215 of 237 pairs), otherwise by self-report (22 of 237 pairs). Details relating to participant selection and MRI acquisition have been reported elsewhere (Van Essen et al., 2012). All analyses completed on the QTIM sample were undertaken on the HCP data, including test-retest reliability on a sub-sample of participants who were scanned twice ($n = 45$, mean duration between first and second scan was 139.30 ± 68.99 days).

5.3 Results

The mean of estimates of mean-standardised genetic variance (I_A) in the QTIM dataset were highest for ventricular structures (6.88% compared to $< 1.40\%$ for cortical and subcortical structure volumes), and considerably higher than for body weight (3.80%) (Figure 5.1a). Further, mean-standardised genetic variance for cortical and subcortical structures was, on average, only slightly higher than for total brain volume ($I_A = 0.90\%$).

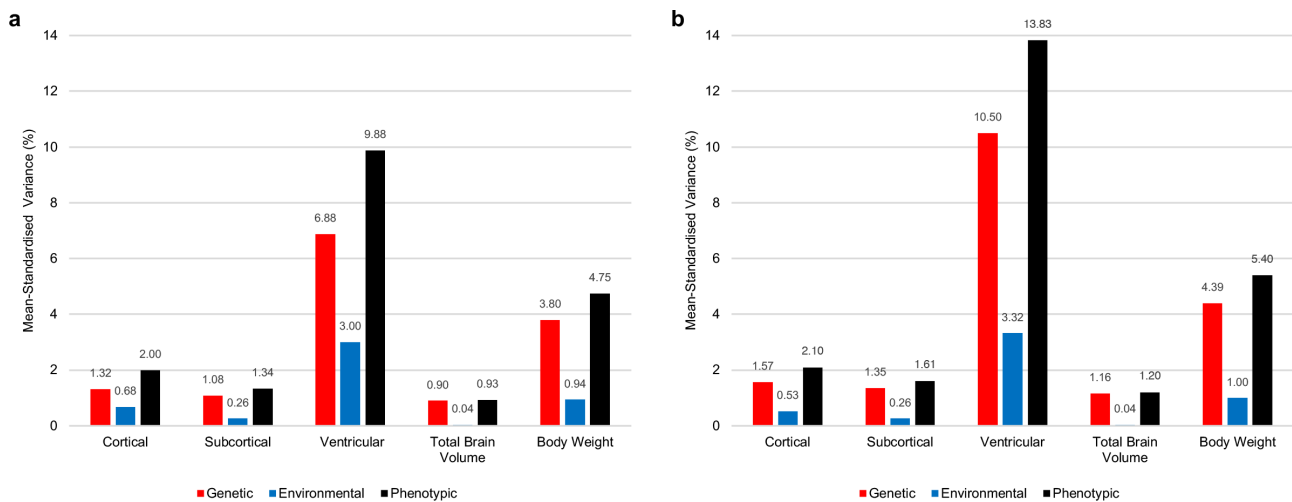


Figure 5.1 Average of mean-standardised variance component estimates in the QTIM and HCP datasets

Average of mean-standardised genetic (I_A), environmental (I_E), and phenotypic (I_P) variances of cortical, subcortical, and ventricular volumes, as well as total brain volume and body weight in the QTIM (a) and HCP (b) datasets. On average, mean-standardised variance estimates were substantially larger for the ventricles compared to other brain structures (cortical, subcortical, total brain). Estimates for body weight were smaller (nearly less than half) than the ventricular structures, but larger (> 2 times) than that for cortical or subcortical structures. Genetic and phenotypic variance components estimates were generally larger in the HCP (b) dataset compared to QTIM (a), whereas environmental estimates were similar.

Figures 5.2a, 5.3a and 5.3d show estimates of I_A ranged from a high of 13.08% for the lateral ventricles to a low of 0.77% for hippocampal volume (Appendix 21), representing a 17-fold range in mean-standardised genetic variance across the brain structure volumes examined. However, this wide range in I_A was substantially reduced when the ventricular structures were excluded (0.77% to 2.22%, 2.88-fold range), and within each of the structural divisions we observed a similar range in I_A : cortical 2.74-fold (Figure 5.2a), subcortical 2.05-fold (Figure 5.3a), ventricular 3.88-fold (Figure 5.3d). We found no evidence for an association between mean-standardised genetic variance and test-retest correlation, mean structure size, or spatial direction (Appendix 22), indicating that regional differences in I_A estimates were not explained by straightforward factors relating to measurement error or simple patterns of brain morphology (e.g. greater I_A estimates for larger structures, greater I_A estimates for anterior than posterior structures). Descriptive statistics and raw/non-standardised variance component estimates are presented in Appendix 20.

For the majority of structures, mean-standardised environmental variance was less than the genetic variance (36/45 structures with non-overlapping 95% confidence intervals; Figure 5.2 and Figure 5.3). An exception to this was the frontal pole, where the mean-standardised environmental variance (which includes measurement error; $I_E \pm 95\% \text{ CI}$: 1.65% (1.39%, 2.01%)) was significantly greater than the corresponding estimate of genetic variance ($I_A \pm 95\% \text{ CI}$: 0.94% (0.59%, 1.31%)). For both cortical and subcortical structure volumes, we also found that estimates of mean-standardised environmental variance were strongly associated with test-retest reliability correlation ($r = -0.71$, $p = 2.84\text{E-}06$ and $r = -0.99$, $p = 2.16\text{E-}05$ respectively; Appendix 22). This suggests that differences in mean-standardised environmental variance is largely due to variation in measurement error. Further, mean-standardised environmental variance for cortical structures correlated with mean volume ($r = -0.65$, $p = 2.81\text{E-}05$), which remained significant after controlling for test-retest correlation ($r = -0.61$, $p = 1.58\text{E-}04$).

There was 2.53-fold range in relative genetic variance estimates (i.e. heritability) across brain structures (frontal pole h^2 36% to putamen h^2 92%; Figure 5.2c; Figure 5.3c/f; Appendix 21); a substantially smaller range compared to the 17-fold range in mean-standardised genetic variance. Cortical and subcortical structures with high relative genetic variance (>75%) generally had more moderate mean-standardised variance (0.77-1.42%), with high mean-standardised and relative genetic variance found only for the pericalcarine cortex (2.22% and 86% respectively). Relative genetic variance estimates for the ventricles, which had significantly higher mean-standardised genetic variance than subcortical/cortical structures (3.37-13.08%), ranged from 66% to 77%. Moderate relative genetic variance (~ 50%) was due to low mean-standardised genetic variance (cortical ROIs: pars triangularis, frontal pole) or high mean-standardised environmental variance (cortical ROIs: entorhinal, temporal pole, caudal anterior cingulate). We also found no correlation between estimates of mean-standardised and relative genetic variance (ventricular $r = -0.70$, $p = .29$; subcortical $r = -0.45$, $p = .31$; cortical $r = 0.13$, $p = .46$).

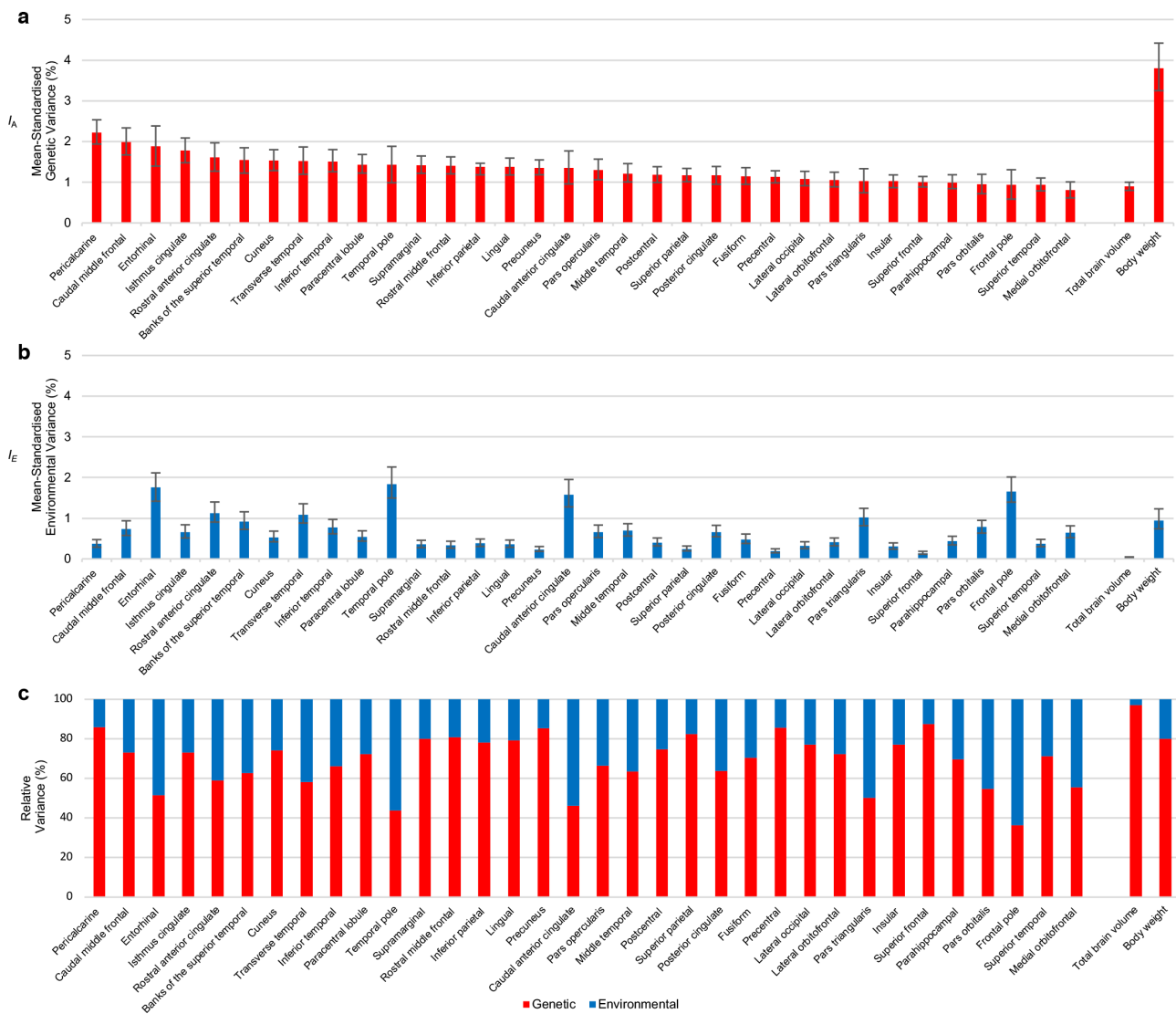


Figure 5.2 Mean-standardised and relative genetic and environmental variances for cortical structures in the QITM dataset

Mean-standardised genetic (a) and environmental (b) variances (with 95% confidence intervals), as well as relative genetic and environmental variance components (c) for cortical structures in the QITM dataset. Estimates are presented in descending order of mean-standardised genetic variance. Mean-standardised genetic variance was largest for the pericalcarine cortex, and smallest for the medial orbitofrontal gyrus (a). Approximately half of the cortical structures had more mean-standardised genetic variance than total brain volume (18/34 structures with non-overlapping 95% confidence intervals with total brain volume, Appendix 20), and all cortical structures had less mean-standardised genetic variance than body weight. Estimates of mean-standardised environmental variance were generally less than genetic variance, with the exception of the frontal pole (b). Moderate relative genetic variance (c; ~ 50%) was due to low mean-standardised genetic variance (pars triangularis, frontal pole) or high mean-standardised environmental variance (entorhinal, temporal pole, caudal anterior cingulate).

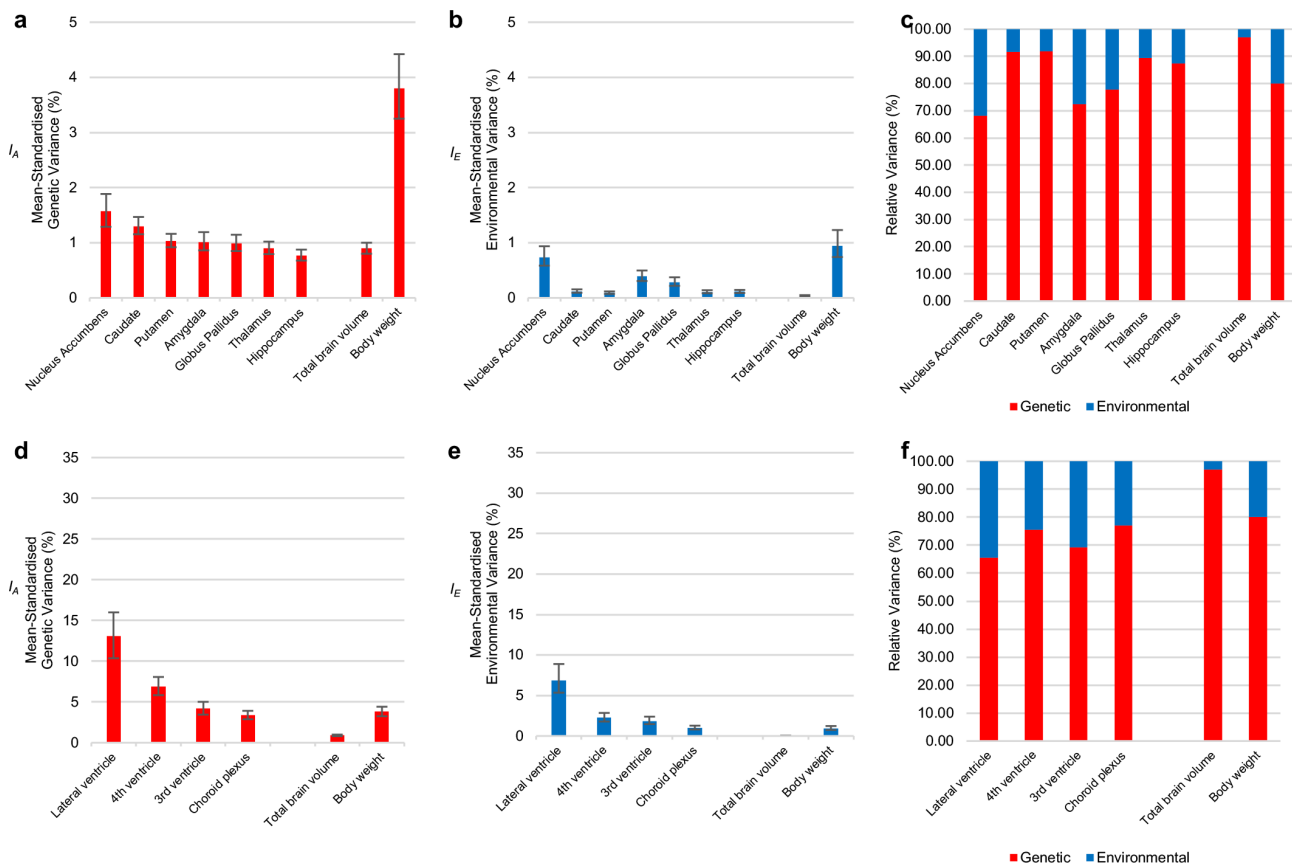


Figure 5.3 Mean-standardised and relative genetic and environmental variances for subcortical and ventricular structures in the QITM dataset

Mean-standardised genetic (a, d) and environmental (b, e) variances (with 95% confidence intervals), as well as relative genetic and environmental variance components (c, f) for subcortical (top row) and ventricular (bottom row) structures in the QITM dataset. Estimates are presented in descending order of mean-standardised genetic variance. For subcortical structures, mean-standardised genetic variance was largest for the nucleus accumbens, and smallest for the hippocampus and thalamus (a). Further, mean-standardised genetic variance for subcortical structures was like that for total brain volume, though estimates for the nucleus accumbens and caudate did not overlap with total brain volume (95% confidence intervals, Appendix 21). For ventricular structures, genetic and environmental variance was largest for the lateral ventricles, and smallest for the choroid plexus (d, e). Mean-standardised environmental variance was smaller than genetic variance for all subcortical (b) and ventricular structures (e). Despite having the highest mean-standardised genetic variance for their structure type, the nucleus accumbens (subcortical) and lateral ventricles (ventricular) had the lowest relative genetic variance (c, f) on account of the large environmental variance for these structures.

5.3.1 Replication Using the HCP Sample

Using the same methodology, estimates of mean-standardised genetic variance were, on average, larger in the HCP dataset (Appendices 23-25) compared to the QITM dataset; however, patterns of mean-standardised genetic variance were similar between two datasets (Figure 5.4). The lateral ventricles had the largest mean-standardised genetic variance in the HCP dataset, though this estimate was substantially larger than in the

QTIM dataset ($I_A \pm 95\%$ CI: HCP 19.43% (15.88%, 23.44%), QTIM 13.08% (10.37%, 16.00%)). Estimates of mean-standardised genetic variance for cortical structures followed a similar pattern for both datasets (Figure 5.4), with some noticeable differences (e.g. rostral anterior cingulate $I_A \pm 95\%$ CI: QTIM 1.61% (1.27%, 1.97%), HCP 2.51% (2.06%, 2.94%). In both samples, mean-standardised genetic variance in subcortical structures was largest for the nucleus accumbens, and smallest for the hippocampus and thalamus, though the ranking of estimates for other subcortical structures differed between the two datasets. The association between mean-standardised environmental variance and mean volume for cortical structures was replicated ($r = -0.69$, $p < .001$; Appendix 26), and remained significant after controlling for test-retest correlation ($r = -0.63$, $p = 7.44E-05$). The finding of high mean-standardised and relative genetic variance for pericalcarine cortex was replicated, and there was no association between mean-standardised and relative variance estimates (cortical structures $r = 0.14$, $p = .43$; subcortical structures $r = -0.45$, $p = .31$; ventricular structures $r = -0.62$, $p = .39$).

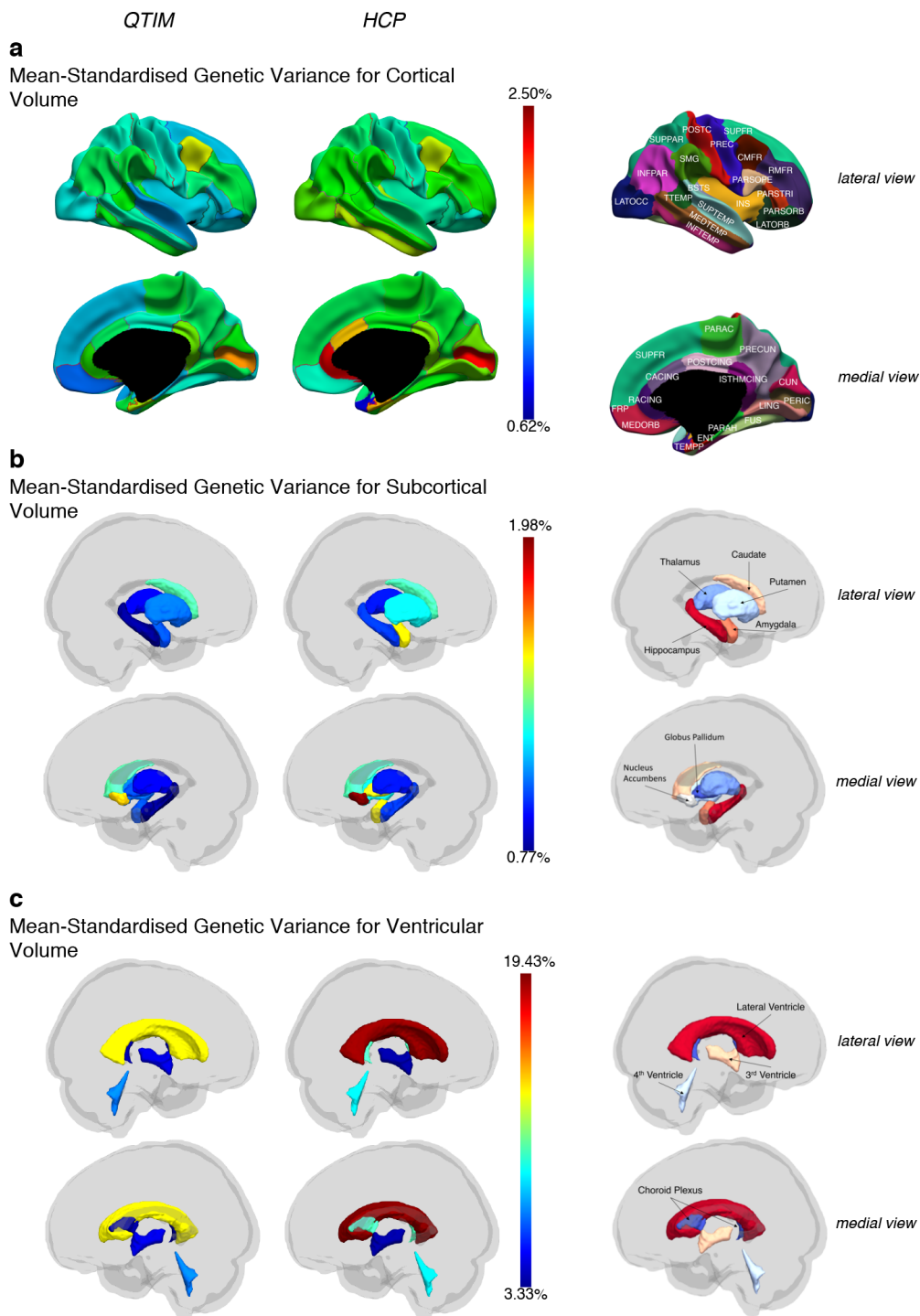


Figure 5.4 Mean-standardised genetic variance estimates for cortical, subcortical, and ventricular structures in the QTIM and HCP datasets

Mean-standardised genetic variance estimates for cortical (a), subcortical (b) and ventricular (c) brain volumes in the QTIM (left column) and HCP (right column) datasets. Estimates of mean-standardised genetic variance for cortical structures followed a similar pattern for both datasets (a), with some noticeable differences (e.g. rostral anterior cingulate (RACING), caudal anterior cingulate (CACING)). In both datasets, mean-standardised genetic variance in subcortical structures was largest for the nucleus accumbens, and smallest for the hippocampus and thalamus (b). The lateral ventricles had the largest mean-standardised genetic variance of any structure in the HCP dataset, and this estimate was substantially larger than in the QTIM dataset (c). Abbreviations for cortical regions listed in Appendix 2.

5.4 Discussion

Here, for the first time, we examine the mean-standardised genetic and environmental variance in the size of cortical, subcortical, and ventricular brain structures in humans. In contrast to relative estimates (e.g. heritability), which have been widely used in neuroimaging genomics studies, the mean-standardised approach does not scale raw/non-standardised variance components to total phenotypic variance. Instead, it estimates the absolute genetic and environmental variance in a trait, and uses the phenotypic mean of the trait to standardise variance components. Thus, estimates of mean-standardised variance are robust to other variance sources, and inform on the strength of factors which maintain or deplete variability in brain anatomy.

The most striking finding was the large mean-standardised variance for the ventricular system (particularly the lateral ventricles) compared to other brain structures, and that this substantial variance in ventricular volume was largely due to genetic factors. This is consistent with studies of mean-standardised phenotypic variance (Allen et al., 2002; Lange et al., 1997), though estimates for lateral ventricle volume were substantially larger (40.32% and 47.75% respectively) than those of the present examination (QTIM 19.96%, HCP 28.60%). This contrast is likely due to the small sample sizes ($n = 115$ and 46 respectively) and superseded imaging methods of past studies. Here we showed that this high phenotypic variance is mainly due to genetic factors, with only a small amount of the variance attributed to the environment. The finding of large mean-standardised genetic variance for ventricular volume (much larger than all other brain structures) is somewhat unexpected, as studies generally report lower amounts of mean-standardised genetic variance for morphological traits compared to life-history and complex behavioural traits (Coltman, O'Donoghue, Hogg, & Festa-Bianchet, 2005; Garcia-Gonzalez et al., 2012; Houle, 1992; Miller & Penke, 2007). For instance, estimates of mean-standardised additive genetic variance for male bighorn sheep bodyweight and reproductive success are 0.27% and 22.09% respectively (Coltman et al., 2005).

Why would a morphological trait such as lateral ventricular volume show such large variation? Ventricular enlargement is often considered a marker of tissue atrophy in both normal ageing and disease (Apostolova et al., 2012; Carmichael et al., 2007; Nestor et al., 2008; Thompson et al., 2006), but estimates in the present study were of healthy adults. Previous studies have suggested the large mean-standardised phenotypic variance in the

volume of the lateral ventricles reflects accumulated variability in surrounding structures (Lange et al., 1997); however, in the present study we did not find large mean-standardised variance for surrounding subcortical structures, namely the hippocampus and caudate (in fact, estimates for these structures were among the smallest found). The large variance found for life-history traits is typically explained by the composite nature of these traits, which integrate variation across the lifespan. Because of this, it is likely that a greater number of loci (and more mutations), more environmental variables, and the interactions between them, contribute to variation in life-history traits (Hansen et al., 2011; Houle, 1992; Miller & Penke, 2007). While not a life-history trait, the early embryonic development of the ventricular system (Lowery & Sive, 2009), if influenced by many more genetic and environmental factors, could explain the large mean-standardised variation in this structure.

The high mean-standardised variance (particularly genetic) for ventricular structures could also represent a lack of selection pressures (stabilising or directional) throughout evolution. All else being equal, brain structures that have been subject to strong selection should show less genetic variance than structures under weaker selection pressures, as selection should deplete additive genetic variance (Barton & Keightley, 2002). Hence, the larger mean-standardised genetic variance for ventricular structures might suggest a lack of strong selection pressures, whereas the small genetic variance found for limbic system structures such as the hippocampus and thalamus might imply that the size of these structures was under stronger selection pressures across evolution. Indeed, the contribution of genetic variants to human hippocampal volume was shown to be significantly greater in evolutionarily conserved regions compared to other functional categories of the genome (Hibar et al., 2017). Small variation for structures could further be interpreted in regards to canalization: a narrowing of variation to increase robustness to genetic (and environmental) perturbations (Waddington, 1942). From this perspective, stabilising selection may have resulted in brain structures that are crucial to physiological and/or cognitive function evolving to a robust optimum. However, the all-else-is-equal assumption is paramount to these inferences. That is, for differences in genetic variance amounts to predict historical associations with selection, the genetic architecture and factors influencing brain structure must be the same.

It is important to also consider the role of ontogenetic (developmental) constraints when comparing variation between traits. For instance, the smaller mean-standardised genetic variance for cortical and subcortical brain structures (I_A range 0.77% to 2.22%) compared to body weight ($I_A = 3.80\%$) might correspond to the stronger physical constraints over brain structure (which is constrained by the skull, dura matter, and subarachnoid space) compared to body weight (which can vary more freely). Interestingly, the larger variation in body weight is likely not entirely due to freely varying composition factors such as muscle, fat, and organ mass, as estimates of mean-standardised phenotypic variance for human skeletal weight (I_P range 1.97% to 4.39%, calculated from data reviewed by Wagner and Heyward (2000)) fall between the estimates for mean-standardised phenotypic variance in cortical/subcortical structures (I_P range 0.88% to 3.64%) and body weight ($I_P = 4.75\%$) in the present study. Further, the physical constraints imposed by the limited space available within the cranium likely impacts the variation of individual brain structures. As the ventricular system arises within the cavities of the primary brain vesicles (Carpenter, 2016; Fujii, Youssefzadeh, Novel, & Neman, 2016; Lowery & Sive, 2009), it begins to develop before subcortical and cortical structures. As a consequence, it may be under less strict physical constraints and vary more freely than later developing structures.

Measures of mean-standardised variance may shed light on the findings of past studies. ENIGMA, a worldwide consortium of brain imaging scientists, has conducted meta-analyses of case-control cohorts for a number of diseases, including major depressive disorder (Schmaal et al., 2017; Schmaal et al., 2016), schizophrenia (van Erp et al., 2016), bipolar disorder (Hibar et al., 2016) and attention deficit hyperactivity disorder (Hoogman et al., 2017). Of the subcortical structures examined so far in these analyses, the hippocampus is the only structure to show a statistically significant difference in the mean volume between patients and matched controls across all disorders (Thompson et al., 2017), and is the only subcortical structure to show a difference for major depressive disorder (Schmaal et al., 2016). This is noteworthy in the context of the present results because mean-standardised phenotypic variance estimates for the hippocampus were the lowest of the subcortical structures examined in the QTIM and HCP datasets. Therefore, the common finding of mean differences in hippocampal volume in all these analyses could reflect in part, the increased statistical power granted by the small variation present in (normal) hippocampal volume, which makes group differences easier to detect. The

effect of normal variation and the sample size required to detect group differences should not be underestimated, especially as the high-price of *in vivo* imaging studies often prohibit large sample sizes. We suggest that future studies could carefully consider their research design and focus on structures with minimal phenotypic variance to maximise their statistical power.

The substantial mean-standardised environmental variance found for several structures should not be disregarded. Negative associations between mean-standardised environmental variance and test-retest reliability correlation or structure size were expected as measurement error is attributed to environmental variance in twin modelling. Though differences in measures of mean-standardised environmental variance might be due to a range of factors (e.g. complexity of the phenotype, developmental constraint, interaction with external environment, measurement error), they are of great importance as they demonstrate that the unusually low relative genetic variance (i.e. heritability) of several brain structures (e.g. caudal anterior cingulate $h^2 = 46.26\%$, entorhinal cortex $h^2 = 51.63\%$) were not a result of unusually low levels of mean-standardised additive genetic variance in these structures (e.g. caudal anterior cingulate $I_A = 1.36\%$, $I_E = 1.58\%$; entorhinal cortex $I_A = 1.88\%$, $I_E = 1.76\%$).

Mean-standardised variance estimates differed between QTIM and HCP, though the patterns of variation were similar. The most prominent difference between the samples was in the lateral ventricles (HCP $I_A = 19.43\%$; QTIM $I_A = 13.08\%$). Interestingly, even if participants are excluded based on their ventricle-to-brain ratio (outliers at ± 3.29 SD excluded), mean-standardised variance estimates for the lateral ventricles remain larger in the HCP dataset ($I_A = 16.66\%$) compared to the QTIM dataset ($I_A = 12.61\%$). Further, these differences in genetic variance could reflect sampling error due to the small sample size of twins used to distinguish genetic from environmental variance. However, estimates of mean-standardised phenotypic variance (which are more stable than genetic/environmental) for the lateral ventricles also differed between the datasets (QTIM $I_P = 19.96\%$, HCP $I_P = 28.60\%$), suggesting that sampling error is unlikely to be the main cause of this difference. As QTIM is a predominantly Caucasian sample, it is possible that differences in variance component estimates reflect the more diverse ethnic and racial composition of the HCP sample, which approximates that of the U.S. population (Van Essen et al., 2013). Differences in test-retest reliability estimates suggest measurement

error differs between the samples, which could additionally lead to differences in structure variability (e.g. temporal pole: QTIM I_P 3.26%, test-retest correlation 0.50, HCP I_P 1.61%, test-retest correlation 0.71).

In the present study, we found no association between mean-standardised and relative measures of genetic variance for brain structure. This is consistent with studies of other biological and life-history traits (Hansen et al., 2011; Houle, 1992), and relates to a common misconception of heritability – that low heritability reflects low genetic variance (Visscher, Hill, et al., 2008). This is an important point, as it has been suggested that low heritability in brain structure relates to a reduction of genetic variance (Lenroot et al., 2009). Low heritability can result from low genetic variance, but conversely, it could also be due to high environmental variance (e.g. despite having the highest mean-standardised genetic variance for subcortical structures, the nucleus accumbens had the lowest relative genetic variance because of the large mean-standardised environmental variance for this structure). Further, as noise due to measurement error inflates estimates of environmental variance, measurement error can also substantially influence heritability. It is important to always consider these points when comparing estimates of heritability.

One limitation of mean-standardised absolute variance measures is that only traits on a true ratio scale can be compared, meaning that many human traits (e.g. intelligence) are unsuitable for mean-standardised measures (Visscher, Hill, et al., 2008). This limitation could be circumvented by future studies examining individual task scores (e.g. number of correct responses) rather than composite, factors scores. Curiously this has been examined in chimpanzees (e.g. spatial memory, $I_A = 20.68\%$) (Woodley Of Menie, Fernandes, & Hopkins, 2015), but not in humans. Further, the confound of variation scaling with dimensionality limits our ability to compare traits of different dimensions (e.g. body height (linear) and brain volume (cubic)).

This was the first comparison of mean-standardised measures of absolute variance (genetic and environmental) in brain structure. We uncovered significant and, in some cases, striking variation in variances across different regions. This variation did not follow any obvious patterns, precluding straightforward explanations. These findings open important new lines of enquiry: namely, understanding the bases of these variance

patterns, and their implications regarding the genetic architecture, evolution, and development of the human brain.

6

A Consistent Pattern of Genetic Parcellations of Cortical Surface Area Across Three Large Twin Datasets

This chapter is based on:

Strike, L. T., Hansell, N. K., Couvy-Duchesne, B., Thompson, P. M., de Zubicaray, G. I., McMahon, K. L., & Wright, M. J. (2017). A consistent pattern of genetic parcellations of cortical surface area across three large twin datasets. *Manuscript in preparation.*

6 A Consistent Pattern of Genetic Parcellations of Cortical Surface Area Across Three Large Twin Datasets

Lachlan T. Strike¹, Narelle K. Hansell¹, Baptiste Couvy-Duchesne², Paul M. Thompson³, Greig de Zubicaray⁴, Katie L. McMahon⁵, Margaret J. Wright^{1,5}

¹Queensland Brain Institute, University of Queensland, Brisbane QLD 4072, Australia. ²Institute for Molecular Bioscience, University of Queensland, Brisbane QLD 4072, Australia. ³Imaging Genetics Center, University of Southern California, Marina del Rey, CA 90292, USA. ⁴Faculty of Health and Institute of Health and Biomedical Innovation, Queensland University of Technology (QUT), Brisbane QLD 4059, Australia. ⁵Centre for Advanced Imaging, University of Queensland, Brisbane QLD 4072, Australia.

Abstract

Structural and functional magnetic resonance imaging measures have provided a variety of means to parcellate the human brain. An alternative method is to map the brain based on genetic correlations (i.e. shared genetic influences), first demonstrated in a sample of middle-aged male twins (Vietnam Era Twin Study of Ageing; VETSA). The replicability of genetic parcellations across different imaging datasets is yet to be determined. Here, we examine cortical genetic patterning of surface area in two large twin datasets: the Queensland Twin IMaging study (QTIM; $N = 1028$, 65% female, mean \pm SD age 22.39 ± 3.32 years, 157/194 MZ/DZ pairs), and the Human Connectome Project (HCP; $N = 1105$, 55% female, mean \pm SD age 29 ± 3.70 years, 152/85 MZ/DZ pairs). We compare the similarity of the parcellations in the QTIM and HCP datasets to the parcellation developed in the VETSA study. Divisions were identified based on cortical surface area, with cortical regions influenced by a common genetic factor grouped together. Twelve genetic divisions of the cortex were identified. These clusters were bilaterally symmetrical, and matched boundaries of structure and function. There was a consistent pattern of genetic parcellations across three large, twin datasets, indicating that genetic parcellations of cortical surface area are robust across sample and methodology. This suggests that delineating the cortical surface based on shared genetic influence is a valid method of cortical parcellation, and one that has the potential to further our understanding of how genes shape the organisation and development of the cerebral cortex.

6.1 Introduction

Integral to our understanding of how the brain works is a coherent and valid division of the structural and functional boundaries of the cerebral cortex. To date, regions of interest (ROI) in the cortex have been delineated predominantly on anatomical characteristics (Brodmann, 1909; Desikan et al., 2006; Destrieux, Fischl, Dale, & Halgren, 2010), functional specialisation (Power et al., 2011; Shen, Tokoglu, Papademetris, & Constable, 2013), and recently, integrated multi-modal data (Fan et al., 2016; Glasser et al., 2016). Another method of mapping the brain, one very much understudied, is to examine how genetic effects have shaped the regionalisation of the cortex.

Several studies have shown that genetic factors account for a significant proportion of variance in cortical structure (Eyler et al., 2012; Schmitt et al., 2008; Strike et al., 2018). Patterns of covariance between cortical structures are predominantly due to a common genetic factor (Strike et al., 2018), and this genetic (co)variance is independent of global genetic factors, suggesting the presence of region-specific genetic patterning. Chen et al. (2012) developed a data-driven, hypothesis free method to examine how the development of distinct cortical regions is genetically influenced. Using a bivariate twin design, they estimated genetic correlations between vertex-wise measures of surface area across the cortex. Genetic correlations provide an estimate of how much the genetic influences on two different cortical regions overlap. Applying a data-driven clustering technique to the matrix of genetic correlations, they divided the cortical surface into 12 clusters of maximal shared genetic influence. These clusters corresponded to biologically meaningful boundaries, and were predominantly bilaterally symmetrical.

In an effort to reduce image dimensionality and increase power, the genetically identified clusters of Chen et al. (2012) have been used as a cortical parcellation atlas in studies examining the genetic architecture of the cortex (Chen et al., 2015; Peng et al., 2016). However, a direct replication of the study design used by Chen et al. (2012), which was restricted to middle-aged males, has not been undertaken. In changing our perspective on cortical delineation to one based on genetic influence, it is important to investigate whether genetically mediated patterns replicate across age, sex, and sample; no matter how valid the results seem, the results of cluster analysis are inappropriate unless they are replicated.

In the current study, we examine genetic patterning of the cortical surface in two large, genetically informative samples of healthy young adults: the Queensland Twin IMaging (QTIM) study, and the Human Connectome Project (HCP). We compare the similarity of the parcellations in the QTIM and HCP datasets to the parcellation developed by Chen et al. (2012), in the Vietnam Era Twin Study of Ageing (VETSA) sample of middle-aged males. Briefly, bivariate twin modelling is used to estimate genetic correlations between vertex-wise surface area measures of the cerebral cortex. A clustering technique is then applied to the genetic correlation matrix to identify genetically similar cortical regions.

6.2 Methods

6.2.1 Study Participants and Imaging Protocols

Genetic parcellations were examined in two genetically informative datasets (QTIM, HCP), and compared with the parcellation developed by Chen et al. (2012), identified in the VETSA surface area dataset. Table 6.1 describes the imaging methodology and main demographic differences across the samples/datasets.

6.2.1.1 QTIM – the Queensland Twin IMaging study

The sample included 1028 healthy, right-handed young adults (65% female, mean age 22.39 ± 3.32 years, age range 15.40 to 30.11 years), consisting of 157 MZ pairs (106 female, 51 male), 191 DZ pairs (88 female, 30 male, 76 opposite sex), 3 triplet trios (all DZ), 221 unpaired twins, and 102 singleton siblings of twins (0-2 per family). Prior to scanning, participants were screened for neurological and psychiatric conditions, including loss of consciousness for more than 5 minutes, and general MRI contraindications. Zygosity of same-sex twin pairs was determined using a commercial kit (AmpFISTR Profiler Plus Amplification Kit, ABI) and later confirmed by genome-wide single nucleotide polymorphism genotyping (Illumina 610K chip). The study was approved by the Human Research Ethics Committees of the University of Queensland, QIMR Berghofer Medical Research Institute, and UnitingCare Health. Written informed consent was obtained from

all participants, including a parent or guardian for those aged under 18 years. Participants received an honorarium for their time and to cover any transport expenses.

Imaging was conducted on a 4T Bruker Medspec (Bruker, Germany) whole-body MRI system paired with a transverse electromagnetic (TEM) head coil. Structural T1-weighted 3D images were acquired (TR=1500 ms, TE=3.35 ms, TI=700 ms, 230 mm FOV, 0.9 mm slice thickness, 256 or 240 slices depending on acquisition orientation (86% coronal (256 slices), 14% sagittal (240 slices))). Cortical surfaces were reconstructed using FreeSurfer (v5.3; <http://surfer.nmr.mgh.harvard.edu/>) previously reported in depth (Fischl & Dale, 2000). Prior to FreeSurfer analysis, the raw T1-weighted images were corrected for intensity inhomogeneity with SPM12 (Wellcome Trust Centre for Neuroimaging, London, UK; <http://www.fil.ion.ucl.ac.uk/spm>).

6.2.1.2 HCP – the Human Connectome Project

Data from the Human Connectome Project (S1200 release) (Glasser et al., 2016; Van Essen et al., 2012) was used as a secondary analysis sample. Here we included 1105 adults (55% female, $M = 28.80$ years, $SD = 3.70$ years, age range 22 – 37 years), consisting of 152 monozygotic (MZ) and 85 dizygotic (DZ) twin pairs, 16 unpaired twins, 208 siblings of twins (0-2 per family), and 407 members of singleton families (1-4 per family). MZ and DZ twin zygosity was determined through genotyping, if available (215 of 237 pairs), otherwise by self-report (22 of 237 pairs). Details relating to participant selection and MRI acquisition have been reported elsewhere (Van Essen et al., 2012). Pre-processed FreeSurfer data was used (Glasser et al., 2013). All analyses completed on QTIM were undertaken on the HCP data.

6.2.2 Vertex-Wise Surface Area

FreeSurfer cortical surfaces are generated as a tessellation (series of triangular meshes), with vertices formed by the meeting point of the triangles. Individual surfaces were resampled to template space (*fsaverage*; 163842 vertices per hemisphere), smoothed with 2819 iterations of nearest neighbour smoothing, then down-sampled by registration to a lower-order template (*fsaverage4*; 2502 vertices per hemisphere). See (Winkler et al., 2018) for further details on the nearest neighbour interpolation used by FreeSurfer when

resampling surfaces. Surface area was calculated by taking the average area of the triangles around each vertex.

Table 6.1 Demographic and imaging information for the three datasets used in this study

	QTIM	HCP	VETSA
Participants	1028 (157/194 MZ/DZ pairs, 326 unpaired twins/singleton siblings)	1105 (152/85 MZ/DZ pairs, 631 unpaired twins/singleton siblings)	474 (110/93 MZ/DZ pairs, 68 unpaired twins)
Sex	65% female	55% female	100% male
Mean \pm SD age (years)	22.39 \pm 3.32	28.80 \pm 3.70	55.80 \pm 2.60
Age range (years)	15-30	22-37	51-59
Scanner	4T Bruker Medspec	3T Custom Siemens Skyra	1.5T Siemens
N-acquisitions	1 x T1-weighted	2 x T1-weighted, 2 x T2-weighted	2 x T1-weighted
Voxel-size (mm)	0.9375 x 0.9375 x 0.9 mm	0.7 mm isotropic	1.3 x 1.0 x 1.3 mm
Reference	(Strike et al., 2018)	Glasser et al. (2016)	Chen et al. (2012)

6.2.3 Statistical Analysis

Genetic correlations of vertex-wise surface area were estimated using maximum-likelihood structural equation modelling using the *OpenMx 2.7.11* package (Boker et al., 2011; Neale et al., 2016) in *R 3.2.2* (R Core Team, 2015). Bivariate analyses were used to estimate genetic correlations for all possible pairs of vertex-wise surface area measures (4613 in total; medial wall vertices were excluded). These 10,637,578 pairwise AE models populated a 4613 by 4613 correlation matrix. Effects of whole brain total surface area (sum of all vertices), sex, linear and non-linear age effects (modelled through normal splines with three degrees of freedom), interactions between age and sex, and MRI acquisition orientation (QTIM only) were controlled for in all bivariate analyses (regression residuals used as input for model fitting).

In the classic twin model, the variance within a phenotype is partitioned into additive genetic (A), common or shared environment (C) and unique or non-shared environment (E) sources (Neale & Cardon, 1992). Based on our previous findings of non-significant common environmental influences on cortical surface area (Strike et al., 2018), we fitted models which estimated additive genetic (A) and unique or non-shared environment (E)

sources of variance. Correlations between additive genetic factors (A) are fixed to 1 for MZ and 0.5 for DZ twins as MZ and DZ twins share 100% and (on average) 50% of their genetic material respectively, and unique environmental factors (E) are uncorrelated between twin pairs as this represents environmental influences affecting one co-twin only. Estimates of unique environment also include measurement error, as it is random and unrelated to twin similarity.

Bivariate analyses extend the univariate design to decompose the covariance between two traits, as well as the variance in each trait, into genetic and environmental sources. Models were extended to include non-twin siblings to increase statistical power (Posthuma and Boomsma 2000). From the covariance decompositions, we further estimated genetic correlations, which indicate the extent to which two phenotypes share genetic variance (e.g. a genetic correlation of 1 indicates that two traits are influenced by the same set of genes, and a genetic correlation of 0 indicates two traits are genetically unique).

6.2.4 Fuzzy Clustering

Similar to the approach of Chen et al. (2012), we used a fuzzy clustering algorithm to partition the genetic correlation matrix using the *cluster* package (Maechler, Rousseeuw, Struyf, Hubert, & Hornik, 2017) in *R* 3.3.3 (R Core Team, 2017). In fuzzy clustering, each data point is spread out over the number of specified clusters, and the degree to which a data point belongs to a cluster is denoted through the membership coefficient (which ranges from 0 to 1, and sum to 1 for a given data point). A hard clustering is achieved by assigning the data point to the cluster with the highest membership coefficient. The optimal number of clusters was determined using silhouette coefficients, which combine two cluster properties: cohesion (intra-cluster differences) and separation (inter-cluster differences). In both the QTIM and HCP datasets, silhouette coefficients plateaued after 11 to 12 clusters (Figure 6.1). A final solution of 12 clusters was selected for both QTIM and HCP datasets based on the peak of silhouette coefficients and to facilitate comparisons with results in the VETSA sample (Chen et al., 2012).

The similarity of clustering solutions with the neuroanatomical ROIs of the Desikan-Killiany atlas (Desikan et al., 2006), and also the similarity of clusters between datasets, was

illustrated using the *riverplot* package (Weiner, 2017) implemented in R 3.3.3 (R Core Team, 2017). In addition, we measured cluster similarity by calculating the Rand index, which ranges from 0 (no agreement between any vertices) to 1 (identical clustering). To account for clustering similarity due to chance, we additionally calculated the adjusted Rand index. Raw and adjusted Rand indexes were calculated using the *fossil* package (Vavrek, 2011) in R 3.3.3 (R Core Team, 2017).

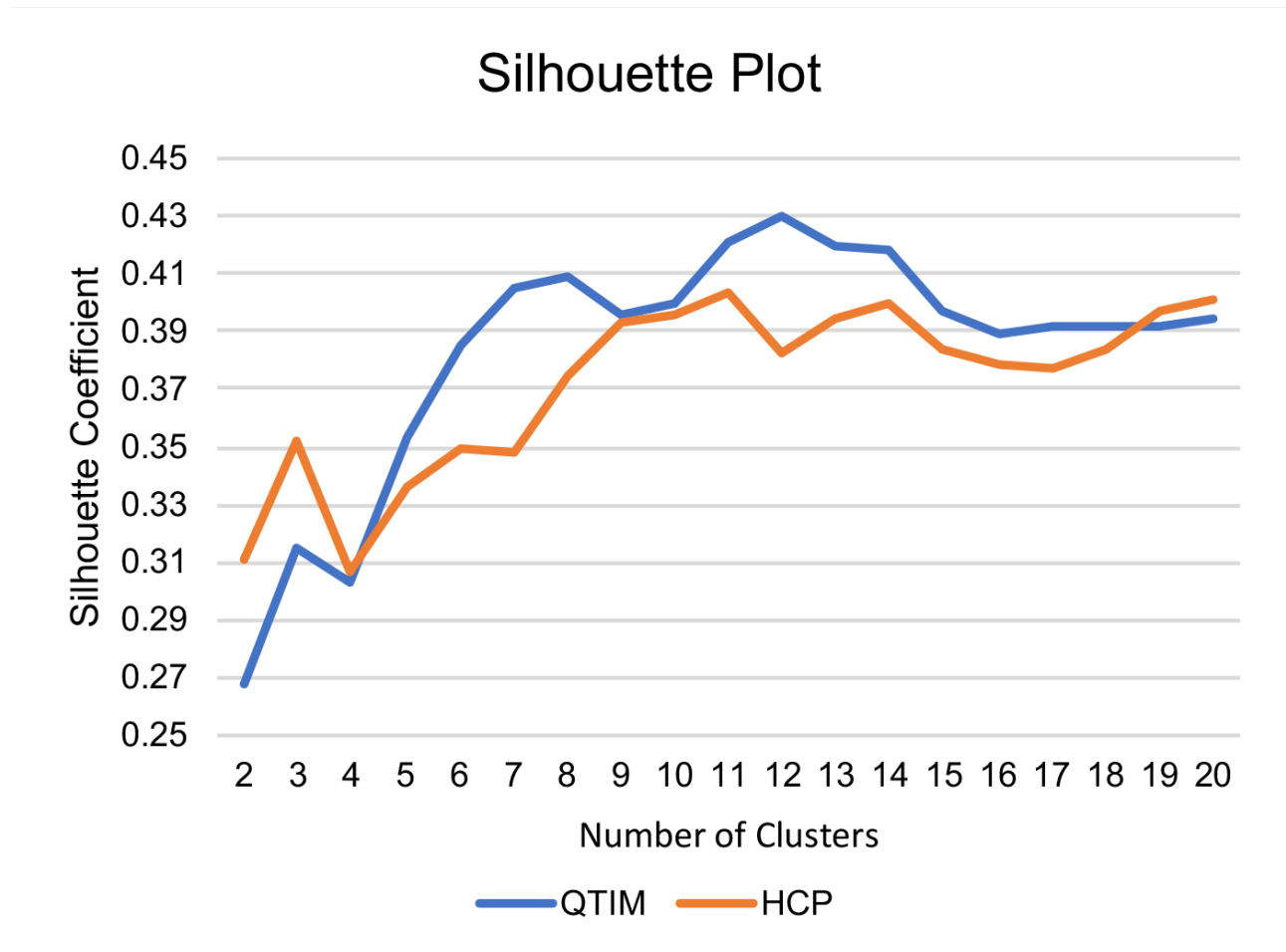


Figure 6.1 Plot of silhouette coefficients for clustering solutions in QTIM and HCP datasets.

6.3 Results

6.3.1 Genetic Parcellations for the QTIM and HCP Datasets

Figure 6.2 displays the genetic parcellations for the QTIM (a) and HCP (b) datasets. Cluster size ranged from 280 (cluster 2) to 587 vertices (cluster 12) for QTIM, and 290 (cluster 4) to 507 (cluster 7) vertices for HCP. Clusters were symmetrical between the left and right hemispheres, though some subtle differences were present (e.g. QTIM cluster 9 – 64 more vertices assigned to the left hemisphere than the right hemisphere). Clusters were generally nested within lobar divisions of the cortex. In Figure 6.3 we show that several clusters had a strong similarity with anatomical ROIs from the Desikan-Killiany atlas (Figure 6.3a/b). For example, there was substantial overlap between cluster 10 and the superior parietal (SUPPR) ROI in both the QTIM and HCP datasets. Some Desikan-Killiany ROIs were completely subsumed by genetic divisions (e.g. pericalcarine (PERIC) and QTIM cluster 12), while other ROIs were split across multiple genetic divisions (e.g. superior frontal gyrus (SUPFR) and QTIM clusters 1,2,3).

6.3.2 Pairwise Cluster Comparisons

Cluster similarity was moderate to high between the QTIM and HCP datasets (Figure 6.4a), except for clusters 4, 5 and 11, where less than 32% of vertices in these clusters corresponded across QTIM and HCP. Even so, this low correspondence was generally due to the assignment of vertices to neighbouring clusters. For example, the lower similarity for cluster 11 is because HCP cluster 11 overlaps with QTIM cluster 10, and QTIM cluster 11 overlaps with HCP cluster 12 (Figure 6.4a, Figure 6.2a/b). A similar pattern of corresponding genetic clusters (i.e. moderate to high similarity between clusters, assignment of vertices to neighbouring clusters) was found between QTIM and VETSA (Figure 6.4b), and between HCP and VETSA datasets (Figure 6.4c). There were no instances in which a cluster in one dataset was associated equally with multiple clusters in another dataset. Cluster similarity between the QTIM and VETSA dataset (Rand index 0.94, adjusted Rand index 0.61) was greater than between the QTIM and HCP dataset or HCP and VETSA dataset (Rand index 0.92, adjusted Rand index 0.52 for both comparisons).

6.3.3 Similarity Across all Three Datasets

Vertices assigned to the same cluster across all three datasets are displayed in Figure 6.2d (VETSA cluster solution used as the reference for percentage overlap). Cluster similarity ranged from 1% (cluster 11) up to 98% (cluster 8). Similarity was greatest in temporal (clusters 7,8), parietal (clusters 9,10) and pre-frontal (cluster 2) cortical regions (similarity > 60%). Clusters 5 and 11 showed the lowest similarity across datasets (similarity < 10%). For cluster 11, the HCP dataset was dissimilar to the delineations found for QTIM and VETSA, while for cluster 5, delineations were different across all three datasets. Differences in delineation for HCP compared with both QTIM and VETSA can be seen in the riverplots in Figure 6.4a and Figure 6.4c.

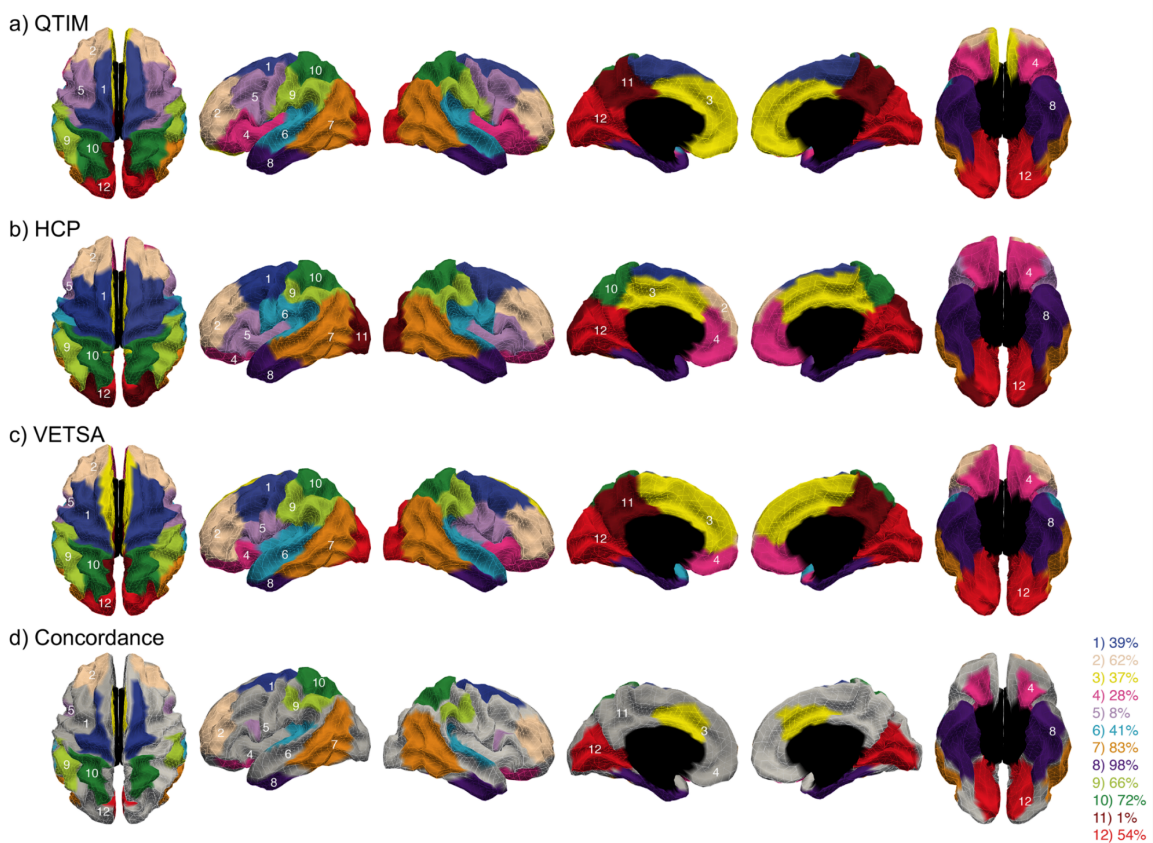


Figure 6.2 12-cluster, genetic parcellations across three datasets

12-cluster, genetic parcellations for the a) QTIM, b) HCP, and c) VETSA datasets (the VETSA parcellation was provided by Chen et al. (2012)). The concordance image (d) shows the vertices assigned to the same cluster across all three datasets. The percentage of vertices in the VETSA cluster which were assigned to the corresponding cluster in both the QTIM and HCP datasets are presented next to the concordance image. Concordance was highest for clusters 2,7,8,9,10 (> 60% of vertices in these clusters were assigned to the same cluster across the three datasets – VETSA used as the reference solution for percentage overlap).

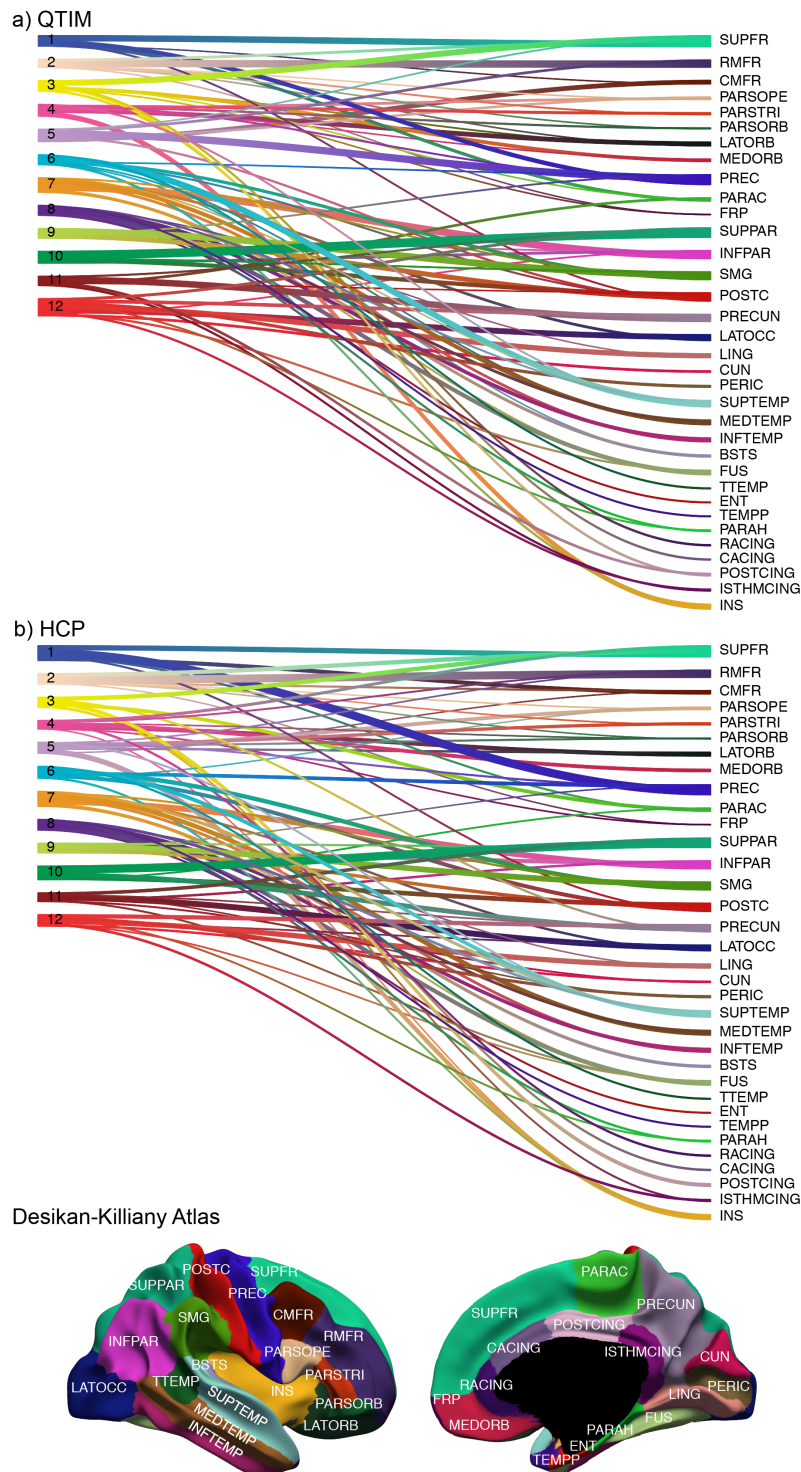


Figure 6.3 Similarity of neuroanatomical and genetic parcellations in the QTIM and HCP datasets

Similarity of vertex-membership between genetic and Desikan-Killiany parcellations for the QTIM (a) and HCP (b) datasets. Lines represent the correspondence of vertices between the genetic and neuroanatomical parcellations, with the width of the lines representing the number of vertices. For example, in the QTIM dataset (a) the thick line from cluster 10 to the Desikan-Killiany ROI superior parietal cortex (SUPPR) indicates a high similarity between the genetic and neuroanatomical region. Line colour corresponds to parcellation colour, shown in Figure 6.2 for genetic ROIs, and at the bottom of Figure 6.3 for Desikan-Killiany ROIs. Abbreviations for cortical regions listed in Appendix 2.

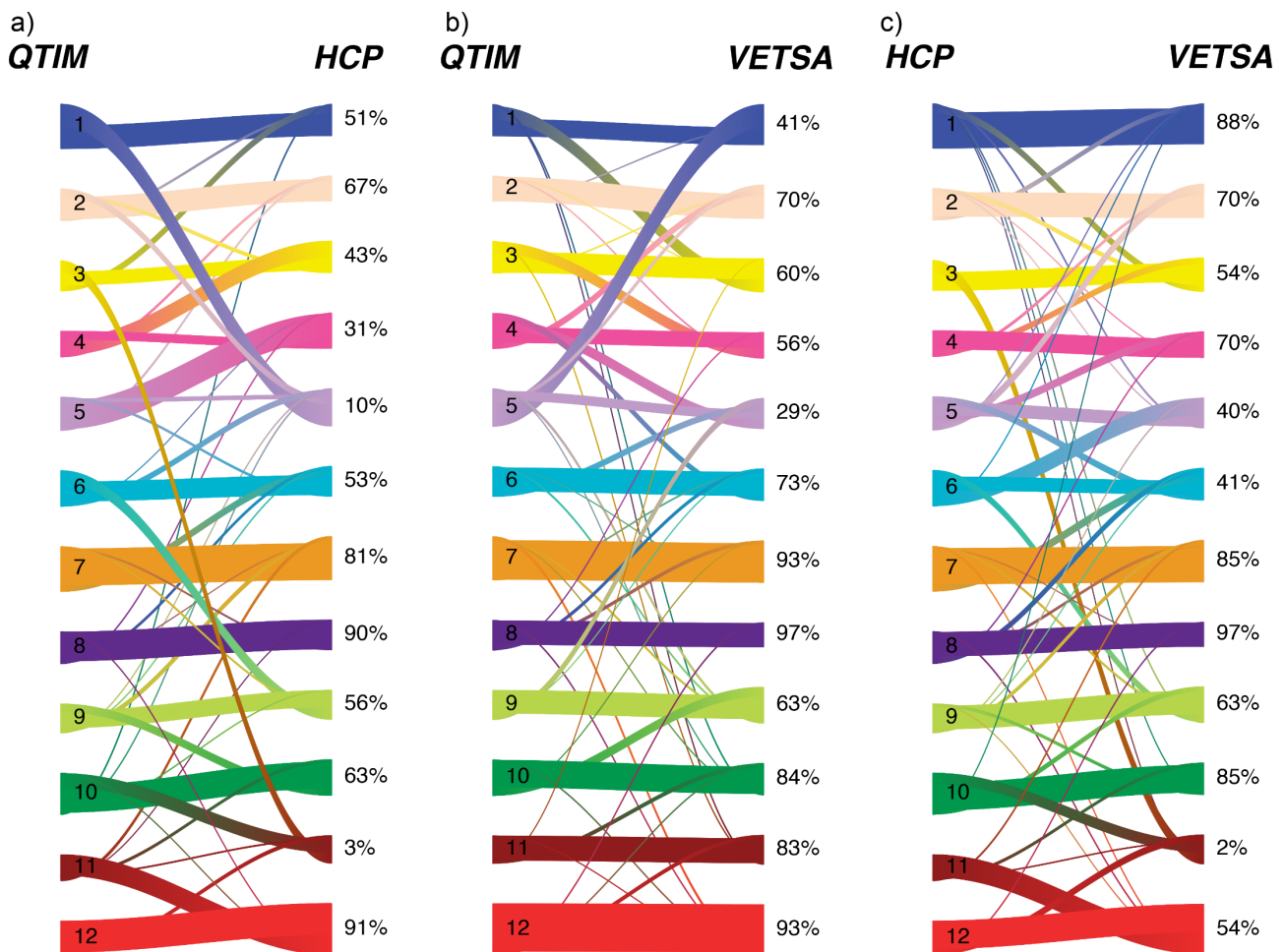


Figure 6.4 Similarity of vertex-membership across datasets

Similarity of vertex-membership for genetic parcellations between a) HCP and QTIM, b) QTIM and VETSA, and c) HCP and VETSA datasets. Percentages denote the proportion of vertices in the second dataset which were assigned to the same cluster in the first dataset. For example, 51% of vertices assigned to cluster 1 in the HCP dataset were assigned to cluster 1 in the QTIM dataset.

6.4 Discussion

We investigated the replicability of a data-driven and hypothesis free, genetically identified parcellation of the cerebral cortex. We found a similar number of clusters in the QTIM and HCP datasets as compared to a previous study of middle-aged males (VETSA).

Genetically identified divisions were predominantly bilaterally symmetrical, and several clusters corresponded to existing neuroanatomical regions. There was a largely consistent pattern of genetic parcellations across three large, twin datasets, indicating that genetic parcellations of cortical surface area are robust across sample and methodology. This suggests that delineating the cortical surface based on shared genetic influence is a valid

method of cortical parcellation, and one that has the potential to further our understanding of how genes shape the organisation and development of the cerebral cortex.

There were several similarities in the cluster solutions across the three datasets. Firstly, the study showed 11-12 to be the optimal number of clusters in the QTIM and HCP datasets, like that found previously in the VETSA dataset (Chen et al., 2012). The selection of number of clusters was primarily driven by the silhouette coefficient metric (an index of cluster validity and cohesion), which showed that 11-12 was the optimal number of clusters in the data. By specifying 12 clusters for both QTIM and HCP, this facilitated a direction comparison to the original VETSA research (Chen et al., 2012). A twelve-cluster solution is substantially less than other cortical atlases (e.g. 34 ROIs - Desikan-Killiany; 210 ROIs - Brainnetome); however, it is imperative to consider that the genetic parcellations within the present study represent the primary structure of genetic patterning. Cortical surfaces were down-sampled and spatially smoothed, which improves the reliability of genetic correlations and decreases computational time, but also precludes us from examining genetic effects at a fine-grained detail. Recently, Cui et al. (2016) used a similar methodology to the present study, but with less down-sampling, to genetically parcellate specific cortical regions into finer subdivisions. Examining genetic parcellations at a higher resolution may provide further insights into cortical regionalization and is an exciting future research direction.

Secondly, we found that predominantly, the clusters were bilaterally symmetrical across all three datasets. This symmetry was found when clustering was applied to genetic correlations considering both hemispheres simultaneously. Interestingly, an earlier iteration of the genetic parcellations in the QTIM and HCP datasets, in which clustering was applied to genetic correlations separately in the left and right hemispheres (Couvry-Duchesne et al., 2018), found a greater level of asymmetry between hemispheres. Genetic correlations between corresponding hemisphere regions are typically stronger than genetic correlations within hemispheres (Strike et al., 2018), and left/right regions are generally merged before neighbouring regions in hierarchical cluster analyses (Docherty et al., 2015; Schmitt et al., 2008). Hence, without these strong left/right associations to drive groupings, it is possible that cluster solutions will be more asymmetrical when derived separately if different patterns of covariance exist within each hemisphere.

Thirdly, we showed that there was a consistent pattern of genetic parcellations across datasets. This is consistent with the results of Cui et al. (2016), who used a similar methodology to genetically parcellate several specific cortical regions, and reproduced these parcellations in an independent dataset. It is reasonable to expect that cluster similarity will worsen with the more datasets considered, because of sample and methodological differences. Indeed, cluster similarity across all three datasets was typically less than between any two datasets. Encouragingly, we show that poor cluster correspondence was largely due to the assignment of vertices to neighbouring clusters, not wholly different clusters. This is important, as it suggests that similarities in genetic patterning are present, and further methodological refinement may result in cortical boundaries that are highly replicable across multiple datasets.

Similarities in genetic parcellations between the QTIM/HCP and VETSA datasets are especially interesting given the substantially older mean age of the VETSA dataset (56 years, compared to 22 and 29 years for QTIM and HCP respectively). Reductions in cortical surface area associated with ageing are well documented (Hogstrom, Westlye, Walhovd, & Fjell, 2013; Lemaitre et al., 2012; Storsve et al., 2014), and the results of the present study suggest that patterns of genetic covariance are stable from young-adulthood to middle-age. However, this inference is drawn from cross-sectional data, and imaging genetics studies with a longitudinal design are required to accurately estimate the stability of these genetic effects.

As the present study took no steps towards data harmonization prior to analyses, comparisons between cluster solutions can be considered as worst-case; they show the similarity between datasets with no additional input. It is likely that, at least to some degree, differences in imaging methodology contributed to dissimilarities between cluster solutions. The three datasets examined here varied in terms of field strength, voxel size and acquisition parameters. Differences in these factors are known to affect structural MRI measurements within the brain (Jovicich et al., 2009; Morey et al., 2010), and could result in differences in patterns of genetic covariance. The number of clusters specified could also impact similarity between datasets. For example, silhouette coefficients showed that the optimal solution for the HCP dataset was 11 clusters (12 was used as it was the most consistent number of clusters across datasets). Though we did not examine cluster similarity between 11 cluster solutions (or between a 11 cluster HCP solution and a 12

cluster QTIM/VETSA solution), it is possible that altering the number of clusters specified could improve the similarity of clustering solutions between datasets. It is also possible that differences in measurement error (which impacts the estimation of genetic correlations) could lead to different cluster solutions between datasets. However, as test-retest reliability correlations are high for surface area measures in both the QTIM and HCP datasets (Strike et al., 2018), measurement error is unlikely to strongly influence the results of the present study.

The results of the present study suggest that a genetically identified parcellation of the cerebral cortex would be a valuable addition to the field of neuroimaging genetics/genomics, and there are likely many advantages to developing such a parcellation. Primarily, a cortical atlas delineated on genetic variance may provide phenotypes that are closer to the level of genetic influence than atlases derived from phenotypic information. These genetic ROIs may improve power for studies seeking to identify behaviours and/or genetic variants associated with cortical surface area. To this end, clusters which showed a high similarity across all three datasets would be excellent phenotypes. Further, genetic parcellation reduces the burden of multiple comparison correction by reducing the dimensionality of the cortical surface (a standard FreeSurfer cortical surface has ~300,000 data points) into 12 clusters of shared genetic influence. Delineating genetic clusters in a larger dataset (possibly through a mega-analysis approach) would be an interesting next step in this area.

6.5 Conclusion

In conclusion, this study provides evidence of a consistent pattern of genetic parcellations of the cortex, which is robust across different samples and methodologies. This suggests that delineating the cortical surface based on shared genetic influence is a valid method of cortical parcellation, and one that has the potential to further our understanding of how genes shape the organisation and development of the cerebral cortex. The present study is an important step in changing our perspective on brain mapping from phenotypically based to genetically based methods.

7

Genetic and Environmental Covariation Between Cortical Brain Structure (Surface Area, Thickness) and Reading Ability

This chapter is based on:

Strike, L. T., Hansell, N. K., McMahon, K. L., Luciano, M., Bates, T. C., Martin, N. G., . . . de Zubicaray, G. I. (2017). Genetic and environmental covariation between cortical brain structure (surface area, thickness) and reading ability. *Manuscript in preparation.*

7 Genetic and Environmental Covariation Between Cortical Brain Structure (Surface Area, Thickness) and Reading Ability

Lachlan T. Strike¹, Narelle K. Hansell¹, Katie L. McMahon², Michelle Luciano³, Timothy C. Bates³, Nicholas G. Martin⁴, Paul M. Thompson⁵, Margaret J. Wright^{1,2}, Greig I. de Zubicaray⁶

¹Queensland Brain Institute, University of Queensland, Brisbane QLD 4072, Australia.

²Centre for Advanced Imaging, University of Queensland, Brisbane, Australia. ³Centre for Cognitive Aging and Cognitive Epidemiology, Department of Psychology, University of Edinburgh, Edinburgh, UK. ⁴Genetic Epidemiology, QIMR Berghofer Medical Research Institute, Brisbane, Australia. ⁵Imaging Genetics Center, Keck School of Medicine, University of Southern California, Marina del Rey, CA, USA. ⁶Institute of Health and Biomedical Innovation and Faculty of Health, Queensland University of Technology, Brisbane, Australia.

Abstract

Language ability, cortical surface area and thickness are all strongly influenced by genetic factors. We investigated genetic and environmental covariation between reading ability and cortical structure in regions previously implicated in language function in 992 twins and singletons from the Human Connectome Project (HCP; mean \pm SD age at reading test and scanning = 28.81 ± 3.71 years). A replication analysis was performed using similar data from an independent sample from the Queensland Twin IMaging study (QTIM; N = 676; mean \pm SD age at reading test = 17.08 years ± 3.05 years; mean \pm SD age at scanning 22.56 ± 3.21 years). In the HCP dataset, reading ability was significantly associated with the surface area, but not the thickness, of several cortical regions in the reading network. These associations were due predominantly to genetic effects shared between brain structure and reading ability. However, when covaried for whole brain total surface area, these associations were no longer significant, suggesting that regional associations are mediated through a global genetic factor shared with whole brain total surface area. These findings were not replicated in the QTIM dataset, perhaps due to the

relatively longer delay between reading assessments and image acquisition in this cohort. The small correlations found suggest larger studies are required to further investigate how structural variation relates to written language ability.

7.1 Introduction

Functional neuroimaging studies have consistently identified a core network of perisylvian brain regions involved in comprehending and producing language (see Friederici (2011); C. J. Price (2012) for overviews). Even so, we do not yet know how structural variation in these regions relates to reading ability. Nor do we know whether such relationships develop because of genetic or environmental influences, or both. Elucidating these associations will guide studies investigating links between brain morphology and genetic variants associated with reading and language ability (Gialluisi, Guadalupe, Francks, & Fisher, 2017; Udden, Snijders, Fisher, & Hagoort, 2017).

Given its importance to cognition, studies of the underlying anatomy and physiology of linguistic ability have typically focused on the cortex. Most work has focussed on more severe developmental reading disabilities (e.g., dyslexia; for a meta-analysis and review, see Linkersdorfer, Lonnemann, Lindberg, Hasselhorn, and Fiebach (2012)); fewer studies examine variation associated with normal skill development. In addition, most of the studies investigating links between brain structure and reading ability (for review, see (Linkersdorfer et al., 2012; Richardson & Price, 2009; Richlan, Kronbichler, & Wimmer, 2013)) have used voxel-based morphometry to examine differences in grey matter volume or density. As grey matter volume is a product of the surface area and thickness of the cortex; variation in grey matter volume can result from changes in either of these measures, or both. Further, cortical surface area and thickness have been shown to be genetically independent (Panizzon et al., 2009; Strike et al., 2018; Winkler et al., 2010). As such, investigating each of these structural measures separately, rather than merging them into a volume index may make it easier to detect specific phenotypic and genetic brain correlates of reading ability.

So far, few studies have related structural measures of the cortex to reading ability. In healthy adults aged 19 to 66 years, Blackmon et al. (2010) report both positive and negative correlations between a single measure of irregular word reading and cortical

thickness of key language regions bilaterally while controlling for age. Greater thickness of the superior temporal and angular gyri was associated with higher scores, while the opposite relationship was observed for the fusiform, inferior frontal and supramarginal gyri. Goldman and Manis (2013) investigated regions within the left hemisphere reading network, in a sample of university students. Cortical thickness of the angular gyrus and pars triangularis of the inferior frontal gyrus was correlated with several measures of regular word reading skill and print exposure (a measure of reading experience). Zhang et al. (2013) also reported positive correlations between regular English and Chinese word and pseudoword reading and left fusiform gyrus thickness in university students. In a sample of children aged 5 to 11 years, Lu et al. (2007) reported greater cortical thickness in the left inferior frontal gyrus to be associated with improved phonological processing.

Twin and family studies have shown variance in reading ability and disability to be moderately to largely influenced by genetic factors (Astrom, Wadsworth, & DeFries, 2007; Bates et al., 2004), and further, genes linked to cortical brain development have been associated with reading and language traits (Bates et al., 2010; Gialluisi et al., 2014; Lind et al., 2010; Luciano et al., 2007). As substantial genetic influence has been identified for structural imaging measures linked to language (Kremen et al., 2010; Lenroot et al., 2009; McKay et al., 2014), it is possible that these measures share a partially overlapping genetic origin. Yet, only one study has examined shared genetic influence between brain structure and reading. In a twin sample of children with and without a history of reading problems (Betjemann et al., 2010), the authors found a low phenotypic correlation between a composite score of reading ability and total brain volume ($r_{ph} = .22$), which was due to genetic influences shared between the two. Furthermore, the authors found suggestive evidence for a genetic factor influencing total brain volume and reading ability, independent of the other cognitive measures examined (performance IQ, verbal IQ, processing speed). Dyslexia studies have suggested that as surface area represents cortical folding patterns determined prenatally, genetic influences may be largely responsible for surface area abnormalities in individuals with reading disability (Black et al., 2012; Frye et al., 2010; Hosseini et al., 2013). However, genetically informative samples have not yet been used to relate cortical surface area and thickness to reading ability in the normal range.

Here we use the Human Connectome Project (HCP) dataset (one of the largest samples including reading and brain phenotypes, $N = 992$) to test whether the genetic factors influencing structural variation in cortical language regions overlap with those influencing measures of reading. We assessed two measures of the cortex (surface area and thickness) and one reading measure. Genetic studies of reading skill often include IQ as a covariate to increase sensitivity of reading ability (Bates et al., 2010; Luciano et al., 2013; Luciano et al., 2007); here, we do likewise. However, as the association between reading ability and IQ may differ between typical and dyslexic readers (Ferrer, Shaywitz, Holahan, Marchione, & Shaywitz, 2010), we performed a secondary analysis without correction for IQ. We selected cortical regions identified as part of the language network in previous studies (see Goldman and Manis (2013) for an overview), examining both left and right hemispheres. We expected to find significant correlations between surface area, cortical thickness, and written language ability, consistent with prior findings. Further, we expected that the genetic factors that influence reading and spelling ability would overlap with the genetic factors influencing cortical thickness and surface area of language network regions. For generalizability, we undertake the same analyses using an independent sample ($N = 676$) from the QTIM study.

7.2 Materials and Methods

7.2.1 Participants

Data from the Human Connectome Project (HCP; S1200 release) (Glasser et al., 2016; Van Essen et al., 2012) was used. The S1200 release contains imaging data for 1113 individuals from families; here, we included only right-handed participants (laterality score > 0). The final sample of 992 adults (55% female, mean age 28.81 ± 3.71 years, age range 22 to 36 years) consisted of 129 MZ pairs (82 female, 47 male), 67 DZ pairs (40 female, 27 male), 51 unpaired twins, 189 singleton siblings of twins (0 – 2 members per family), and 360 members of entirely singleton families (1 – 4 per family). MZ and DZ twin zygosity was determined through genotyping, if available (179 of 196 pairs), otherwise by self-report (17 of 196 pairs). A subset of twins ($n = 45$ individuals) completed the scan protocol and behavioural battery a second time (mean duration between first and second

visit was 139.30 ± 68.99 days). Details relating to participant selection and MRI acquisition have been reported (Van Essen et al., 2012).

7.2.2 Reading Measure

Reading ability was assessed through the NIH Toolbox Oral Reading Recognition Test (TORRT), administered as part of the NIH Toolbox Cognition Battery (NIHTB-CB) (Weintraub et al., 2013). Broadly, this test measures participants' ability to pronounce single printed words, and/or ability to recognize letters. Letters and words are presented one at a time on a computer screen, and participants are instructed to read them aloud. Unadjusted, standardised (mean 100, standard deviation 15) scores were used. To control for general cognitive ability, a composite total intelligence score was derived from the NIHTB-CB with TORRT scores excluded (i.e. the average of the unadjusted standardised scores for Picture Vocabulary, Flanker, Dimensional Change Card Sort, Picture Sequence Memory, List Sorting, and Pattern Comparison tests). Past-year personal income was used as an indicator of socio-economic status (Bucholz et al., 1994). The test-retest reliability of the TORRT was estimated by calculating the Pearson correlation coefficient between TORRT scores from time one and time two visits.

7.2.3 Cortical Surface Area and Thickness Measures

High resolution T1-weighted and T2-weighted images (0.7mm isotropic) were collected on a customised 3 T Siemens Skyra (details pertaining to acquisition have been previously discussed in detail Glasser et al. (2013); Van Essen et al. (2012)). Pre-processed FreeSurfer cortical surface area and thickness measures (Glasser et al., 2013) were used. Regions of interest (ROIs) examined here were based on the reading network adopted by Goldman and Manis (2012) (see Figure 7.1), with a measure of total surface area and mean cortical thickness produced for each ROI. Measures for whole brain, global variables (total surface area, mean cortical thickness) were also extracted. Covariate effects and test-retest reliability are discussed elsewhere (Strike et al., 2018).

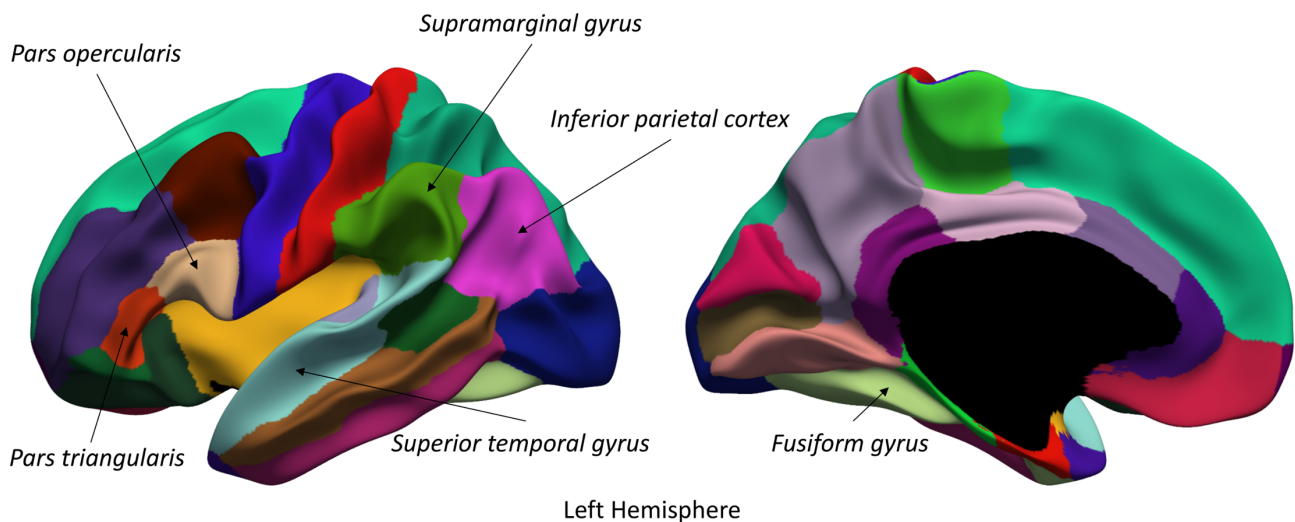


Figure 7.1 Regions of interest involved in the written language network investigated in the present study.

Regions of interest were based on the reading network adopted by Goldman and Manis (2012).

7.2.4 Heritability of Reading Ability

Genetic and environmental influences on reading ability were examined through twin analyses using the maximum-likelihood structural equation modelling package *OpenMx* 2.7.12 (Neale et al., 2016) in *R* 3.3.3 (R Core Team, 2017). MZ and DZ/twin-sibling correlations were estimated for reading ability through saturated models in which means and variances were equated within MZ and DZ/twin-sibling pairs. Next, the heritability of reading ability was estimated in a univariate ACE model. Briefly, the classic twin model partitions the variance within a phenotype into additive genetic (A), common or shared environment (C) and unique or non-shared environment (E) sources (Neale & Cardon, 1992) (Appendix 4). Correlations between additive genetic factors (A) are fixed to 1 for MZ and 0.5 for DZ twins as MZ and DZ twins share 100% and (on average) 50% of their genetic material respectively. For common environment factors (C), correlations are fixed at 1 for both MZ and DZ twins (the model assumes MZ and DZ twins raised together experience similar environments), and the unique environment factors (E) are uncorrelated between twin pairs as this represents environmental influence affecting one twin only. Estimates of unique environment also include measurement error, as it is random and unrelated to twin similarity. Here, the classic twin model was extended to include non-twin siblings (maximum of two per family) in order to increase statistical power (Posthuma & Boomsma, 2000). The saturated and univariate model included a simultaneous means

regression to adjust for effects of sex, linear and non-linear age effects (modelled through normal splines with three degrees of freedom), interactions between age and sex, and past-year personal income. To determine the most parsimonious model, nested models containing AE, CE, or E sources of variance were compared to the ACE decomposition. We assessed the fit of the constrained models by examining the -2 log likelihood difference between the ACE model and the reduced model (AE, CE or E). The difference in the maximum likelihood (assessed through the -2 log likelihood difference) is distributed as a chi-squared statistic for a given number of degrees of freedom (equal to the difference in the number of free parameters estimated), which denotes whether the parameter is significant. If a reduced model is significant, this indicates that the parameter removed from the model accounted for a significant proportion of the phenotypic variance. Maximum-likelihood 95% confidence-intervals were estimated for all model parameters. The significance of covariate effects was tested by fitting reduced ACE models in which the covariate of interest was dropped from the model (i.e. the regression coefficient was set to zero), but all other covariates remained, and comparing the model fit with the full (i.e. all covariates included) ACE model.

7.2.5 Associations Between Brain Structure and Reading Ability

Phenotypic correlations between cortical structure and reading ability were estimated by extending the univariate design to decompose the variance in a trait, and the covariance between two traits, into genetic and unique environmental sources (Appendix 4). As effects of common environment (C) were not significant for reading ability in the univariate model, or a previous examination of cortical surface area and thickness in both the HCP and QTIM datasets (Strike et al., 2018), they were not assessed in bivariate analyses. The significance of the phenotypic correlation was assessed by setting both the genetic and environmental covariances between cortical structure and reading ability to zero and assessing whether this reduced model fit. To control for the multiple comparisons, we applied a Bonferroni correction by a factor of 13 (reflecting one global and 12 ROI measures) to obtain a significance threshold of 0.0038 (0.05/13) for phenotypic associations.

When a significant phenotypic correlation was found, we further estimated the genetic and unique or non-shared environmental (from this point forward referred to as environmental) correlations. Genetic (environmental) correlations indicate the extent to which two phenotypes share genetic (environmental) variance. Both genetic and unique environmental correlations underlie the phenotypic correlation. As a high genetic correlation between two traits can be observed, even if the traits themselves have low heritability, a high genetic correlation can be misleading when genes explain only a small portion of the phenotypic variance. Hence, we examined shared genetic influence between cortical structure and reading ability by calculating the genetic contribution to the phenotypic correlation (r_{ph-a}):

$$\sqrt{(ROI\ 1\ heritability)} \times \text{genetic correlation} \times \sqrt{(ROI\ 2\ heritability)}$$

r_{ph-a} is easily conceptualised as the phenotypic correlation (r_{ph}) between two traits based only on the shared genetic variance. We similarly calculated the environmental contribution to the phenotypic correlation (r_{ph-e}). Both r_{ph-a} and r_{ph-e} were computed using variance estimates from the bivariate model in which the genetic (environmental) correlations were estimated. Bivariate models included a simultaneous means regression to adjust for effects of sex, linear and non-linear age effects (modelled through normal splines with three degrees of freedom), interactions between age and sex, past-year personal income (reading ability only), and IQ (total intelligence composite score excluding TORRT; reading ability only).

7.2.6 Replication in an Independent Sample (QTIM)

Participants in the replication sample were drawn from the Queensland Twin IMaging (QTIM) study of brain structure and function (for example (Blokland et al., 2014; Chiang et al., 2009; de Zubicaray et al., 2008) for whom measures of reading (Bates et al., 2004; Bates et al., 2007) and general cognitive ability (Wainwright et al., 2004) were also available. The present sample (i.e., participants with brain imaging and reading measures) consisted of 676 healthy, right-handed young adults (58% female), comprising of 78 MZ pairs (51 female, 27 male), 161 DZ pairs (62 female, 32 male, 67 opposite sex), 127 unpaired twins, and 71 singleton siblings of twins (0 – 2 members per family). Mean \pm SD age at scanning was 22.56 years \pm 3.21 years (range 16.02 – 30.11 years), with reading

and cognition assessed on average, five and a half years earlier (range 12.27 – 24.83 years). Zygosity was determined from DNA using a commercial kit (AmpFISTR Profiler Plus Amplification Kit, ABI) and was later confirmed on a genome-wide single nucleotide polymorphism genotyping platform (Illumina 610K chip). The study was approved by the Human Research Ethics Committees of the QIMR Berghofer Medical Research Institute, The University of Queensland, and Uniting Health Care. Written informed consent was obtained from all participants, including a parent or guardian for those aged under 18 years. Participants received an honorarium for each study.

Imaging was conducted on a 4 T Bruker Medspec (Bruker, Germany) whole-body MRI system paired with a transverse electromagnetic (TEM) head coil. Structural T1-weighted 3D images were acquired (TR=1500ms, TE=3.35ms, TI=700ms, 230mm FOV, 0.9mm slice thickness, 256 or 240 slices depending on acquisition orientation (86% coronal (256 slices), 14% sagittal (240 slices))). Cortical thickness and surface area measurements were extracted using the FreeSurfer software package (v5.3), <http://surfer.nmr.mgh.harvard.edu/> previously reported in depth (Desikan et al., 2006; Fischl & Dale, 2000). Prior to FreeSurfer analysis, the raw T1-weighted images were corrected for intensity inhomogeneity with SPM (SPM12; Wellcome Trust Centre for Neuroimaging, London, UK; <http://www.fil.ion.ucl.ac.uk/spm>). Cortical reconstructions and ROI labelling were checked using the ENIGMA quality checking procedure (enigma.ini.usc.edu).

Measures of reading ability were collected several years prior to scanning. The Components of Reading Examination (CORE) (Bates et al., 2004; Castles & Coltheart, 1993), provides scores for regular, irregular, and non-word reading ability. CORE measures were collected through two separate studies. Test scores were calculated as the number of correct responses for the individual component subtests and were Box-Cox transformed to attain normality. A principal component factor score (CORE-PC) was derived from individual subtests, explaining 79% of the variance. Performance IQ was collected at age 16 years using the Multidimensional Aptitude Battery (Jackson, 1984). SES was assessed through the AUSEI06 (McMillan et al., 2009). QTIM measures were corrected for the same covariates as HCP measures, additionally controlling for slice acquisition direction (structural MRI measures only) and study source (CORE-PC score only). Duration between brain scanning and language testing was included as a covariate

for all bivariate analyses. All analyses completed on the HCP dataset were undertaken in the QTIM dataset.

7.3 Results

7.3.1 Demographics, Heritability, Covariate Effects, and Reliability of Reading Ability

Descriptive statistics, heritability estimates and covariate effects for reading ability in the HCP and QTIM datasets are presented in Table 7.1. Twin correlations for reading ability score for MZ and DZ pairs were 0.64 and 0.37 respectively (HCP), and 0.75 and 0.23 respectively (QTIM). Heritability estimates ('A'; 95% CI) for reading ability were significant in both samples: HCP 0.52 (0.29, 0.70), QTIM 0.72 (0.58, 0.81). Estimates of common environmental influence ('C'; 95% CI) were small for both datasets and could be dropped from models without significantly worse model fit: HCP 0.09 (0.00, 0.26); QTIM 0.00, (0.00, 0.08). Unique environmental effects ('E'; 95% CI) accounted for 0.38 (0.30, 0.49) and 0.28 (0.19, 0.40) of the total phenotypic variance in the HCP and QTIM datasets respectively. Socioeconomic status and IQ were significant covariates in both datasets. A 1 SD increase in the socio-economic status measure was associated with a 0.10 SD and 0.15 SD increase in reading ability score in the HCP and QTIM datasets respectively, while a 1 SD increase in IQ was associated with a 0.36 SD and 0.29 SD increase in reading ability score in the QTIM and HCP datasets respectively, all other variables held constant). The test-retest reliability correlation of reading ability (controlling for covariate effects) was 0.65 in the HCP dataset.

7.3.2 Associations Between Cortical Structure and Reading Ability

There was a significant phenotypic correlation between TORRT score and whole brain total surface area ($r_{ph} = 0.15$, $p = 2.35E-05$), which was due to a genetic contribution ($r_{ph-a} = 0.13$, $r_{ph-e} = 0.02$; Appendix 27). As shown in Figure 7.2, there was a significant phenotypic correlation between TORRT score and cortical surface area for six reading network ROIs (r_{ph} range 0.10 to 0.15). For three of these ROIs (superior temporal gyrus

left, fusiform gyrus left and right), the significant phenotypic association was due to genetic effects shared between reading ability and cortical surface area (Appendix 27). Phenotypic correlations between mean cortical thickness (whole brain or ROI) and reading ability were not significant (Appendix 27). Heritability estimates for individual cortical measures ranged from 0.41 to 0.70 for surface area, and from 0.54 to 0.76 for cortical thickness (Appendix 27), and heritability estimates for global measures were 0.93 (total surface area) and 0.86 (mean cortical thickness); heritability estimates taken from bivariate AE models between cortical structure and reading ability. Analyses without IQ as a covariate yielded similar findings to those controlling for IQ (results not shown).

Table 7.1 Descriptive statistics for the HCP and QTIM datasets

	HCP	QTIM
<i>N</i>	992	676
Reading Age (Mean ± SD)	28.81 ± 3.71 years	17.08 ± 3.05 years
Reading Age (Range)	22 - 36 years	12 - 25 years
MRI Age (Mean ± SD)	<i>Same as reading</i>	22.56 ± 3.21 years
MRI Age (Range)	<i>Same as reading</i>	16 - 30 years
% Female	55%	60%
Reading Ability Heritability*	0.52	0.72
<u>Reading Ability Covariates†</u>	<u>Beta (p value)</u>	<u>Beta (p value)</u>
Age	-0.03 (0.58)	0.29 (1.77E-04)
Age ²	0.17 (5.96E-04)	0.32 (5.95E-05)
Age ³	0.22 (1.33E-03)	0.15 (0.10)
Sex	0.09 (0.63)	0.37 (0.19)
Age x sex	0.04 (0.43)	0.01 (0.92)
Age ² x sex	-0.25 (0.02)	-0.13 (0.44)
Age ³ x sex	-0.19 (4.63E-03)	0.03 (0.76)
SEI	0.10 (4.90E-04)	0.15 (2.37E-04)
IQ	0.36 (2.24E-31)	0.29 (1.42E-15)
Reading Test Source‡	NA	0.48 (9.03E-06)

*Heritability estimate for reading ability from univariate ACE model. Heritability estimates from the AE model were 0.63 (HCP) and 0.72 (QTIM).

†Dummy variables were coded sex (male = 0, female = 1), reading test source (study 1 = 0, study 2 = 1); all other variables were standardised prior to analysis. The significance of covariate effects was tested by fitting ACE models in which the covariate of interest was dropped from the model (i.e. the regression coefficient was set to zero), but all other covariates remained, and assessing the significance of the covariate via likelihood ratio test.

‡Reading measures in the QTIM datasets were collected through two separate studies

7.3.3 The Influence of Global Effects

When whole brain total surface area was included as a covariate in models, associations between regional surface area and reading ability were no longer significant (results not shown), indicating that genetic covariance between TORRT score and ROI surface area

was not region-specific (i.e. it was shared with whole brain surface area). Phenotypic correlations between regional cortical thickness and TORRT score remained not significant after correction for whole brain average cortical thickness (results not shown). Analyses without IQ as a covariate yielded similar findings to those controlling for IQ (results not shown).

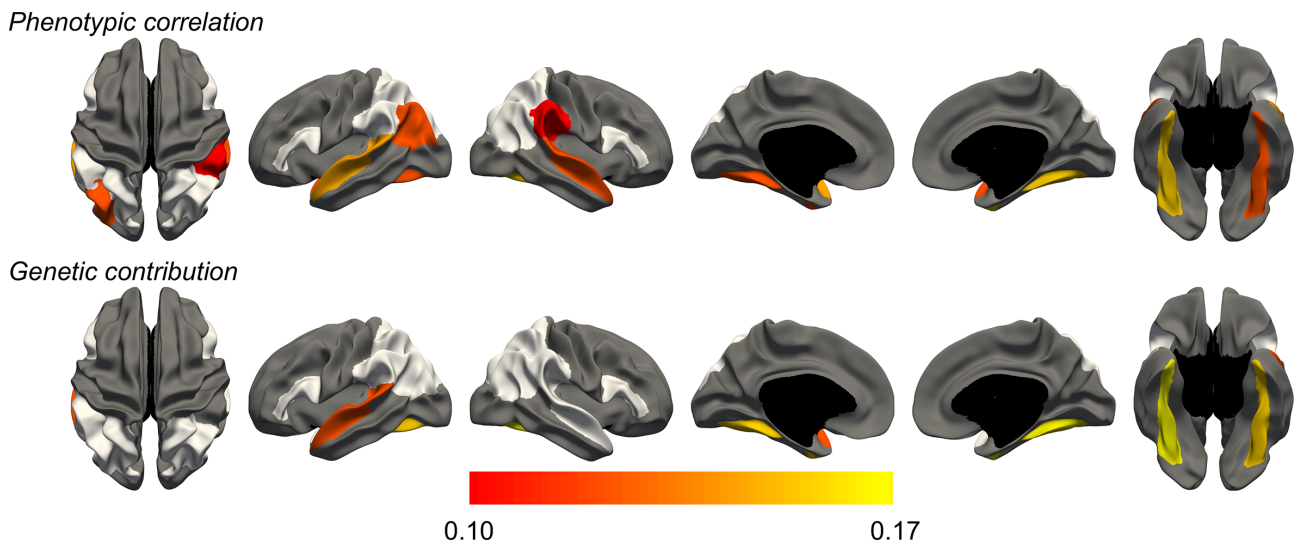


Figure 7.2 Phenotypic correlations, with genetic and environmental contributions, between surface area of reading network ROIs and TORRT score in the HCP dataset.

Cortical regions in dark grey are not part of the reading network, and regions in silver are reading network ROIs for which a non-significant phenotypic correlation was found.

7.3.4 Replication of Associations in QTIM

The phenotypic and genetic association between total surface area and reading ability was not replicated in the QTIM dataset, neither were associations between regional cortical surface area (ROIs: inferior parietal left, supramarginal gyrus right, superior temporal gyrus left and right, fusiform gyrus left and right) and reading ability (Appendix 28). Moreover, there were no significant phenotypic associations between cortical surface area or thickness and reading ability (CORE-PC score) for any reading network ROIs. In addition, all phenotypic correlations were not significant when corrected for global effects, or not corrected for IQ.

7.4 Discussion

Here we determined whether brain structure and reading ability are linked, and if so, whether this association results from shared genetic influences. This is the first study to examine genetic associations between measures of cortical structure (i.e. surface area and cortical thickness), and reading skill in non-impaired individuals. Whole brain total surface area showed a positive phenotypic association with reading ability, independent of general cognitive ability and socio-economic status. This association was underpinned by genetic factors shared between surface area and reading ability. However, this association was not replicated in an independent sample. In both datasets, no region-specific associations (i.e. independent of global effects) were found between reading ability and the surface area/cortical thickness of individual brain structures.

The estimate of heritability for reading ability in the HCP dataset (52%; ACE model) was less than the estimate for QTIM (72%; ACE model), as well as other published estimates (Betjemann et al., 2010; Davis et al., 2014)(66% and 72% respectively; both estimates from ACE models). This was likely due to the older age of the HCP sample (mean 29 years) compared to other datasets (17 years (QTIM); 11 years (Betjemann et al., 2010); 12 years (Davis et al., 2014)). The phenotypic association between reading ability and whole brain surface area in the HCP dataset ($r_{ph} = 0.21$) is consistent with the results of Betjemann et al. (2010), in which an association was reported between total brain volume and reading ability ($r_{ph} = 0.22$) in a paediatric sample of good and poor readers. Further, in both the HCP dataset and the results of Betjemann et al. (2010), the phenotypic association between brain structure and reading ability was due to genetic influence shared between the two. The failure to replicate this association in an independent sample (QTIM) could relate to the substantial duration between brain imaging and reading assessment (mean duration 5.5 years) in the QTIM sample. Further, the strong negative skew of raw reading subtests in the QTIM sample could reflect a sampling bias of good readers (i.e. variation in written language ability was not adequately measured in the sample, making it difficult to detect associations with variation in cortical structure).

Previous studies that related reading ability to cortical structure reported a thicker cortex in primarily left-hemisphere regions (Blackmon et al., 2010; Goldman & Manis, 2013; Zhang et al., 2013), and thinner cortex bilaterally to be associated with irregular word reading proficiency (Blackmon et al., 2010). Yet, in our comparatively large adult samples we failed

to observe *any* significant correlations between reading ability and cortical thickness. One possibility is that prior reports reflected, at least in part, contributions from IQ. However, in both the HCP and QTIM samples, region-specific associations between reading skill and brain structure were not significant with or without the inclusion of IQ as a covariate. More likely, the lack of consistency with past studies may relate to their substantially smaller sample sizes (Blackmon et al., 2010; Goldman & Manis, 2013; Zhang et al., 2013), $N = 60, 28, 226$ respectively). It is also possible that associations between reading ability and cortical thickness vary across developmental stages (as reported for general intelligence (Menary et al., 2013)) and/or are specific to the measures of reading skill utilised.

Brain imaging studies of dyslexia - a developmental disorder of reading – have reported cortical abnormalities in the language network bilaterally, primarily using measures of regular word and pseudoword reading, and grey matter volume (a function of cortical surface area and thickness). Meta-analyses implicated inferior frontal, occipitotemporal (fusiform gyrus) and inferior parietal (supramarginal gyrus) regions bilaterally (see Linkersdörfer, Lonnemann, Lindberg, Hasselhorn, & Fiebach, 2012; Richlan, Kronbichler, & Wimmer, 2013). Further, reduced inferior frontal and fusiform gyrus surface areas have been reported in adults with dyslexia as compared to controls (Frye et al., 2010), and Welcome, Chiarello, Thompson, and Sowell (2011) demonstrated reduced radial expansion (a measure similar to surface area) of multiple brain regions in poor compared to proficient adult readers. Surface area reductions have also been associated with maternal history of reading disability (Black et al., 2012), as have differences in structural brain networks constructed from surface area measures in individuals with familial risk for dyslexia (Hosseini et al., 2013). As most neuroimaging studies of dyslexia were conducted with children or adults who have experienced reading difficulty over a number of years, the cortical abnormalities reported could reflect either an etiological mechanism, or they could result from impoverished reading experience (Norton, Beach, & Gabrieli, 2014). This may explain why, in our sample of typical readers, no regional associations between reading ability and surface area were found.

Researchers face many issues when assessing the phenotypic and genetic relationships between brain structure and language. For example, developmental timing differs between cortical regions, with higher-order association cortices maturing after lower-order sensorimotor cortices (Gogtay et al., 2004; Stiles & Jernigan, 2010). Further, genetic

influence on cortical thickness may gradually increase throughout late childhood and adolescence; there may also be sex differences in the maturation of language centres (including Broca's and Wernicke's areas) (Schmitt et al., 2014). By contrast, genetic influence on reading and spelling is greater during middle childhood years (7 to 9 years), possibly due to formal education in primary school reducing environmental influence (Byrne et al., 2013; Kovas et al., 2013). Consequently, the age(s) at which brain structure and language measures are acquired will affect the phenotypic and genetic relationships reported, so a longitudinal approach would be ideal.

The results suggest some further steps. Firstly, as reading ability involves multiple processes, a single measure of reading ability may not adequately disentangle the underlying sub-components that contribute to variation in reading ability. Hence, future studies could use multiple measures of reading ability, each indexing different sub-processes of reading ability, when examining associations with cortical structure (He et al., 2013). Similarly, structural equation modelling could be used to decompose language ability into latent factors to enhance the detection of the neural substrates of language ability (Hoffman et al., 2017). Secondly, ROIs in the current study were based on standard anatomical delineations. These may not map directly onto functional and/or genetic divisions of the brain. A next step in this research could use ROIs based on brain functional networks, genetic networks, or structural connectivity. Such regions may show stronger associations than those based on anatomical divisions. Further, expanding analyses to include measures of white-matter integrity would allow testing the role of regional connectivity in language. In addition, although we controlled our written-language measures for domain general cognitive ability, associations found between reading ability may also represent other domain general cognitive abilities, such as working memory. It would be valuable to assess such associations through multivariate twin modelling, in which multiple cognitive abilities could be entered. Then the unique genetic covariance associated with brain structure and reading / spelling ability (and not general cognitive ability) could be estimated. Lastly, although our sample is one of the larger cohorts with both imaging and language measures, our ability to detect significant covariation is limited by sample size. Further, our analyses lack the power to fully explore potential common environmental influences, such as lateralised effects of family-level environment on brain structure or brain-behaviour linkages. These await larger studies.

7.5 Conclusion

We found a significant association between whole brain total surface area and performance on the NIH Toolbox Oral Reading Recognition Test, independent of general cognitive ability and socio-economic status. This phenotypic association was due to genetic influences shared between the two. However, we were unable to replicate this finding in an independent sample using similar but not identical reading measures, possibly due to the substantial duration between language testing and brain imaging in that sample. In both datasets, region specific associations between cortical structure (i.e. independent of global effects) and reading ability were weak and not significant. We conclude that previously reported associations between cortical structure and reading ability may reflect, at least in part, confounding factors such as general cognitive ability and/or socio-economic status, and suggest that larger studies are required to further investigate associations between variation in reading ability and cortical structure.

8

Discussion and Conclusion

8 Discussion and Conclusion

8.1 Overview

This thesis aimed to examine genetic and non-genetic (i.e. environmental) contributions to normal variation in the structure of the human brain. Past studies show heritability estimates for global brain phenotypes (e.g. total brain volume) are well established, but the robustness of genetic effects for cortical structures are yet to be completely demonstrated. This is likely because of differences in the datasets used (sample size, participant age, study design (twin or family), and/or imaging methodology). Further, studies had not evaluated the reliability of their imaging measures, a critical step as measurement error typically sets the upper limit for heritability. To provide a normative reference of healthy brain structure for future studies of neurological and psychiatric disorders, a reliable and robust map of genetic and environmental influences on the brain is required.

To this end, I followed two main lines of study: firstly, quantifying the strength of genetic and environmental influences on phenotypic variance in brain structure (Chapters 4-5), and secondly, examining the genetic and environmental covariance between different brain structures, as well as between brain structure and cognitive ability (Chapters 5-7). Importantly, two independent imaging datasets, consisting of participants of a comparable age, were used to investigate similarities in patterns of genetic and environmental variance across samples and imaging methodology. Further, estimates of test-retest reliability for imaging measures were considered in conjunction with estimates of genetic and environmental variance to better evaluate differences in variance components within and between datasets. The following sections summarise the main findings from the above chapters (Table 8.1), and discuss their implications within the broader context of this thesis.

Table 8.1 Aims and findings of empirical thesis chapters

Chapter	Aim/s	Findings
4. Genetic Complexity of Cortical Structure: Differences in Genetic and Environmental Factors Influencing Cortical Surface Area and Thickness	<ul style="list-style-type: none"> • Estimate heritability of cortical surface area and thickness for 68 ROIs • Test for associations across ROIs for cortical surface area and/or cortical thickness • Estimate the genetic and environmental contributions to phenotypic associations across ROIs • Conduct the same analyses within an independent sample (HCP) to check for consistent patterns and whether effects are robust • Examine the reliability of imaging measures, and the degree to which they affect estimates of heritability 	<ul style="list-style-type: none"> • A wide range of region-specific heritability estimates (up to 65% (surface area) and 55% (cortical thickness)) • Heritability largely independent of test-retest reliability • For most ROIs, residual variance (i.e. not attributed to genetics) largely due to unique environmental influence, not measurement error • Wide variety in phenotypic correlations between corresponding left/right ROIs • Sparse phenotypic correlations across surface area measures, more moderate correlations across cortical thickness measures (covaried for global effects) • Genetic covariance responsible for phenotypic associations within surface area and cortical thickness ROIs, some environmental contributions to phenotypic associations for cortical thickness, indicating region-specific genetically mediated networks are strongest for cortical thickness • Very little association between surface area and cortical thickness, replicating past studies showing surface area and thickness to be distinct characteristics of the cerebral cortex • Patterns of genetic variance similar in an independent dataset (HCP)
5. Mean-Standardised and Relative Estimates of Genetic and Environmental Influence on Brain Structure Volume	<ul style="list-style-type: none"> • Examine absolute amounts of variance components (standardised by the phenotypic mean) for ventricular, subcortical, and cortical volumes • Compare mean-standardised and relative measures of genetic variance • Use an independent sample (HCP) to examine whether findings can be replicated 	<ul style="list-style-type: none"> • A wide overall range in mean-standardised phenotypic variance (17-fold range), largest for the lateral ventricles, smallest for the hippocampus • Within structural divisions (ventricular, subcortical, cortical), ranges were more moderate, and similar across divisions (2 to 4-fold range) • No association between mean-standardised and relative genetic variance

6. A Consistent Pattern of Genetic Parcellations of Cortical Surface Area Across Three Large Twin Datasets

- Parcellate the cortical surface based on genetic covariance in cortical surface area
- Compare genetic parcellations across datasets (QTIM, HCP, VETSA)

7. Genetic and Environmental Covariation Between Cortical Brain Structure (Surface Area, Thickness) and Reading Ability

- Estimate phenotypic associations between reading ability and regional surface area/thickness of reading network ROIs
- Quantify genetic and environmental contributions to phenotypic associations
- Use an independent sample (QTIM) to examine whether findings can be replicated

- Patterns of mean-standardised genetic variance not explained by differences in measurement error or structure size
 - Results were similar in an independent sample (i.e. significantly larger mean-standardised genetic variance for the lateral ventricles compared to cortical/subcortical structures, moderate range in estimates across divisions (cortical, subcortical, ventricular)
 - Genetic covariance best explained by 11-12 clusters in QTIM and HCP datasets
 - Clusters bilaterally symmetrical, matched boundaries of structure and function
 - Consistent pattern of genetic parcellations across three large, twin datasets, indicating that genetic parcellations of cortical surface area are robust across sample and methodology
 - HCP: significant phenotypic associations between surface area of several reading network ROIs and reading ability score, due to genetic covariance
 - Associations shared with whole brain total surface area (i.e. not region specific)
 - Findings not replicated in QTIM, suggesting the effects is not robust across sample and methodology, or not reliable
-

8.2 Genetic Variance

Understanding the role of genetic influence on the brain is critical to understanding the regionalisation of the cortex (i.e. distinctions of structure/function). This thesis shows that at both the univariate and bivariate level (Chapter 4), there is significant, region-specific genetic influence on cerebral cortex variation (surface area, thickness) in the QTIM dataset. The strength of these genetic effects was not equal across ROIs, giving rise to a wide range of heritability estimates (surface area up to 65%; cortical thickness up to 55%), and regionalised, genetically mediated networks across the cortex. Importantly, these regional differences in genetic influences were largely independent of measurement error. Hence, dissimilarities in region-specific variance across the brain may reflect differences in function, maturational timing, evolution, experienced-related plasticity, and/or trophic influences (Eyler et al., 2011; Lenroot et al., 2009; Mechelli et al., 2005). Further, these findings were replicated in an independent sample of twins and singletons (HCP), indicating these region-specific effects are robust across sample and imaging methodology (discussed in more detail below).

In Chapter 5 we found no association between mean-standardised and relative measures of genetic variance for brain structure. Though this was expected based on studies of other biological and life-history traits (Hansen et al., 2011; Houle, 1992), it was important to empirically demonstrate this for human brain morphology. This lack of association is significant, as it indicates that new insights into brain development could be gained from changing the way in which the variance components of brain structure are considered. For example, investigating amounts of mean-standardised variance (genetic/environmental) in brain structure for healthy controls and patients could reflect differences in the histogenetic processes underlying brain development between these groups. While further research is required to understand the implications of differences in mean-standardised absolute variance amounts, their usefulness may lie in elucidating patterns of genetic variance in the brain not visible through heritability estimates.

Building upon the results of Chapter 4, we estimated genetic associations across the cortical surface at a finer detail (i.e. vertex-wise), using a clustering algorithm to create a genetic parcellation of the cerebral cortex (Chapter 6). Despite the presence of greater genetic covariance for cortical thickness than surface area at the ROI level (Chapter 4), we

focused on the more reliable cortical measure, surface area, to maximise our ability to detect genetic covariance. The finding of generally weak, region-specific genetic associations across the cortex for surface area (Chapter 4) appear in contrast to the findings of Chapter 6, in which 12, maximally genetically correlated divisions of the cortical surface area were identified based on vertex-wise surface area measures. How could genetic covariance in cortical surface area be best explained by a 12-cluster solution, when the results of Chapter 4 suggest that outside of the occipital lobe, there is little region-specific genetic covariance between regional surface area?

Firstly, vertex-based measures of surface area are more heritable than ROI-based measures, possibly due to the degree of spatial averaging in vertex-based approaches (Eyler et al., 2012), which could result in higher genetic covariance. Secondly, similarities in the genetic associations between cortical locations for ROI and vertex-wise measures suggest that both approaches tell a similar story, albeit in different ways. For example, in the QTIM dataset, the strong genetic covariance at the ROI level found in the occipital lobe (Chapter 4, Figure 4.3b) was reflected in the delineation of Cluster 12, which consisted largely of the four bilateral occipital ROIs (Chapter 6, Figure 6.2a and Figure 6.3a). Further, low genetic covariance was found between the superior temporal and inferior/middle temporal gyri (Chapter 4, Figure 4.3b), which is mirrored in the delineation of Cluster 6 (which includes vertices from the superior temporal ROI) and Cluster 7 (which includes vertices from the middle and inferior temporal ROIs; Chapter 6, Figure 6.2a and Figure 6.3a). Though it is difficult to compare results from ROI and vertex-wise analyses (as vertex-wise measures are not constrained to the predefined boundaries of ROI measures), the similarities between the approaches support the existence of genetically-mediated cortical networks.

8.3 Environmental Variance

While imaging genetics studies typically focus on genetic effects, it is equally important to consider non-genetic (i.e. environmental) influence on individual differences in brain structure. At the univariate level, we found significant and substantial environmental influence on variation for cortical surface area and thickness (Chapter 4), and cortical, subcortical, and ventricular volumes (Chapter 5). In-line with previous twin imaging

studies, these environmental effects were predominantly attributed to unique or non-shared environment ('E') rather than common or shared environment factors ('C') (Blokland et al., 2012; Kremen et al., 2010; Schmitt et al., 2008). However, it is important to consider that the sample size of twin imaging studies is typically underpowered to detect common environment effects; using theoretical predictions, Visscher, Gordon, and Neale (2008) estimate sample sizes into the thousands to detect small to moderate effects of common environment. Hence, the non-significant estimates of variance attributed to common environment sources by studies (the present thesis included) is likely due to a lack of power rather than the absence of 'C' effects. Increasing the number of twin pairs improves the ability to detect 'C' effects, but this is generally not possible for imaging studies due to the prohibitive cost of MRI acquisition. In the absence of large sample sizes and/or very strong 'C' effects, it may be more pertinent to use models specifying only additive genetic and unique-environment variance sources (AE), and possibly use 'non-traditional' study designs to detect common environment effects (see Burt (2014) for a further discussion of 'non-traditional' designs).

We found that inter-regional associations across the cortex were predominantly due to genetic, not environmental covariation (Chapter 4). This is interesting given that univariate analyses showed that a substantial proportion of variance in brain structure was attributed to environmental factors. This would suggest that the sparse environmental associations found were not due to a lack of environmental variance (which would reduce our ability to detect environmental associations). The lack of environmental associations may indicate that a large proportion of variance attributed to unique environmental sources represents stochastic biological effects or experiences that do not relate to structural covariance networks in the cortex. Additionally, the rarity of non-genetic covariance might indicate that environmentally mediated structural networks are limited, or not detected at the macroscale.

While the genome provides a limited search space for identifying the causes of genetic variation, the causes of environmental variation are inherently more difficult to elucidate. Individual differences due to environmental factors could relate to any number of factors (e.g. drug and alcohol use, childhood adverse events), as well as stochastic biological effects that cannot be predicted. However, elucidating the causes of environmental variance in the brain can be greatly assisted by collecting data on high quality,

environmental variables. In this regard, the Human Connectome Project (Van Essen et al., 2013) is an excellent example.

8.4 Robustness of Findings Across Datasets

As meta/mega-analysis approaches become more common in imaging genetics (e.g. ENIGMA (Thompson et al., 2014), CHARGE (Psaty et al., 2009)), it is important to consider the replicability of findings from different samples, field strengths, and acquisition parameters. Encouragingly, in this thesis we show that patterns of genetic variance, at both the univariate (Chapters 4, 5) and bivariate (Chapters 4, 6, 7) level were generally robust across different samples and methodologies. Importantly in Chapter 6, we found that patterns of genetic parcellations of cortical surface area were similar across three independent twin datasets. Studies like Chapter 6 are critical to our understanding of the consistency of genetic effects across different samples with different MRI acquisition parameters.

That is not to say that results were identical between the two datasets. Most notably, the association between cortical structure and reading ability in the HCP dataset was not replicated in the QTIM dataset (Chapter 7). This finding could indicate that associations between cortical structure and reading ability are not robust across sample and methodology. Conversely, if samples and measures are equivalent between datasets, then shared genetic effects between brain structure and written language ability may not be reliable.

It is important to learn the lessons of imaging candidate gene studies, where many underpowered studies reported associations between candidate genes and brain measures that were never replicated. As imaging datasets like the HCP are publicly available, replicability should be a focus for imaging genetics studies.

8.5 Test-Retest Reliability

One of the advantages of software suites such as FreeSurfer is that it provides reproducible measures of brain structure (Han et al., 2006; Jovicich et al., 2009; Madan &

Kensinger, 2017; Morey et al., 2010), which tend to show high consistency with expert, manual delineations (Desikan et al., 2006; Morey et al., 2009; Ochs et al., 2015; Perlaki et al., 2017). However, we cannot assume that all brain measures extracted from automated segmentations are highly accurate and reliable; we must consider that measurement reliability is likely region-specific. The importance of considering the test-retest reliability of imaging measures alongside estimates of (co)variance in brain morphology was stated many times throughout this thesis, and should not be undervalued. Measurement error artificially reduces the similarity between MZ twins, in turn reducing our ability to detect genetic variance. Phenotypes with high test-retest reliability provide greater confidence that heritability estimates are not limited by measurement reliability (i.e. estimates would not be larger if the phenotype was more reliably measured), and that variance attributed to residual sources represents the effect of unique environmental factors and not measurement error.

The results of this thesis suggest that indeed, estimates of variance components for region-specific cortical surface area/thickness are largely independent of measurement error (Chapter 4). This is encouraging, particularly as the imaging datasets used (QTIM, HCP) varied in terms of their imaging methodology. Morphological measures in the QTIM dataset were extracted from a single T1 weighted image, whereas the corresponding measures for the HCP dataset were extracted from multiple T1 and T2 weighted images. A comparison of the test-retest correlations from the QTIM and HCP datasets (Chapter 4) shows that test-retest correlations are higher for HCP measurements, particularly for cortical thickness. MRI measures of cortical thickness are especially sensitive to variability in tissue contrast, and it is likely that the higher quality acquisition parameters of the HCP dataset are reflected in the higher test-retest correlations for that dataset.

Future studies should focus on maximising the test-retest reliability of their imaging phenotypes to maximise their ability to detect genetic and environmental effects. This is particularly relevant for studies seeking to use novel image acquisition or analysis techniques that are not as widely used and validated as existing methodologies such as FreeSurfer morphometry statistics.

8.6 Genes, Brain, and Behaviour

In Chapter 7, we found significant associations between reading ability and the surface area of several cortical regions in the reading network. This association is influenced by a common genetic factor; however, this genetic factor is not region-specific (i.e. effects are shared with whole brain total surface area). Evidence of region-specific associates between brain structure and cognition have been difficult to elucidate, with genetic variance between individual brain structures and cognitive phenotypes typically shared with a global brain phenotype (Bohlken et al., 2014; Bohlken et al., 2016). The genetic association between brain structure and cognitive ability appears to be influenced by a complex configuration of brain development (Vuoksima et al., 2016), and is unlikely to be detected using broad measures of brain morphology. Large samples, using a multivariate, whole brain approach will likely be required to detect an association between individual differences in brain structure and cognition (Ritchie et al., 2015).

Patterns of structural covariance (Chapters 4, 6) may recapitulate functional networks in the brain, as synaptic connectivity and/or use-dependent growth between brain regions may lead to brain structures covarying in their morphology (Alexander-Bloch, Giedd, et al., 2013). However, further studies are required to quantify the relationship between structural covariance and brain function to advance the use of structural covariance as a metric to understand behavioural and mental illness.

Elucidating pathways between genes, brain, and behaviour is an incredibly difficult task, and the field of neuroimaging genetics is very much still in the early stages of understanding these relationships. It is hoped that the insights provided by this thesis into the genetic and environmental factors underlying anatomical organisation advance our understanding of the structure of neural circuits underlying brain function.

8.7 The Continuing Importance of Twin Imaging Studies

At a time when the sample size of brain imaging GWAS are increasing to over 20,000 participants (Adams et al., 2016; Hibar et al., 2017), one might wonder if twin studies are still relevant to the field of neuroimaging genetics/genomics. However, we argue that there

is still much to learn about genetic (and non-genetic) influences on the brain from twin and family imaging studies.

As mentioned in Chapter 2, heritability can be estimated directly from the genome through GCTA (Yang et al., 2011). However, GCTA requires very large sample sizes (i.e. thousands) to produce accurate heritability estimates. While this approach is feasible for consortia and biobanks, imaging studies are generally too small to accurately estimate GCTA heritability (without data sharing, which is not always possible). Hence, the classical twin design provides a methodology to estimate heritability in a much smaller sample size.

The smaller sample sizes required for twin studies compared to studies of unrelated individuals allow twin studies to collect extensive phenotypic data. Hence, twin studies provide a powerful method to establish the heritability of novel imaging phenotypes (e.g. complex task fMRI, connectome imaging) and/or examine the genetic overlap between neuroimaging measures and behavioural phenotypes (e.g. substance use, diet, sleep, risk-taking). In this way, twin studies can provide the crucial, first evidence of genetic contributions to the complexities of the brain and behaviour, which later, larger studies can expand upon.

The discordant MZ twin design is another strong example of the usefulness of twin studies. As MZ twin pairs are naturally matched on genetic and shared environmental backgrounds, they provide a powerful method to examine the influence of unique environmental factors in situations where a characteristic/disease is present in one twin pair member but not the other (van Dongen, Slagboom, Draisma, Martin, & Boomsma, 2012; Vitaro, Brendgen, & Arseneault, 2009). The value of this approach lies in its ability to distinguish phenotypic associations that are due to causation (one phenotype influences another) from associations due to overlapping effects (two phenotypes are influenced by the same genetic or environmental influences). Though this method is constrained by the availability of MZ twin pairs discordant for a phenotype, it may be able to provide important insights into the biological pathways underlying complex traits that standard case-control studies cannot. Another possible extension of twin analysis is to examine causal relationships through family confounding (Hopper et al., 2012). This approach, like Mendelian randomisation (Greenland, 2000), aims to determine if observed relationships are causal, and if so, infer the direction of this causality. However, the applicability of this

technique to twin imaging studies is yet to be examined, and the discordant MZ twin design is likely the best method to examine causality in twin studies of brain and function.

8.8 Potential Limitations

Though both the QTIM and HCP datasets have the benefit of comprising of healthy young adult participants with extensive imaging and non-imaging phenotyping, there are several potential limitations of these datasets. Foremost is the suggestion that results based on twin studies are not generalizable to the wider population (i.e. singletons) due to differences in intrauterine and family environments in twins compared to singletons (Hay & O'Brien, 1983; B. Price, 1950). However, studies have demonstrated that twin designs provide valid measures of heritability for brain morphometry, and importantly, that these results are generalizable to the non-twin population (Ordaz et al., 2010; Pol et al., 2002).

There is likely a slight sampling/participation bias in both datasets. Females outweigh males in both datasets (approximately 65% and 55% of participants were female in the QTIM and HCP datasets respectively). To control for this bias, sex (and sex by age interactions) were included as covariates in all analyses. Further, participants from the QTIM and HCP datasets were, on average, more intelligent than the general population (based on intelligence composite scores). As structural differences have been observed in individuals with high intelligence (Brant et al., 2013), this is a limitation that cannot be dismissed. However, the inclusion of global brain measures (i.e. total surface area, mean cortical thickness) as covariates may have reduced effects of high intelligence. This topic awaits further research.

Lastly, it must be noted that while sample sizes in this thesis are large for imaging studies, they are small for twin studies. Both the QTIM and HCP datasets would benefit from increased sample sizes, which would improve the accuracy of variance components estimates, particularly for common environment estimates (Visscher, Gordon, et al., 2008).

8.9 Future Directions

Future twin studies should use high-level MRI acquisition techniques to measure brain structure at a finer detail, and focus on measures of structural connectivity and/or complex task fMRI to demarcate neural networks. At the same time, future studies should examine the reliability of their imaging measures to ensure that their ability to detect genetic effects is not limited by measurement error. If so, studies should seek to improve the test-retest reliability of their measures (e.g. altering acquisition parameters, using the average of multiple scans).

Longitudinal studies are required to investigate the stability of genetic effects across the lifespan, particularly during critical neurodevelopmental periods like infancy and adolescence. Further, longitudinal studies provide a valuable method to evaluate changes in behavioural measures and possible corresponding changes in brain structure. Importantly, longitudinal studies should also examine group differences (e.g. sex, socioeconomic status) across neurodevelopment.

In Chapter 4, we investigated region-specific variance by using a whole brain covariate (total surface area/mean cortical thickness) to remove variance explained by a common, whole brain factor. However, a better methodology may be to use multivariate (as opposed to bivariate) twin modelling, as used by Renteria et al. (2014) when investigating the genetic architecture of subcortical structures. Multivariate models allow for the identification of common and region-specific variance sources, and may further quantify the extent that genetic and/or environmental effects are shared across, or unique to, individual cortical regions. Further extending multivariate studies to include subcortical, cerebellar, and white matter structures is a promising future direction which may help in detecting associations with behavioural phenotypes (Ritchie et al., 2015; Sabuncu et al., 2012).

At the genomics level, measures sharing genetic covariance (Chapter 4) could be used as phenotypes in multivariate GWAS, which would likely increase statistical power to identify genetic variants (Couvy-Duchesne et al., 2016), a valuable addition to neuroimaging genetics studies, which are typically underpowered. Additionally, the genetic clusters that showed high similarity across datasets (Chapter 6) are interesting phenotypes for future GWAS, as they may be closer to the level of genetic function than neuroanatomical

regions. Further, using genomic techniques to investigate the genetic architecture of structures with low and high mean-standardised absolute genetic variance could elucidate what underlies the wide range of variability in brain morphology (Chapter 5). Lastly, it is important to look beyond common genetic variants in seeking to understand the complexity of the brain; the characterisation of epigenetic modifications (Wiers, 2012), copy number variants (Redon et al., 2006), and gene expression (Kang et al., 2011) in the brain are likely to shed new light on individual differences in brain morphology.

8.10 Conclusion

This thesis illustrates a complex pattern of genetic and environmental influences on human brain morphology. Encouragingly, these patterns of genetic and environmental influence were largely similar between two independent datasets of healthy young adults, and further, differences in measurement error are unlikely to underlie these complexities. Future work should focus on more sophisticated MRI analysis, and collect dense genetic and environmental variables, to facilitate the next wave of studies investigating the aetiology of variation in brain morphology.

9 Bibliography

- Adams, H. H., Hibar, D. P., Chouraki, V., Stein, J. L., Nyquist, P. A., Renteria, M. E., . . . Thompson, P. M. (2016). Novel genetic loci underlying human intracranial volume identified through genome-wide association. *Nat Neurosci*, *19*(12), 1569-1582. doi:10.1038/nn.4398
- Adib-Samii, P., Devan, W., Traylor, M., Lanfranconi, S., Zhang, C. R., Cloonan, L., . . . Markus, H. S. (2015). Genetic architecture of white matter hyperintensities differs in hypertensive and nonhypertensive ischemic stroke. *Stroke*, *46*(2), 348-353. doi:10.1161/STROKEAHA.114.006849
- Alexander-Bloch, A., Giedd, J. N., & Bullmore, E. (2013). Imaging structural co-variance between human brain regions. *Nat Rev Neurosci*, *14*(5), 322-336. doi:10.1038/nrn3465
- Alexander-Bloch, A., Raznahan, A., Bullmore, E., & Giedd, J. (2013). The convergence of maturational change and structural covariance in human cortical networks. *J Neurosci*, *33*(7), 2889-2899. doi:10.1523/JNEUROSCI.3554-12.2013
- Allen, J. S., Damasio, H., & Grabowski, T. J. (2002). Normal neuroanatomical variation in the human brain: an MRI-volumetric study. *Am J Phys Anthropol*, *118*(4), 341-358. doi:10.1002/ajpa.10092
- Andrews, T. J., Halpern, S. D., & Purves, D. (1997). Correlated size variations in human visual cortex, lateral geniculate nucleus, and optic tract. *J Neurosci*, *17*(8), 2859-2868.
- Apostolova, L. G., Green, A. E., Babakchian, S., Hwang, K. S., Chou, Y. Y., Toga, A. W., & Thompson, P. M. (2012). Hippocampal atrophy and ventricular enlargement in normal aging, mild cognitive impairment (MCI), and Alzheimer Disease. *Alzheimer Dis Assoc Disord*, *26*(1), 17-27. doi:10.1097/WAD.0b013e3182163b62
- Astrom, R. L., Wadsworth, S. J., & DeFries, J. C. (2007). Etiology of the stability of reading difficulties: the longitudinal twin study of reading disabilities. *Twin Res Hum Genet*, *10*(3), 434-439. doi:10.1375/twin.10.3.434

- Baare, W. F., Hulshoff Pol, H. E., Boomsma, D. I., Posthuma, D., de Geus, E. J., Schnack, H. G., . . . Kahn, R. S. (2001). Quantitative genetic modeling of variation in human brain morphology. *Cereb Cortex*, *11*(9), 816-824.
- Bakken, T. E., Roddey, J. C., Djurovic, S., Akshoomoff, N., Amaral, D. G., Bloss, C. S., . . . Carlson, H. (2012). Association of common genetic variants in GPCPD1 with scaling of visual cortical surface area in humans. *Proc Natl Acad Sci U S A*, *109*(10), 3985-3990. doi:10.1073/pnas.1105829109
- Bartley, A. J., Jones, D. W., & Weinberger, D. R. (1997). Genetic variability of human brain size and cortical gyral patterns. *Brain*, *120* (Pt 2), 257-269.
- Barton, N. H., & Keightley, P. D. (2002). Understanding quantitative genetic variation. *Nat Rev Genet*, *3*(1), 11-21. doi:10.1038/nrg700
- Bates, T. C., Castles, A., Coltheart, M., Gillespie, N., Wright, M., & Martin, N. G. (2004). Behaviour genetic analyses of reading and spelling: A component processes approach. *Australian Journal of Psychology*, *56*(2), 115-126. doi:10.1080/00049530410001734847
- Bates, T. C., Castles, A., Luciano, M., Wright, M. J., Coltheart, M., & Martin, N. G. (2007). Genetic and environmental bases of reading and spelling: A unified genetic dual route model. *Reading and Writing*, *20*(1-2), 147-171. doi:10.1007/s11145-006-9022-1
- Bates, T. C., Lewis, G. J., & Weiss, A. (2013). Childhood socioeconomic status amplifies genetic effects on adult intelligence. *Psychol Sci*, *24*(10), 2111-2116. doi:10.1177/0956797613488394
- Bates, T. C., Lind, P. A., Luciano, M., Montgomery, G. W., Martin, N. G., & Wright, M. J. (2010). Dyslexia and DYX1C1: deficits in reading and spelling associated with a missense mutation. *Mol Psychiatry*, *15*(12), 1190-1196. doi:10.1038/mp.2009.120
- Batouli, S. A., Sachdev, P. S., Wen, W., Wright, M. J., Ames, D., & Trollor, J. N. (2014). Heritability of brain volumes in older adults: the Older Australian Twins Study. *Neurobiol Aging*, *35*(4), 937 e935-918. doi:10.1016/j.neurobiolaging.2013.10.079
- Benjamini, Y., & Hochberg, Y. (1995). Controlling the False Discovery Rate - a Practical and Powerful Approach to Multiple Testing. *Journal of the Royal Statistical Society Series B-Methodological*, *57*(1), 289-300.
- Betjemann, R. S., Johnson, E. P., Barnard, H., Boada, R., Filley, C. M., Filipek, P. A., . . . Pennington, B. F. (2010). Genetic covariation between brain volumes and IQ,

- reading performance, and processing speed. *Behav Genet*, *40*(2), 135-145.
doi:10.1007/s10519-009-9328-2
- Black, J. M., Tanaka, H., Stanley, L., Nagamine, M., Zakerani, N., Thurston, A., . . . Hoefft, F. (2012). Maternal history of reading difficulty is associated with reduced language-related gray matter in beginning readers. *Neuroimage*, *59*(3), 3021-3032.
doi:10.1016/j.neuroimage.2011.10.024
- Blackmon, K., Barr, W. B., Kuzniecky, R., Dubois, J., Carlson, C., Quinn, B. T., . . . Thesen, T. (2010). Phonetically irregular word pronunciation and cortical thickness in the adult brain. *Neuroimage*, *51*(4), 1453-1458.
doi:10.1016/j.neuroimage.2010.03.028
- Blokland, G. A., de Zubicaray, G. I., McMahon, K. L., & Wright, M. J. (2012). Genetic and environmental influences on neuroimaging phenotypes: a meta-analytical perspective on twin imaging studies. *Twin Res Hum Genet*, *15*(3), 351-371.
doi:10.1017/thg.2012.11
- Blokland, G. A., McMahon, K. L., Thompson, P. M., Hickie, I. B., Martin, N. G., de Zubicaray, G. I., & Wright, M. J. (2014). Genetic effects on the cerebellar role in working memory: same brain, different genes? *Neuroimage*, *86*(C), 392-403.
doi:10.1016/j.neuroimage.2013.10.006
- Blokland, G. A., McMahon, K. L., Thompson, P. M., Martin, N. G., de Zubicaray, G. I., & Wright, M. J. (2011). Heritability of working memory brain activation. *J Neurosci*, *31*(30), 10882-10890. doi:10.1523/JNEUROSCI.5334-10.2011
- Bochud, M. (2012). Estimating Heritability from Nuclear Family and Pedigree Data. In R. C. Elston, J. M. Satagopan, & S. Sun (Eds.), *Statistical Human Genetics* (Vol. 850, pp. 171-186): Humana Press.
- Bohlken, M. M., Brouwer, R. M., Mandl, R. C., van Haren, N. E., Brans, R. G., van Baal, G. C., . . . Hulshoff Pol, H. E. (2014). Genes contributing to subcortical volumes and intellectual ability implicate the thalamus. *Hum Brain Mapp*, *35*(6), 2632-2642.
doi:10.1002/hbm.22356
- Bohlken, M. M., Brouwer, R. M., Mandl, R. C. W., Hedman, A. M., van den Heuvel, M. P., van Haren, N. E. M., . . . Hulshoff Pol, H. E. (2016). Topology of genetic associations between regional gray matter volume and intellectual ability: Evidence for a high capacity network. *Neuroimage*, *124*(Pt A), 1044-1053.
doi:10.1016/j.neuroimage.2015.09.046

- Boker, S., Neale, M., Maes, H., Wilde, M., Spiegel, M., Brick, T., . . . Fox, J. (2011). OpenMx: An Open Source Extended Structural Equation Modeling Framework. *Psychometrika*, *76*(2), 306-317. doi:10.1007/s11336-010-9200-6
- Boyd, R., Richerson, P. J., & Henrich, J. (2011). The cultural niche: why social learning is essential for human adaptation. *Proc Natl Acad Sci U S A*, *108 Suppl 2*, 10918-10925. doi:10.1073/pnas.1100290108
- Brans, R. G., Kahn, R. S., Schnack, H. G., van Baal, G. C., Posthuma, D., van Haren, N. E., . . . Hulshoff Pol, H. E. (2010). Brain plasticity and intellectual ability are influenced by shared genes. *J Neurosci*, *30*(16), 5519-5524. doi:10.1523/JNEUROSCI.5841-09.2010
- Brant, A. M., Munakata, Y., Boomsma, D. I., Defries, J. C., Haworth, C. M., Keller, M. C., . . . Hewitt, J. K. (2013). The nature and nurture of high IQ: an extended sensitive period for intellectual development. *Psychol Sci*, *24*(8), 1487-1495. doi:10.1177/0956797612473119
- Brodmann, K. (1909). *Vergleichende Lokalisationslehre der Grosshirnrinde in ihren Prinzipien dargestellt auf Grund des Zellenbaues*. Leipzig: Barth.
- Brouwer, R. M., Glahn, D. C., Hibar, D. P., Hua, X., Jahanshad, N., Franz, C. E., . . . Panizzon, M. S. (2015). *Genetic influences on longitudinal changes in subcortical volumes: results of the ENIGMA Plasticity Working Group*. Paper presented at the Organization for Human Brain Mapping 2015.
- Brouwer, R. M., Hedman, A. M., van Haren, N. E., Schnack, H. G., Brans, R. G., Smit, D. J., . . . Hulshoff Pol, H. E. (2014). Heritability of brain volume change and its relation to intelligence. *Neuroimage*, *100*, 676-683. doi:10.1016/j.neuroimage.2014.04.072
- Brouwer, R. M., Panizzon, M. S., Glahn, D. C., Hibar, D. P., Hua, X., Jahanshad, N., . . . Hulshoff Pol, H. E. (2017). Genetic influences on individual differences in longitudinal changes in global and subcortical brain volumes: Results of the ENIGMA plasticity working group. *Hum Brain Mapp*, *38*(9), 4444-4458. doi:10.1002/hbm.23672
- Brouwer, R. M., van Soelen, I. L., Swagerman, S. C., Schnack, H. G., Ehli, E. A., Kahn, R. S., . . . Boomsma, D. I. (2014). Genetic associations between intelligence and cortical thickness emerge at the start of puberty. *Hum Brain Mapp*, *35*(8), 3760-3773. doi:10.1002/hbm.22435

- Bryant, C., Giovanello, K. S., Ibrahim, J. G., Chang, J., Shen, D., Peterson, B. S., . . . Alzheimer's Disease Neuroimaging, I. (2013). Mapping the genetic variation of regional brain volumes as explained by all common SNPs from the ADNI study. *PLoS One*, 8(8), e71723. doi:10.1371/journal.pone.0071723
- Bucholz, K. K., Cadoret, R., Cloninger, C. R., Dinwiddie, S. H., Hesselbrock, V. M., Nurnberger, J. I., Jr., . . . Schuckit, M. A. (1994). A new, semi-structured psychiatric interview for use in genetic linkage studies: a report on the reliability of the SSAGA. *J Stud Alcohol*, 55(2), 149-158.
- Burt, S. A. (2014). Research review: the shared environment as a key source of variability in child and adolescent psychopathology. *J Child Psychol Psychiatry*, 55(4), 304-312. doi:10.1111/jcpp.12173
- Carmelli, D., Reed, T., & DeCarli, C. (2002). A bivariate genetic analysis of cerebral white matter hyperintensities and cognitive performance in elderly male twins. *Neurobiol Aging*, 23(3), 413-420.
- Carmelli, D., Swan, G. E., DeCarli, C., & Reed, T. (2002). Quantitative genetic modeling of regional brain volumes and cognitive performance in older male twins. *Biol Psychol*, 61(1-2), 139-155.
- Carmichael, O. T., Kuller, L. H., Lopez, O. L., Thompson, P. M., Dutton, R. A., Lu, A., . . . Becker, J. T. (2007). Ventricular volume and dementia progression in the Cardiovascular Health Study. *Neurobiol Aging*, 28(3), 389-397. doi:10.1016/j.neurobiolaging.2006.01.006
- Carpenter, E. M. (2016). Development of Brain Ventricles and Choroid Plexus. In T. C. Chen (Ed.), *The Choroid Plexus and Cerebrospinal Fluid* (pp. 15-27). San Diego: Academic Press.
- Castles, A., & Coltheart, M. (1993). Varieties of developmental dyslexia. *Cognition*, 47(2), 149-180.
- Charlesworth, B. (1984). The evolutionary genetics of life histories. In B. Shorrocks (Ed.), *Evolutionary Ecology*. Oxford: Blackwell Publishers.
- Charlesworth, B. (1987). The heritability of fitness. In J. W. Bradbury & M. B. Andersson (Eds.), *Sexual selection: testing the alternatives* (pp. 21-40). New York: John Wiley & Sons Limited.

- Chen, C. H., Fiecas, M., Gutierrez, E. D., Panizzon, M. S., Eyler, L. T., Vuoksima, E., . . . Kremen, W. S. (2013). Genetic topography of brain morphology. *Proc Natl Acad Sci U S A*, *110*(42), 17089-17094. doi:10.1073/pnas.1308091110
- Chen, C. H., Gutierrez, E. D., Thompson, W., Panizzon, M. S., Jernigan, T. L., Eyler, L. T., . . . Dale, A. M. (2012). Hierarchical genetic organization of human cortical surface area. *Science*, *335*(6076), 1634-1636. doi:10.1126/science.1215330
- Chen, C. H., Panizzon, M. S., Eyler, L. T., Jernigan, T. L., Thompson, W., Fennema-Notestine, C., . . . Dale, A. M. (2011). Genetic influences on cortical regionalization in the human brain. *Neuron*, *72*(4), 537-544. doi:10.1016/j.neuron.2011.08.021
- Chen, C. H., Peng, Q., Schork, A. J., Lo, M. T., Fan, C. C., Wang, Y., . . . Alzheimer's Disease Neuroimaging, I. (2015). Large-scale genomics unveil polygenic architecture of human cortical surface area. *Nat Commun*, *6*, 7549. doi:10.1038/ncomms8549
- Chiang, M. C., Barysheva, M., McMahon, K. L., de Zubicaray, G. I., Johnson, K., Montgomery, G. W., . . . Thompson, P. M. (2012). Gene network effects on brain microstructure and intellectual performance identified in 472 twins. *J Neurosci*, *32*(25), 8732-8745. doi:10.1523/JNEUROSCI.5993-11.2012
- Chiang, M. C., Barysheva, M., Shattuck, D. W., Lee, A. D., Madsen, S. K., Avedissian, C., . . . Thompson, P. M. (2009). Genetics of brain fiber architecture and intellectual performance. *J Neurosci*, *29*(7), 2212-2224. doi:10.1523/JNEUROSCI.4184-08.2009
- Chiang, M. C., McMahon, K. L., de Zubicaray, G. I., Martin, N. G., Hickie, I., Toga, A. W., . . . Thompson, P. M. (2011). Genetics of white matter development: a DTI study of 705 twins and their siblings aged 12 to 29. *Neuroimage*, *54*(3), 2308-2317. doi:10.1016/j.neuroimage.2010.10.015
- Coltman, D. W., O'Donoghue, P., Hogg, J. T., & Festa-Bianchet, M. (2005). Selection and genetic (co)variance in bighorn sheep. *Evolution*, *59*(6), 1372-1382. doi:10.1111/j.0014-3820.2005.tb01786.x
- Couvy-Duchesne, B., Strike, L., Hansell, N., Martin, N., McMahon, K., de Zubicaray, G., . . . Wright, M. (2016). Power of multivariate GWAS: real case scenarios using brain phenotypes from MRI. *Behavior Genetics*, *46*(6), 777-777.
- Couvy-Duchesne, B., Strike, L. T., de Zubicaray, G. I., McMahon, K. L., Thompson, P. M., Hickie, I. B., . . . Wright, M. J. (2018). Lingual Gyrus Surface Area Is Associated

- with Anxiety-Depression Severity in Young Adults: A Genetic Clustering Approach. *eneuro*, 5(1). doi:10.1523/ENEURO.0153-17.2017
- Crow, J. F. (1958). Some possibilities for measuring selection intensities in man. *Hum Biol*, 30(1), 1-13.
- Cui, Y., Liu, B., Zhou, Y., Fan, L., Li, J., Zhang, Y., . . . Jiang, T. (2016). Genetic Effects on Fine-Grained Human Cortical Regionalization. *Cereb Cortex*, 26(9), 3732-3743. doi:10.1093/cercor/bhv176
- Davis, O. S., Band, G., Pirinen, M., Haworth, C. M., Meaburn, E. L., Kovas, Y., . . . Spencer, C. C. (2014). The correlation between reading and mathematics ability at age twelve has a substantial genetic component. *Nat Commun*, 5, 4204. doi:10.1038/ncomms5204
- de Geus, E. J. (2010). From genotype to EEG endophenotype: a route for post-genomic understanding of complex psychiatric disease? *Genome Med*, 2(9), 63. doi:10.1186/gm184
- de Zubicaray, G. I., Chiang, M. C., McMahon, K. L., Shattuck, D. W., Toga, A. W., Martin, N. G., . . . Thompson, P. M. (2008). Meeting the Challenges of Neuroimaging Genetics. *Brain Imaging Behav*, 2(4), 258-263. doi:10.1007/s11682-008-9029-0
- Deary, I. J., Penke, L., & Johnson, W. (2010). The neuroscience of human intelligence differences. *Nat Rev Neurosci*, 11(3), 201-211. doi:10.1038/nrn2793
- den Braber, A., Bohlken, M. M., Brouwer, R. M., van 't Ent, D., Kanai, R., Kahn, R. S., . . . Boomsma, D. I. (2013). Heritability of subcortical brain measures: a perspective for future genome-wide association studies. *Neuroimage*, 83, 98-102. doi:10.1016/j.neuroimage.2013.06.027
- Dennison, M., Whittle, S., Yucel, M., Vijayakumar, N., Kline, A., Simmons, J., & Allen, N. B. (2013). Mapping subcortical brain maturation during adolescence: evidence of hemisphere- and sex-specific longitudinal changes. *Dev Sci*, 16(5), 772-791. doi:10.1111/desc.12057
- Desikan, R. S., Segonne, F., Fischl, B., Quinn, B. T., Dickerson, B. C., Blacker, D., . . . Killiany, R. J. (2006). An automated labeling system for subdividing the human cerebral cortex on MRI scans into gyral based regions of interest. *Neuroimage*, 31(3), 968-980. doi:10.1016/j.neuroimage.2006.01.021
- DeStefano, A. L., Seshadri, S., Beiser, A., Atwood, L. D., Massaro, J. M., Au, R., . . . DeCarli, C. (2009). Bivariate heritability of total and regional brain volumes: the

- Framingham Study. *Alzheimer Dis Assoc Disord*, 23(3), 218-223.
doi:10.1097/WAD.0b013e31819cadd8
- Destrieux, C., Fischl, B., Dale, A., & Halgren, E. (2010). Automatic parcellation of human cortical gyri and sulci using standard anatomical nomenclature. *Neuroimage*, 53(1), 1-15. doi:10.1016/j.neuroimage.2010.06.010
- Docherty, A. R., Sawyers, C. K., Panizzon, M. S., Neale, M. C., Eyler, L. T., Fennema-Notestine, C., . . . Kremen, W. S. (2015). Genetic network properties of the human cortex based on regional thickness and surface area measures. *Front Hum Neurosci*, 9, 440. doi:10.3389/fnhum.2015.00440
- Dohm, M. R. (2002). Repeatability estimates do not always set an upper limit to heritability. *Functional Ecology*, 16(2), 273-280.
- Erickson, K. I., Leckie, R. L., & Weinstein, A. M. (2014). Physical activity, fitness, and gray matter volume. *Neurobiol Aging*, 35 Suppl 2, S20-28.
doi:10.1016/j.neurobiolaging.2014.03.034
- Evans, A. C. (2013). Networks of anatomical covariance. *Neuroimage*, 80, 489-504.
doi:10.1016/j.neuroimage.2013.05.054
- Evans, D. M., Gillespie, N. A., & Martin, N. G. (2002). Biometrical genetics. *Biol Psychol*, 61(1-2), 33-51.
- Eyler, L. T., Chen, C. H., Panizzon, M. S., Fennema-Notestine, C., Neale, M. C., Jak, A., . . . Kremen, W. S. (2012). A comparison of heritability maps of cortical surface area and thickness and the influence of adjustment for whole brain measures: a magnetic resonance imaging twin study. *Twin Res Hum Genet*, 15(3), 304-314.
doi:10.1017/thg.2012.3
- Eyler, L. T., Prom-Wormley, E., Fennema-Notestine, C., Panizzon, M. S., Neale, M. C., Jernigan, T. L., . . . Kremen, W. S. (2011). Genetic patterns of correlation among subcortical volumes in humans: results from a magnetic resonance imaging twin study. *Hum Brain Mapp*, 32(4), 641-653. doi:10.1002/hbm.21054
- Eyler, L. T., Vuoksima, E., Panizzon, M. S., Fennema-Notestine, C., Neale, M. C., Chen, C. H., . . . Kremen, W. S. (2014). Conceptual and data-based investigation of genetic influences and brain asymmetry: a twin study of multiple structural phenotypes. *J Cogn Neurosci*, 26(5), 1100-1117. doi:10.1162/jocn_a_00531

- Fan, L., Li, H., Zhuo, J., Zhang, Y., Wang, J., Chen, L., . . . Jiang, T. (2016). The Human Brainnetome Atlas: A New Brain Atlas Based on Connectional Architecture. *Cereb Cortex*, 26(8), 3508-3526. doi:10.1093/cercor/bhw157
- Ferrer, E., Shaywitz, B. A., Holahan, J. M., Marchione, K., & Shaywitz, S. E. (2010). Uncoupling of reading and IQ over time: empirical evidence for a definition of dyslexia. *Psychol Sci*, 21(1), 93-101. doi:10.1177/0956797609354084
- Fischl, B., & Dale, A. M. (2000). Measuring the thickness of the human cerebral cortex from magnetic resonance images. *Proc Natl Acad Sci U S A*, 97(20), 11050-11055. doi:10.1073/pnas.200033797
- Fjell, A. M., Grydeland, H., Krogstad, S. K., Amlie, I., Rohani, D. A., Ferschmann, L., . . . Walhovd, K. B. (2015). Development and aging of cortical thickness correspond to genetic organization patterns. *Proc Natl Acad Sci U S A*, 112(50), 15462-15467. doi:10.1073/pnas.1508831112
- Frangou, S. (2014). *Developing Individualized Diagnostic and Therapeutic Tools with Images: The IMAGEMEND Network*. Paper presented at the Biol Psychiatry.
- Friederici, A. D. (2011). The brain basis of language processing: from structure to function. *Physiol Rev*, 91(4), 1357-1392. doi:10.1152/physrev.00006.2011
- Frye, R. E., Liederman, J., Malmberg, B., McLean, J., Strickland, D., & Beauchamp, M. S. (2010). Surface area accounts for the relation of gray matter volume to reading-related skills and history of dyslexia. *Cereb Cortex*, 20(11), 2625-2635. doi:10.1093/cercor/bhq010
- Fujii, T., Youssefzadeh, J., Novel, M., & Neman, J. (2016). Introduction to the Ventricular System and Choroid Plexus. In J. Neman & T. C. Chen (Eds.), *The Choroid Plexus and Cerebrospinal Fluid* (1st ed., pp. 1-13). San Diego: Academic Press.
- Garcia-Gonzalez, F., Simmons, L. W., Tomkins, J. L., Kotiaho, J. S., & Evans, J. P. (2012). Comparing evolvabilities: common errors surrounding the calculation and use of coefficients of additive genetic variation. *Evolution*, 66(8), 2341-2349. doi:10.1111/j.1558-5646.2011.01565.x
- Gatt, J. M., Korgaonkar, M. S., Schofield, P. R., Harris, A., Clark, C. R., Oakley, K. L., . . . Williams, L. M. (2012). The TWIN-E project in emotional wellbeing: study protocol and preliminary heritability results across four MRI and DTI measures. *Twin Res Hum Genet*, 15(3), 419-441. doi:10.1017/thg.2012.12

- Geschwind, D. H., & Rakic, P. (2013). Cortical evolution: judge the brain by its cover. *Neuron*, *80*(3), 633-647. doi:10.1016/j.neuron.2013.10.045
- Gialluisi, A., Guadalupe, T., Francks, C., & Fisher, S. E. (2017). Neuroimaging genetic analyses of novel candidate genes associated with reading and language. *Brain Lang*, *172*, 9-15. doi:10.1016/j.bandl.2016.07.002
- Gialluisi, A., Newbury, D. F., Wilcutt, E. G., Olson, R. K., DeFries, J. C., Brandler, W. M., . . . Fisher, S. E. (2014). Genome-wide screening for DNA variants associated with reading and language traits. *Genes Brain Behav*, *13*(7), 686-701. doi:10.1111/gbb.12158
- Giedd, J. N., Schmitt, J. E., & Neale, M. C. (2007). Structural brain magnetic resonance imaging of pediatric twins. *Hum Brain Mapp*, *28*(6), 474-481. doi:10.1002/hbm.20403
- Gilmore, J. H., Schmitt, J. E., Knickmeyer, R. C., Smith, J. K., Lin, W., Styner, M., . . . Neale, M. C. (2010). Genetic and environmental contributions to neonatal brain structure: A twin study. *Hum Brain Mapp*, *31*(8), 1174-1182. doi:10.1002/hbm.20926
- Glahn, D. C., Kent, J. W., Jr., Sprooten, E., Diego, V. P., Winkler, A. M., Curran, J. E., . . . Blangero, J. (2013). Genetic basis of neurocognitive decline and reduced white-matter integrity in normal human brain aging. *Proc Natl Acad Sci U S A*, *110*(47), 19006-19011. doi:10.1073/pnas.1313735110
- Glahn, D. C., Thompson, P. M., & Blangero, J. (2007). Neuroimaging endophenotypes: strategies for finding genes influencing brain structure and function. *Hum Brain Mapp*, *28*(6), 488-501. doi:10.1002/hbm.20401
- Glasser, M. F., Coalson, T. S., Robinson, E. C., Hacker, C. D., Harwell, J., Yacoub, E., . . . Van Essen, D. C. (2016). A multi-modal parcellation of human cerebral cortex. *Nature*, *536*(7615), 171-178. doi:10.1038/nature18933
- Glasser, M. F., Sotiropoulos, S. N., Wilson, J. A., Coalson, T. S., Fischl, B., Andersson, J. L., . . . Consortium, W. U.-M. H. (2013). The minimal preprocessing pipelines for the Human Connectome Project. *Neuroimage*, *80*, 105-124. doi:10.1016/j.neuroimage.2013.04.127
- Goldman, J. G., & Manis, F. R. (2013). Relationships Among Cortical Thickness, Reading Skill, and Print Exposure in Adults. *Scientific Studies of Reading*, *17*(3), 163-176. doi:10.1080/10888438.2011.620673

- Gomez-Robles, A., Hopkins, W. D., Schapiro, S. J., & Sherwood, C. C. (2015). Relaxed genetic control of cortical organization in human brains compared with chimpanzees. *Proc Natl Acad Sci U S A*, *112*(48), 14799-14804. doi:10.1073/pnas.1512646112
- Gottesman, II, & Gould, T. D. (2003). The endophenotype concept in psychiatry: etymology and strategic intentions. *Am J Psychiatry*, *160*(4), 636-645. doi:10.1176/appi.ajp.160.4.636
- Gottesman, II, & Shields, J. (1967). A polygenic theory of schizophrenia. *Proc Natl Acad Sci U S A*, *58*(1), 199-205.
- Greenland, S. (2000). An introduction to instrumental variables for epidemiologists. *International Journal of Epidemiology*, *29*(4), 722-729. doi:10.1093/ije/29.4.722
- Greenough, W. T., Black, J. E., & Wallace, C. S. (1987). Experience and brain development. *Child Dev*, *58*(3), 539-559.
- Gronenschild, E. H., Habets, P., Jacobs, H. I., Mengelers, R., Rozendaal, N., van Os, J., & Marcelis, M. (2012). The effects of FreeSurfer version, workstation type, and Macintosh operating system version on anatomical volume and cortical thickness measurements. *PLoS One*, *7*(6), e38234. doi:10.1371/journal.pone.0038234
- Gu, J., & Kanai, R. (2014). What contributes to individual differences in brain structure? *Front Hum Neurosci*, *8*, 262. doi:10.3389/fnhum.2014.00262
- Guadalupe, T., Mathias, S. R., vanErp, T. G. M., Whelan, C. D., Zwiers, M. P., Abe, Y., . . . Francks, C. (2017). Human subcortical brain asymmetries in 15,847 people worldwide reveal effects of age and sex. *Brain Imaging Behav*, *11*(5), 1497-1514. doi:10.1007/s11682-016-9629-z
- Han, X., Jovicich, J., Salat, D., van der Kouwe, A., Quinn, B., Czanner, S., . . . Fischl, B. (2006). Reliability of MRI-derived measurements of human cerebral cortical thickness: the effects of field strength, scanner upgrade and manufacturer. *Neuroimage*, *32*(1), 180-194. doi:10.1016/j.neuroimage.2006.02.051
- Hansen, T. F., Pelabon, C., Armbruster, W. S., & Carlson, M. L. (2003). Evolvability and genetic constraint in *Dalechampia* blossoms: components of variance and measures of evolvability. *J Evol Biol*, *16*(4), 754-766.
- Hansen, T. F., Pélabon, C., & Houle, D. (2011). Heritability is not evolvability. *Evolutionary Biology*, *38*(3), 258-277.

- Hay, D. A., & O'Brien, P. J. (1983). The La Trobe Twin Study: a genetic approach to the structure and development of cognition in twin children. *Child Dev*, *54*(2), 317-330. doi:10.2307/1129694
- He, Q., Xue, G., Chen, C., Chen, C., Lu, Z. L., & Dong, Q. (2013). Decoding the neuroanatomical basis of reading ability: a multivoxel morphometric study. *J Neurosci*, *33*(31), 12835-12843. doi:10.1523/JNEUROSCI.0449-13.2013
- Hibar, D. P., Adams, H. H. H., Jahanshad, N., Chauhan, G., Stein, J. L., Hofer, E., . . . Ikram, M. A. (2017). Novel genetic loci associated with hippocampal volume. *Nat Commun*, *8*, 13624. doi:10.1038/ncomms13624
- Hibar, D. P., Stein, J. L., Renteria, M. E., Arias-Vasquez, A., Desrivieres, S., Jahanshad, N., . . . Medland, S. E. (2015). Common genetic variants influence human subcortical brain structures. *Nature*, *520*(7546), 224-229. doi:10.1038/nature14101
- Hibar, D. P., Westlye, L. T., van Erp, T. G., Rasmussen, J., Leonardo, C. D., Faskowitz, J., . . . Andreassen, O. A. (2016). Subcortical volumetric abnormalities in bipolar disorder. *Mol Psychiatry*, *21*(12), 1710-1716. doi:10.1038/mp.2015.227
- Hoffman, P., Cox, S. R., Dykiert, D., Munoz Maniega, S., Valdes Hernandez, M. C., Bastin, M. E., . . . Deary, I. J. (2017). Brain grey and white matter predictors of verbal ability traits in older age: The Lothian Birth Cohort 1936. *Neuroimage*, *156*, 394-402. doi:10.1016/j.neuroimage.2017.05.052
- Hogstrom, L. J., Westlye, L. T., Walhovd, K. B., & Fjell, A. M. (2013). The structure of the cerebral cortex across adult life: age-related patterns of surface area, thickness, and gyrification. *Cereb Cortex*, *23*(11), 2521-2530. doi:10.1093/cercor/bhs231
- Hoogman, M., Bralten, J., Hibar, D. P., Mennes, M., Zwiers, M. P., Schweren, L. S. J., . . . Franke, B. (2017). Subcortical brain volume differences in participants with attention deficit hyperactivity disorder in children and adults: a cross-sectional mega-analysis. *Lancet Psychiatry*, *4*(4), 310-319. doi:10.1016/S2215-0366(17)30049-4
- Hopper, J. L., Bui, Q. M., Erbas, B., Matheson, M. C., Gurrin, L. C., Burgess, J. A., . . . Dharmage, S. C. (2012). Does eczema in infancy cause hay fever, asthma, or both in childhood? Insights from a novel regression model of sibling data. *J Allergy Clin Immunol*, *130*(5), 1117-1122 e1111. doi:10.1016/j.jaci.2012.08.003
- Hosseini, S. M., Black, J. M., Soriano, T., Bugescu, N., Martinez, R., Raman, M. M., . . . Hoefft, F. (2013). Topological properties of large-scale structural brain networks in

- children with familial risk for reading difficulties. *Neuroimage*, 71, 260-274.
doi:10.1016/j.neuroimage.2013.01.013
- Houle, D. (1992). Comparing evolvability and variability of quantitative traits. *Genetics*, 130(1), 195-204.
- Hulshoff Pol, H. E., Schnack, H. G., Posthuma, D., Mandl, R. C., Baare, W. F., van Oel, C., . . . Kahn, R. S. (2006). Genetic contributions to human brain morphology and intelligence. *J Neurosci*, 26(40), 10235-10242. doi:10.1523/JNEUROSCI.1312-06.2006
- Iacono, W. G., Vaidyanathan, U., Vrieze, S. I., & Malone, S. M. (2014). Knowns and unknowns for psychophysiological endophenotypes: integration and response to commentaries. *Psychophysiology*, 51(12), 1339-1347. doi:10.1111/psyp.12358
- Insel, T. R., & Wang, P. S. (2010). Rethinking mental illness. *JAMA*, 303(19), 1970-1971. doi:10.1001/jama.2010.555
- Jackson, D. (1984). Manual for the multidimensional aptitude battery. In: Port Huron, MI: Research Psychologists Press.
- Jahanshad, N., Bhatt, P., Hibar, D. P., Villalon, J. E., Nir, T. M., Toga, A. W., . . . Thompson, P. M. (2013). Bivariate Genome-Wide Association Study of Genetically Correlated Neuroimaging Phenotypes from DTI and MRI through a Seemingly Unrelated Regression Model. In L. Shen, T. Liu, P.-T. Yap, H. Huang, D. Shen, & C.-F. Westin (Eds.), *Multimodal Brain Image Analysis* (Vol. 8159, pp. 189-201): Springer International Publishing.
- Jancke, L. (2009). The plastic human brain. *Restor Neurol Neurosci*, 27(5), 521-538. doi:10.3233/RNN-2009-0519
- Jansen, A. G., Mous, S. E., White, T., Posthuma, D., & Polderman, T. J. (2015). What twin studies tell us about the heritability of brain development, morphology, and function: a review. *Neuropsychol Rev*, 25(1), 27-46. doi:10.1007/s11065-015-9278-9
- Jhaveri, D. J., Tedoldi, A., Hunt, S., Sullivan, R., Watts, N. R., Power, J. M., . . . Sah, P. (2018). Evidence for newly generated interneurons in the basolateral amygdala of adult mice. *Mol Psychiatry*, 23(3), 521-532. doi:10.1038/mp.2017.134
- Joshi, A. A., Lepore, N., Joshi, S. H., Lee, A. D., Barysheva, M., Stein, J. L., . . . Thompson, P. M. (2011). The contribution of genes to cortical thickness and volume. *Neuroreport*, 22(3), 101-105. doi:10.1097/WNR.0b013e3283424c84

- Jovicich, J., Czanner, S., Han, X., Salat, D., van der Kouwe, A., Quinn, B., . . . Fischl, B. (2009). MRI-derived measurements of human subcortical, ventricular and intracranial brain volumes: Reliability effects of scan sessions, acquisition sequences, data analyses, scanner upgrade, scanner vendors and field strengths. *Neuroimage*, *46*(1), 177-192. doi:10.1016/j.neuroimage.2009.02.010
- Kang, H. J., Kawasawa, Y. I., Cheng, F., Zhu, Y., Xu, X., Li, M., . . . Sestan, N. (2011). Spatio-temporal transcriptome of the human brain. *Nature*, *478*(7370), 483-489. doi:10.1038/nature10523
- Karlsgodt, K. H., Kochunov, P., Winkler, A. M., Laird, A. R., Almasy, L., Duggirala, R., . . . Glahn, D. C. (2010). A multimodal assessment of the genetic control over working memory. *J Neurosci*, *30*(24), 8197-8202. doi:10.1523/JNEUROSCI.0359-10.2010
- Kendler, K. S. (2013). What psychiatric genetics has taught us about the nature of psychiatric illness and what is left to learn. *Mol Psychiatry*, *18*(10), 1058-1066. doi:10.1038/mp.2013.50
- Kennedy, D. N., Lange, N., Makris, N., Bates, J., Meyer, J., & Caviness, V. S., Jr. (1998). Gyri of the human neocortex: an MRI-based analysis of volume and variance. *Cereb Cortex*, *8*(4), 372-384.
- Kochunov, P., Glahn, D., Winkler, A., Duggirala, R., Olvera, R. L., Cole, S., . . . Blangero, J. (2009). Analysis of genetic variability and whole genome linkage of whole-brain, subcortical, and ependymal hyperintense white matter volume. *Stroke*, *40*(12), 3685-3690. doi:10.1161/STROKEAHA.109.565390
- Kochunov, P., Glahn, D. C., Lancaster, J. L., Winkler, A. M., Smith, S., Thompson, P. M., . . . Blangero, J. (2010). Genetics of microstructure of cerebral white matter using diffusion tensor imaging. *Neuroimage*, *53*(3), 1109-1116. doi:10.1016/j.neuroimage.2010.01.078
- Kochunov, P., Glahn, D. C., Nichols, T. E., Winkler, A. M., Hong, E. L., Holcomb, H. H., . . . Blangero, J. (2011). Genetic analysis of cortical thickness and fractional anisotropy of water diffusion in the brain. *Front Neurosci*, *5*, 120. doi:10.3389/fnins.2011.00120
- Kochunov, P., Jahanshad, N., Sprooten, E., Nichols, T. E., Mandl, R. C., Almasy, L., . . . Glahn, D. C. (2014). Multi-site study of additive genetic effects on fractional anisotropy of cerebral white matter: Comparing meta and mega-analytical approaches for data pooling. *Neuroimage*, *95*, 136-150. doi:10.1016/j.neuroimage.2014.03.033

- Koolschijn, P. C., & Crone, E. A. (2013). Sex differences and structural brain maturation from childhood to early adulthood. *Dev Cogn Neurosci*, 5, 106-118.
doi:10.1016/j.dcn.2013.02.003
- Koten, J. W., Jr., Wood, G., Hagoort, P., Goebel, R., Propping, P., Willmes, K., & Boomsma, D. I. (2009). Genetic contribution to variation in cognitive function: an fMRI study in twins. *Science*, 323(5922), 1737-1740. doi:10.1126/science.1167371
- Kremen, W. S., Franz, C. E., & Lyons, M. J. (2013). VETSA: the Vietnam Era Twin Study of Aging. *Twin Res Hum Genet*, 16(1), 399-402. doi:10.1017/thg.2012.86
- Kremen, W. S., Panizzon, M. S., Neale, M. C., Fennema-Notestine, C., Prom-Wormley, E., Eyler, L. T., . . . Dale, A. M. (2012). Heritability of brain ventricle volume: converging evidence from inconsistent results. *Neurobiol Aging*, 33(1), 1-8.
doi:10.1016/j.neurobiolaging.2010.02.007
- Kremen, W. S., Prom-Wormley, E., Panizzon, M. S., Eyler, L. T., Fischl, B., Neale, M. C., . . . Fennema-Notestine, C. (2010). Genetic and environmental influences on the size of specific brain regions in midlife: the VETSA MRI study. *Neuroimage*, 49(2), 1213-1223. doi:10.1016/j.neuroimage.2009.09.043
- Kuhn, S., Gleich, T., Lorenz, R. C., Lindenberger, U., & Gallinat, J. (2014). Playing Super Mario induces structural brain plasticity: gray matter changes resulting from training with a commercial video game. *Mol Psychiatry*, 19(2), 265-271.
doi:10.1038/mp.2013.120
- Kuntsi, J., Rogers, H., Swinard, G., Borger, N., van der Meere, J., Rijdsdijk, F., & Asherson, P. (2006). Reaction time, inhibition, working memory and 'delay aversion' performance: genetic influences and their interpretation. *Psychol Med*, 36(11), 1613-1624. doi:10.1017/S0033291706008580
- Lande, R. (1977). On Comparing Coefficients of Variation. *Systematic Zoology*, 26(2), 214.
doi:10.2307/2412845
- Lange, N., Giedd, J. N., Castellanos, F. X., Vaituzis, A. C., & Rapoport, J. L. (1997). Variability of human brain structure size: ages 4-20 years. *Psychiatry Res*, 74(1), 1-12. doi:[https://doi.org/10.1016/S0925-4927\(96\)03054-5](https://doi.org/10.1016/S0925-4927(96)03054-5)
- Lemaitre, H., Goldman, A. L., Sambataro, F., Verchinski, B. A., Meyer-Lindenberg, A., Weinberger, D. R., & Mattay, V. S. (2012). Normal age-related brain morphometric changes: nonuniformity across cortical thickness, surface area and gray matter

volume? *Neurobiol Aging*, 33(3), 617 e611-619.

doi:10.1016/j.neurobiolaging.2010.07.013

- Lendvai, B., Stern, E. A., Chen, B., & Svoboda, K. (2000). Experience-dependent plasticity of dendritic spines in the developing rat barrel cortex in vivo. *Nature*, 404(6780), 876-881. doi:10.1038/35009107
- Lenroot, R. K., & Giedd, J. N. (2008). The changing impact of genes and environment on brain development during childhood and adolescence: initial findings from a neuroimaging study of pediatric twins. *Dev Psychopathol*, 20(4), 1161-1175. doi:10.1017/S0954579408000552
- Lenroot, R. K., & Giedd, J. N. (2010). Sex differences in the adolescent brain. *Brain Cogn*, 72(1), 46-55. doi:10.1016/j.bandc.2009.10.008
- Lenroot, R. K., Schmitt, J. E., Ordaz, S. J., Wallace, G. L., Neale, M. C., Lerch, J. P., . . . Giedd, J. N. (2009). Differences in genetic and environmental influences on the human cerebral cortex associated with development during childhood and adolescence. *Hum Brain Mapp*, 30(1), 163-174. doi:10.1002/hbm.20494
- Leuner, B., & Gould, E. (2010). Structural plasticity and hippocampal function. *Annu Rev Psychol*, 61, 111-140, C111-113. doi:10.1146/annurev.psych.093008.100359
- Lind, P. A., Luciano, M., Wright, M. J., Montgomery, G. W., Martin, N. G., & Bates, T. C. (2010). Dyslexia and DCDC2: normal variation in reading and spelling is associated with DCDC2 polymorphisms in an Australian population sample. *Eur J Hum Genet*, 18(6), 668-673. doi:10.1038/ejhg.2009.237
- Linkersdorfer, J., Lonnemann, J., Lindberg, S., Hasselhorn, M., & Fiebach, C. J. (2012). Grey matter alterations co-localize with functional abnormalities in developmental dyslexia: an ALE meta-analysis. *PLoS One*, 7(8), e43122. doi:10.1371/journal.pone.0043122
- Loehlin, J. C. (1996). The Cholesky approach: A cautionary note. *Behavior Genetics*, 26(1), 65-69. doi:Doi 10.1007/Bf02361160
- Lowery, L. A., & Sive, H. (2009). Totally tubular: the mystery behind function and origin of the brain ventricular system. *Bioessays*, 31(4), 446-458. doi:10.1002/bies.200800207
- Lu, L., Leonard, C., Thompson, P., Kan, E., Jolley, J., Welcome, S., . . . Sowell, E. (2007). Normal developmental changes in inferior frontal gray matter are associated with

- improvement in phonological processing: a longitudinal MRI analysis. *Cereb Cortex*, 17(5), 1092-1099. doi:10.1093/cercor/bhl019
- Luciano, M., Evans, D. M., Hansell, N. K., Medland, S. E., Montgomery, G. W., Martin, N. G., . . . Bates, T. C. (2013). A genome-wide association study for reading and language abilities in two population cohorts. *Genes Brain Behav*, 12(6), 645-652. doi:10.1111/gbb.12053
- Luciano, M., Lind, P. A., Duffy, D. L., Castles, A., Wright, M. J., Montgomery, G. W., . . . Bates, T. C. (2007). A haplotype spanning KIAA0319 and TTRAP is associated with normal variation in reading and spelling ability. *Biol Psychiatry*, 62(7), 811-817. doi:10.1016/j.biopsych.2007.03.007
- Luciano, M., Wright, M. J., Smith, G. A., Geffen, G. M., Geffen, L. B., & Martin, N. G. (2001). Genetic covariance among measures of information processing speed, working memory, and IQ. *Behavior Genetics*, 31(6), 581-592. doi:10.1023/A:1013397428612
- Madan, C. R., & Kensinger, E. A. (2017). Test-retest reliability of brain morphology estimates. *Brain Inform*, 4(2), 107-121. doi:10.1007/s40708-016-0060-4
- Maechler, M., Rousseeuw, P., Struyf, A., Hubert, M., & Hornik, K. (2017). cluster: Cluster Analysis Basics and Extensions.
- Martin, N. G., Eaves, L. J., Kearsley, M. J., & Davies, P. (1978). The power of the classical twin study. *Heredity (Edinb)*, 40(1), 97-116.
- McEwen, B. S., & Morrison, J. H. (2013). The brain on stress: vulnerability and plasticity of the prefrontal cortex over the life course. *Neuron*, 79(1), 16-29. doi:10.1016/j.neuron.2013.06.028
- McKay, D. R., Knowles, E. E., Winkler, A. A., Sprooten, E., Kochunov, P., Olvera, R. L., . . . Glahn, D. C. (2014). Influence of age, sex and genetic factors on the human brain. *Brain Imaging Behav*, 8(2), 143-152. doi:10.1007/s11682-013-9277-5
- McMillan, J., Beavis, A., & Jones, F. L. (2009). The AUSEI06. *Journal of Sociology*, 45(2), 123-149. doi:10.1177/1440783309103342
- Mechelli, A., Friston, K. J., Frackowiak, R. S., & Price, C. J. (2005). Structural covariance in the human cortex. *J Neurosci*, 25(36), 8303-8310. doi:10.1523/JNEUROSCI.0357-05.2005
- Menary, K., Collins, P. F., Porter, J. N., Muetzel, R., Olson, E. A., Kumar, V., . . . Luciana, M. (2013). Associations between cortical thickness and general intelligence in

- children, adolescents and young adults. *Intelligence*, 41(5), 597-606.
doi:10.1016/j.intell.2013.07.010
- Miller, G. F., & Penke, L. (2007). The evolution of human intelligence and the coefficient of additive genetic variance in human brain size. *Intelligence*, 35(2), 97-114.
doi:10.1016/j.intell.2006.08.008
- Morey, R. A., Petty, C. M., Xu, Y., Hayes, J. P., Wagner, H. R., 2nd, Lewis, D. V., . . .
McCarthy, G. (2009). A comparison of automated segmentation and manual tracing
for quantifying hippocampal and amygdala volumes. *Neuroimage*, 45(3), 855-866.
doi:10.1016/j.neuroimage.2008.12.033
- Morey, R. A., Selgrade, E. S., Wagner, H. R., 2nd, Huettel, S. A., Wang, L., & McCarthy,
G. (2010). Scan-rescan reliability of subcortical brain volumes derived from
automated segmentation. *Hum Brain Mapp*, 31(11), 1751-1762.
doi:10.1002/hbm.20973
- Mountcastle, V. B. (1997). The columnar organization of the neocortex. *Brain*, 120 (Pt 4),
701-722.
- Neale, M. C., & Cardon, L. R. (1992). *Methodology for genetic studies of twins and
families*: Springer.
- Neale, M. C., Hunter, M. D., Pritikin, J. N., Zahery, M., Brick, T. R., Kirkpatrick, R. M., . . .
Boker, S. M. (2016). OpenMx 2.0: Extended Structural Equation and Statistical
Modeling. *Psychometrika*, 81(2), 535-549. doi:10.1007/s11336-014-9435-8
- Nestor, S. M., Rupsingh, R., Borrie, M., Smith, M., Accomazzi, V., Wells, J. L., . . .
Alzheimer's Disease Neuroimaging, I. (2008). Ventricular enlargement as a possible
measure of Alzheimer's disease progression validated using the Alzheimer's
disease neuroimaging initiative database. *Brain*, 131(Pt 9), 2443-2454.
doi:10.1093/brain/awn146
- Nugent, A. C., Luckenbaugh, D. A., Wood, S. E., Bogers, W., Zarate, C. A., Jr., & Drevets,
W. C. (2013). Automated subcortical segmentation using FIRST: test-retest
reliability, interscanner reliability, and comparison to manual segmentation. *Hum
Brain Mapp*, 34(9), 2313-2329. doi:10.1002/hbm.22068
- Ochs, A. L., Ross, D. E., Zannoni, M. D., Abildskov, T. J., Bigler, E. D., & Alzheimer's
Disease Neuroimaging, I. (2015). Comparison of Automated Brain Volume
Measures obtained with NeuroQuant and FreeSurfer. *J Neuroimaging*, 25(5), 721-
727. doi:10.1111/jon.12229

- Ordaz, S. J., Lenroot, R. K., Wallace, G. L., Clasen, L. S., Blumenthal, J. D., Schmitt, J. E., & Giedd, J. N. (2010). Are there differences in brain morphometry between twins and unrelated singletons? A pediatric MRI study. *Genes Brain Behav*, *9*(3), 288-295. doi:10.1111/j.1601-183X.2009.00558.x
- Panizzon, M. S., Fennema-Notestine, C., Eyler, L. T., Jernigan, T. L., Prom-Wormley, E., Neale, M., . . . Kremen, W. S. (2009). Distinct genetic influences on cortical surface area and cortical thickness. *Cereb Cortex*, *19*(11), 2728-2735. doi:10.1093/cercor/bhp026
- Panizzon, M. S., Fennema-Notestine, C., Kubarych, T. S., Chen, C. H., Eyler, L. T., Fischl, B., . . . Kremen, W. S. (2012). Genetic and environmental influences of white and gray matter signal contrast: a new phenotype for imaging genetics? *Neuroimage*, *60*(3), 1686-1695. doi:10.1016/j.neuroimage.2012.01.122
- Pantev, C., Engelien, A., Candia, V., & Elbert, T. (2001). Representational cortex in musicians. Plastic alterations in response to musical practice. *Ann N Y Acad Sci*, *930*(1), 300-314.
- Pascual-Leone, A., Amedi, A., Fregni, F., & Merabet, L. B. (2005). The plastic human brain cortex. *Annu Rev Neurosci*, *28*, 377-401. doi:10.1146/annurev.neuro.27.070203.144216
- Peng, Q., Schork, A., Bartsch, H., Lo, M. T., Panizzon, M. S., Pediatric Imaging, N., . . . Chen, C. H. (2016). Conservation of Distinct Genetically-Mediated Human Cortical Pattern. *PLoS Genet*, *12*(7), e1006143. doi:10.1371/journal.pgen.1006143
- Pennington, B. F., Filipek, P. A., Lefly, D., Chhabildas, N., Kennedy, D. N., Simon, J. H., . . . DeFries, J. C. (2000). A twin MRI study of size variations in human brain. *J Cogn Neurosci*, *12*(1), 223-232.
- Perlaki, G., Horvath, R., Nagy, S. A., Bogner, P., Doczi, T., Janszky, J., & Orsi, G. (2017). Comparison of accuracy between FSL's FIRST and Freesurfer for caudate nucleus and putamen segmentation. *Sci Rep*, *7*(1), 2418. doi:10.1038/s41598-017-02584-5
- Pfefferbaum, A., Sullivan, E. V., Swan, G. E., & Carmelli, D. (2000). Brain structure in men remains highly heritable in the seventh and eighth decades of life. *Neurobiol Aging*, *21*(1), 63-74.
- Plomin, R., DeFries, J. C., & Loehlin, J. C. (1977). Genotype-environment interaction and correlation in the analysis of human behavior. *Psychol Bull*, *84*(2), 309-322.

- Pol, H. E. H., Posthuma, D., Baare, W. F. C., De Geus, E. J. C., Schnack, H. G., van Haren, N. E. M., . . . Boomsma, D. I. (2002). Twin-singleton differences in brain structure using structural equation modelling. *Brain*, *125*, 384-390. doi:DOI 10.1093/brain/awf035
- Posthuma, D., Baare, W. F., Hulshoff Pol, H. E., Kahn, R. S., Boomsma, D. I., & De Geus, E. J. (2003). Genetic correlations between brain volumes and the WAIS-III dimensions of verbal comprehension, working memory, perceptual organization, and processing speed. *Twin Res*, *6*(2), 131-139. doi:10.1375/136905203321536254
- Posthuma, D., & Boomsma, D. I. (2000). A note on the statistical power in extended twin designs. *Behav Genet*, *30*(2), 147-158. doi:10.1023/a:1001959306025
- Posthuma, D., De Geus, E. J., Baare, W. F., Hulshoff Pol, H. E., Kahn, R. S., & Boomsma, D. I. (2002). The association between brain volume and intelligence is of genetic origin. *Nat Neurosci*, *5*(2), 83-84. doi:10.1038/nn0202-83
- Posthuma, D., de Geus, E. J., Neale, M. C., Hulshoff Pol, H. E., Baare, W. E. C., Kahn, R. S., & Boomsma, D. (2000). Multivariate genetic analysis of brain structure in an extended twin design. *Behav Genet*, *30*(4), 311-319.
- Power, J. D., Cohen, A. L., Nelson, S. M., Wig, G. S., Barnes, K. A., Church, J. A., . . . Petersen, S. E. (2011). Functional network organization of the human brain. *Neuron*, *72*(4), 665-678. doi:10.1016/j.neuron.2011.09.006
- Price, B. (1950). Primary biases in twin studies; a review of prenatal and natal difference-producing factors in monozygotic pairs. *Am J Hum Genet*, *2*(4), 293-352.
- Price, C. J. (2012). A review and synthesis of the first 20 years of PET and fMRI studies of heard speech, spoken language and reading. *Neuroimage*, *62*(2), 816-847. doi:10.1016/j.neuroimage.2012.04.062
- Psaty, B. M., O'Donnell, C. J., Gudnason, V., Lunetta, K. L., Folsom, A. R., Rotter, J. I., . . . Consortium, C. (2009). Cohorts for Heart and Aging Research in Genomic Epidemiology (CHARGE) Consortium: Design of prospective meta-analyses of genome-wide association studies from 5 cohorts. *Circ Cardiovasc Genet*, *2*(1), 73-80. doi:10.1161/CIRCGENETICS.108.829747
- R Core Team. (2015). R: A language and environment for statistical computing. Vienna, Austria. Retrieved from <http://www.R-project.org/>

- R Core Team. (2017). R: A language and environment for statistical computing. Vienna, Austria: R Foundation for Statistical Computing. Retrieved from <http://www.R-project.org/>
- Rabl, U., Meyer, B. M., Diers, K., Bartova, L., Berger, A., Mandorfer, D., . . . Pezawas, L. (2014). Additive gene-environment effects on hippocampal structure in healthy humans. *J Neurosci*, *34*(30), 9917-9926. doi:10.1523/JNEUROSCI.3113-13.2014
- Rakic, P. (1988). Specification of cerebral cortical areas. *Science*, *241*(4862), 170-176.
- Rakic, P. (2009). Evolution of the neocortex: a perspective from developmental biology. *Nat Rev Neurosci*, *10*(10), 724-735. doi:10.1038/nrn2719
- Redon, R., Ishikawa, S., Fitch, K. R., Feuk, L., Perry, G. H., Andrews, T. D., . . . Hurles, M. E. (2006). Global variation in copy number in the human genome. *Nature*, *444*(7118), 444-454. doi:10.1038/nature05329
- Renteria, M. E., Hansell, N. K., Strike, L. T., McMahon, K. L., de Zubicaray, G. I., Hickie, I. B., . . . Wright, M. J. (2014). Genetic architecture of subcortical brain regions: common and region-specific genetic contributions. *Genes Brain Behav*, *13*(8), 821-830. doi:10.1111/gbb.12177
- Renteria, M. E., Schmaal, L., Hibar, D. P., Couvy-Duchesne, B., Strike, L. T., Mills, N. T., . . . Hickie, I. B. (2017). Subcortical brain structure and suicidal behaviour in major depressive disorder: a meta-analysis from the ENIGMA-MDD working group. *Transl Psychiatry*, *7*(5), e1116. doi:10.1038/tp.2017.84
- Richardson, F. M., & Price, C. J. (2009). Structural MRI studies of language function in the undamaged brain. *Brain Struct Funct*, *213*(6), 511-523. doi:10.1007/s00429-009-0211-y
- Richlan, F., Kronbichler, M., & Wimmer, H. (2013). Structural abnormalities in the dyslexic brain: a meta-analysis of voxel-based morphometry studies. *Hum Brain Mapp*, *34*(11), 3055-3065. doi:10.1002/hbm.22127
- Richmond, S., Johnson, K. A., Seal, M. L., Allen, N. B., & Whittle, S. (2016). Development of brain networks and relevance of environmental and genetic factors: A systematic review. *Neurosci Biobehav Rev*, *71*, 215-239. doi:10.1016/j.neubiorev.2016.08.024
- Rijsdijk, F. V., Viding, E., De Brito, S., Forgiarini, M., Mechelli, A., Jones, A. P., & McCrory, E. (2010). Heritable variations in gray matter concentration as a potential endophenotype for psychopathic traits. *Arch Gen Psychiatry*, *67*(4), 406-413. doi:10.1001/archgenpsychiatry.2010.20

- Rimol, L. M., Panizzon, M. S., Fennema-Notestine, C., Eyer, L. T., Fischl, B., Franz, C. E., . . . Dale, A. M. (2010). Cortical thickness is influenced by regionally specific genetic factors. *Biol Psychiatry*, *67*(5), 493-499. doi:10.1016/j.biopsych.2009.09.032
- Ritchie, S. J., Booth, T., Valdes Hernandez, M. D., Corley, J., Maniega, S. M., Gow, A. J., . . . Deary, I. J. (2015). Beyond a bigger brain: Multivariable structural brain imaging and intelligence. *Intelligence*, *51*(Supplement C), 47-56. doi:10.1016/j.intell.2015.05.001
- Rogers, J., Kochunov, P., Zilles, K., Shelledy, W., Lancaster, J., Thompson, P., . . . Glahn, D. C. (2010). On the genetic architecture of cortical folding and brain volume in primates. *Neuroimage*, *53*(3), 1103-1108. doi:10.1016/j.neuroimage.2010.02.020
- Rousson, V., Gasser, T., & Seifert, B. (2002). Assessing intrarater, interrater and test-retest reliability of continuous measurements. *Stat Med*, *21*(22), 3431-3446. doi:10.1002/sim.1253
- Sabuncu, M. R., Buckner, R. L., Smoller, J. W., Lee, P. H., Fischl, B., Sperling, R. A., & Alzheimer's Disease Neuroimaging, I. (2012). The association between a polygenic Alzheimer score and cortical thickness in clinically normal subjects. *Cereb Cortex*, *22*(11), 2653-2661. doi:10.1093/cercor/bhr348
- Sachdev, P. S., Lammell, A., Trollor, J. N., Lee, T., Wright, M. J., Ames, D., . . . team, O. r. (2009). A comprehensive neuropsychiatric study of elderly twins: the Older Australian Twins Study. *Twin Res Hum Genet*, *12*(6), 573-582. doi:10.1375/twin.12.6.573
- Sahay, A., Scobie, K. N., Hill, A. S., O'Carroll, C. M., Kheirbek, M. A., Burghardt, N. S., . . . Hen, R. (2011). Increasing adult hippocampal neurogenesis is sufficient to improve pattern separation. *Nature*, *472*(7344), 466-470. doi:10.1038/nature09817
- Salat, D. H., Buckner, R. L., Snyder, A. Z., Greve, D. N., Desikan, R. S., Busa, E., . . . Fischl, B. (2004). Thinning of the cerebral cortex in aging. *Cereb Cortex*, *14*(7), 721-730. doi:10.1093/cercor/bhh032
- Schmaal, L., Hibar, D. P., Samann, P. G., Hall, G. B., Baune, B. T., Jahanshad, N., . . . Veltman, D. J. (2017). Cortical abnormalities in adults and adolescents with major depression based on brain scans from 20 cohorts worldwide in the ENIGMA Major Depressive Disorder Working Group. *Mol Psychiatry*, *22*(6), 900-909. doi:10.1038/mp.2016.60

- Schmaal, L., Veltman, D. J., van Erp, T. G., Samann, P. G., Frodl, T., Jahanshad, N., . . . Hibar, D. P. (2016). Subcortical brain alterations in major depressive disorder: findings from the ENIGMA Major Depressive Disorder working group. *Mol Psychiatry*, *21*(6), 806-812. doi:10.1038/mp.2015.69
- Schmitt, J. E., Lenroot, R. K., Ordaz, S. E., Wallace, G. L., Lerch, J. P., Evans, A. C., . . . Giedd, J. N. (2009). Variance decomposition of MRI-based covariance maps using genetically informative samples and structural equation modeling. *Neuroimage*, *47*(1), 56-64. doi:10.1016/j.neuroimage.2008.06.039
- Schmitt, J. E., Lenroot, R. K., Wallace, G. L., Ordaz, S., Taylor, K. N., Kabani, N., . . . Giedd, J. N. (2008). Identification of genetically mediated cortical networks: a multivariate study of pediatric twins and siblings. *Cereb Cortex*, *18*(8), 1737-1747. doi:10.1093/cercor/bhm211
- Schmitt, J. E., Neale, M. C., Fassassi, B., Perez, J., Lenroot, R. K., Wells, E. M., & Giedd, J. N. (2014). The dynamic role of genetics on cortical patterning during childhood and adolescence. *Proc Natl Acad Sci U S A*, *111*(18), 6774-6779. doi:10.1073/pnas.1311630111
- Schmitt, J. E., Wallace, G. L., Lenroot, R. K., Ordaz, S. E., Greenstein, D., Clasen, L., . . . Giedd, J. N. (2010). A twin study of intracerebral volumetric relationships. *Behav Genet*, *40*(2), 114-124. doi:10.1007/s10519-010-9332-6
- Schmitt, J. E., Wallace, G. L., Rosenthal, M. A., Molloy, E. A., Ordaz, S., Lenroot, R., . . . Giedd, J. N. (2007). A multivariate analysis of neuroanatomic relationships in a genetically informative pediatric sample. *Neuroimage*, *35*(1), 70-82. doi:10.1016/j.neuroimage.2006.04.232
- Schnack, H. G., van Haren, N. E., Brouwer, R. M., Evans, A., Durston, S., Boomsma, D. I., . . . Hulshoff Pol, H. E. (2015). Changes in thickness and surface area of the human cortex and their relationship with intelligence. *Cereb Cortex*, *25*(6), 1608-1617. doi:10.1093/cercor/bht357
- Sham, P. (1998). *Statistics in Human Genetics (Arnold Applications of Statistics Series)*. Edward Arnold, London.
- Shen, X., Tokoglu, F., Papademetris, X., & Constable, R. T. (2013). Groupwise whole-brain parcellation from resting-state fMRI data for network node identification. *Neuroimage*, *82*(Supplement C), 403-415. doi:10.1016/j.neuroimage.2013.05.081

- Sowell, E. R., Peterson, B. S., Kan, E., Woods, R. P., Yoshii, J., Bansal, R., . . . Toga, A. W. (2007). Sex differences in cortical thickness mapped in 176 healthy individuals between 7 and 87 years of age. *Cereb Cortex*, *17*(7), 1550-1560. doi:10.1093/cercor/bhl066
- Stein, J. L., Medland, S. E., Vasquez, A. A., Hibar, D. P., Senstad, R. E., Winkler, A. M., Enhancing Neuro Imaging Genetics through Meta-Analysis, C. (2012). Identification of common variants associated with human hippocampal and intracranial volumes. *Nat Genet*, *44*(5), 552-561. doi:10.1038/ng.2250
- Storsve, A. B., Fjell, A. M., Tamnes, C. K., Westlye, L. T., Overbye, K., Aasland, H. W., & Walhovd, K. B. (2014). Differential longitudinal changes in cortical thickness, surface area and volume across the adult life span: regions of accelerating and decelerating change. *J Neurosci*, *34*(25), 8488-8498. doi:10.1523/JNEUROSCI.0391-14.2014
- Strike, L. T., Hansell, N. K., Couvy-Duchesne, B., Thompson, P. M., de Zubicaray, G. I., McMahon, K. L., & Wright, M. J. (2018). Genetic Complexity of Cortical Structure: Differences in Genetic and Environmental Factors Influencing Cortical Surface Area and Thickness. *Cereb Cortex*. doi:10.1093/cercor/bhy002
- Tamnes, C. K., Ostby, Y., Fjell, A. M., Westlye, L. T., Due-Tønnessen, P., & Walhovd, K. B. (2010). Brain maturation in adolescence and young adulthood: regional age-related changes in cortical thickness and white matter volume and microstructure. *Cereb Cortex*, *20*(3), 534-548. doi:10.1093/cercor/bhp118
- Thompson, P. M., Andreassen, O. A., Arias-Vasquez, A., Bearden, C. E., Boedhoe, P. S., Brouwer, R. M., . . . Consortium, E. (2017). ENIGMA and the individual: Predicting factors that affect the brain in 35 countries worldwide. *Neuroimage*, *145*(Pt B), 389-408. doi:10.1016/j.neuroimage.2015.11.057
- Thompson, P. M., Cannon, T. D., Narr, K. L., van Erp, T., Poutanen, V. P., Huttunen, M., . . . Toga, A. W. (2001). Genetic influences on brain structure. *Nat Neurosci*, *4*(12), 1253-1258. doi:10.1038/nn758
- Thompson, P. M., Dutton, R. A., Hayashi, K. M., Lu, A., Lee, S. E., Lee, J. Y., . . . Becker, J. T. (2006). 3D mapping of ventricular and corpus callosum abnormalities in HIV/AIDS. *Neuroimage*, *31*(1), 12-23. doi:10.1016/j.neuroimage.2005.11.043
- Thompson, P. M., Stein, J. L., Medland, S. E., Hibar, D. P., Vasquez, A. A., Renteria, M. E., . . . Alzheimer's Disease Neuroimaging Initiative, E. C. I. C. S. Y. S. G. (2014).

- The ENIGMA Consortium: large-scale collaborative analyses of neuroimaging and genetic data. *Brain Imaging Behav*, 8(2), 153-182. doi:10.1007/s11682-013-9269-5
- Trachtenberg, J. T., Chen, B. E., Knott, G. W., Feng, G., Sanes, J. R., Welker, E., & Svoboda, K. (2002). Long-term in vivo imaging of experience-dependent synaptic plasticity in adult cortex. *Nature*, 420(6917), 788-794. doi:10.1038/nature01273
- Tucker-Drob, E. M., Rhemtulla, M., Harden, K. P., Turkheimer, E., & Fask, D. (2011). Emergence of a Gene x socioeconomic status interaction on infant mental ability between 10 months and 2 years. *Psychol Sci*, 22(1), 125-133. doi:10.1177/0956797610392926
- Turkheimer, E., Haley, A., Waldron, M., D'Onofrio, B., & Gottesman, I. I. (2003). Socioeconomic status modifies heritability of IQ in young children. *Psychol Sci*, 14(6), 623-628. doi:10.1046/j.0956-7976.2003.psci_1475.x
- Udden, J., Snijders, T. M., Fisher, S. E., & Hagoort, P. (2017). A common variant of the CNTNAP2 gene is associated with structural variation in the left superior occipital gyrus. *Brain Lang*, 172, 16-21. doi:10.1016/j.bandl.2016.02.003
- van Dongen, J., Slagboom, P. E., Draisma, H. H., Martin, N. G., & Boomsma, D. I. (2012). The continuing value of twin studies in the omics era. *Nat Rev Genet*, 13(9), 640-653. doi:10.1038/nrg3243
- van Erp, T. G., Hibar, D. P., Rasmussen, J. M., Glahn, D. C., Pearlson, G. D., Andreassen, O. A., . . . Turner, J. A. (2016). Subcortical brain volume abnormalities in 2028 individuals with schizophrenia and 2540 healthy controls via the ENIGMA consortium. *Mol Psychiatry*, 21(4), 547-553. doi:10.1038/mp.2015.63
- Van Essen, D. C., Smith, S. M., Barch, D. M., Behrens, T. E., Yacoub, E., Ugurbil, K., & Consortium, W. U.-M. H. (2013). The WU-Minn Human Connectome Project: an overview. *Neuroimage*, 80, 62-79. doi:10.1016/j.neuroimage.2013.05.041
- Van Essen, D. C., Ugurbil, K., Auerbach, E., Barch, D., Behrens, T. E., Bucholz, R., . . . Consortium, W. U.-M. H. (2012). The Human Connectome Project: a data acquisition perspective. *Neuroimage*, 62(4), 2222-2231. doi:10.1016/j.neuroimage.2012.02.018
- van Leeuwen, M., Peper, J. S., van den Berg, S. M., Brouwer, R. M., Hulshoff Pol, H. E., Kahn, R. S., & Boomsma, D. I. (2009). A genetic analysis of brain volumes and IQ in children. *Intelligence*, 37(2), 181-191.

- van Soelen, I. L., Brouwer, R. M., van Baal, G. C., Schnack, H. G., Peper, J. S., Chen, L., . . . Hulshoff Pol, H. E. (2013). Heritability of volumetric brain changes and height in children entering puberty. *Hum Brain Mapp*, *34*(3), 713-725. doi:10.1002/hbm.21468
- van Soelen, I. L., Brouwer, R. M., van Baal, G. C., Schnack, H. G., Peper, J. S., Collins, D. L., . . . Hulshoff Pol, H. E. (2012). Genetic influences on thinning of the cerebral cortex during development. *Neuroimage*, *59*(4), 3871-3880. doi:10.1016/j.neuroimage.2011.11.044
- van Soelen, I. L., Brouwer, R. M., van Leeuwen, M., Kahn, R. S., Hulshoff Pol, H. E., & Boomsma, D. I. (2011). Heritability of verbal and performance intelligence in a pediatric longitudinal sample. *Twin Res Hum Genet*, *14*(2), 119-128. doi:10.1375/twin.14.2.119
- Vavrek, M. J. (2011). fossil: Palaeoecological and palaeogeographical analysis tools. *Palaeontologia Electronica*, *14*(1), 1T.
- Vertes, P. E., & Bullmore, E. T. (2015). Annual research review: Growth connectomics--the organization and reorganization of brain networks during normal and abnormal development. *J Child Psychol Psychiatry*, *56*(3), 299-320. doi:10.1111/jcpp.12365
- Verweij, K. J., Mosing, M. A., Zietsch, B. P., & Medland, S. E. (2012). Estimating heritability from twin studies. *Methods Mol Biol*, *850*, 151-170. doi:10.1007/978-1-61779-555-8_9
- Vinkhuyzen, A. A., Wray, N. R., Yang, J., Goddard, M. E., & Visscher, P. M. (2013). Estimation and partition of heritability in human populations using whole-genome analysis methods. *Annu Rev Genet*, *47*, 75-95. doi:10.1146/annurev-genet-111212-133258
- Visscher, P. M., Gordon, S., & Neale, M. C. (2008). Power of the classical twin design revisited: II detection of common environmental variance. *Twin Res Hum Genet*, *11*(1), 48-54. doi:10.1375/twin.11.1.48
- Visscher, P. M., Hill, W. G., & Wray, N. R. (2008). Heritability in the genomics era-- concepts and misconceptions. *Nat Rev Genet*, *9*(4), 255-266. doi:10.1038/nrg2322
- Vitaro, F., Brendgen, M., & Arseneault, L. (2009). The discordant MZ-twin method: One step closer to the holy grail of causality. *International Journal of Behavioral Development*, *33*(4), 376-382. doi:10.1177/0165025409340805

- Vuoksima, E., Panizzon, M. S., Chen, C. H., Fiecas, M., Eyer, L. T., Fennema-Notestine, C., . . . Kremen, W. S. (2015). The Genetic Association Between Neocortical Volume and General Cognitive Ability Is Driven by Global Surface Area Rather Than Thickness. *Cereb Cortex*, 25(8), 2127-2137. doi:10.1093/cercor/bhu018
- Vuoksima, E., Panizzon, M. S., Chen, C. H., Fiecas, M., Eyer, L. T., Fennema-Notestine, C., . . . Kremen, W. S. (2016). Is bigger always better? The importance of cortical configuration with respect to cognitive ability. *Neuroimage*, 129, 356-366. doi:10.1016/j.neuroimage.2016.01.049
- Waddington, C. H. (1942). Canalization of development and the inheritance of acquired characters. *Nature*, 150(3811), 563-565. doi:DOI 10.1038/150563a0
- Wagner, D. R., & Heyward, V. H. (2000). Measures of body composition in blacks and whites: a comparative review. *Am J Clin Nutr*, 71(6), 1392-1402. doi:10.1093/ajcn/71.6.1392
- Wainwright, M., Wright, M. J., Geffen, G. M., Geffen, L. B., Luciano, M., & Martin, N. G. (2004). Genetic and environmental sources of covariance between reading tests used in neuropsychological assessment and IQ subtests. *Behav Genet*, 34(4), 365-376. doi:10.1023/B:BEGE.0000023642.34853.cb
- Wallace, G. L., Eric Schmitt, J., Lenroot, R., Viding, E., Ordaz, S., Rosenthal, M. A., . . . Giedd, J. N. (2006). A pediatric twin study of brain morphometry. *J Child Psychol Psychiatry*, 47(10), 987-993. doi:10.1111/j.1469-7610.2006.01676.x
- Wallace, G. L., Lee, N. R., Prom-Wormley, E. C., Medland, S. E., Lenroot, R. K., Clasen, L. S., . . . Giedd, J. N. (2010). A bivariate twin study of regional brain volumes and verbal and nonverbal intellectual skills during childhood and adolescence. *Behav Genet*, 40(2), 125-134. doi:10.1007/s10519-009-9329-1
- Warnes, G. R., Bolker, B., Bonebakker, L., Gentleman, R., Huber, W., Liaw, A., . . . Venables, B. (2016). gplots: Various R Programming Tools for Plotting Data: <https://CRAN.R-project.org/package=gplots>.
- Wei, T., & Simko, V. (2016). corrplot: Visualization of a correlation matrix. Retrieved from <https://CRAN.R-project.org/package=corrplot>
- Weiner, J. (2017). riverplot: Sankey or Ribbon Plots. Retrieved from <https://CRAN.R-project.org/package=riverplot>

- Weintraub, S., Dikmen, S. S., Heaton, R. K., Tulsky, D. S., Zelazo, P. D., Bauer, P. J., . . . Gershon, R. C. (2013). Cognition assessment using the NIH Toolbox. *Neurology*, *80*(11 Suppl 3), S54-64. doi:10.1212/WNL.0b013e3182872ded
- Wen, W., Thalamuthu, A., Mather, K. A., Zhu, W., Jiang, J., de Micheaux, P. L., . . . Sachdev, P. S. (2016). Distinct Genetic Influences on Cortical and Subcortical Brain Structures. *Sci Rep*, *6*, 32760. doi:10.1038/srep32760
- Whelan, C. D., Hibar, D. P., van Velzen, L. S., Zannas, A. S., Carrillo-Roa, T., McMahon, K., . . . Alzheimer's Disease Neuroimaging, I. (2016). Heritability and reliability of automatically segmented human hippocampal formation subregions. *Neuroimage*, *128*, 125-137. doi:10.1016/j.neuroimage.2015.12.039
- Wiers, C. E. (2012). Methylation and the human brain: towards a new discipline of imaging epigenetics. *Eur Arch Psychiatry Clin Neurosci*, *262*(3), 271-273. doi:10.1007/s00406-011-0261-z
- Winkler, A. M., Greve, D. N., Bjuvand, K. J., Nichols, T. E., Sabuncu, M. R., Haberg, A. K., . . . Rimol, L. M. (2018). Joint Analysis of Cortical Area and Thickness as a Replacement for the Analysis of the Volume of the Cerebral Cortex. *Cereb Cortex*, *28*(2), 738-749. doi:10.1093/cercor/bhx308
- Winkler, A. M., Kochunov, P., Blangero, J., Almasy, L., Zilles, K., Fox, P. T., . . . Glahn, D. C. (2010). Cortical thickness or grey matter volume? The importance of selecting the phenotype for imaging genetics studies. *Neuroimage*, *53*(3), 1135-1146. doi:10.1016/j.neuroimage.2009.12.028
- Woodley Of Menie, M. A., Fernandes, H. B. F., & Hopkins, W. D. (2015). The more g-loaded, the more heritable, evolvable, and phenotypically variable: Homology with humans in chimpanzee cognitive abilities. *Intelligence*, *50*, 159-163. doi:10.1016/j.intell.2015.04.002
- Wray, N. R., Lee, S. H., Mehta, D., Vinkhuyzen, A. A., Dudbridge, F., & Middeldorp, C. M. (2014). Research review: Polygenic methods and their application to psychiatric traits. *J Child Psychol Psychiatry*, *55*(10), 1068-1087. doi:10.1111/jcpp.12295
- Wright, I. C., Sham, P., Murray, R. M., Weinberger, D. R., & Bullmore, E. T. (2002). Genetic contributions to regional variability in human brain structure: methods and preliminary results. *Neuroimage*, *17*(1), 256-271.

- Wright, M. J., & Martin, N. G. (2004). Brisbane adolescent twin study: Outline of study methods and research projects. *Australian Journal of Psychology*, 56(2), 65-78. doi:10.1080/00049530410001734865
- Yang, J., Lee, S. H., Goddard, M. E., & Visscher, P. M. (2011). GCTA: a tool for genome-wide complex trait analysis. *Am J Hum Genet*, 88(1), 76-82. doi:10.1016/j.ajhg.2010.11.011
- Yoon, U., Fahim, C., Perusse, D., & Evans, A. C. (2010). Lateralized genetic and environmental influences on human brain morphology of 8-year-old twins. *Neuroimage*, 53(3), 1117-1125. doi:10.1016/j.neuroimage.2010.01.007
- Zatorre, R. J., Fields, R. D., & Johansen-Berg, H. (2012). Plasticity in gray and white: neuroimaging changes in brain structure during learning. *Nat Neurosci*, 15(4), 528-536. doi:10.1038/nn.3045
- Zhang, M., Li, J., Chen, C., Mei, L., Xue, G., Lu, Z., . . . Dong, Q. (2013). The contribution of the left mid-fusiform cortical thickness to Chinese and English reading in a large Chinese sample. *Neuroimage*, 65, 250-256. doi:10.1016/j.neuroimage.2012.09.045
- Zhao, Y., & Castellanos, F. X. (2016). Annual Research Review: Discovery science strategies in studies of the pathophysiology of child and adolescent psychiatric disorders--promises and limitations. *J Child Psychol Psychiatry*, 57(3), 421-439. doi:10.1111/jcpp.12503

Appendix 1 Ethics Approval for QTIM and HCP Datasets



THE UNIVERSITY OF QUEENSLAND
Institutional Human Research Ethics Approval

Project Title: Genetics Of Brain Structure And Function - 08/10/2015 - AMENDMENT

Chief Investigator: A/Prof Margaret Wright

Supervisor: None

Co-Investigator(s): Prof Greig de Zubicaray, A/Prof Katie McMahon, Prof Paul Thompson, Prof Nick Martin

School(s): QBI

Approval Number: 2004000185

Granting Agency/Degree: NIH

Duration: 31st December 2018

Comments/Conditions:

MREC (40)

APPROVES


Note: if this approval is for amendments to an originally submitted, then the researchers must submit Information Sheets & Consent Forms as a resubmission.

Name of responsible Committee:
Medical Research Ethics C
This project complies with the *Ethical Conduct in Human Research* and will not involve any experimentation on humans.

Name of Ethics Committee Chairperson:
Professor Bill Vicenzino
Chairperson
Medical Research Ethics C

Form was participant

on
ning

Signature 

Date 13/10/2015



THE UNIVERSITY OF QUEENSLAND
Institutional Approval Form For Experiments On Humans
Including Behavioural Research

Chief Investigator: Dr Margie Wright
Project Title: Genes For Cognition - 15/03/2012 - AMENDMENT
Supervisor: None
Co-Investigator(s): Prof Nick Martin, Dr Narelle Hansell, Prof Graeme Halford, Prof David Shum, Dr Glenda Andrews, Prof Gina Geffen, Nico Martin
Department(s): Queensland Institute of Medical Research (QIMR)
Project Number: 2008001873
Granting Agency/Degree: ARC
Duration: 31st December 2028

Comments:

**Name of responsible Committee:-
Medical Research Ethics Committee**

This project complies with the provisions contained in the *National Statement on Ethical Conduct in Human Research* and complies with the regulations governing experimentation on humans.

**Name of Ethics Committee representative:-
Professor Bill Vicenzino
Chairperson
Medical Research Ethics Committee**

Date: 21/3/12

Signature: 



THE UNIVERSITY OF QUEENSLAND

Institutional Human Research Ethics Approval

Project Title: Data Sharing using the Human Connectome Project (HCP)
Databases: Replication and Meta/Mega-analyses

Chief Investigator: A/Prof Margie Wright

Supervisor: None

Co-Investigator(s): A/Prof Katie McMahon, Dr Narelle Hansell, Mr Baptiste Couvy-Duchesne, Mr Lachlan Strike, Mr Liang-Dar (Daniel) Hwang, Ms Liza van Eijk, Ms Victoria O'Callaghan

School(s): QBI

Approval Number: 2017000229

Granting Agency/Degree: NHMRC Project APP1078756; NIH Award 1U54EB020403-01

Duration: 30th April 2022

Comments/Conditions:

Expedited Review - Low Risk

- Application, 22/02/2017
- Protocol, 22/02/2017
- Certification Data Term Use Queensland
- Data Use Terms HCP Restricted Access 26Jan2016

Note: if this approval is for amendments to an already approved protocol for which a UQ Clinical Trials Protection/Insurance Form was originally submitted, then the researchers must directly notify the UQ Insurance Office of any changes to that Form and Participant Information Sheets & Consent Forms as a result of the amendments, before action.

Name of responsible Committee:

University of Queensland Human Research Ethics Committee B

This project complies with the provisions contained in the *National Statement on Ethical Conduct in Human Research* and complies with the regulations governing experimentation on humans.

Name of Ethics Committee representative:

Dr. Frederick Khafagi

Chairperson

University of Queensland Human Research Ethics Committee

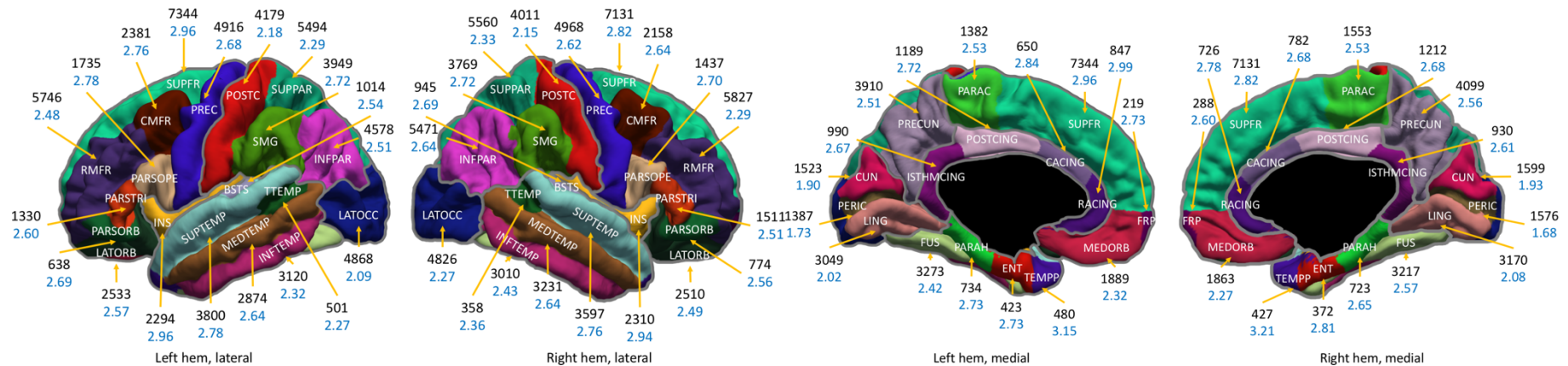
Registration: EC00457

11/04/2017

Signature _____

Date _____

Appendix 2 The Desikan-Killiany Atlas, with Total Surface Area and Mean Cortical Thickness Estimates in the QTIM Dataset



Total surface area (mm²; black) and mean cortical thickness (mm; blue) for 34 regions of interest (per hemisphere) of the Desikan-Killiany atlas. Grey outline denotes lobar divisions (frontal, parietal, occipital, temporal, cingulate, insular).

BSTS banks of the superior temporal sulcus; *CACING* caudal anterior cingulate; *CMFR* caudal middle frontal gyrus; *CUN* cuneus cortex; *ENT* entorhinal cortex; *FRP* frontal pole; *FUS* fusiform gyrus; *INFPAR* inferior parietal cortex; *INTEMP* inferior temporal gyrus; *INS* insular cortex; *ISTHMCING* isthmus cingulate; *LATOCC* lateral occipital cortex; *LATORB* lateral orbitofrontal cortex; *LING* lingual gyrus; *MEDORB* medial orbitofrontal cortex; *MIDTEMP* middle temporal gyrus; *PARAC* paracentral lobule; *PARAH* parahippocampal gyrus; *PARSOPE* pars opercularis; *PARSORB* pars orbitalis; *PARSTR* pars triangularis; *PERIC* pericalcarine cortex; *POSTC* postcentral gyrus; *POSTCING* posterior cingulate; *PREC* precentral gyrus; *PRECUN*; precuneus cortex; *RACING* rostral anterior cingulate; *RMFR* rostral

middle frontal gyrus; *SUPFR* superior frontal gyrus; *SUPPAR* superior parietal cortex; *SUPTEMP* superior temporal gyrus; *SMG* supramarginal cortex; *TEMPP* temporal pole; *TTEMP* transverse temporal cortex.

Appendix 3 Descriptive Statistics for Surface Area and Cortical Thickness in the QTIM Dataset

Number of excluded measures, mean (SD), minimum, maximum, percentage difference between male and female raw means, and number of outliers (± 3.29 SD) for QTIM surface area and cortical thickness ($N = 923$).

	Excluded [†]	Surface Area (mm ²)					Cortical Thickness (mm)				
		Mean (SD)	Minimum	Maximum	M/F Diff [†]	Outliers [‡]	Mean (SD)	Minimum	Maximum	M/F Diff [†]	Outliers [‡]
<i>Frontal</i>											
Superior frontal gyrus left	0	7344 (860)	5068	10177	11.81	2	2.96 (0.15)	2.49	3.47	-1.97	2
Superior frontal gyrus right	1	7131 (846)	4843	10094	11.23	2	2.82 (0.14)	2.35	3.31	-1.33	3
Rostral middle frontal gyrus left	1	5746 (797)	3708	8977	13.47	2	2.48 (0.13)	2.08	2.9	-1.49	1
Rostral middle frontal gyrus right	2	5827 (794)	3903	9376	12.75	4	2.29 (0.12)	1.95	2.7	-2.04	2
Caudal middle frontal gyrus left	1	2381 (383)	1315	3528	10.82	0	2.76 (0.15)	2.17	3.33	0.53	2
Caudal middle frontal gyrus right	0	2158 (400)	1187	3554	12.25	3	2.64 (0.15)	2.17	3.26	-0.31	3
Pars opercularis left	1	1735 (267)	1020	2619	9.80	1	2.78 (0.15)	2.33	3.49	1.13	2
Pars opercularis right	3	1437 (236)	803	2342	9.85	3	2.7 (0.16)	2.3	3.23	0.16	2
Pars triangularis left	1	1330 (205)	791	2064	11.49	2	2.6 (0.16)	2.08	3.06	-2.16	1
Pars triangularis right	3	1511 (250)	913	2422	10.60	2	2.51 (0.15)	2.14	2.96	-1.13	0
Pars orbitalis left	1	638 (83)	425	937	9.67	1	2.69 (0.24)	1.94	3.65	-3.45	2
Pars orbitalis right	0	774 (101)	493	1169	11.21	1	2.56 (0.23)	1.87	3.29	-3.03	0
Lateral orbitofrontal cortex left	1	2535 (318)	1663	3557	9.17	0	2.57 (0.17)	2.03	3.07	-2.63	1
Lateral orbitofrontal cortex right	0	2510 (329)	1668	3837	10.30	1	2.49 (0.17)	1.94	3.06	-1.39	3
Medial orbitofrontal cortex left	0	1889 (250)	1147	2826	9.19	2	2.32 (0.18)	1.74	2.9	-3.54	1
Medial orbitofrontal cortex right	0	1863 (235)	1147	2604	8.13	0	2.27 (0.19)	1.7	2.99	-3.88	1
Precentral gyrus left	4	4916 (598)	3508	7128	13.35	3	2.68 (0.13)	2.19	3.08	-0.05	5
Precentral gyrus right	8	4968 (609)	3588	7148	12.79	1	2.62 (0.13)	2.06	3.15	-0.59	7
Paracentral lobule left	2	1382 (189)	810	2079	7.20	2	2.53 (0.15)	2.08	3.07	-0.30	1
Paracentral lobule right	1	1553 (236)	995	2459	9.98	5	2.53 (0.16)	1.97	3.05	-0.03	2
Frontal pole left	0	219 (35)	110	339	7.56	1	2.73 (0.35)	1.82	4.01	-8.28	3
Frontal pole right	0	288 (43)	172	451	7.45	1	2.6 (0.33)	1.74	3.73	-7.89	2
<i>Parietal</i>											
Superior parietal cortex left	0	5494 (668)	3762	8565	10.94	2	2.29 (0.11)	1.95	2.66	1.19	0
Superior parietal cortex right	0	5560 (678)	3747	7867	11.65	1	2.33 (0.12)	1.92	2.66	0.95	1
Inferior parietal cortex left	0	4578 (646)	2973	6903	12.62	2	2.51 (0.13)	2.16	3.02	1.94	3
Inferior parietal cortex right	1	5471 (755)	3766	8327	13.54	4	2.64 (0.13)	2.13	3.14	1.10	4
Supramarginal cortex left	8	3949 (590)	2438	6328	13.48	3	2.72 (0.14)	2.23	3.19	1.96	4
Supramarginal cortex right	10	3769 (532)	2335	6024	12.12	4	2.72 (0.13)	2.31	3.1	1.16	0

Postcentral gyrus left	4	4179 (508)	3029	6023	11.69	2	2.18 (0.12)	1.85	2.52	0.94	0
Postcentral gyrus right	8	4011 (513)	2791	5841	11.88	4	2.15 (0.12)	1.74	2.58	0.55	5
Precuneus cortex left	0	3910 (497)	2684	5696	12.53	4	2.51 (0.13)	2.07	2.95	1.78	2
Precuneus cortex right	0	4099 (545)	2802	5887	13.07	1	2.56 (0.13)	2.09	3	1.44	2
<i>Occipital</i>											
Lateral occipital cortex left	0	4868 (578)	3398	6782	11.97	1	2.09 (0.11)	1.71	2.52	0.11	3
Lateral occipital cortex right	0	4826 (616)	3167	7003	12.62	1	2.27 (0.12)	1.94	2.7	-0.09	1
Lingual gyrus left	0	3049 (411)	1965	4210	10.90	0	2.02 (0.11)	1.66	2.43	1.70	3
Lingual gyrus right	0	3170 (392)	2013	4512	9.78	1	2.08 (0.12)	1.72	2.57	1.39	3
Cuneus cortex left	0	1523 (215)	916	2332	11.71	3	1.9 (0.13)	1.55	2.43	0.03	1
Cuneus cortex right	1	1599 (222)	803	2275	12.76	2	1.93 (0.14)	1.53	2.43	-0.60	2
Pericalcarine cortex left	0	1387 (231)	766	2160	10.88	2	1.73 (0.13)	1.33	2.15	-0.54	1
Pericalcarine cortex right	0	1576 (243)	797	2262	11.53	0	1.68 (0.14)	1.33	2.15	-1.17	2
<i>Temporal</i>											
Superior temporal gyrus left	2	3800 (471)	2528	5993	11.59	5	2.78 (0.18)	2.24	3.31	-0.29	0
Superior temporal gyrus right	2	3597 (414)	2573	5172	9.50	3	2.76 (0.17)	2.19	3.36	0.22	2
Middle temporal gyrus left	2	2874 (417)	1788	4228	12.40	0	2.64 (0.2)	2.12	3.31	-1.02	1
Middle temporal gyrus right	2	3231 (438)	2153	4732	12.31	2	2.64 (0.19)	2.11	3.35	-2.19	3
Inferior temporal gyrus left	2	3120 (484)	1881	4897	12.89	4	2.32 (0.18)	1.83	2.99	-1.70	2
Inferior temporal gyrus right	2	3010 (473)	1888	4994	12.45	4	2.43 (0.18)	1.82	3.05	-2.73	2
Banks of the superior temporal sulcus left	0	1014 (175)	569	1792	11.62	6	2.54 (0.18)	1.91	3.14	2.58	2
Banks of the superior temporal sulcus right	0	945 (148)	592	1546	11.21	3	2.69 (0.17)	2.17	3.33	0.91	2
Fusiform gyrus left	1	3273 (432)	1967	5049	11.50	3	2.42 (0.17)	1.88	3.05	-1.33	1
Fusiform gyrus right	2	3217 (438)	1849	4703	12.72	1	2.57 (0.15)	2.09	3.07	-0.84	1
Transverse temporal cortex left	1	501 (85)	298	861	8.38	4	2.27 (0.23)	1.35	3.05	-0.75	2
Transverse temporal cortex right	0	358 (62)	228	573	7.93	3	2.36 (0.22)	1.6	2.97	0.41	1
Entorhinal cortex left	1	423 (87)	170	759	13.94	5	2.73 (0.43)	1.57	4.24	-0.47	2
Entorhinal cortex right	3	372 (97)	109	814	9.24	10	2.81 (0.47)	1.69	4.45	0.44	2
Temporal pole left	3	480 (62)	279	676	7.80	1	3.15 (0.48)	1.63	4.42	-7.31	0
Temporal pole right	4	427 (69)	189	661	3.44	3	3.21 (0.53)	1.36	4.56	-2.31	1
Parahippocampal gyrus left	3	734 (107)	483	1103	8.87	3	2.73 (0.26)	1.96	3.47	0.06	0
Parahippocampal gyrus right	1	723 (102)	437	1190	9.19	8	2.65 (0.23)	1.98	3.4	0.36	2
<i>Cingulate</i>											
Rostral anterior cingulate left	0	847 (165)	363	1499	13.28	2	2.99 (0.22)	2.23	3.73	-2.42	2
Rostral anterior cingulate right	1	726 (145)	349	1301	13.07	5	2.78 (0.23)	2	3.51	-1.40	1
Caudal anterior cingulate left	1	650 (135)	336	1148	8.64	4	2.84 (0.22)	2.19	3.73	-1.82	5
Caudal anterior cingulate right	1	782 (158)	322	1488	9.62	5	2.68 (0.22)	2.11	3.43	-0.73	2
Posterior cingulate left	0	1189 (183)	674	1875	9.44	1	2.72 (0.17)	2.2	3.42	0.46	2
Posterior cingulate right	1	1212 (183)	767	1797	10.23	0	2.68 (0.15)	2.18	3.31	1.43	2
Isthmus cingulate left	1	990 (179)	570	1636	14.15	4	2.67 (0.21)	2.04	3.52	0.65	3
Isthmus cingulate right	0	930 (161)	535	1712	10.75	2	2.61 (0.22)	2	3.27	1.26	0
<i>Insular</i>											
Insular cortex left	1	2294 (297)	1543	3533	9.69	7	2.96 (0.17)	2.41	3.4	2.07	0

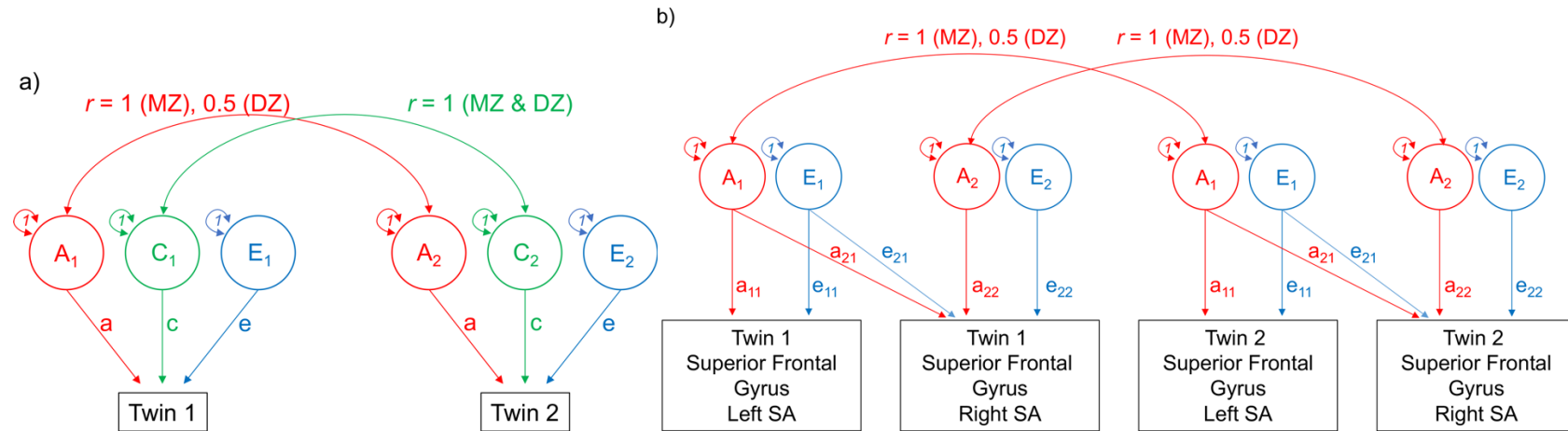
Insular cortex right	1	2310 (296)	1644	3582	10.31	4	2.94 (0.19)	2.27	3.49	1.48	2
----------------------	---	------------	------	------	-------	---	-------------	------	------	------	---

*Variables were excluded based on visual inspection of the accuracy of cortical parcellations as per ENIGMA protocols (enigma.ini.usc.edu).

†Percentage difference between male and female raw means; positive (negative) percentage denotes larger/thicker value for males (females).

‡Outliers ± 3.29 SD from the mean were replaced by the corresponding threshold value (i.e. ± 3.29).

Appendix 4 The Classic Twin Design and the AE Bivariate Twin Design



(a) The classic twin (ACE) model. The model partitions the variance in a phenotype into additive genetic (A), common or shared environment (C) and unique or non-shared environment (E) sources (Neale and Cardon 1992). Estimates of unique environment also include measurement error, as it is random and unrelated to twin similarity. The additive genetic factors (A) correlate at 1 for MZ and 0.5 for DZ twins (who share 100% and (on average) 50% of their genetic material respectively), the common environment factors (C) correlate at 1 for both MZ and DZ (the model assumes MZ and DZ twins raised together experience similar environments), and the unique environment factors (E) are uncorrelated between twin pairs as this represents environmental influence affecting one twin only. To determine the most parsimonious model, nested models containing AE, CE, or E sources of variance were compared to the fully saturated ACE decomposition. We assessed the fit of the constrained models by examining the $-2 \log$ likelihood difference between the ACE model and the reduced model (AE, CE or E). The difference in the maximum likelihood (assessed through the $-2 \log$ likelihood difference) is distributed as a chi-squared statistic for a given number of degrees of freedom (equal to the difference in the number of free parameters estimated), which denotes whether the parameter is significant. If a reduced model is significant, this indicates that the

parameter removed from the model accounted for a significant proportion of the phenotypic variance. (b) The AE bivariate twin design. The variance in the observed variables (phenotypes; denoted as rectangles) is partitioned into additive genetic (A) and unique environment (E) sources; represented as circles. Effects of common environment (C) were not assessed in this model. The correlation between genetic components is equal to 1 for MZ and 0.5 for DZ twins respectively. Double headed arrows represent the covariance between variables, or the covariance of a variance with itself. Unique environment components are uncorrelated. The design assumes that the first genetic variable (A_1) explains genetic variance in the first phenotype (superior frontal gyrus left surface area) and the second phenotype (superior frontal gyrus right surface area). Any variance in the second phenotype (i.e. specific variance) which is not due to the first latent variable is assumed to be due to a second latent variable (A_2). Latent variables are specified for each source of variance specified in the model. It is important to note that while the first genetic variable (A_1) explains variance in the first and second phenotype, it cannot be interpreted as a common factor as it includes both common (a_{21}) and specific (a_{11}) variance (Loehlin, 1996). From the covariance decompositions, we further estimated genetic, environmental, and phenotypic correlations. Genetic (environmental) correlations indicate the extent to which two phenotypes share genetic (environmental) variance. Both genetic and environmental correlations underlie the phenotypic correlation. As a high genetic correlation between two traits can be observed, even if the traits themselves have low heritability, a high genetic correlation can be misleading when genes explain only a small portion of the phenotypic variance. Hence, we examined shared genetic influence between ROIs by calculating the genetic contribution to the phenotypic correlation (r_{ph-a}):

$$\sqrt{(ROI\ 1\ heritability)} \times \text{genetic correlation} \times \sqrt{(ROI\ 2\ heritability)}$$

r_{ph-a} is easily conceptualised as the phenotypic correlation (r_{ph}) between two traits based only on the shared genetic variance. We similarly calculated the environmental contribution to the phenotypic correlation (r_{ph-e}). Both r_{ph-a} and r_{ph-e} were computed using variance estimates from the bivariate model in which the genetic (environmental) correlations were estimated. The significance of the genetic or

environmental contribution to the phenotypic correlation was assessed by fitting a reduced model in which the genetic or unique environmental covariance between ROIs (a_{21} or e_{21} respectively) was set to zero and assessing model fit. The significance of the phenotypic correlation was assessed by setting both the genetic and environmental covariances between ROIs to zero.

Appendix 5 Regression Coefficients and *q* values for Surface Area Covariates in the QTIM Dataset

	Total Surface Area		Age		Age2		Age3		Sex		Age x Sex		Age2 x Sex		Age3 x Sex		Acquisition Orientation [†]	
	Regression Coefficient	<i>q</i> value	Regression Coefficient	<i>q</i> value	Regression Coefficient	<i>q</i> value	Regression Coefficient	<i>q</i> value	Regression Coefficient	<i>q</i> value	Regression Coefficient	<i>q</i> value	Regression Coefficient	<i>q</i> value	Regression Coefficient	<i>q</i> value	Regression Coefficient	<i>q</i> value
<i>Frontal</i>																		
Superior frontal gyrus left	0.85	3.44E-187	-0.04	0.51	-0.07	0.19	-0.10	0.06	-6.73E-04	1.00	0.03	0.76	0.01	0.98	0.03	0.76	-0.13	0.09
Superior frontal gyrus right	0.86	1.23E-180	-0.01	0.90	-0.06	0.32	-0.09	0.15	0.13	0.68	0.02	0.78	-0.03	0.89	0.02	0.89	1.02E-03	1.00
Rostral middle frontal gyrus left	0.82	2.19E-157	0.01	0.93	-0.02	0.86	-0.07	0.33	0.14	0.68	-0.03	0.72	-0.04	0.84	6.83E-04	1.00	-0.25	2.89E-04
Rostral middle frontal gyrus right	0.81	5.98E-142	0.02	0.84	0.02	0.87	0.03	0.81	0.18	0.60	-0.03	0.78	-0.09	0.67	-0.07	0.38	-0.19	0.02
Caudal middle frontal gyrus left	0.61	1.52E-58	-0.14	0.03	-0.02	0.91	0.05	0.71	-0.21	0.67	0.19	4.05E-03	0.01	0.98	-0.10	0.36	0.10	0.55
Caudal middle frontal gyrus right	0.66	5.81E-67	-3.46E-03	0.98	0.04	0.78	-0.03	0.86	0.11	0.84	-1.42E-03	1.00	0.01	0.99	3.02E-03	0.99	-0.17	0.17
Pars opercularis left	0.61	8.65E-56	0.03	0.84	-0.01	0.96	-0.09	0.46	0.34	0.35	-0.02	0.87	-0.10	0.74	0.06	0.73	-0.14	0.32
Pars opercularis right	0.61	4.26E-56	0.06	0.55	-0.03	0.84	-0.07	0.60	0.07	0.90	-0.09	0.34	0.09	0.77	0.07	0.68	-0.08	0.71
Pars triangularis left	0.60	1.43E-56	0.08	0.38	-0.06	0.61	-0.09	0.38	0.03	0.96	-0.10	0.23	0.07	0.84	0.11	0.36	-0.07	0.74
Pars triangularis right	0.58	3.67E-51	0.03	0.84	0.04	0.80	7.86E-04	1.00	0.19	0.72	-0.03	0.87	-0.06	0.86	0.03	0.89	0.01	0.96
Pars orbitalis left	0.64	2.24E-68	0.05	0.61	-0.11	0.12	-0.03	0.83	-0.05	0.93	-0.08	0.33	0.08	0.79	-0.02	0.90	0.11	0.46
Pars orbitalis right	0.57	7.91E-55	0.05	0.69	0.04	0.79	0.05	0.74	0.14	0.78	-0.02	0.87	-0.21	0.27	-0.09	0.50	0.19	0.11
Lateral orbitofrontal cortex left	0.78	5.29E-119	0.05	0.52	-0.06	0.54	-0.01	0.91	0.10	0.83	-0.08	0.30	0.08	0.72	0.03	0.85	0.53	4.47E-13
Lateral orbitofrontal cortex right	0.70	9.17E-87	0.05	0.68	1.02E-03	1.00	0.02	0.87	0.22	0.59	-0.06	0.60	-0.08	0.78	-0.06	0.67	-0.27	3.04E-03
Medial orbitofrontal cortex left	0.69	2.09E-81	0.05	0.68	-0.09	0.25	-3.06E-04	1.00	-0.18	0.71	-0.03	0.85	0.20	0.26	0.02	0.91	-0.17	0.12
Medial orbitofrontal cortex right	0.79	3.61E-113	0.13	0.03	0.05	0.61	0.03	0.86	0.40	0.13	-0.11	0.11	0.02	0.96	0.07	0.58	0.29	4.32E-04
Precentral gyrus left	0.73	2.07E-121	0.06	0.40	-0.11	0.06	-0.09	0.18	-0.36	0.11	-0.02	0.84	0.10	0.58	0.05	0.66	0.07	0.66
Precentral gyrus right	0.72	6.40E-108	3.00E-03	0.98	-0.02	0.83	-0.10	0.17	-0.04	0.93	0.02	0.89	-0.06	0.78	0.05	0.71	0.15	0.10
Paracentral lobule left	0.63	2.20E-64	-0.04	0.74	-0.14	0.07	-0.08	0.53	-0.10	0.86	0.02	0.90	0.19	0.35	-6.43E-04	1.00	-0.02	0.93
Paracentral lobule right	0.62	4.96E-62	0.01	0.96	-0.15	0.03	-0.14	0.13	-0.24	0.60	-0.02	0.90	0.22	0.22	0.07	0.60	-0.09	0.60
Frontal pole left	0.48	1.58E-33	-0.16	0.03	-0.03	0.84	0.01	0.96	-0.10	0.87	0.11	0.21	0.08	0.79	0.03	0.87	-0.34	1.05E-03
Frontal pole right	0.40	9.32E-25	-0.02	0.89	0.08	0.47	-0.05	0.74	0.29	0.54	0.01	0.96	-0.14	0.66	0.05	0.78	-0.27	0.02
<i>Parietal</i>																		
Superior parietal cortex left	0.76	2.04E-110	-0.03	0.78	0.03	0.83	3.53E-03	0.98	-0.12	0.78	0.07	0.38	0.04	0.87	-0.01	0.96	-0.03	0.87
Superior parietal cortex right	0.79	6.92E-126	-0.08	0.25	0.13	0.02	0.15	0.01	0.10	0.81	0.09	0.16	-0.15	0.34	-0.09	0.27	0.20	0.02
Inferior parietal cortex left	0.74	1.07E-103	-0.01	0.97	0.02	0.89	0.05	0.67	0.02	0.98	0.02	0.89	-0.05	0.86	-0.08	0.41	-0.14	0.21
Inferior parietal cortex right	0.72	4.74E-102	-0.03	0.76	0.01	0.90	-0.04	0.72	0.16	0.69	0.02	0.86	-0.20	0.19	-0.02	0.89	0.11	0.36
Supramarginal cortex left	0.74	3.61E-106	-0.02	0.84	-0.02	0.86	2.38E-04	1.00	-0.10	0.84	0.04	0.73	0.01	0.96	-0.01	0.93	0.02	0.93
Supramarginal cortex right	0.70	1.82E-89	-0.11	0.08	-0.12	0.08	-0.01	0.94	-0.45	0.07	0.08	0.27	0.22	0.14	0.05	0.73	0.21	0.02
Postcentral gyrus left	0.80	3.78E-139	-0.08	0.14	-0.04	0.72	0.03	0.79	-0.06	0.89	0.09	0.11	-0.01	0.96	4.24E-03	0.98	0.05	0.72
Postcentral gyrus right	0.78	2.92E-122	-0.08	0.17	0.02	0.84	0.02	0.89	0.16	0.68	0.07	0.30	-0.14	0.38	-0.05	0.67	0.17	0.08
Precuneus cortex left	0.79	3.19E-135	-0.02	0.83	0.05	0.60	0.08	0.33	0.01	0.99	4.19E-03	0.97	-0.06	0.78	-0.06	0.59	0.06	0.72
Precuneus cortex right	0.78	1.34E-131	0.01	0.93	0.02	0.89	0.03	0.81	-0.03	0.94	0.01	0.93	-0.04	0.89	-0.04	0.78	0.14	0.13
<i>Occipital</i>																		
Lateral occipital cortex left	0.67	7.46E-88	-0.05	0.63	-0.04	0.72	0.05	0.72	-0.47	0.05	0.06	0.49	0.13	0.54	2.05E-03	1.00	-0.29	4.77E-04
Lateral occipital cortex right	0.64	5.92E-77	0.01	0.93	-0.09	0.26	0.02	0.89	-0.63	0.01	-0.03	0.84	0.25	0.10	1.11E-03	1.00	-0.25	0.01
Lingual gyrus left	0.60	2.58E-59	-0.03	0.79	0.04	0.78	-0.02	0.89	-0.20	0.68	-0.01	0.92	0.11	0.68	0.05	0.74	-0.59	6.76E-11
Lingual gyrus right	0.63	6.76E-64	-0.04	0.74	-0.02	0.91	0.05	0.72	-0.45	0.13	-0.02	0.90	0.25	0.14	0.02	0.89	-0.11	0.52
Cuneus cortex left	0.55	1.11E-49	0.07	0.51	-0.03	0.86	0.05	0.74	-0.47	0.11	-0.05	0.68	0.20	0.32	-0.01	0.96	-0.23	0.06

Cuneus cortex right	0.66	3.12E-78	-0.06	0.45	0.03	0.84	0.08	0.46	-0.43	0.11	0.08	0.32	0.14	0.53	1.17E-03	1.00	-0.12	0.36
Pericalcarine cortex left	0.45	6.36E-30	0.02	0.90	0.04	0.78	0.03	0.87	-0.10	0.87	-0.04	0.79	0.03	0.93	-3.77E-03	0.99	-0.56	7.62E-08
Pericalcarine cortex right	0.51	2.90E-39	-0.05	0.72	0.05	0.74	0.06	0.68	-0.39	0.27	0.04	0.79	0.15	0.55	0.02	0.90	-0.35	1.16E-03
<i>Temporal</i>																		
Superior temporal gyrus left	0.79	4.73E-136	-0.01	0.96	0.02	0.84	0.01	0.96	0.10	0.79	1.32E-03	1.00	-0.07	0.76	-0.01	0.91	0.17	0.06
Superior temporal gyrus right	0.81	1.51E-136	0.05	0.52	0.06	0.46	-0.04	0.77	0.52	0.01	-0.08	0.24	-0.16	0.30	0.02	0.90	0.20	0.02
Middle temporal gyrus left	0.71	3.38E-96	0.12	0.03	0.10	0.13	0.01	0.96	0.30	0.31	-0.06	0.51	-0.14	0.47	0.05	0.72	0.48	7.09E-10
Middle temporal gyrus right	0.79	5.34E-136	0.12	0.01	0.03	0.76	-0.05	0.66	-0.02	0.97	-0.08	0.20	0.11	0.58	0.09	0.23	0.31	1.27E-05
Inferior temporal gyrus left	0.69	1.99E-85	0.02	0.85	0.05	0.67	0.01	0.96	0.15	0.74	-0.05	0.63	-0.06	0.84	0.04	0.79	0.15	0.21
Inferior temporal gyrus right	0.67	1.80E-84	-0.03	0.78	0.11	0.10	0.07	0.53	0.23	0.54	-2.22E-03	0.99	-0.16	0.36	-0.03	0.84	0.43	1.55E-07
Banks of the superior temporal sulcus left	0.55	4.08E-48	-0.05	0.68	0.10	0.26	0.11	0.26	0.19	0.71	-0.02	0.90	-0.14	0.60	-0.11	0.36	-0.03	0.90
Banks of the superior temporal sulcus right	0.57	3.65E-54	0.04	0.76	0.04	0.77	-0.04	0.81	0.14	0.79	-0.05	0.72	-0.06	0.85	0.01	0.97	0.03	0.90
Fusiform gyrus left	0.75	6.24E-103	-1.39E-03	1.00	-2.89E-03	0.99	0.11	0.18	-0.08	0.87	0.01	0.96	0.04	0.90	-0.07	0.51	-0.27	1.47E-03
Fusiform gyrus right	0.74	7.78E-99	-0.04	0.68	0.11	0.12	0.14	0.05	0.23	0.53	0.03	0.81	-0.24	0.11	-0.11	0.19	0.03	0.87
Transverse temporal cortex left	0.59	9.62E-50	0.07	0.51	-0.06	0.66	-0.05	0.74	0.17	0.75	-0.02	0.89	0.04	0.90	0.03	0.87	0.15	0.32
Transverse temporal cortex right	0.67	5.15E-67	-0.01	0.97	-0.01	0.93	0.14	0.13	0.37	0.29	-0.03	0.81	-0.01	0.97	-0.07	0.67	-0.03	0.89
Entorhinal cortex left	0.39	2.83E-23	-0.09	0.33	-0.01	0.93	0.10	0.46	-0.13	0.84	0.06	0.68	-0.11	0.74	-0.11	0.36	-0.42	4.16E-05
Entorhinal cortex right	0.26	4.88E-10	-0.02	0.90	0.02	0.90	0.06	0.72	0.06	0.93	0.04	0.82	-0.16	0.60	-0.11	0.43	0.75	3.11E-13
Temporal pole left	0.50	4.55E-36	0.03	0.81	0.05	0.68	-0.03	0.89	0.27	0.58	-0.02	0.92	-0.10	0.76	0.09	0.51	-0.06	0.79
Temporal pole right	0.37	9.62E-20	0.05	0.68	0.07	0.63	0.01	0.96	0.27	0.59	0.06	0.68	-0.06	0.86	0.04	0.85	0.63	1.14E-10
Parahippocampal gyrus left	0.51	2.15E-39	-0.05	0.67	0.02	0.90	0.04	0.84	4.63E-03	1.00	0.08	0.44	-0.04	0.91	-0.04	0.83	-0.21	0.10
Parahippocampal gyrus right	0.55	1.89E-46	0.05	0.69	0.05	0.72	0.01	0.98	0.35	0.36	-0.05	0.74	-0.19	0.41	-0.04	0.84	0.09	0.66
<i>Cingulate</i>																		
Rostral anterior cingulate left	0.71	6.92E-87	-0.01	0.95	0.04	0.74	0.09	0.40	0.26	0.50	0.02	0.90	-0.07	0.79	-0.06	0.68	-0.04	0.85
Rostral anterior cingulate right	0.58	8.84E-52	-0.03	0.81	0.01	0.96	0.02	0.89	0.07	0.90	0.06	0.66	-0.06	0.86	-0.04	0.84	-0.06	0.76
Caudal anterior cingulate left	0.57	4.12E-44	0.01	0.98	-0.01	0.97	0.03	0.87	0.17	0.77	-1.24E-04	1.00	0.02	0.96	-0.06	0.74	0.11	0.58
Caudal anterior cingulate right	0.54	6.18E-43	-0.05	0.67	0.12	0.16	0.15	0.10	0.53	0.10	0.05	0.74	-0.28	0.14	-0.14	0.18	-0.11	0.50
Posterior cingulate left	0.62	3.44E-57	0.05	0.68	-0.02	0.91	-0.04	0.82	0.06	0.91	-0.04	0.78	0.06	0.85	0.02	0.90	-0.02	0.93
Posterior cingulate right	0.71	7.42E-83	0.11	0.13	-0.04	0.74	-0.06	0.60	0.17	0.72	-0.10	0.17	0.08	0.78	0.06	0.68	0.02	0.94
Isthmus cingulate left	0.67	6.68E-74	0.02	0.89	0.01	0.96	-0.01	0.93	-0.01	1.00	-0.01	0.94	0.04	0.90	0.07	0.59	0.06	0.78
Isthmus cingulate right	0.68	3.62E-74	0.10	0.17	0.02	0.89	-0.05	0.74	0.26	0.53	-0.09	0.32	0.05	0.89	0.08	0.51	-0.04	0.87
<i>Insular</i>																		
Insular cortex left	0.69	3.44E-87	0.05	0.66	0.01	0.96	-0.04	0.77	0.05	0.92	-0.10	0.19	0.14	0.49	0.16	0.04	0.07	0.72
Insular cortex right	0.71	3.24E-95	0.09	0.19	4.20E-03	0.98	-0.01	0.96	0.04	0.94	-0.07	0.42	0.10	0.68	0.14	0.10	0.15	0.16

Note. Estimates significant at $q < 0.05$ appear in bold. A positive estimate for sex indicates a larger surface area for females. ROIs are grouped in lobar divisions (Frontal, Parietal, Occipital, Temporal, Cingulate, Insular). A positive estimate for acquisition orientation indicates a larger surface area for sagittal acquisitions. Dummy variables were coded sex (male = 0, female = 1), acquisition orientation (coronal = 0, sagittal = 1), and all other variables were standardised prior to analyses.

* There were many significant acquisition orientation effects for surface area ROIs. To ensure that differences in acquisition orientation were not adversely affecting our results we compared heritability estimates in the full sample (351 pairs) to the subsample in which scans were collected using the same acquisition orientation (287 pairs, coronal orientation). Results (not shown) were very similar between the two samples (average difference in heritability estimates 5%); some moderate differences were observed, though 95% confidence intervals overlapped for all estimates between the two samples.

Appendix 6 Regression Coefficients and q values for Cortical Thickness Covariates in the QTIM Dataset

	Average Thickness		Age		Age ²		Age ³		Sex		Age x Sex		Age ² x Sex		Age ³ x Sex		Acquisition Orientation		
	Regression Coefficient	q value	Regression Coefficient	q value	Regression Coefficient	q value	Regression Coefficient	q value	Regression Coefficient	q value	Regression Coefficient	q value	Regression Coefficient	q value	Regression Coefficient	q value	Regression Coefficient	q value	
<i>Frontal</i>																			
Superior frontal gyrus left	0.73	1.21E-148	-0.04	0.57	-0.15	4.54E-03	-0.08	0.24	0.17	0.51	-0.04	0.52	0.16	0.24	0.05	0.58	-0.34	6.02E-06	
Superior frontal gyrus right	0.76	1.12E-143	0.09	0.13	-0.03	0.73	0.01	0.90	0.30	0.23	-0.15	3.16E-03	0.07	0.68	0.03	0.76	-0.48	1.73E-10	
Rostral middle frontal gyrus left	0.64	4.85E-95	0.03	0.68	-0.16	0.01	-0.11	0.19	0.07	0.84	-2.82E-03	0.98	0.11	0.56	-2.39E-03	0.98	-0.12	0.29	
Rostral middle frontal gyrus right	0.56	4.72E-64	0.13	0.07	-0.05	0.62	-0.02	0.84	0.49	0.09	-0.10	0.21	-0.01	0.96	0.02	0.85	-0.31	4.35E-03	
Caudal middle frontal gyrus left	0.63	2.61E-90	-0.08	0.26	-0.17	0.01	-0.08	0.38	-0.31	0.29	0.07	0.38	0.06	0.76	-0.06	0.58	-0.49	1.28E-08	
Caudal middle frontal gyrus right	0.60	6.55E-81	-0.01	0.90	-0.14	0.03	-0.06	0.52	-0.31	0.29	0.06	0.45	0.15	0.41	0.01	0.90	0.21	0.04	
Pars opercularis left	0.61	3.91E-82	1.28E-04	1.00	-0.11	0.15	-0.14	0.07	-0.29	0.33	-0.02	0.86	0.07	0.73	0.04	0.73	-0.48	8.06E-08	
Pars opercularis right	0.60	8.93E-77	0.06	0.46	2.61E-03	0.98	-4.05E-03	0.97	0.33	0.26	-0.01	0.94	-0.26	0.09	-0.13	0.16	0.01	0.93	
Pars triangularis left	0.58	1.16E-73	-0.02	0.80	-0.09	0.28	-0.03	0.76	0.18	0.58	0.13	0.07	-0.03	0.90	-0.12	0.19	-0.21	0.05	
Pars triangularis right	0.57	3.33E-66	0.15	0.02	0.05	0.61	-0.05	0.65	0.41	0.17	-0.07	0.39	-0.11	0.58	-0.02	0.87	-0.01	0.97	
Pars orbitalis left	0.46	1.48E-45	0.03	0.72	-0.02	0.83	-0.07	0.52	0.33	0.29	-0.03	0.73	0.01	0.97	0.01	0.91	0.41	1.44E-05	
Pars orbitalis right	0.35	8.89E-23	0.06	0.55	-0.05	0.67	-0.07	0.52	0.40	0.25	-0.10	0.28	0.03	0.90	0.08	0.49	0.07	0.67	
Lateral orbitofrontal cortex left	0.54	2.03E-71	-0.01	0.88	-0.02	0.82	-0.03	0.80	0.29	0.31	0.02	0.79	-0.01	0.97	-0.01	0.93	0.54	2.38E-10	
Lateral orbitofrontal cortex right	0.49	5.62E-51	0.07	0.38	0.08	0.39	0.02	0.84	0.08	0.08	-0.04	0.67	-0.20	0.27	-0.03	0.83	0.53	4.03E-08	
Medial orbitofrontal cortex left	0.40	2.12E-31	0.03	0.75	-0.09	0.31	-0.06	0.57	0.38	0.26	-0.05	0.64	0.06	0.81	0.03	0.83	-0.13	0.35	
Medial orbitofrontal cortex right	0.44	5.50E-37	0.04	0.67	0.09	0.32	0.06	0.58	0.74	0.01	-0.07	0.46	-0.18	0.38	-0.08	0.47	-0.22	0.08	
Precentral gyrus left	0.69	1.83E-107	-0.03	0.76	0.02	0.87	0.07	0.46	-0.01	0.97	7.74E-06	1.00	-0.05	0.81	-0.11	0.21	-0.40	5.29E-06	
Precentral gyrus right	0.67	7.93E-103	0.04	0.58	-0.03	0.75	0.09	0.30	-0.19	0.55	0.01	0.90	0.12	0.51	-0.10	0.29	-0.43	1.62E-06	
Paracentral lobule left	0.59	1.38E-71	-0.10	0.16	-0.07	0.40	-0.05	0.65	-0.05	0.89	0.08	0.33	0.01	0.97	-0.01	0.91	-0.55	5.81E-09	
Paracentral lobule right	0.62	7.13E-81	-0.08	0.30	-0.14	0.04	-0.06	0.52	-0.43	0.11	0.11	0.14	0.17	0.32	-0.03	0.83	-0.39	5.89E-05	
Frontal pole left	0.29	3.05E-17	0.04	0.71	0.08	0.43	0.12	0.25	0.61	0.04	-0.13	0.12	0.07	0.79	-0.04	0.79	-0.35	1.11E-03	
Frontal pole right	0.34	6.76E-22	0.05	0.62	0.14	0.11	0.16	0.09	0.59	0.06	0.02	0.85	-0.01	0.96	-0.08	0.52	-0.34	3.31E-03	
<i>Parietal</i>																			
Superior parietal cortex left	0.68	1.01E-122	-0.15	2.61E-03	-0.11	0.06	-0.04	0.66	-0.70	4.68E-04	0.09	0.17	0.21	0.12	0.08	0.32	0.02	0.88	
Superior parietal cortex right	0.70	5.43E-117	-0.09	0.17	-0.03	0.68	0.02	0.82	-0.52	0.02	0.06	0.47	0.16	0.32	0.04	0.67	-0.33	1.84E-04	
Inferior parietal cortex left	0.70	2.82E-118	-0.11	0.05	-0.14	0.02	-0.02	0.82	-0.87	1.18E-05	0.11	0.08	0.21	0.15	0.02	0.84	-0.18	0.06	
Inferior parietal cortex right	0.81	1.44E-174	-0.03	0.62	-0.05	0.39	0.06	0.40	-0.36	0.08	0.01	0.88	0.02	0.90	-0.10	0.16	-0.38	3.01E-08	
Supramarginal cortex left	0.70	3.66E-120	-0.08	0.22	-0.07	0.32	-0.08	0.35	-0.48	0.03	4.23E-03	0.97	0.04	0.84	0.01	0.90	-0.54	6.65E-12	
Supramarginal cortex right	0.75	6.95E-138	-0.01	0.89	-0.04	0.57	0.02	0.86	-0.40	0.08	-0.01	0.89	0.05	0.76	-0.03	0.79	-0.25	2.70E-03	
Postcentral gyrus left	0.63	4.72E-86	-0.02	0.80	0.09	0.27	0.02	0.86	-0.24	0.45	0.04	0.63	0.02	0.91	0.05	0.62	-0.56	1.69E-09	
Postcentral gyrus right	0.56	9.71E-63	-0.02	0.87	0.03	0.79	-0.09	0.33	-0.23	0.51	-0.07	0.46	0.16	0.41	0.17	0.07	-0.52	1.54E-07	
Precuneus cortex left	0.69	3.01E-124	-0.13	0.01	-0.17	1.77E-03	-0.13	0.05	-0.74	1.40E-04	0.04	0.58	0.21	0.11	0.07	0.41	-0.25	2.95E-03	
Precuneus cortex right	0.73	1.06E-126	-0.10	0.07	-0.07	0.28	-0.08	0.28	-0.43	0.06	0.06	0.39	0.06	0.76	0.03	0.76	-0.56	2.68E-13	
<i>Occipital</i>																			
Lateral occipital cortex left	0.62	5.84E-82	-0.02	0.84	0.18	4.89E-03	0.12	0.16	0.14	0.68	0.03	0.79	-0.11	0.57	0.04	0.72	-0.03	0.87	
Lateral occipital cortex right	0.69	1.57E-109	-0.03	0.76	0.09	0.18	0.07	0.46	-0.29	0.29	0.05	0.51	0.13	0.46	0.09	0.34	0.30	6.29E-04	
Lingual gyrus left	0.50	3.36E-52	-0.08	0.31	0.02	0.83	-0.03	0.77	-0.17	0.63	0.04	0.68	-0.03	0.89	0.09	0.39	-0.79	6.14E-16	
Lingual gyrus right	0.50	6.66E-51	-0.07	0.39	-0.11	0.19	-0.12	0.21	-0.59	0.03	0.04	0.67	0.22	0.22	0.09	0.38	-0.80	3.11E-16	
Cuneus cortex left	0.41	2.17E-30	-0.07	0.49	-0.09	0.34	-0.03	0.84	-0.36	0.30	0.04	0.72	0.21	0.29	0.12	0.28	-0.02	0.89	
Cuneus cortex right	0.43	1.09E-34	-0.08	0.34	-0.04	0.73	-0.06	0.57	-0.22	0.57	0.06	0.57	0.16	0.46	0.07	0.55	-0.17	0.23	
Pericalcarine cortex left	0.34	2.64E-21	0.02	0.86	0.08	0.41	0.03	0.83	0.09	0.84	0.01	0.90	0.01	0.97	0.07	0.57	-0.13	0.43	

Pericalcarine cortex right	0.34	4.66E-21	-0.03	0.80	-0.06	0.58	-0.06	0.62	-0.20	0.61	0.06	0.55	0.21	0.32	0.09	0.46	-0.20	0.17	
<i>Temporal</i>																			
Superior temporal gyrus left	0.67	4.83E-118	0.02	0.80	0.24	1.91E-06	0.17	0.01	0.36	0.13	-9.31E-04	0.99	-0.26	0.05	-0.08	0.38	0.62	6.84E-16	
Superior temporal gyrus right	0.65	1.22E-105	0.15	4.26E-03	0.21	1.45E-04	0.14	0.05	0.15	0.61	-0.05	0.48	-0.15	0.34	-0.04	0.67	0.79	5.16E-23	
Middle temporal gyrus left	0.47	8.97E-55	0.03	0.70	0.12	0.07	0.09	0.29	0.48	0.06	-0.05	0.52	-0.25	0.11	-0.02	0.83	1.04	1.71E-32	
Middle temporal gyrus right	0.50	3.80E-65	0.16	3.64E-03	0.08	0.32	0.09	0.28	0.43	0.08	-0.11	0.08	-0.12	0.51	-0.10	0.28	1.03	1.87E-33	
Inferior temporal gyrus left	0.48	1.15E-43	-2.15E-03	0.98	0.09	0.32	0.07	0.52	0.58	0.05	-0.01	0.89	-0.23	0.23	-0.02	0.88	0.13	0.39	
Inferior temporal gyrus right	0.52	3.34E-63	1.91E-03	0.98	0.10	0.22	0.08	0.39	0.41	0.14	0.06	0.44	-0.14	0.46	-0.08	0.39	0.71	2.61E-15	
Banks of the superior temporal sulcus left	0.44	6.30E-38	-0.06	0.49	-0.08	0.38	-0.07	0.51	-0.46	0.14	0.02	0.84	0.01	0.97	-0.07	0.55	-0.31	4.55E-03	
Banks of the superior temporal sulcus right	0.52	4.17E-53	-0.03	0.73	-0.03	0.74	0.07	0.51	-0.53	0.07	0.06	0.51	0.13	0.51	-0.09	0.38	-0.20	0.08	
Fusiform gyrus left	0.54	2.73E-57	-0.03	0.74	0.09	0.31	0.06	0.58	0.44	0.15	-0.02	0.88	-0.15	0.46	4.93E-03	0.97	0.04	0.80	
Fusiform gyrus right	0.62	2.79E-87	-0.02	0.80	0.04	0.68	0.03	0.80	0.07	0.84	1.71E-04	1.00	-0.03	0.90	-0.06	0.52	0.35	8.53E-05	
Transverse temporal cortex left	0.50	1.89E-46	-0.02	0.86	0.21	2.87E-03	0.09	0.38	0.09	0.83	0.04	0.74	-0.06	0.80	-0.02	0.90	0.11	0.46	
Transverse temporal cortex right	0.48	1.61E-44	0.03	0.73	0.17	0.02	-0.02	0.87	-0.03	0.93	2.60E-03	0.98	-0.01	0.98	0.06	0.63	-0.04	0.83	
Entorhinal cortex left	0.19	1.14E-10	0.10	0.14	0.15	0.02	0.06	0.56	0.12	0.74	-0.06	0.45	-0.05	0.80	0.09	0.37	1.46	2.57E-54	
Entorhinal cortex right	0.16	4.44E-06	0.08	0.34	0.12	0.13	0.14	0.14	-0.12	0.76	-3.88E-03	0.97	-0.01	0.96	-0.02	0.87	1.27	2.08E-36	
Temporal pole left	0.33	9.32E-27	0.12	0.07	0.16	0.02	0.06	0.52	0.42	0.13	-0.03	0.76	-0.03	0.89	-0.01	0.92	1.00	2.54E-28	
Temporal pole right	0.34	7.65E-26	0.19	2.39E-03	0.31	7.53E-07	0.23	3.12E-03	0.47	0.12	-0.06	0.47	-0.24	0.19	-0.08	0.49	1.00	1.77E-25	
Parahippocampal gyrus left	0.31	3.00E-17	-0.04	0.68	0.10	0.32	0.05	0.67	0.51	0.13	-3.25E-04	1.00	-0.32	0.09	-0.09	0.46	-0.38	1.63E-03	
Parahippocampal gyrus right	0.33	3.22E-19	-0.03	0.80	0.08	0.46	0.06	0.63	0.06	0.89	0.06	0.58	-0.13	0.57	-0.08	0.51	-0.04	0.84	
<i>Cingulate</i>																			
Rostral anterior cingulate left	0.51	2.11E-51	0.09	0.30	0.04	0.71	0.06	0.61	0.20	0.58	-0.03	0.76	0.05	0.83	-0.04	0.76	-0.12	0.41	
Rostral anterior cingulate right	0.45	1.51E-39	0.07	0.46	0.23	8.22E-04	0.14	0.14	0.55	0.07	-0.01	0.91	-0.25	0.17	-0.11	0.33	-0.49	1.65E-06	
Caudal anterior cingulate left	0.34	4.76E-23	0.04	0.66	-0.02	0.87	-0.01	0.94	0.18	0.65	-0.02	0.87	-0.01	0.97	-0.04	0.79	0.42	8.83E-05	
Caudal anterior cingulate right	0.37	3.82E-24	0.04	0.73	0.05	0.61	-0.07	0.57	0.10	0.82	0.03	0.76	2.66E-03	0.99	0.09	0.46	-0.30	0.01	
Posterior cingulate left	0.44	2.52E-42	-0.10	0.16	-0.17	0.02	-0.22	4.35E-03	-0.35	0.27	0.08	0.32	0.12	0.56	0.07	0.54	0.37	2.69E-04	
Posterior cingulate right	0.44	2.11E-39	-0.16	0.02	-0.10	0.25	-0.08	0.46	-0.40	0.21	0.06	0.54	0.03	0.90	-0.07	0.55	-0.53	6.40E-08	
Isthmus cingulate left	0.32	5.07E-19	-0.18	0.02	-0.01	0.97	0.04	0.79	-0.02	0.96	0.08	0.41	-0.09	0.71	-0.05	0.73	-0.15	0.32	
Isthmus cingulate right	0.30	6.00E-17	-0.12	0.17	-0.03	0.82	0.06	0.62	-0.29	0.46	0.05	0.62	0.04	0.88	-0.07	0.57	-0.58	2.05E-07	
<i>Insular</i>																			
Insular cortex left	0.55	6.44E-61	0.09	0.25	0.13	0.10	0.01	0.91	-0.03	0.95	0.05	0.57	-0.21	0.25	0.03	0.80	-0.10	0.46	
Insular cortex right	0.52	3.94E-59	0.11	0.12	0.13	0.08	0.05	0.60	-0.11	0.77	-0.05	0.56	-0.08	0.69	0.02	0.88	0.63	1.88E-12	

Note. Estimates significant at $q < 0.05$ appear in bold. ROIs are grouped in lobar divisions (Frontal, Parietal, Occipital, Temporal, Cingulate, Insular). A positive estimate for sex indicates a thicker cortex for females. A positive estimate for acquisition orientation indicates a thicker cortex for sagittal acquisitions. Dummy variables were coded sex (male = 0, female = 1), acquisition orientation (coronal = 0, sagittal = 1), and all other variables were standardised prior to analyses.

* There were many significant acquisition orientation effects for cortical thickness ROIs. To ensure that differences in acquisition orientation were not adversely affecting our results we compared heritability estimates in the full sample (351 pairs) to the subsample in which scans were collected using the same acquisition orientation (287 pairs, coronal orientation). Results (not shown) were very similar between the two samples (average difference in heritability estimates was 5%); some moderate differences were observed, though 95% confidence intervals overlapped for all estimates between the two samples.

Appendix 7 Variance Component Estimates for QTIM Surface Area and Cortical Thickness

Twin correlations, estimates of variance components, model fit comparisons, and test-retest correlations for surface area and cortical thickness of left and right cortical regions in the QTIM dataset.

	Twin Correlations (95% CI)		a^2	Variance Components (95% CI)			g value			Test-Retest Reliability	
	MZ	DZ		c^2	e^2	No A	No C	No AC	r trt	1 - r ² trt	
<i>Surface Area</i>											
<i>Frontal</i>											
Superior frontal gyrus left	0.46 (0.33, 0.57)	0.15 (0.02, 0.27)	0.41 (0.17, 0.52)	0.00 (0.00, 0.00)	0.59 (0.48, 0.71)	0.01	1.00	4.68E-08	0.90	0.19	
Superior frontal gyrus right	0.32 (0.18, 0.45)	0.32 (0.18, 0.44)	0.03 (0.00, 0.40)	0.30 (0.00, 0.41)	0.67 (0.55, 0.78)	1.00	0.11	8.21E-08	0.96	0.08	
Rostral middle frontal gyrus left	0.27 (0.12, 0.41)	0.19 (0.05, 0.32)	0.22 (0.00, 0.43)	0.08 (0.00, 0.31)	0.71 (0.57, 0.86)	0.48	0.89	3.21E-04	0.95	0.11	
Rostral middle frontal gyrus right	0.28 (0.13, 0.42)	0.23 (0.09, 0.35)	0.19 (0.00, 0.44)	0.12 (0.00, 0.33)	0.69 (0.56, 0.84)	0.54	0.67	4.72E-05	0.92	0.15	
Caudal middle frontal gyrus left	0.36 (0.22, 0.49)	0.15 (-0.01, 0.31)	0.38 (0.07, 0.50)	0.00 (0.00, 0.00)	0.62 (0.50, 0.76)	0.05	1.00	1.36E-05	0.95	0.11	
Caudal middle frontal gyrus right	0.37 (0.23, 0.50)	0.02 (-0.13, 0.17)	0.31 (0.10, 0.43)	0.00 (0.00, 0.14)	0.69 (0.57, 0.83)	0.03	1.00	3.86E-04	0.91	0.16	
Pars opercularis left	0.34 (0.20, 0.47)	0.17 (0.03, 0.31)	0.31 (0.00, 0.45)	0.02 (0.00, 0.31)	0.67 (0.55, 0.81)	0.23	1.00	1.85E-05	0.94	0.12	
Pars opercularis right	0.16 (-0.00, 0.31)	0.11 (-0.03, 0.24)	0.09 (0.00, 0.29)	0.06 (0.00, 0.23)	0.85 (0.71, 0.97)	0.94	0.95	0.11	0.94	0.12	
Pars triangularis left	0.32 (0.18, 0.45)	0.12 (-0.02, 0.25)	0.30 (0.00, 0.41)	0.00 (0.00, 0.23)	0.70 (0.59, 0.83)	0.12	1.00	1.93E-04	0.93	0.13	
Pars triangularis right	0.28 (0.12, 0.41)	0.04 (-0.09, 0.17)	0.24 (0.01, 0.37)	0.00 (0.00, 0.15)	0.76 (0.63, 0.90)	0.10	1.00	0.01	0.95	0.10	
Pars orbitalis left	0.14 (-0.01, 0.29)	0.15 (0.00, 0.29)	0.00 (0.00, 0.28)	0.15 (0.00, 0.25)	0.85 (0.72, 0.96)	1.00	0.54	0.06	0.85	0.28	
Pars orbitalis right	0.39 (0.24, 0.51)	0.08 (-0.07, 0.23)	0.33 (0.07, 0.45)	0.00 (0.00, 0.00)	0.67 (0.55, 0.80)	0.05	1.00	5.97E-05	0.80	0.37	
Lateral orbitofrontal cortex left	0.38 (0.24, 0.51)	0.08 (-0.06, 0.22)	0.35 (0.14, 0.47)	0.00 (0.00, 0.14)	0.65 (0.53, 0.78)	0.02	1.00	3.62E-05	0.72	0.48	
Lateral orbitofrontal cortex right	0.39 (0.25, 0.52)	0.05 (-0.10, 0.20)	0.34 (0.13, 0.46)	0.00 (0.00, 0.14)	0.66 (0.54, 0.80)	0.02	1.00	8.16E-05	0.41	0.83	
Medial orbitofrontal cortex left	0.16 (0.00, 0.30)	0.10 (-0.05, 0.24)	0.14 (0.00, 0.30)	0.02 (0.00, 0.22)	0.83 (0.70, 0.97)	0.77	1.00	0.12	0.40	0.84	
Medial orbitofrontal cortex right	0.19 (0.03, 0.34)	0.07 (-0.07, 0.21)	0.20 (0.00, 0.32)	0.00 (0.00, 0.23)	0.80 (0.68, 0.94)	0.48	1.00	0.04	0.64	0.59	
Precentral gyrus left	0.51 (0.37, 0.61)	0.27 (0.13, 0.40)	0.50 (0.16, 0.61)	0.01 (0.00, 0.28)	0.48 (0.39, 0.61)	0.01	1.00	2.19E-11	0.95	0.11	
Precentral gyrus right	0.43 (0.29, 0.55)	0.21 (0.07, 0.35)	0.44 (0.10, 0.55)	0.00 (0.00, 0.25)	0.56 (0.45, 0.70)	0.03	1.00	1.06E-07	0.95	0.10	
Paracentral lobule left	0.35 (0.21, 0.47)	0.28 (0.14, 0.41)	0.09 (0.00, 0.44)	0.24 (0.00, 0.40)	0.66 (0.54, 0.78)	0.89	0.23	1.06E-07	0.91	0.17	
Paracentral lobule right	0.21 (0.06, 0.36)	0.16 (0.02, 0.28)	0.21 (0.00, 0.39)	0.04 (0.00, 0.27)	0.75 (0.61, 0.91)	0.52	1.00	4.97E-03	0.82	0.32	
Frontal pole left	0.12 (-0.04, 0.27)	0.06 (-0.08, 0.20)	0.12 (0.00, 0.25)	0.00 (0.00, 0.18)	0.88 (0.75, 1.00)	0.80	1.00	0.42	0.39	0.85	
Frontal pole right	-0.01 (-0.18, 0.15)	-0.02 (-0.15, 0.11)	0.00 (0.00, 0.13)	0.00 (0.00, 0.09)	1.00 (0.87, 1.00)	1.00	1.00	1.00	0.55	0.70	
<i>Parietal</i>											
Superior parietal cortex left	0.51 (0.38, 0.61)	0.22 (0.08, 0.35)	0.48 (0.16, 0.57)	0.00 (0.00, 0.26)	0.52 (0.43, 0.63)	0.01	1.00	1.82E-11	0.94	0.12	
Superior parietal cortex right	0.41 (0.27, 0.53)	0.19 (0.06, 0.32)	0.31 (0.00, 0.48)	0.06 (0.00, 0.36)	0.62 (0.52, 0.75)	0.19	0.95	6.01E-08	0.95	0.09	
Inferior parietal cortex left	0.47 (0.33, 0.58)	0.31 (0.18, 0.43)	0.28 (0.00, 0.56)	0.18 (0.00, 0.43)	0.54 (0.43, 0.67)	0.19	0.37	7.11E-12	0.93	0.13	
Inferior parietal cortex right	0.43 (0.29, 0.55)	0.27 (0.14, 0.39)	0.47 (0.12, 0.59)	0.02 (0.00, 0.28)	0.51 (0.41, 0.65)	0.03	1.00	6.94E-10	0.89	0.22	
Supramarginal cortex left	0.40 (0.26, 0.53)	0.17 (0.04, 0.30)	0.40 (0.11, 0.51)	0.00 (0.00, 0.21)	0.60 (0.49, 0.73)	0.03	1.00	6.63E-07	0.97	0.05	
Supramarginal cortex right	0.25 (0.09, 0.40)	0.19 (0.04, 0.32)	0.15 (0.00, 0.40)	0.11 (0.00, 0.31)	0.74 (0.60, 0.88)	0.72	0.74	1.51E-03	0.91	0.17	
Postcentral gyrus left	0.16 (-0.00, 0.31)	0.08 (-0.06, 0.21)	0.16 (0.00, 0.29)	0.00 (0.00, 0.21)	0.84 (0.71, 0.98)	0.66	1.00	0.16	0.97	0.06	
Postcentral gyrus right	0.39 (0.24, 0.51)	0.25 (0.11, 0.38)	0.28 (0.00, 0.51)	0.11 (0.00, 0.38)	0.61 (0.49, 0.75)	0.27	0.70	1.18E-07	0.93	0.13	
Precuneus cortex left	0.46 (0.33, 0.58)	0.33 (0.21, 0.45)	0.27 (0.00, 0.56)	0.20 (0.00, 0.44)	0.53 (0.43, 0.67)	0.23	0.27	4.98E-12	0.94	0.12	
Precuneus cortex right	0.40 (0.26, 0.52)	0.18 (0.04, 0.31)	0.40 (0.11, 0.51)	0.00 (0.00, 0.22)	0.60 (0.49, 0.73)	0.03	1.00	4.77E-07	0.86	0.27	
<i>Occipital</i>											
Lateral occipital cortex left	0.41 (0.27, 0.53)	0.16 (0.02, 0.29)	0.39 (0.12, 0.50)	0.00 (0.00, 0.20)	0.61 (0.50, 0.74)	0.03	1.00	7.80E-07	0.85	0.28	
Lateral occipital cortex right	0.42 (0.28, 0.54)	0.18 (0.04, 0.31)	0.41 (0.11, 0.52)	0.00 (0.00, 0.23)	0.59 (0.48, 0.72)	0.03	1.00	3.81E-07	0.93	0.13	
Lingual gyrus left	0.52 (0.40, 0.62)	0.17 (0.03, 0.30)	0.50 (0.29, 0.59)	0.00 (0.00, 0.15)	0.50 (0.41, 0.62)	7.71E-04	1.00	6.39E-11	0.93	0.13	

Lingual gyrus right	0.57 (0.46, 0.67)	0.21 (0.07, 0.35)	0.56 (0.34, 0.64)	0.00 (0.00, 0.17)	0.44 (0.36, 0.55)	2.34E-04	1.00	4.49E-14	0.88	0.23
Cuneus cortex left	0.40 (0.26, 0.52)	0.31 (0.18, 0.43)	0.08 (0.00, 0.43)	0.29 (0.00, 0.44)	0.62 (0.51, 0.73)	0.90	0.11	3.82E-10	0.86	0.27
Cuneus cortex right	0.28 (0.13, 0.42)	0.09 (-0.05, 0.23)	0.27 (0.00, 0.39)	0.00 (0.00, 0.22)	0.73 (0.61, 0.87)	0.16	1.00	3.30E-03	0.77	0.41
Pericalcarine cortex left	0.61 (0.50, 0.69)	0.36 (0.23, 0.47)	0.48 (0.19, 0.68)	0.12 (0.00, 0.36)	0.40 (0.32, 0.50)	4.01E-03	0.56	1.24E-20	0.95	0.10
Pericalcarine cortex right	0.66 (0.57, 0.74)	0.27 (0.14, 0.39)	0.65 (0.46, 0.72)	0.00 (0.00, 0.00)	0.35 (0.28, 0.44)	1.78E-06	1.00	1.65E-22	0.90	0.19
<i>Temporal</i>										
Superior temporal gyrus left	0.53 (0.41, 0.63)	0.18 (0.04, 0.31)	0.50 (0.28, 0.60)	0.00 (0.00, 0.00)	0.50 (0.40, 0.62)	1.25E-03	1.00	8.24E-11	0.83	0.31
Superior temporal gyrus right	0.51 (0.38, 0.61)	0.33 (0.20, 0.44)	0.39 (0.08, 0.61)	0.13 (0.00, 0.37)	0.48 (0.39, 0.60)	0.04	0.52	1.31E-14	0.63	0.60
Middle temporal gyrus left	0.45 (0.31, 0.56)	0.20 (0.06, 0.32)	0.42 (0.08, 0.53)	0.00 (0.00, 0.27)	0.58 (0.47, 0.71)	0.04	1.00	2.23E-08	0.86	0.26
Middle temporal gyrus right	0.40 (0.27, 0.52)	0.06 (-0.09, 0.20)	0.34 (0.14, 0.46)	0.00 (0.00, 0.15)	0.66 (0.54, 0.78)	0.02	1.00	5.83E-06	0.78	0.39
Inferior temporal gyrus left	0.37 (0.22, 0.49)	0.23 (0.10, 0.35)	0.25 (0.00, 0.48)	0.11 (0.00, 0.36)	0.64 (0.52, 0.78)	0.32	0.72	5.84E-07	0.78	0.40
Inferior temporal gyrus right	0.31 (0.17, 0.44)	0.28 (0.13, 0.41)	0.08 (0.00, 0.43)	0.23 (0.00, 0.39)	0.68 (0.56, 0.81)	0.94	0.27	2.86E-06	0.81	0.35
Banks of the superior temporal sulcus left	0.31 (0.15, 0.46)	0.04 (-0.09, 0.17)	0.25 (0.00, 0.38)	0.00 (0.00, 0.17)	0.75 (0.62, 0.89)	0.11	1.00	0.01	0.94	0.11
Banks of the superior temporal sulcus right	0.18 (0.01, 0.33)	-0.02 (-0.15, 0.12)	0.12 (0.00, 0.26)	0.00 (0.00, 0.14)	0.88 (0.74, 1.00)	0.38	1.00	0.40	0.80	0.36
Fusiform gyrus left	0.29 (0.13, 0.43)	0.15 (-0.00, 0.29)	0.21 (0.00, 0.40)	0.06 (0.00, 0.31)	0.73 (0.60, 0.87)	0.52	1.00	9.54E-04	0.87	0.25
Fusiform gyrus right	0.38 (0.24, 0.50)	0.13 (-0.01, 0.26)	0.36 (0.08, 0.47)	0.00 (0.00, 0.21)	0.64 (0.53, 0.77)	0.04	1.00	4.86E-06	0.87	0.24
Transverse temporal cortex left	0.41 (0.28, 0.53)	0.09 (-0.05, 0.23)	0.35 (0.11, 0.46)	0.00 (0.00, 0.19)	0.65 (0.54, 0.77)	0.03	1.00	3.10E-06	0.89	0.21
Transverse temporal cortex right	0.31 (0.15, 0.44)	0.18 (0.04, 0.31)	0.30 (0.00, 0.46)	0.03 (0.00, 0.31)	0.67 (0.54, 0.83)	0.27	1.00	7.56E-05	0.88	0.22
Entorhinal cortex left	0.17 (0.02, 0.32)	0.04 (-0.10, 0.19)	0.16 (0.00, 0.29)	0.00 (0.00, 0.00)	0.84 (0.71, 0.98)	0.44	1.00	0.16	0.59	0.65
Entorhinal cortex right	0.30 (0.14, 0.44)	0.13 (-0.01, 0.26)	0.26 (0.00, 0.39)	0.02 (0.00, 0.28)	0.73 (0.61, 0.87)	0.36	1.00	6.57E-04	0.50	0.75
Temporal pole left	0.12 (-0.03, 0.26)	0.09 (-0.05, 0.22)	0.08 (0.00, 0.27)	0.05 (0.00, 0.20)	0.87 (0.73, 1.00)	0.96	1.00	0.25	0.31	0.90
Temporal pole right	0.14 (-0.02, 0.29)	-0.04 (-0.18, 0.10)	0.09 (0.00, 0.22)	0.00 (0.00, 0.13)	0.91 (0.78, 1.00)	0.52	1.00	0.67	0.45	0.80
Parahippocampal gyrus left	0.40 (0.26, 0.52)	0.17 (0.01, 0.31)	0.39 (0.07, 0.50)	0.00 (0.00, 0.25)	0.61 (0.50, 0.74)	0.05	1.00	1.78E-06	0.78	0.40
Parahippocampal gyrus right	0.39 (0.24, 0.52)	0.18 (0.04, 0.31)	0.39 (0.06, 0.50)	0.00 (0.00, 0.25)	0.61 (0.50, 0.75)	0.06	1.00	1.78E-06	0.69	0.53
<i>Cingulate</i>										
Rostral anterior cingulate left	0.37 (0.23, 0.49)	0.19 (0.05, 0.33)	0.38 (0.01, 0.49)	0.00 (0.00, 0.29)	0.62 (0.51, 0.75)	0.10	1.00	4.43E-07	0.85	0.27
Rostral anterior cingulate right	0.10 (-0.06, 0.25)	0.08 (-0.07, 0.22)	0.01 (0.00, 0.23)	0.08 (0.00, 0.19)	0.91 (0.77, 1.00)	1.00	0.92	0.43	0.79	0.37
Caudal anterior cingulate left	0.48 (0.35, 0.59)	0.06 (-0.09, 0.20)	0.42 (0.25, 0.53)	0.00 (0.00, 0.11)	0.58 (0.47, 0.71)	1.54E-03	1.00	3.09E-07	0.95	0.10
Caudal anterior cingulate right	0.07 (-0.08, 0.22)	0.04 (-0.12, 0.19)	0.08 (0.00, 0.22)	0.00 (0.00, 0.16)	0.92 (0.78, 1.00)	0.95	1.00	0.80	0.97	0.07
Posterior cingulate left	0.32 (0.16, 0.46)	0.11 (-0.03, 0.25)	0.29 (0.00, 0.41)	0.00 (0.00, 0.25)	0.71 (0.59, 0.85)	0.16	1.00	7.26E-04	0.92	0.15
Posterior cingulate right	0.31 (0.17, 0.44)	0.11 (-0.03, 0.25)	0.29 (0.00, 0.40)	0.00 (0.00, 0.26)	0.71 (0.60, 0.84)	0.18	1.00	2.26E-04	0.91	0.17
Isthmus cingulate left	0.41 (0.27, 0.53)	0.30 (0.16, 0.42)	0.27 (0.00, 0.54)	0.16 (0.00, 0.41)	0.57 (0.46, 0.72)	0.26	0.48	4.38E-09	0.84	0.29
Isthmus cingulate right	0.41 (0.27, 0.53)	0.22 (0.07, 0.35)	0.41 (0.04, 0.53)	0.01 (0.00, 0.29)	0.58 (0.47, 0.72)	0.07	1.00	6.07E-08	0.83	0.32
<i>Insular</i>										
Insular cortex left	0.34 (0.18, 0.48)	0.15 (0.00, 0.29)	0.32 (0.00, 0.44)	0.00 (0.00, 0.30)	0.68 (0.56, 0.83)	0.25	1.00	2.74E-04	0.57	0.68
Insular cortex right	0.34 (0.20, 0.47)	0.12 (-0.02, 0.25)	0.33 (0.06, 0.45)	0.00 (0.00, 0.20)	0.67 (0.55, 0.80)	0.06	1.00	7.72E-05	0.32	0.90
<u>Cortical Thickness</u>										
<i>Frontal</i>										
Superior frontal gyrus left	0.47 (0.34, 0.58)	0.34 (0.21, 0.46)	0.19 (0.00, 0.53)	0.26 (0.00, 0.47)	0.55 (0.44, 0.67)	0.40	0.16	3.88E-12	0.82	0.33
Superior frontal gyrus right	0.37 (0.22, 0.50)	0.15 (0.01, 0.28)	0.36 (0.05, 0.47)	0.00 (0.00, 0.23)	0.64 (0.53, 0.78)	0.06	1.00	2.83E-05	0.69	0.53
Rostral middle frontal gyrus left	0.30 (0.15, 0.43)	0.18 (0.05, 0.31)	0.26 (0.00, 0.44)	0.05 (0.00, 0.30)	0.69 (0.56, 0.84)	0.32	0.94	9.88E-05	0.57	0.67
Rostral middle frontal gyrus right	0.55 (0.43, 0.64)	0.28 (0.15, 0.40)	0.44 (0.12, 0.61)	0.08 (0.00, 0.34)	0.48 (0.39, 0.59)	0.02	0.79	5.06E-15	0.65	0.57
Caudal middle frontal gyrus left	0.37 (0.22, 0.49)	0.04 (-0.09, 0.18)	0.29 (0.08, 0.41)	0.00 (0.00, 0.15)	0.71 (0.59, 0.84)	0.03	1.00	3.47E-04	0.82	0.33
Caudal middle frontal gyrus right	0.29 (0.14, 0.43)	0.17 (0.03, 0.31)	0.32 (0.00, 0.45)	0.01 (0.00, 0.29)	0.67 (0.55, 0.83)	0.21	1.00	1.77E-04	0.75	0.44
Pars opercularis left	0.35 (0.21, 0.47)	0.18 (0.03, 0.32)	0.27 (0.00, 0.45)	0.06 (0.00, 0.34)	0.67 (0.55, 0.80)	0.29	0.94	8.34E-06	0.63	0.60
Pars opercularis right	0.23 (0.08, 0.36)	0.23 (0.09, 0.36)	0.00 (0.00, 0.35)	0.23 (0.00, 0.33)	0.77 (0.64, 0.87)	1.00	0.24	2.86E-04	0.75	0.43
Pars triangularis left	0.08 (-0.07, 0.23)	0.10 (-0.05, 0.24)	0.00 (0.00, 0.00)	0.09 (0.00, 0.19)	0.91 (0.76, 1.00)	1.00	0.75	0.38	0.76	0.42
Pars triangularis right	0.37 (0.24, 0.49)	0.09 (-0.04, 0.23)	0.35 (0.14, 0.46)	0.00 (0.00, 0.14)	0.65 (0.54, 0.78)	0.01	1.00	1.15E-05	0.70	0.50
Pars orbitalis left	0.28 (0.12, 0.42)	0.04 (-0.10, 0.19)	0.23 (0.00, 0.36)	0.00 (0.00, 0.21)	0.77 (0.64, 0.90)	0.16	1.00	0.01	0.68	0.54
Pars orbitalis right	0.48 (0.36, 0.59)	0.09 (-0.05, 0.23)	0.42 (0.22, 0.52)	0.00 (0.00, 0.15)	0.58 (0.48, 0.70)	3.19E-03	1.00	5.89E-09	0.71	0.50

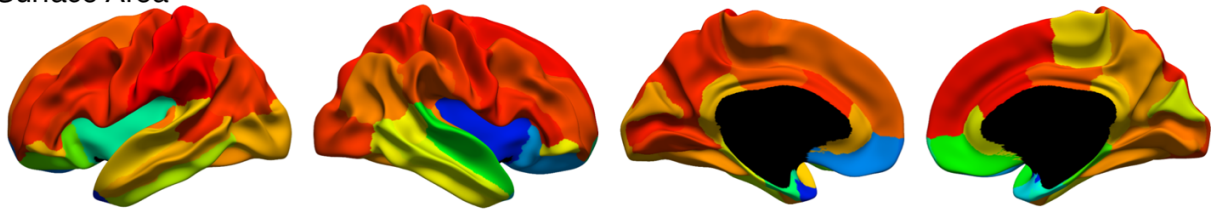
Lateral orbitofrontal cortex left	0.31 (0.16, 0.44)	0.15 (0.01, 0.29)	0.32 (0.00, 0.44)	0.00 (0.00, 0.27)	0.68 (0.56, 0.83)	0.16	1.00	1.47E-04	0.62	0.62
Lateral orbitofrontal cortex right	0.38 (0.24, 0.50)	0.21 (0.06, 0.34)	0.31 (0.00, 0.48)	0.06 (0.00, 0.34)	0.63 (0.52, 0.76)	0.18	0.94	4.43E-07	0.56	0.69
Medial orbitofrontal cortex left	0.35 (0.20, 0.47)	0.21 (0.08, 0.33)	0.25 (0.00, 0.45)	0.09 (0.00, 0.34)	0.66 (0.55, 0.80)	0.31	0.76	2.12E-06	0.63	0.60
Medial orbitofrontal cortex right	0.45 (0.32, 0.56)	0.23 (0.10, 0.35)	0.41 (0.07, 0.54)	0.03 (0.00, 0.30)	0.56 (0.46, 0.69)	0.04	1.00	8.59E-10	0.51	0.74
Precentral gyrus left	0.48 (0.35, 0.59)	0.18 (0.03, 0.32)	0.45 (0.14, 0.55)	0.00 (0.00, 0.24)	0.55 (0.45, 0.67)	0.02	1.00	3.70E-09	0.88	0.22
Precentral gyrus right	0.49 (0.36, 0.60)	0.32 (0.18, 0.43)	0.36 (0.03, 0.59)	0.14 (0.00, 0.39)	0.50 (0.40, 0.63)	0.07	0.49	7.02E-13	0.74	0.45
Paracentral lobule left	0.38 (0.24, 0.50)	0.13 (-0.01, 0.26)	0.36 (0.11, 0.47)	0.00 (0.00, 0.18)	0.64 (0.53, 0.76)	0.02	1.00	3.73E-06	0.68	0.53
Paracentral lobule right	0.44 (0.31, 0.55)	0.26 (0.12, 0.38)	0.35 (0.00, 0.54)	0.09 (0.00, 0.36)	0.57 (0.46, 0.69)	0.11	0.77	6.58E-10	0.78	0.40
Frontal pole left	0.08 (-0.08, 0.23)	0.06 (-0.08, 0.21)	0.05 (0.00, 0.23)	0.04 (0.00, 0.18)	0.92 (0.77, 1.00)	1.00	1.00	0.60	0.57	0.67
Frontal pole right	0.27 (0.13, 0.41)	0.20 (0.06, 0.33)	0.14 (0.00, 0.40)	0.13 (0.00, 0.32)	0.73 (0.60, 0.86)	0.69	0.60	1.86E-04	0.71	0.50
<i>Parietal</i>										
Superior parietal cortex left	0.44 (0.30, 0.55)	0.13 (-0.02, 0.27)	0.40 (0.17, 0.51)	0.00 (0.00, 0.18)	0.60 (0.49, 0.72)	0.01	1.00	2.24E-07	0.85	0.28
Superior parietal cortex right	0.46 (0.33, 0.57)	0.25 (0.12, 0.37)	0.43 (0.09, 0.57)	0.03 (0.00, 0.30)	0.53 (0.43, 0.66)	0.03	1.00	1.60E-10	0.86	0.26
Inferior parietal cortex left	0.26 (0.12, 0.40)	0.07 (-0.07, 0.21)	0.24 (0.00, 0.36)	0.00 (0.00, 0.22)	0.76 (0.64, 0.89)	0.18	1.00	0.01	0.58	0.66
Inferior parietal cortex right	0.35 (0.21, 0.48)	-0.03 (-0.16, 0.11)	0.27 (0.10, 0.39)	0.00 (0.00, 0.10)	0.73 (0.61, 0.87)	0.02	1.00	3.19E-03	0.78	0.39
Supramarginal cortex left	0.37 (0.23, 0.50)	0.16 (0.03, 0.29)	0.35 (0.00, 0.46)	0.00 (0.00, 0.29)	0.65 (0.54, 0.79)	0.13	1.00	6.50E-06	0.80	0.37
Supramarginal cortex right	0.25 (0.10, 0.39)	0.12 (-0.02, 0.25)	0.27 (0.00, 0.39)	0.00 (0.00, 0.23)	0.73 (0.61, 0.89)	0.20	1.00	4.68E-03	0.87	0.24
Postcentral gyrus left	0.54 (0.43, 0.64)	0.25 (0.11, 0.38)	0.55 (0.29, 0.64)	0.00 (0.00, 0.20)	0.45 (0.36, 0.56)	7.14E-04	1.00	2.57E-14	0.88	0.23
Postcentral gyrus right	0.42 (0.29, 0.54)	0.24 (0.09, 0.37)	0.32 (0.00, 0.52)	0.09 (0.00, 0.37)	0.59 (0.48, 0.72)	0.16	0.79	8.18E-09	0.78	0.39
Precuneus cortex left	0.38 (0.24, 0.50)	0.21 (0.07, 0.33)	0.33 (0.00, 0.49)	0.05 (0.00, 0.33)	0.62 (0.51, 0.76)	0.15	0.94	2.52E-07	0.82	0.32
Precuneus cortex right	0.38 (0.24, 0.50)	0.04 (-0.10, 0.18)	0.32 (0.14, 0.44)	0.00 (0.00, 0.12)	0.68 (0.56, 0.81)	0.01	1.00	6.83E-05	0.75	0.43
<i>Occipital</i>										
Lateral occipital cortex left	0.45 (0.31, 0.56)	0.31 (0.18, 0.43)	0.24 (0.00, 0.54)	0.19 (0.00, 0.43)	0.56 (0.45, 0.69)	0.27	0.29	5.79E-11	0.61	0.63
Lateral occipital cortex right	0.32 (0.17, 0.45)	0.13 (-0.00, 0.27)	0.33 (0.05, 0.46)	0.00 (0.00, 0.19)	0.67 (0.54, 0.81)	0.06	1.00	2.19E-04	0.77	0.41
Lingual gyrus left	0.49 (0.37, 0.59)	0.23 (0.09, 0.35)	0.48 (0.16, 0.57)	0.00 (0.00, 0.26)	0.52 (0.43, 0.64)	0.01	1.00	4.43E-12	0.79	0.38
Lingual gyrus right	0.35 (0.21, 0.47)	0.30 (0.17, 0.42)	0.15 (0.00, 0.47)	0.22 (0.00, 0.41)	0.63 (0.51, 0.76)	0.58	0.20	4.75E-09	0.82	0.33
Cuneus cortex left	0.44 (0.31, 0.54)	0.12 (-0.01, 0.25)	0.41 (0.22, 0.51)	0.00 (0.00, 0.13)	0.59 (0.49, 0.71)	2.80E-03	1.00	3.71E-08	0.77	0.41
Cuneus cortex right	0.38 (0.25, 0.51)	0.05 (-0.09, 0.18)	0.34 (0.16, 0.46)	0.00 (0.00, 0.11)	0.66 (0.54, 0.80)	0.01	1.00	8.25E-05	0.82	0.33
Pericalcarine cortex left	0.52 (0.40, 0.62)	0.30 (0.18, 0.41)	0.48 (0.17, 0.63)	0.06 (0.00, 0.30)	0.46 (0.37, 0.58)	0.01	0.87	2.57E-14	0.73	0.46
Pericalcarine cortex right	0.49 (0.36, 0.60)	0.33 (0.21, 0.44)	0.36 (0.03, 0.60)	0.15 (0.00, 0.39)	0.50 (0.40, 0.62)	0.07	0.41	5.61E-13	0.72	0.48
<i>Temporal</i>										
Superior temporal gyrus left	0.40 (0.26, 0.52)	0.20 (0.06, 0.33)	0.36 (0.00, 0.49)	0.02 (0.00, 0.32)	0.62 (0.51, 0.75)	0.12	1.00	2.98E-07	0.71	0.49
Superior temporal gyrus right	0.33 (0.19, 0.46)	0.14 (-0.00, 0.27)	0.31 (0.00, 0.42)	0.00 (0.00, 0.27)	0.69 (0.58, 0.82)	0.16	1.00	6.92E-05	0.70	0.51
Middle temporal gyrus left	0.40 (0.26, 0.52)	0.09 (-0.05, 0.23)	0.36 (0.15, 0.48)	0.00 (0.00, 0.15)	0.64 (0.52, 0.77)	0.01	1.00	7.60E-06	0.76	0.42
Middle temporal gyrus right	0.38 (0.24, 0.50)	0.20 (0.07, 0.33)	0.30 (0.00, 0.47)	0.06 (0.00, 0.34)	0.64 (0.53, 0.77)	0.19	0.91	2.52E-07	0.61	0.63
Inferior temporal gyrus left	0.38 (0.24, 0.50)	0.28 (0.15, 0.40)	0.21 (0.00, 0.49)	0.18 (0.00, 0.40)	0.62 (0.50, 0.75)	0.38	0.35	7.30E-09	0.43	0.81
Inferior temporal gyrus right	0.32 (0.17, 0.45)	0.24 (0.11, 0.36)	0.27 (0.00, 0.49)	0.09 (0.00, 0.34)	0.64 (0.51, 0.80)	0.30	0.74	3.73E-06	0.52	0.73
Banks of the superior temporal sulcus left	0.19 (0.04, 0.33)	0.17 (0.03, 0.30)	0.01 (0.00, 0.31)	0.17 (0.00, 0.28)	0.82 (0.68, 0.92)	1.00	0.44	0.01	0.74	0.45
Banks of the superior temporal sulcus right	0.18 (0.03, 0.32)	0.13 (-0.02, 0.26)	0.14 (0.00, 0.33)	0.05 (0.00, 0.24)	0.81 (0.67, 0.95)	0.73	0.94	0.04	0.76	0.42
Fusiform gyrus left	0.38 (0.25, 0.49)	0.23 (0.09, 0.35)	0.34 (0.00, 0.50)	0.05 (0.00, 0.32)	0.61 (0.50, 0.74)	0.12	0.94	5.14E-08	0.54	0.71
Fusiform gyrus right	0.32 (0.17, 0.46)	0.18 (0.04, 0.32)	0.27 (0.00, 0.45)	0.05 (0.00, 0.32)	0.68 (0.55, 0.83)	0.31	0.94	7.63E-05	0.30	0.91
Transverse temporal cortex left	0.36 (0.21, 0.48)	0.17 (0.03, 0.30)	0.35 (0.00, 0.46)	0.00 (0.00, 0.29)	0.65 (0.54, 0.79)	0.14	1.00	9.97E-06	0.49	0.76
Transverse temporal cortex right	0.41 (0.27, 0.52)	0.11 (-0.02, 0.24)	0.37 (0.16, 0.48)	0.00 (0.00, 0.15)	0.63 (0.52, 0.76)	0.01	1.00	1.69E-06	0.78	0.40
Entorhinal cortex left	0.26 (0.11, 0.40)	0.21 (0.07, 0.34)	0.07 (0.00, 0.38)	0.18 (0.00, 0.33)	0.75 (0.62, 0.87)	0.94	0.40	2.35E-04	0.49	0.76
Entorhinal cortex right	0.35 (0.21, 0.48)	0.14 (-0.00, 0.27)	0.33 (0.00, 0.44)	0.00 (0.00, 0.00)	0.67 (0.56, 0.80)	0.11	1.00	3.15E-05	0.48	0.77
Temporal pole left	0.32 (0.18, 0.45)	0.04 (-0.09, 0.17)	0.26 (0.04, 0.38)	0.00 (0.00, 0.16)	0.74 (0.62, 0.86)	0.06	1.00	9.58E-04	0.43	0.81
Temporal pole right	0.29 (0.14, 0.43)	-0.03 (-0.18, 0.11)	0.22 (0.02, 0.35)	0.00 (0.00, 0.13)	0.78 (0.65, 0.92)	0.07	1.00	0.02	0.45	0.80
Parahippocampal gyrus left	0.40 (0.26, 0.52)	0.15 (-0.00, 0.29)	0.40 (0.13, 0.51)	0.00 (0.00, 0.19)	0.60 (0.49, 0.73)	0.02	1.00	1.77E-06	0.92	0.15
Parahippocampal gyrus right	0.47 (0.34, 0.58)	0.27 (0.13, 0.39)	0.51 (0.17, 0.60)	0.00 (0.00, 0.26)	0.49 (0.40, 0.62)	0.01	1.00	1.22E-10	0.84	0.30
<i>Cingulate</i>										
Rostral anterior cingulate left	0.26 (0.12, 0.39)	0.20 (0.06, 0.33)	0.07 (0.00, 0.36)	0.18 (0.00, 0.32)	0.76 (0.64, 0.87)	0.94	0.41	1.80E-04	0.56	0.69

Rostral anterior cingulate right	0.30 (0.15, 0.43)	0.14 (0.00, 0.27)	0.25 (0.00, 0.39)	0.03 (0.00, 0.29)	0.73 (0.61, 0.86)	0.35	1.00	4.24E-04	0.66	0.56
Caudal anterior cingulate left	0.37 (0.23, 0.49)	0.10 (-0.05, 0.24)	0.35 (0.13, 0.47)	0.00 (0.00, 0.15)	0.65 (0.53, 0.78)	0.02	1.00	3.05E-05	0.69	0.52
Caudal anterior cingulate right	0.34 (0.20, 0.47)	0.04 (-0.10, 0.18)	0.29 (0.09, 0.41)	0.00 (0.00, 0.14)	0.71 (0.59, 0.84)	0.03	1.00	5.03E-04	0.78	0.39
Posterior cingulate left	0.22 (0.07, 0.36)	0.24 (0.10, 0.37)	0.00 (0.00, 0.34)	0.23 (0.00, 0.33)	0.77 (0.64, 0.87)	1.00	0.19	4.15E-04	0.85	0.28
Posterior cingulate right	0.25 (0.10, 0.39)	0.19 (0.05, 0.32)	0.20 (0.00, 0.42)	0.08 (0.00, 0.30)	0.72 (0.58, 0.87)	0.49	0.81	5.03E-04	0.86	0.27
Isthmus cingulate left	0.38 (0.24, 0.50)	0.33 (0.19, 0.45)	0.15 (0.00, 0.49)	0.24 (0.00, 0.43)	0.61 (0.49, 0.73)	0.57	0.18	1.74E-09	0.91	0.17
Isthmus cingulate right	0.39 (0.26, 0.51)	0.28 (0.14, 0.40)	0.26 (0.00, 0.51)	0.14 (0.00, 0.39)	0.60 (0.49, 0.74)	0.26	0.51	8.51E-09	0.83	0.31
<i>Insular</i>										
Insular cortex left	0.21 (0.06, 0.35)	0.19 (0.05, 0.32)	0.00 (0.00, 0.32)	0.20 (0.00, 0.29)	0.80 (0.67, 0.90)	1.00	0.34	2.01E-03	0.62	0.62
Insular cortex right	0.35 (0.20, 0.48)	-0.01 (-0.15, 0.14)	0.29 (0.09, 0.41)	0.00 (0.00, 0.13)	0.71 (0.59, 0.85)	0.03	1.00	9.17E-04	0.43	0.82

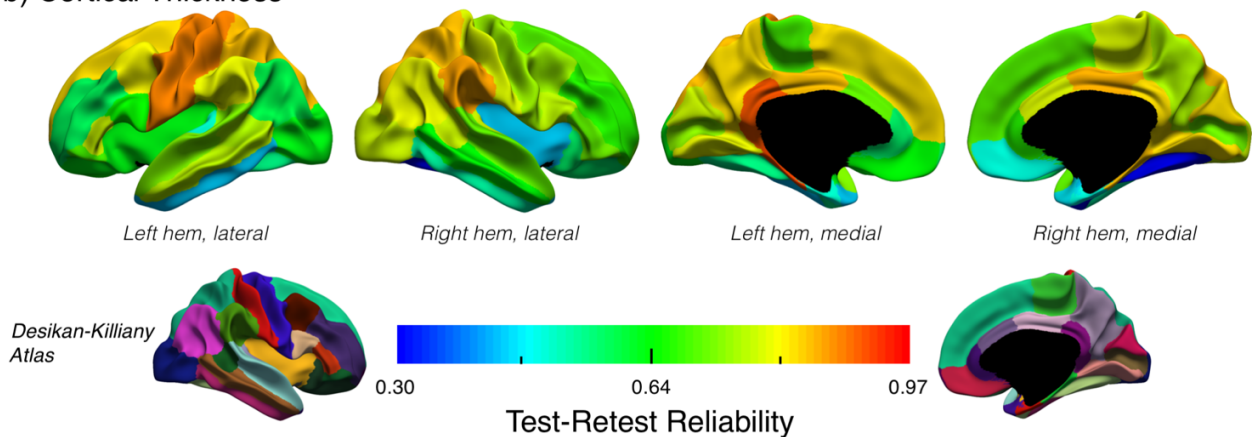
Note. Surface area and cortical thickness of each region is adjusted for total surface area/mean cortical thickness, linear and non-linear age effects, sex, interactions between age and sex, and acquisition orientation. ROIs are grouped in lobar divisions (Frontal, Parietal, Occipital, Temporal, Cingulate, Insular). a^2 = additive genetic influences; c^2 common or shared environmental influences; e^2 unique or non-shared environmental influences; No A = test of CE model (no additive genetic influence); No C = test of AE model (no common environmental influence); No AC = test of E model (no additive genetic or common environmental influence). Heritability estimates (a^2) significantly different from zero (significant 'No A'; q value < 0.05) appear in bold. Variance explained by measurement error ($1 - r^2$ test-retest correlation) was greater than non-shared environment (e^2) in the following ROIs: surface area – lateral orbitofrontal right, medial orbitofrontal left, superior temporal right, entorhinal right, temporal pole left, insula right, cortical thickness – rostral middle frontal right, lateral orbitofrontal right, medial orbitofrontal right, lateral occipital left, inferior temporal left and right, fusiform left and right, transverse temporal left, entorhinal left and right, temporal pole left and right, insular right.

Appendix 8 Test-Retest Correlations for QTIM Surface Area and Cortical Thickness

a) Surface Area

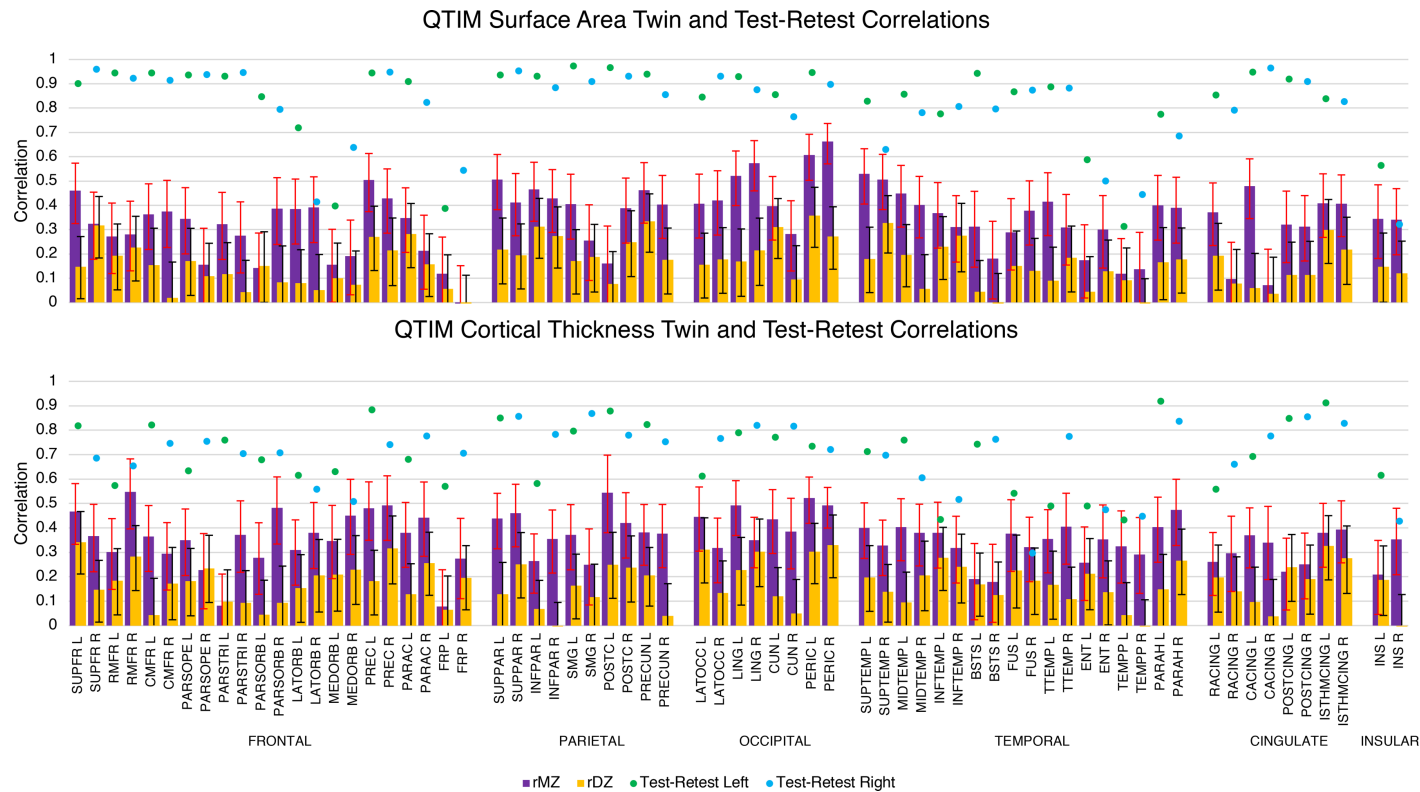


b) Cortical Thickness



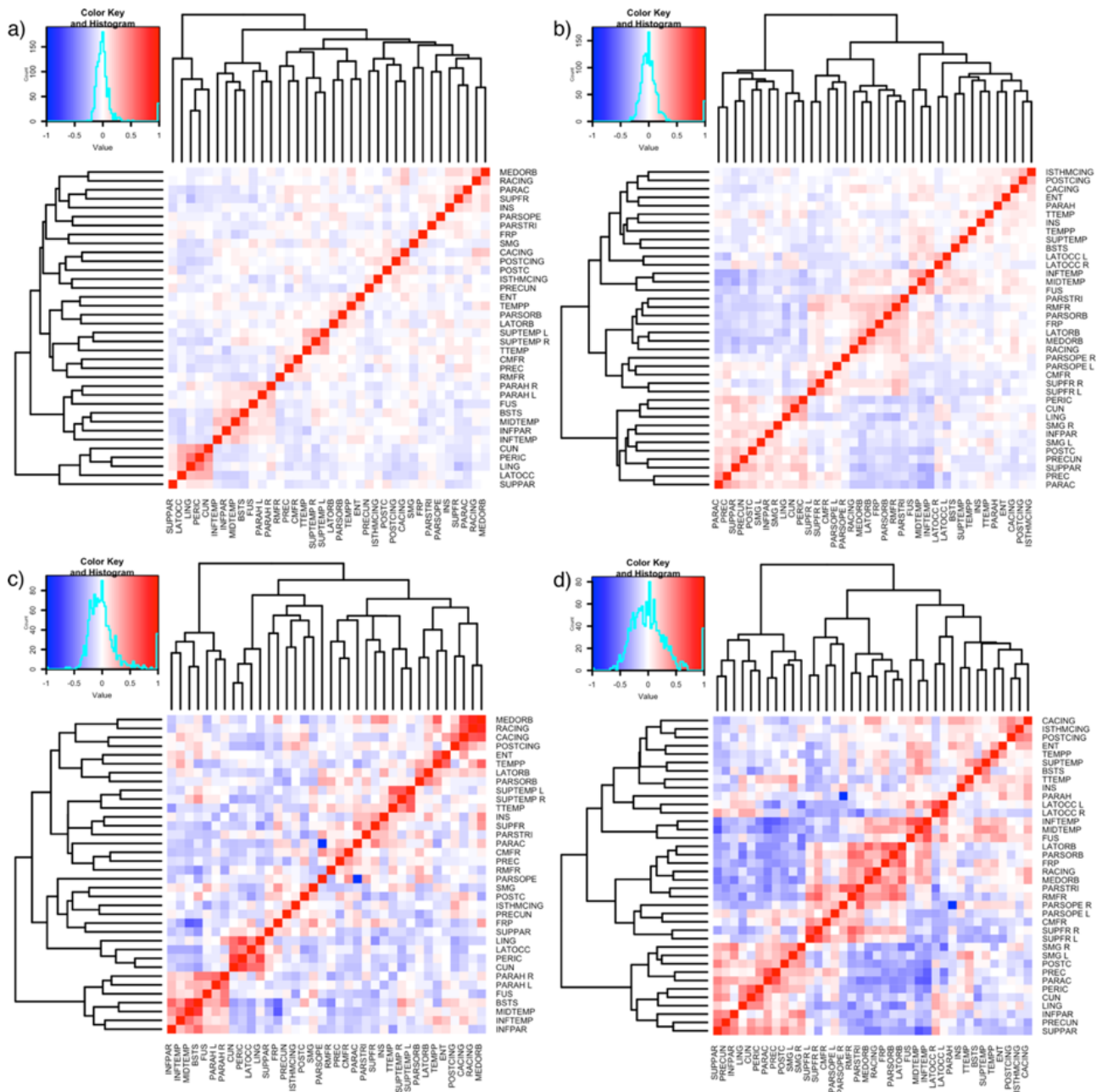
Test-retest reliability correlations varied across ROIs, ranging from 0.30 to 0.97, and were generally high for surface area (a) (reliability >70% for 55/68 ROIs) and more moderate for cortical thickness (b) (reliability >70% for 39/68 ROIs), with the mean reliability estimate (weighted by ROI size) being higher for surface area (0.84) than cortical thickness (0.72). Reliability was generally similar for corresponding left/right regions, though there were some exceptions (insular surface area, lateral orbitofrontal surface area, middle temporal gyrus cortical thickness, transverse temporal cortical thickness, fusiform cortical thickness). Poor reliability estimates (less than 50%) were generally limited to small (e.g. entorhinal, temporal pole) and difficult to measure ROIs (e.g. insular, orbitofrontal). Test-retest reliability was estimated by calculating the Pearson's correlation coefficient between surface area/cortical thickness measures from time one and time two scans (covariate effects were removed by using regression residuals; same covariates as for heritability estimates). The test-retest sample consisted 53 participants who were scanned a second time (mean duration between first and second scan was 113.36 ± 52.25 days).

Appendix 9 Twin and Test-Retest Correlations for QTIM Surface Area and Cortical



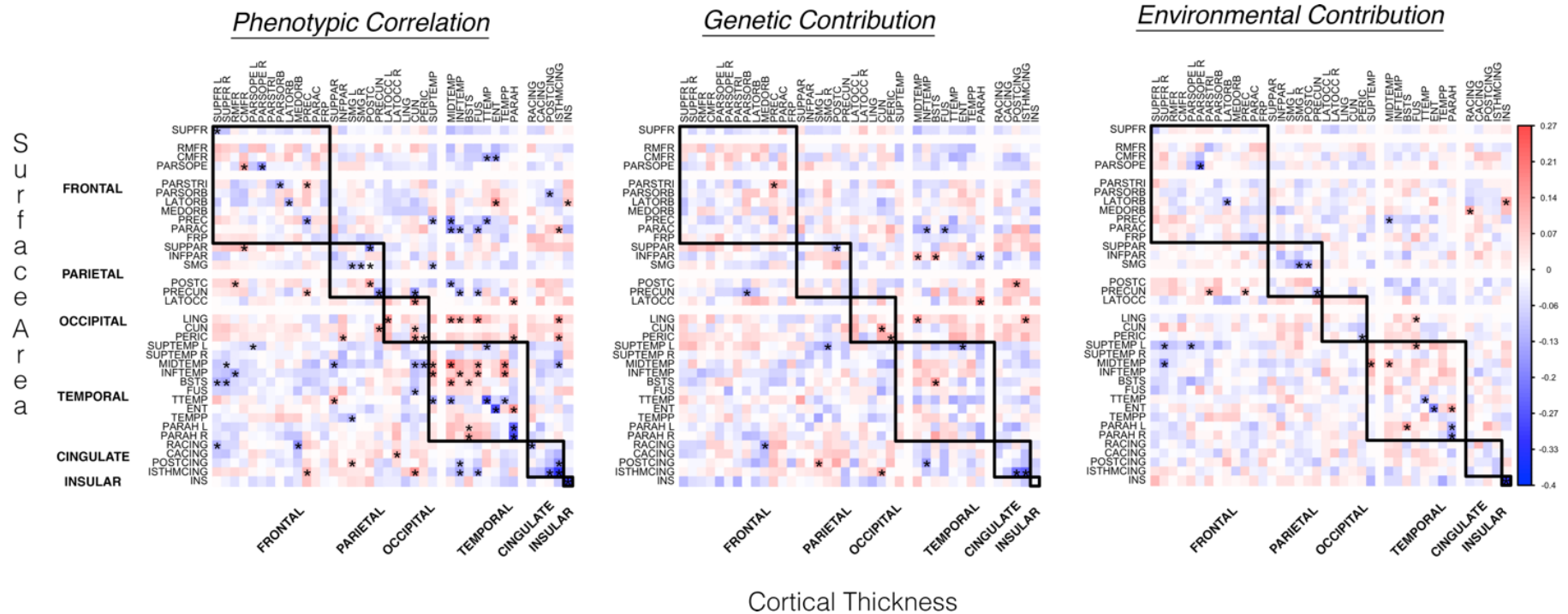
Twin correlations with 95% confidence intervals, and test-retest reliability correlations for surface area (top) and cortical thickness (bottom) for 68 ROIs (34 in each of the left (L) and right (R) hemisphere in the QTIM sample). For almost all ROIs, for both surface area (65/68) and cortical thickness (65/68) the MZ twin correlations were higher than the DZ correlations, suggesting individual variation in surface area and cortical thickness is genetically influenced.

Appendix 10 Heatmaps of Genetic Correlations Across ROIs for QTIM Surface Area and Cortical Thickness



Heatmaps, with hierarchical clustering applied, of the genetic correlations across ROIs (weighted by heritability) for a) surface area and b) cortical thickness, and genetic correlations across ROIs (not weighted by heritability) for c) surface area and d) cortical thickness in the QTIM dataset.

Appendix 11 Phenotypic Correlations with Genetic and Environmental Contributions, between QTIM Surface Area and Cortical Thickness



Phenotypic correlations (left), with genetic (middle) and environmental (right) contributions, between surface area and cortical thickness across regions in the QTIM sample. * denotes a significant correlation (q value < 0.05).

Appendix 12 Descriptive Statistics for Surface Area and Cortical Thickness in the HCP Dataset

Number of excluded measures, mean (SD), minimum, maximum, percentage difference between male and female raw means, and number of outliers (± 3.29 SD) for HCP surface area and cortical thickness ($N = 698$).

	Excluded [†]	Surface Area (mm ²)					Cortical Thickness (mm)				
		Mean (SD)	Minimum	Maximum	M/F Diff [‡]	Outliers [‡]	Mean (SD)	Minimum	Maximum	M/F Diff [‡]	Outliers [‡]
<i>Frontal</i>											
Superior frontal gyrus left	0	7374 (916)	5405	10695	13.20	4	2.84 (0.12)	2.49	3.26	-0.23	1
Superior frontal gyrus right	0	7237 (916)	5221	11507	13.57	2	2.87 (0.12)	2.47	3.29	0.09	1
Rostral middle frontal gyrus left	0	6020 (788)	4049	8461	14.04	0	2.57 (0.11)	2.27	3.01	0.90	1
Rostral middle frontal gyrus right	0	6237 (829)	4311	8773	13.67	0	2.58 (0.11)	2.22	2.96	0.79	0
Caudal middle frontal gyrus left	0	2404 (429)	1405	4114	13.90	4	2.73 (0.11)	2.43	3.15	0.88	1
Caudal middle frontal gyrus right	0	2226 (412)	1176	3666	13.89	3	2.75 (0.11)	2.38	3.08	0.47	0
Pars opercularis left	0	1710 (279)	1128	2868	11.75	2	2.79 (0.11)	2.45	3.25	1.10	1
Pars opercularis right	0	1445 (250)	859	2864	12.22	5	2.83 (0.12)	2.41	3.23	0.98	2
Pars triangularis left	0	1302 (212)	865	2098	12.54	5	2.63 (0.12)	2.31	3.01	0.79	0
Pars triangularis right	0	1518 (253)	913	2393	11.87	2	2.70 (0.12)	2.29	3.20	1.03	2
Pars orbitalis left	1	639 (87)	399	902	12.90	0	2.78 (0.14)	2.39	3.18	-0.61	0
Pars orbitalis right	0	797 (104)	485	1097	12.50	0	2.84 (0.15)	2.24	3.50	0.17	2
Lateral orbitofrontal cortex left	0	2643 (317)	1706	3672	12.21	0	2.82 (0.11)	2.48	3.33	1.29	1
Lateral orbitofrontal cortex right	0	2571 (325)	1647	3828	12.70	3	2.84 (0.12)	2.48	3.22	1.09	0
Medial orbitofrontal cortex left	0	1985 (304)	1239	2980	12.89	1	2.57 (0.15)	2.17	3.18	1.02	2
Medial orbitofrontal cortex right	0	1849 (231)	1161	2886	11.56	2	2.74 (0.13)	2.40	3.22	0.81	2
Precentral gyrus left	1	4809 (560)	3547	6962	11.78	2	2.73 (0.10)	2.42	3.10	0.76	1
Precentral gyrus right	1	4893 (575)	3359	7027	12.50	3	2.73 (0.11)	2.19	3.11	0.69	4
Paracentral lobule left	0	1317 (191)	879	2068	10.29	1	2.56 (0.12)	2.19	2.90	-0.39	0
Paracentral lobule right	0	1506 (223)	1009	2378	12.22	2	2.58 (0.13)	2.22	3.00	-0.22	0
Frontal pole left	0	203 (35)	111	317	11.72	0	2.84 (0.20)	2.30	3.65	-0.46	1
Frontal pole right	0	279 (47)	159	465	12.89	1	2.87 (0.20)	2.29	3.68	-0.44	1
<i>Parietal</i>											
Superior parietal cortex left	0	5502 (702)	3694	8020	11.45	2	2.29 (0.10)	1.99	2.54	-0.42	0
Superior parietal cortex right	0	5511 (686)	3758	7727	12.05	0	2.33 (0.10)	2.04	2.61	-0.26	0
Inferior parietal cortex left	0	4627 (680)	2917	6753	14.48	0	2.58 (0.10)	2.24	2.97	-0.15	1
Inferior parietal cortex right	0	5578 (803)	3599	8234	16.06	2	2.65 (0.10)	2.23	2.99	0.33	4
Supramarginal cortex left	0	3930 (573)	2664	6190	15.37	1	2.66 (0.11)	2.25	3.03	-0.01	2
Supramarginal cortex right	0	3694 (539)	2207	5570	13.17	1	2.70 (0.11)	2.36	3.02	0.17	0
Postcentral gyrus left	1	4141 (507)	2872	6136	12.92	1	2.22 (0.09)	1.87	2.55	0.09	2
Postcentral gyrus right	1	3961 (491)	2744	6076	12.08	5	2.24 (0.10)	1.92	2.64	0.20	3
Precuneus cortex left	0	3850 (499)	2554	5685	13.65	1	2.53 (0.10)	2.24	2.83	0.30	0
Precuneus cortex right	0	4068 (562)	2664	6051	14.08	3	2.56 (0.11)	2.21	2.88	0.34	0
<i>Occipital</i>											
Lateral occipital cortex left	0	4739 (614)	3197	6703	13.29	0	2.30 (0.10)	1.97	2.56	0.32	0
Lateral occipital cortex right	0	4621 (630)	3042	6438	13.42	0	2.35 (0.10)	2.03	2.64	0.78	0

Lingual gyrus left	0	3093 (442)	1876	4880	12.49	2	2.18 (0.10)	1.89	2.48	1.15	0
Lingual gyrus right	0	3120 (431)	1955	4921	12.33	2	2.20 (0.11)	1.77	2.57	0.76	1
Cuneus cortex left	0	1466 (215)	837	2241	13.43	1	2.09 (0.11)	1.77	2.45	0.32	1
Cuneus cortex right	0	1501 (236)	536	2292	13.44	6	2.10 (0.11)	1.74	2.44	-0.25	0
Pericalcarine cortex left	0	1477 (245)	733	2203	12.22	0	2.01 (0.11)	1.65	2.40	0.03	2
Pericalcarine cortex right	0	1614 (261)	896	2438	11.94	0	2.01 (0.12)	1.63	2.40	0.51	0
<i>Temporal</i>											
Superior temporal gyrus left	0	3833 (460)	2622	5359	12.39	0	2.90 (0.12)	2.55	3.30	1.12	1
Superior temporal gyrus right	0	3643 (420)	2665	5245	10.96	1	2.95 (0.13)	2.51	3.34	1.63	1
Middle temporal gyrus left	0	3146 (435)	1979	4750	13.52	3	2.99 (0.12)	2.66	3.36	0.34	0
Middle temporal gyrus right	0	3493 (462)	2259	5225	13.12	1	3.06 (0.13)	2.67	3.41	1.16	0
Inferior temporal gyrus left	0	3410 (517)	2210	5703	14.60	2	2.94 (0.12)	2.60	3.31	0.94	0
Inferior temporal gyrus right	0	3270 (486)	1969	4812	14.01	0	2.98 (0.12)	2.60	3.31	0.87	0
Banks of the superior temporal sulcus left	0	1054 (171)	665	1660	11.65	2	2.68 (0.13)	2.31	3.03	0.64	0
Banks of the superior temporal sulcus right	0	974 (143)	609	1487	11.10	2	2.80 (0.14)	2.24	3.25	0.75	1
Fusiform gyrus left	0	3375 (461)	2335	5288	13.98	3	2.89 (0.10)	2.54	3.29	0.20	1
Fusiform gyrus right	0	3270 (459)	2151	5018	14.66	2	2.90 (0.11)	2.49	3.27	0.44	3
Transverse temporal cortex left	0	453 (77)	285	700	12.41	0	2.68 (0.16)	2.23	3.17	-0.21	0
Transverse temporal cortex right	0	333 (55)	196	545	11.17	3	2.75 (0.16)	2.18	3.39	0.89	2
Entorhinal cortex left	6	427 (79)	276	685	15.48	1	3.31 (0.25)	2.50	4.32	0.32	2
Entorhinal cortex right	0	366 (85)	195	720	18.12	3	3.42 (0.25)	2.66	4.22	0.25	0
Temporal pole left	0	501 (60)	331	725	9.25	2	3.43 (0.28)	2.62	4.26	-1.41	0
Temporal pole right	0	437 (58)	280	621	6.85	0	3.67 (0.29)	2.77	4.46	0.23	0
Parahippocampal gyrus left	1	727 (113)	435	1233	10.10	4	2.74 (0.26)	2.01	3.40	-0.41	0
Parahippocampal gyrus right	0	699 (110)	412	1232	12.15	4	2.71 (0.21)	2.00	3.31	-0.53	0
<i>Cingulate</i>											
Rostral anterior cingulate left	2	873 (169)	441	1457	16.97	1	3.04 (0.18)	2.51	3.63	0.84	1
Rostral anterior cingulate right	20	672 (140)	321	1128	16.62	0	3.02 (0.20)	2.37	3.64	1.30	0
Caudal anterior cingulate left	2	691 (145)	393	1263	12.02	4	2.70 (0.17)	2.26	3.25	0.55	2
Caudal anterior cingulate right	20	803 (161)	428	1588	11.03	1	2.54 (0.17)	2.04	3.13	-0.68	1
Posterior cingulate left	2	1215 (179)	794	1869	11.82	2	2.57 (0.11)	2.23	2.91	0.61	0
Posterior cingulate right	20	1243 (195)	841	2015	12.26	2	2.54 (0.11)	2.20	2.89	0.97	0
Isthmus cingulate left	35	1049 (191)	641	1642	17.36	0	2.34 (0.16)	1.84	2.80	-0.10	0
Isthmus cingulate right	23	971 (158)	597	1536	13.59	4	2.34 (0.15)	1.83	2.87	1.58	2
<i>Insular</i>											
Insular cortex left	5	2267 (261)	1701	3189	10.86	1	3.06 (0.14)	2.58	3.44	2.81	1
Insular cortex right	0	2412 (295)	1710	3401	12.07	1	3.02 (0.14)	2.53	3.44	2.69	1

Note. ROIs are grouped in lobar divisions (Frontal, Parietal, Occipital, Temporal, Cingulate, Insular)

*Variables were excluded based on visual inspection of the accuracy of cortical parcellations as per ENIGMA protocols (enigma.ini.usc.edu).

+Percentage difference between male and female raw means; positive (negative) percentage denotes larger/thicker value for males (females).

‡Outliers ± 3.29 SD from the mean were replaced by the corresponding threshold value (i.e. ± 3.29).

Appendix 13 Covariate Effects for Surface Area Measures in the HCP Dataset

Regression coefficients and *q* values for surface area covariates in the HCP sample.

	Total Surface Area		Age		Age ²		Age ³		Sex		Age x Sex		Age ² x Sex		Age ³ x Sex	
	Regression Coefficient	<i>q</i> value	Regression Coefficient	<i>q</i> value	Regression Coefficient	<i>q</i> value	Regression Coefficient	<i>q</i> value	Regression Coefficient	<i>q</i> value	Regression Coefficient	<i>q</i> value	Regression Coefficient	<i>q</i> value	Regression Coefficient	<i>q</i> value
<i>Frontal</i>																
Superior frontal gyrus left	0.89	1.50E-134	0.02	0.83	-0.03	0.76	0.03	0.87	-0.18	0.67	-0.01	0.98	0.11	0.66	-0.07	0.51
Superior frontal gyrus right	0.88	3.35E-127	0.01	0.93	-0.03	0.80	0.01	0.98	-0.18	0.67	-0.02	0.90	0.12	0.59	-0.01	0.98
Rostral middle frontal gyrus left	0.82	4.29E-106	-0.02	0.93	0.04	0.69	0.12	0.18	0.04	0.98	-0.04	0.80	-0.06	0.85	-0.13	0.09
Rostral middle frontal gyrus right	0.84	2.11E-104	0.01	0.97	0.03	0.81	0.03	0.89	0.01	0.98	-0.05	0.67	0.03	0.98	-0.04	0.83
Caudal middle frontal gyrus left	0.70	3.61E-50	-0.02	0.92	0.01	0.98	1.34E-03	1.00	0.06	0.98	0.01	0.98	0.01	0.98	0.01	0.98
Caudal middle frontal gyrus right	0.70	4.41E-50	-0.09	0.33	0.01	0.98	-0.01	0.98	0.22	0.78	0.10	0.34	-0.10	0.81	-0.03	0.92
Pars opercularis left	0.68	8.78E-50	-0.15	0.03	0.08	0.46	0.05	0.86	0.24	0.76	0.11	0.31	-0.11	0.81	-0.02	0.98
Pars opercularis right	0.66	7.40E-49	-0.04	0.80	4.87E-03	0.98	-0.05	0.86	0.11	0.93	-0.01	0.98	0.06	0.93	0.08	0.67
Pars triangularis left	0.59	4.50E-33	0.07	0.60	-4.82E-04	1.00	0.02	0.98	0.15	0.89	-0.04	0.87	-0.11	0.82	-0.04	0.92
Pars triangularis right	0.55	1.80E-29	-0.05	0.79	0.04	0.83	0.12	0.54	0.11	0.95	0.02	0.98	-0.12	0.81	-0.06	0.84
Pars orbitalis left	0.65	1.34E-49	-0.04	0.80	0.02	0.95	0.13	0.29	-0.32	0.58	0.01	0.98	0.05	0.95	-0.10	0.48
Pars orbitalis right	0.65	2.89E-54	0.01	0.98	-4.63E-03	0.98	-1.03E-03	1.00	-0.40	0.38	0.01	0.98	0.14	0.67	-1.39E-03	1.00
Lateral orbitofrontal cortex left	0.87	8.51E-116	-0.06	0.32	0.10	0.09	0.19	0.01	0.17	0.74	0.06	0.48	-0.17	0.37	-0.18	0.01
Lateral orbitofrontal cortex right	0.82	5.04E-96	-0.03	0.84	0.09	0.17	0.17	0.03	0.55	0.05	-0.02	0.96	-0.36	0.01	-0.21	2.92E-03
Medial orbitofrontal cortex left	0.70	6.78E-55	-0.01	0.98	0.05	0.71	-0.02	0.98	-0.10	0.93	0.03	0.87	0.06	0.93	0.06	0.80
Medial orbitofrontal cortex right	0.82	8.53E-90	3.53E-03	0.98	0.11	0.08	0.15	0.11	0.05	0.98	0.02	0.93	-0.06	0.91	-0.14	0.15
Precentral gyrus left	0.80	5.76E-83	0.01	0.98	-0.04	0.80	0.05	0.79	-0.33	0.41	0.01	0.98	0.14	0.65	-0.03	0.91
Precentral gyrus right	0.80	2.11E-91	-0.02	0.90	-3.59E-04	1.00	0.07	0.67	-0.46	0.12	0.03	0.82	0.17	0.44	-0.04	0.82
Paracentral lobule left	0.67	9.25E-46	-0.01	0.98	0.03	0.89	0.23	0.03	-0.21	0.80	0.05	0.80	0.08	0.89	-0.13	0.37
Paracentral lobule right	0.67	2.36E-51	0.05	0.67	0.03	0.87	0.15	0.24	-0.18	0.82	-0.04	0.84	0.09	0.83	-0.06	0.79
Frontal pole left	0.52	1.18E-28	0.04	0.82	-0.04	0.82	-0.11	0.59	0.11	0.95	-0.07	0.69	0.02	0.98	0.05	0.87
Frontal pole right	0.53	1.65E-31	0.03	0.89	-0.02	0.93	0.01	0.98	-0.09	0.97	-0.11	0.37	0.05	0.95	-0.03	0.96
<i>Parietal</i>																
Superior parietal cortex left	0.78	5.46E-75	0.03	0.82	-0.02	0.92	-0.21	0.01	0.28	0.58	-0.02	0.92	-0.01	0.98	0.19	0.02
Superior parietal cortex right	0.75	2.05E-73	-0.05	0.67	0.05	0.67	-0.12	0.27	0.47	0.14	0.01	0.98	-0.22	0.25	0.06	0.69
Inferior parietal cortex left	0.76	1.43E-79	-0.01	0.98	-0.05	0.67	-0.06	0.78	0.02	0.98	0.02	0.97	1.22E-03	1.00	0.10	0.45
Inferior parietal cortex right	0.73	2.83E-75	-0.06	0.48	-0.01	0.98	0.01	0.98	-0.21	0.71	0.06	0.59	-0.03	0.97	-0.02	0.95
Supramarginal cortex left	0.73	4.40E-82	0.02	0.92	0.02	0.95	0.01	0.98	-0.12	0.87	-0.01	0.98	0.03	0.97	0.03	0.93
Supramarginal cortex right	0.73	3.48E-68	0.09	0.22	0.01	0.98	-0.02	0.98	0.25	0.67	-0.07	0.55	-0.07	0.87	0.06	0.76
Postcentral gyrus left	0.80	3.16E-97	-0.08	0.19	0.01	0.98	0.10	0.34	-0.17	0.79	0.08	0.36	-0.01	0.98	-0.11	0.27
Postcentral gyrus right	0.79	3.71E-87	-9.05E-05	1.00	-0.04	0.80	-0.03	0.89	-0.12	0.88	0.05	0.69	0.05	0.92	0.01	0.98
Precuneus cortex left	0.80	2.85E-102	0.01	0.98	-0.07	0.31	-0.08	0.48	0.03	0.98	-0.03	0.86	0.01	0.98	0.02	0.95
Precuneus cortex right	0.81	1.45E-92	0.03	0.82	0.01	0.98	-0.03	0.92	0.07	0.95	-0.02	0.96	-0.02	0.98	0.02	0.94
<i>Occipital</i>																
Lateral occipital cortex left	0.74	1.27E-69	-0.02	0.96	0.11	0.18	0.06	0.76	0.08	0.95	0.01	0.98	-0.13	0.69	-0.03	0.92
Lateral occipital cortex right	0.73	5.76E-70	1.78E-03	1.00	0.07	0.48	0.08	0.67	-0.13	0.87	0.05	0.69	-0.03	0.98	-0.08	0.61
Lingual gyrus left	0.64	4.15E-45	0.11	0.19	-0.04	0.82	-0.11	0.49	0.40	0.42	-0.09	0.48	-0.15	0.69	0.06	0.80
Lingual gyrus right	0.66	4.05E-51	0.07	0.55	0.01	0.98	-0.16	0.17	0.48	0.23	-0.06	0.67	-0.18	0.58	0.08	0.66
Cuneus cortex left	0.62	1.60E-42	0.02	0.92	-0.08	0.51	-0.12	0.38	-0.24	0.72	-0.01	0.98	0.11	0.80	0.04	0.87
Cuneus cortex right	0.62	7.18E-42	0.01	0.98	0.02	0.97	3.87E-03	0.99	0.29	0.67	-5.40E-04	1.00	-0.20	0.51	-0.08	0.70
Pericalcarine cortex left	0.54	2.89E-28	0.05	0.76	0.01	0.98	-0.03	0.97	0.06	0.98	-0.04	0.88	0.02	0.98	0.03	0.96

Pericalcarine cortex right	0.56	1.42E-30	0.01	0.98	0.05	0.79	0.01	0.98	0.24	0.79	0.01	0.98	-0.12	0.81	-0.03	0.94
<i>Temporal</i>																
Superior temporal gyrus left	0.80	2.04E-99	0.03	0.83	0.08	0.27	0.01	0.98	0.12	0.84	0.01	0.98	-0.08	0.80	1.78E-03	1.00
Superior temporal gyrus right	0.86	7.58E-115	0.02	0.87	0.02	0.87	0.01	0.98	0.21	0.67	-0.01	0.98	-0.03	0.98	0.01	0.98
Middle temporal gyrus left	0.83	1.30E-94	0.02	0.92	-0.03	0.80	-0.05	0.80	0.12	0.87	-0.06	0.60	0.02	0.98	0.06	0.70
Middle temporal gyrus right	0.82	6.60E-99	0.01	0.98	-0.08	0.23	-0.08	0.51	0.01	0.98	-0.02	0.92	0.07	0.83	0.08	0.51
Inferior temporal gyrus left	0.75	4.36E-73	-4.89E-03	0.98	-0.10	0.23	-0.07	0.67	-0.41	0.29	-7.94E-04	1.00	0.23	0.27	0.08	0.67
Inferior temporal gyrus right	0.77	3.59E-79	-0.08	0.32	-0.07	0.51	0.07	0.69	-0.36	0.40	0.09	0.33	0.15	0.59	-0.04	0.87
Banks of the superior temporal sulcus left	0.55	1.15E-31	0.02	0.96	-0.07	0.67	-0.02	0.98	-0.02	0.98	-0.03	0.90	0.04	0.98	0.04	0.92
Banks of the superior temporal sulcus right	0.61	1.75E-40	-0.06	0.69	-0.03	0.92	-0.06	0.82	-0.02	0.98	0.06	0.69	0.02	0.98	0.06	0.80
Fusiform gyrus left	0.70	3.18E-72	-0.09	0.18	-0.05	0.69	-0.03	0.90	-0.35	0.38	0.12	0.11	0.08	0.84	-0.01	0.98
Fusiform gyrus right	0.76	2.02E-88	0.03	0.84	-0.12	0.04	-0.10	0.34	-0.14	0.82	-0.04	0.80	0.12	0.68	0.09	0.40
Transverse temporal cortex left	0.60	1.75E-38	-0.01	0.98	0.11	0.27	0.14	0.37	-0.20	0.81	0.07	0.69	0.03	0.98	-0.12	0.48
Transverse temporal cortex right	0.65	7.92E-44	0.07	0.61	0.06	0.71	0.06	0.80	-0.02	0.98	-0.04	0.83	0.08	0.89	0.02	0.98
Entorhinal cortex left	0.52	9.28E-29	-0.03	0.92	1.78E-03	1.00	-0.12	0.48	-0.36	0.59	0.01	0.98	0.14	0.74	0.16	0.24
Entorhinal cortex right	0.39	3.29E-15	-0.03	0.93	-0.02	0.96	-0.13	0.48	-0.30	0.69	0.02	0.95	0.05	0.97	0.14	0.40
Temporal pole left	0.42	4.82E-18	0.13	0.18	-0.13	0.21	-0.27	0.02	-0.42	0.48	-0.08	0.67	0.24	0.46	0.22	0.06
Temporal pole right	0.42	2.98E-16	0.01	0.98	-0.13	0.29	-0.12	0.59	-0.63	0.22	0.01	0.98	0.40	0.11	0.18	0.23
Parahippocampal gyrus left	0.60	5.17E-39	0.06	0.65	-0.03	0.90	-0.14	0.28	-0.13	0.90	0.01	0.98	0.18	0.60	0.14	0.32
Parahippocampal gyrus right	0.72	4.21E-56	0.11	0.14	-0.01	0.98	-0.06	0.80	0.24	0.70	-0.07	0.59	1.06E-03	1.00	0.06	0.80
<i>Cingulate</i>																
Rostral anterior cingulate left	0.83	3.92E-87	0.05	0.67	0.09	0.27	0.06	0.74	0.61	0.04	-0.07	0.51	-0.24	0.22	-0.07	0.67
Rostral anterior cingulate right	0.58	6.45E-37	0.06	0.65	-0.02	0.95	-0.07	0.79	-0.21	0.80	-0.03	0.93	0.12	0.80	0.11	0.49
Caudal anterior cingulate left	0.59	1.71E-36	0.01	0.98	-0.02	0.94	-0.02	0.98	0.29	0.69	-0.01	0.98	-0.04	0.98	0.01	0.98
Caudal anterior cingulate right	0.57	5.63E-35	0.01	0.98	-0.01	0.98	-0.03	0.93	0.32	0.67	-0.07	0.69	-3.61E-03	1.00	0.05	0.87
Posterior cingulate left	0.65	1.67E-48	-0.05	0.69	0.05	0.79	0.12	0.46	0.16	0.86	0.06	0.67	-0.13	0.72	-0.07	0.74
Posterior cingulate right	0.73	1.11E-58	0.03	0.91	-0.09	0.34	-0.05	0.86	-0.14	0.87	-0.04	0.81	0.21	0.46	0.07	0.69
Isthmus cingulate left	0.71	1.57E-55	0.04	0.79	-0.05	0.70	-0.12	0.42	0.04	0.98	-0.04	0.82	-0.02	0.98	0.08	0.68
Isthmus cingulate right	0.71	1.73E-57	-0.08	0.37	-7.25E-04	1.00	0.08	0.67	0.17	0.82	0.01	0.98	-0.08	0.86	-0.07	0.72
<i>Insular</i>																
Insular cortex left	0.76	3.68E-79	0.06	0.51	-0.05	0.67	0.08	0.61	-0.55	0.07	0.02	0.94	0.26	0.17	-0.05	0.82
Insular cortex right	0.73	2.70E-71	0.11	0.08	0.05	0.67	0.10	0.46	-0.34	0.44	-0.04	0.80	0.12	0.70	-1.40E-03	1.00

Note. Estimates significant at $q < 0.05$ appear in bold. ROIs are grouped in lobar divisions (Frontal, Parietal, Occipital, Temporal, Cingulate, Insular). A positive estimate for sex indicates a larger surface area for females. Dummy variables were coded sex (male = 0, female = 1), and all other variables were standardised prior to analyses.

Appendix 14 Covariate Effects for Cortical Thickness Measures in the HCP Dataset

Regression coefficients and q values for cortical thickness covariates in the HCP sample.

	Average Thickness		Age		Age ²		Age ³		Sex		Age x Sex		Age ² x Sex		Age ³ x Sex	
	Regression Coefficient	q value	Regression Coefficient	q value	Regression Coefficient	q value	Regression Coefficient	q value	Regression Coefficient	q value	Regression Coefficient	q value	Regression Coefficient	q value	Regression Coefficient	q value
<i>Frontal</i>																
Superior frontal gyrus left	0.73	2.35E-107	-0.07	0.37	-0.10	0.16	-0.15	0.08	0.22	0.64	-0.03	0.83	0.09	0.75	0.14	0.15
Superior frontal gyrus right	0.77	6.23E-122	-0.08	0.22	-0.05	0.58	-0.07	0.61	0.21	0.64	-0.01	0.97	0.01	0.97	0.05	0.72
Rostral middle frontal gyrus left	0.75	3.48E-110	-0.05	0.61	-0.10	0.16	-0.10	0.41	-0.01	0.97	-0.01	0.95	0.04	0.94	0.10	0.41
Rostral middle frontal gyrus right	0.75	1.57E-109	-0.07	0.33	-0.07	0.41	-0.08	0.56	-0.10	0.86	0.01	0.97	0.08	0.80	0.07	0.57
Caudal middle frontal gyrus left	0.71	2.19E-93	-0.06	0.50	-0.01	0.95	-0.06	0.73	0.20	0.69	-0.06	0.60	-0.07	0.84	0.01	0.97
Caudal middle frontal gyrus right	0.76	1.84E-108	-0.13	0.02	0.01	0.97	0.02	0.96	0.11	0.85	-0.01	0.96	-0.02	0.97	0.01	0.97
Pars opercularis left	0.71	7.05E-90	-0.12	0.06	-0.04	0.79	-0.04	0.85	-0.06	0.95	0.04	0.82	-0.03	0.97	0.05	0.82
Pars opercularis right	0.69	1.08E-80	-0.06	0.58	-0.02	0.90	-0.03	0.93	-0.30	0.56	0.06	0.62	0.07	0.85	0.04	0.85
Pars triangularis left	0.67	9.99E-76	-0.07	0.50	-0.05	0.72	-0.07	0.70	0.24	0.65	0.06	0.66	-0.18	0.53	-0.02	0.95
Pars triangularis right	0.72	2.61E-89	-0.14	0.03	-0.05	0.64	-0.02	0.95	-0.26	0.61	0.10	0.36	0.06	0.91	0.02	0.95
Pars orbitalis left	0.56	8.12E-48	-0.07	0.60	-0.02	0.92	-0.03	0.94	0.09	0.95	0.11	0.41	0.02	0.97	-0.01	0.97
Pars orbitalis right	0.67	1.12E-75	3.48E-03	0.97	-0.03	0.85	-0.06	0.75	-0.06	0.96	-0.03	0.84	0.14	0.65	0.11	0.44
Lateral orbitofrontal cortex left	0.59	9.82E-61	-0.08	0.43	-0.12	0.16	-0.14	0.30	-0.55	0.16	0.03	0.84	0.23	0.38	0.11	0.44
Lateral orbitofrontal cortex right	0.63	4.89E-66	-0.01	0.95	-0.05	0.68	-0.07	0.69	-0.38	0.44	-0.02	0.95	0.17	0.57	0.07	0.69
Medial orbitofrontal cortex left	0.37	3.98E-18	-0.03	0.88	-0.14	0.22	0.02	0.97	-0.89	0.04	0.01	0.97	0.44	0.09	0.05	0.85
Medial orbitofrontal cortex right	0.48	2.69E-33	-0.10	0.37	-0.05	0.75	0.04	0.91	-0.19	0.82	0.04	0.86	0.03	0.97	-0.08	0.69
Precentral gyrus left	0.77	7.58E-114	-0.01	0.97	0.04	0.65	-0.03	0.85	0.17	0.73	-0.04	0.74	-0.07	0.83	0.06	0.67
Precentral gyrus right	0.78	5.02E-109	-0.02	0.90	0.03	0.85	0.01	0.96	0.32	0.44	-0.03	0.82	-0.17	0.50	-0.01	0.97
Paracentral lobule left	0.68	5.12E-78	-0.04	0.75	0.03	0.85	0.09	0.57	-0.02	0.97	0.09	0.41	0.05	0.93	-0.02	0.95
Paracentral lobule right	0.68	3.93E-74	0.04	0.79	0.01	0.97	-0.07	0.67	0.44	0.33	-0.02	0.96	-0.12	0.73	0.04	0.84
Frontal pole left	0.47	8.08E-31	-0.08	0.54	-0.14	0.16	-0.13	0.48	-0.40	0.51	0.03	0.93	0.36	0.16	0.12	0.52
Frontal pole right	0.47	5.55E-33	-0.09	0.42	-0.07	0.59	-0.07	0.75	0.08	0.95	0.02	0.96	0.07	0.90	0.01	0.97
<i>Parietal</i>																
Superior parietal cortex left	0.77	4.35E-113	0.04	0.66	0.07	0.42	0.08	0.59	0.50	0.11	-3.05E-03	0.97	-0.20	0.38	-0.06	0.69
Superior parietal cortex right	0.80	7.10E-131	0.04	0.61	0.09	0.21	0.10	0.41	0.27	0.50	0.06	0.57	-0.14	0.54	-0.07	0.56
Inferior parietal cortex left	0.83	2.21E-124	0.10	0.10	2.03E-03	0.98	-0.07	0.62	0.71	0.01	-0.12	0.12	-0.22	0.26	-0.01	0.96
Inferior parietal cortex right	0.87	3.58E-151	0.05	0.56	0.07	0.40	0.02	0.92	0.49	0.06	-0.06	0.51	-0.22	0.18	-0.04	0.81
Supramarginal cortex left	0.83	2.27E-131	0.02	0.91	0.02	0.93	-0.01	0.97	0.31	0.42	-0.03	0.82	-0.07	0.81	-0.01	0.97
Supramarginal cortex right	0.86	6.80E-147	-0.08	0.21	0.06	0.50	0.10	0.37	0.16	0.74	0.06	0.57	-0.10	0.69	-0.09	0.44
Postcentral gyrus left	0.72	5.12E-91	0.04	0.75	0.02	0.95	2.73E-03	0.98	-0.14	0.83	0.02	0.95	0.12	0.68	0.03	0.89
Postcentral gyrus right	0.70	8.70E-85	0.06	0.60	0.10	0.25	0.08	0.62	0.05	0.96	-0.03	0.84	-0.01	0.97	-1.02E-03	0.99
Precuneus cortex left	0.78	1.23E-121	0.02	0.88	0.06	0.49	0.08	0.53	0.35	0.37	-0.02	0.91	-0.19	0.37	-0.08	0.52
Precuneus cortex right	0.78	6.65E-113	5.49E-04	0.99	0.10	0.19	0.07	0.62	0.46	0.19	-0.01	0.97	-0.27	0.15	-0.10	0.43
<i>Occipital</i>																
Lateral occipital cortex left	0.70	1.83E-91	0.11	0.06	0.03	0.84	-0.02	0.94	-0.09	0.91	-0.06	0.61	0.09	0.75	0.04	0.85
Lateral occipital cortex right	0.72	2.15E-101	0.03	0.75	0.10	0.18	0.10	0.41	-0.04	0.97	0.02	0.92	-0.07	0.84	-0.05	0.75
Lingual gyrus left	0.49	2.73E-37	-0.01	0.97	0.07	0.62	0.13	0.41	0.13	0.89	0.09	0.53	-0.24	0.42	-0.12	0.48
Lingual gyrus right	0.47	6.80E-34	-0.04	0.83	0.05	0.75	0.07	0.70	0.22	0.75	0.10	0.42	-0.25	0.41	-0.17	0.21
Cuneus cortex left	0.52	9.17E-40	-0.02	0.95	0.12	0.23	0.09	0.61	0.04	0.97	0.07	0.61	-0.11	0.79	-0.08	0.66
Cuneus cortex right	0.56	4.56E-45	0.03	0.84	0.14	0.14	0.10	0.58	0.36	0.55	0.05	0.79	-0.23	0.46	-0.08	0.65

Pericalcarine cortex left	0.41	1.06E-23	-0.06	0.69	4.43E-03	0.97	-0.05	0.86	-0.04	0.97	0.14	0.21	-0.01	0.97	-0.02	0.96
Pericalcarine cortex right	0.40	5.02E-22	0.02	0.94	-0.03	0.89	-1.32E-03	0.99	-0.32	0.65	0.09	0.57	0.09	0.85	-0.05	0.85
<i>Temporal</i>																
Superior temporal gyrus left	0.75	1.47E-98	0.03	0.81	0.01	0.97	-0.01	0.97	-0.22	0.67	0.02	0.95	0.03	0.95	-0.02	0.95
Superior temporal gyrus right	0.80	6.00E-114	-4.17E-03	0.97	0.08	0.41	0.08	0.56	-0.07	0.95	0.00	1.00	-0.14	0.60	-0.08	0.56
Middle temporal gyrus left	0.78	1.22E-102	0.07	0.42	0.05	0.65	0.02	0.95	0.68	0.02	-0.06	0.62	-0.35	0.04	-0.12	0.35
Middle temporal gyrus right	0.80	1.33E-113	0.03	0.75	0.08	0.35	0.05	0.75	0.06	0.95	-0.05	0.68	-0.12	0.68	-0.04	0.85
Inferior temporal gyrus left	0.73	2.95E-88	0.10	0.21	0.06	0.58	0.06	0.71	-0.10	0.91	-0.04	0.79	-0.02	0.97	-0.05	0.83
Inferior temporal gyrus right	0.76	1.27E-96	0.07	0.46	0.05	0.65	0.06	0.70	-0.30	0.55	-0.03	0.85	0.10	0.75	-0.01	0.97
Banks of the superior temporal sulcus left	0.63	5.83E-59	0.04	0.79	0.05	0.71	0.13	0.41	0.27	0.64	0.02	0.95	-0.24	0.38	-0.20	0.07
Banks of the superior temporal sulcus right	0.62	1.50E-61	0.06	0.61	0.04	0.79	-0.02	0.97	0.42	0.41	-0.08	0.58	-0.22	0.44	-0.02	0.97
Fusiform gyrus left	0.72	1.24E-88	0.14	0.03	0.07	0.52	-0.01	0.97	0.03	0.97	-0.11	0.26	0.07	0.85	0.08	0.58
Fusiform gyrus right	0.73	2.66E-91	0.08	0.41	0.02	0.93	0.03	0.93	-0.13	0.85	-0.05	0.66	0.09	0.81	0.02	0.96
Transverse temporal cortex left	0.48	5.96E-33	-0.01	0.97	-0.03	0.89	0.07	0.75	-0.09	0.94	0.11	0.41	0.02	0.97	-0.11	0.52
Transverse temporal cortex right	0.50	8.36E-39	3.72E-03	0.97	0.04	0.82	0.05	0.84	0.09	0.94	-4.53E-03	0.97	-0.11	0.78	-0.10	0.57
Entorhinal cortex left	0.37	2.81E-17	0.06	0.73	0.08	0.59	0.01	0.97	0.13	0.92	-0.04	0.89	-0.04	0.96	0.02	0.96
Entorhinal cortex right	0.33	3.43E-14	0.07	0.65	0.03	0.89	0.06	0.83	-0.87	0.06	0.08	0.66	0.37	0.21	-0.08	0.72
Temporal pole left	0.38	2.06E-18	0.07	0.62	0.01	0.97	-0.05	0.85	-0.04	0.97	0.01	0.97	0.16	0.72	0.11	0.62
Temporal pole right	0.38	1.57E-20	-0.01	0.97	0.10	0.43	0.11	0.59	-0.20	0.82	0.12	0.40	-2.69E-03	0.99	-0.09	0.65
Parahippocampal gyrus left	0.30	2.64E-12	-0.02	0.93	0.07	0.68	0.06	0.85	0.15	0.89	0.06	0.73	-0.06	0.94	0.02	0.96
Parahippocampal gyrus right	0.32	4.02E-13	-0.08	0.60	-0.01	0.97	0.02	0.97	-0.49	0.44	0.15	0.21	0.24	0.52	0.01	0.97
<i>Cingulate</i>																
Rostral anterior cingulate left	0.39	3.50E-19	0.07	0.62	-0.12	0.41	-0.18	0.29	-0.62	0.24	-0.02	0.96	0.35	0.23	0.11	0.61
Rostral anterior cingulate right	0.29	1.06E-10	-0.09	0.56	-0.01	0.97	-0.01	0.97	-0.20	0.83	0.07	0.69	2.10E-03	0.99	-0.02	0.97
Caudal anterior cingulate left	0.29	6.28E-12	-0.13	0.21	-0.03	0.89	3.58E-03	0.98	-0.20	0.83	0.10	0.52	0.07	0.93	0.01	0.97
Caudal anterior cingulate right	0.29	1.03E-10	-0.09	0.52	-0.07	0.69	0.01	0.97	-0.04	0.97	0.02	0.95	0.12	0.82	0.02	0.97
Posterior cingulate left	0.44	8.52E-30	-0.13	0.16	-0.10	0.41	-0.07	0.74	-0.19	0.81	0.06	0.69	0.08	0.86	-0.02	0.95
Posterior cingulate right	0.48	2.52E-34	-0.09	0.44	-0.08	0.55	-0.01	0.97	0.23	0.74	-0.01	0.97	-0.18	0.60	-0.08	0.69
Isthmus cingulate left	0.29	2.30E-11	-0.01	0.97	-0.08	0.60	-0.01	0.97	0.07	0.97	-0.04	0.89	0.06	0.94	0.02	0.96
Isthmus cingulate right	0.21	6.62E-06	-0.04	0.84	-0.04	0.86	0.01	0.97	0.03	0.97	-0.02	0.95	-0.10	0.85	-0.05	0.86
<i>Insular</i>																
Insular cortex left	0.40	4.73E-25	0.04	0.83	-0.02	0.92	-0.09	0.68	-0.04	0.97	-0.08	0.58	-0.20	0.56	0.02	0.96
Insular cortex right	0.41	2.48E-25	-0.01	0.97	-0.12	0.32	-0.14	0.43	-0.23	0.75	1.47E-03	0.99	-0.10	0.83	0.04	0.89

Note. Estimates significant at $q < 0.05$ appear in bold. ROIs are grouped in lobar divisions (Frontal, Parietal, Occipital, Temporal, Cingulate, Insular). A positive estimate for sex indicates a thicker cortex for females. Dummy variables were coded sex (male = 0, female = 1), and all other variables were standardised prior to analyses.

Appendix 15 Variance Component Estimates for HCP Surface Area and Cortical Thickness

Twin Correlations, Estimates of Variance Components, Model Fit Comparisons, and Test-Retest Correlations for Surface Area and Cortical Thickness of Left and Right Cortical Regions in the HCP Dataset.

	Twin Correlations (95% CI)		Variance Components (95% CI)			No A	q value		Test-Retest Reliability	
	MZ	DZ/twin-sibling	a ²	c ²	e ²		No C	No AC	r trt	1 - r ² trt
<i>Surface Area</i>										
<i>Frontal</i>										
Superior frontal gyrus left	0.46 (0.32, 0.58)	0.17 (0.07, 0.28)	0.43 (0.24, 0.55)	0.00 (0.00, 0.12)	0.57 (0.45, 0.70)	1.09E-03	1.00	1.08E-08	0.96	0.07
Superior frontal gyrus right	0.38 (0.23, 0.51)	0.11 (0.02, 0.21)	0.35 (0.17, 0.48)	0.00 (0.00, 0.11)	0.65 (0.52, 0.78)	0.01	1.00	6.00E-06	0.94	0.11
Rostral middle frontal gyrus left	0.37 (0.22, 0.50)	0.14 (0.04, 0.24)	0.35 (0.12, 0.47)	0.00 (0.00, 0.14)	0.65 (0.53, 0.78)	0.01	1.00	2.66E-06	0.97	0.06
Rostral middle frontal gyrus right	0.34 (0.19, 0.47)	0.24 (0.15, 0.34)	0.21 (0.00, 0.47)	0.13 (0.00, 0.33)	0.65 (0.53, 0.80)	0.29	0.36	3.39E-09	0.97	0.06
Caudal middle frontal gyrus left	0.27 (0.12, 0.42)	0.13 (0.03, 0.22)	0.28 (0.00, 0.41)	0.00 (0.00, 0.19)	0.72 (0.59, 0.86)	0.11	1.00	1.29E-04	0.98	0.05
Caudal middle frontal gyrus right	0.25 (0.10, 0.39)	0.32 (0.22, 0.42)	0.00 (0.00, 0.19)	0.30 (0.15, 0.39)	0.70 (0.60, 0.79)	1.00	1.94E-03	2.69E-10	0.98	0.04
Pars opercularis left	0.30 (0.14, 0.44)	0.02 (-0.06, 0.12)	0.20 (0.03, 0.34)	0.00 (0.00, 0.09)	0.80 (0.66, 0.93)	0.06	1.00	0.02	0.97	0.06
Pars opercularis right	0.09 (-0.06, 0.24)	0.08 (0.00, 0.17)	0.05 (0.00, 0.27)	0.06 (0.00, 0.18)	0.89 (0.73, 0.98)	1.00	0.82	0.11	0.94	0.12
Pars triangularis left	0.41 (0.28, 0.53)	0.28 (0.19, 0.37)	0.38 (0.08, 0.58)	0.09 (0.00, 0.29)	0.53 (0.42, 0.67)	0.03	0.59	1.01E-13	0.97	0.05
Pars triangularis right	0.24 (0.09, 0.39)	0.15 (0.07, 0.24)	0.24 (0.00, 0.41)	0.04 (0.00, 0.24)	0.72 (0.59, 0.88)	0.25	0.97	3.52E-05	0.96	0.07
Pars orbitalis left	0.32 (0.17, 0.46)	0.26 (0.15, 0.36)	0.14 (0.00, 0.45)	0.18 (0.00, 0.36)	0.67 (0.54, 0.81)	0.57	0.21	1.55E-08	0.88	0.23
Pars orbitalis right	0.11 (-0.05, 0.26)	0.17 (0.07, 0.27)	0.00 (0.00, 0.22)	0.15 (0.00, 0.24)	0.85 (0.74, 0.93)	1.00	0.11	1.94E-03	0.92	0.15
Lateral orbitofrontal cortex left	0.48 (0.35, 0.59)	0.32 (0.23, 0.42)	0.34 (0.08, 0.57)	0.14 (0.00, 0.33)	0.52 (0.42, 0.64)	0.03	0.29	3.50E-18	0.92	0.15
Lateral orbitofrontal cortex right	0.32 (0.17, 0.46)	0.21 (0.11, 0.31)	0.28 (0.00, 0.45)	0.05 (0.00, 0.26)	0.67 (0.55, 0.81)	0.14	0.86	2.16E-07	0.74	0.45
Medial orbitofrontal cortex left	0.22 (0.06, 0.37)	0.12 (0.03, 0.22)	0.21 (0.00, 0.36)	0.02 (0.00, 0.22)	0.77 (0.64, 0.92)	0.37	1.00	2.24E-03	0.43	0.81
Medial orbitofrontal cortex right	0.41 (0.28, 0.54)	0.12 (0.02, 0.23)	0.37 (0.17, 0.48)	0.00 (0.00, 0.13)	0.63 (0.52, 0.75)	0.01	1.00	1.00E-07	0.88	0.23
Precentral gyrus left	0.38 (0.24, 0.51)	0.25 (0.15, 0.35)	0.33 (0.03, 0.51)	0.06 (0.00, 0.27)	0.61 (0.49, 0.75)	0.06	0.77	1.17E-09	0.97	0.05
Precentral gyrus right	0.44 (0.31, 0.56)	0.16 (0.07, 0.25)	0.42 (0.25, 0.54)	0.00 (0.00, 0.10)	0.58 (0.46, 0.70)	8.07E-04	1.00	1.02E-09	0.92	0.15
Paracentral lobule left	0.32 (0.18, 0.46)	0.15 (0.06, 0.24)	0.32 (0.05, 0.44)	0.00 (0.00, 0.18)	0.68 (0.56, 0.82)	0.05	1.00	5.52E-06	0.94	0.11
Paracentral lobule right	0.33 (0.18, 0.46)	0.08 (-0.01, 0.17)	0.28 (0.09, 0.41)	0.00 (0.00, 0.10)	0.72 (0.59, 0.85)	0.02	1.00	5.42E-04	0.91	0.18
Frontal pole left	0.10 (-0.05, 0.26)	0.06 (-0.03, 0.15)	0.11 (0.00, 0.24)	0.00 (0.00, 0.15)	0.89 (0.76, 1.00)	0.77	1.00	0.34	0.57	0.68
Frontal pole right	0.10 (-0.06, 0.25)	0.01 (-0.09, 0.10)	0.06 (0.00, 0.19)	0.00 (0.00, 0.11)	0.94 (0.81, 1.00)	0.68	1.00	0.81	0.71	0.50
<i>Parietal</i>										
Superior parietal cortex left	0.54 (0.42, 0.65)	0.28 (0.18, 0.38)	0.54 (0.27, 0.65)	0.02 (0.00, 0.22)	0.44 (0.35, 0.56)	4.21E-04	1.00	5.59E-17	0.98	0.04
Superior parietal cortex right	0.45 (0.32, 0.57)	0.30 (0.19, 0.40)	0.28 (0.00, 0.54)	0.16 (0.00, 0.36)	0.56 (0.45, 0.69)	0.09	0.27	1.01E-13	0.90	0.19
Inferior parietal cortex left	0.39 (0.24, 0.51)	0.19 (0.10, 0.29)	0.42 (0.14, 0.53)	0.00 (0.00, 0.19)	0.58 (0.47, 0.72)	0.01	1.00	3.92E-09	0.98	0.05
Inferior parietal cortex right	0.34 (0.19, 0.47)	0.11 (0.02, 0.21)	0.34 (0.13, 0.46)	0.00 (0.00, 0.13)	0.66 (0.54, 0.79)	0.01	1.00	4.01E-06	0.97	0.06
Supramarginal cortex left	0.32 (0.17, 0.45)	0.16 (0.07, 0.26)	0.33 (0.00, 0.44)	0.00 (0.00, 0.22)	0.67 (0.56, 0.82)	0.09	1.00	3.80E-06	0.98	0.04
Supramarginal cortex right	0.27 (0.12, 0.41)	0.14 (0.05, 0.24)	0.29 (0.00, 0.41)	0.00 (0.00, 0.21)	0.71 (0.59, 0.87)	0.15	1.00	1.27E-04	0.97	0.05
Postcentral gyrus left	0.22 (0.06, 0.37)	0.07 (-0.02, 0.17)	0.19 (0.00, 0.31)	0.00 (0.00, 0.17)	0.81 (0.69, 0.94)	0.24	1.00	0.02	0.98	0.04
Postcentral gyrus right	0.20 (0.05, 0.35)	0.13 (0.04, 0.22)	0.17 (0.00, 0.35)	0.04 (0.00, 0.22)	0.79 (0.65, 0.93)	0.52	0.96	2.24E-03	0.95	0.10
Precuneus cortex left	0.41 (0.27, 0.53)	0.30 (0.20, 0.39)	0.24 (0.00, 0.51)	0.17 (0.00, 0.37)	0.59 (0.47, 0.73)	0.20	0.21	3.94E-13	0.96	0.08
Precuneus cortex right	0.49 (0.36, 0.60)	0.19 (0.08, 0.30)	0.46 (0.24, 0.56)	0.00 (0.00, 0.15)	0.54 (0.44, 0.66)	1.08E-03	1.00	1.17E-11	0.97	0.05
<i>Occipital</i>										
Lateral occipital cortex left	0.50 (0.37, 0.61)	0.19 (0.09, 0.30)	0.46 (0.27, 0.57)	0.00 (0.00, 0.00)	0.54 (0.43, 0.66)	4.34E-04	1.00	2.42E-11	0.96	0.07
Lateral occipital cortex right	0.48 (0.34, 0.59)	0.16 (0.06, 0.26)	0.43 (0.26, 0.54)	0.00 (0.00, 0.11)	0.57 (0.46, 0.70)	5.42E-04	1.00	3.75E-09	0.92	0.15
Lingual gyrus left	0.58 (0.47, 0.68)	0.21 (0.11, 0.31)	0.58 (0.43, 0.68)	0.00 (0.00, 0.10)	0.42 (0.32, 0.53)	2.17E-06	1.00	1.46E-16	0.93	0.14
Lingual gyrus right	0.63 (0.53, 0.72)	0.29 (0.19, 0.38)	0.63 (0.44, 0.71)	0.00 (0.00, 0.15)	0.37 (0.29, 0.47)	6.33E-07	1.00	5.91E-23	0.81	0.34

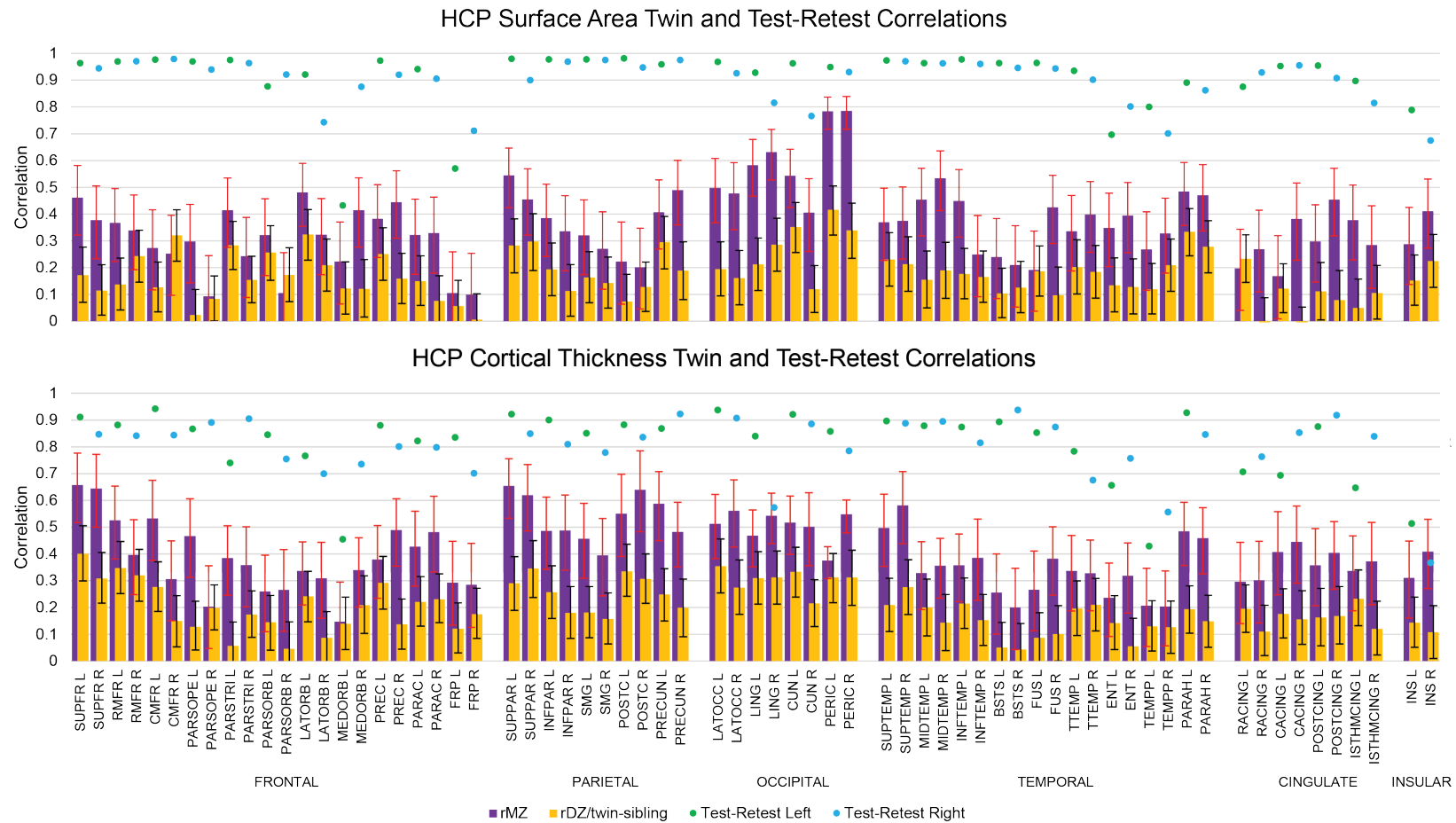
Cuneus cortex left	0.54 (0.42, 0.64)	0.35 (0.26, 0.44)	0.40 (0.14, 0.63)	0.15 (0.00, 0.34)	0.45 (0.35, 0.57)	0.01	0.22	6.34E-22	0.96	0.07
Cuneus cortex right	0.41 (0.26, 0.53)	0.12 (0.03, 0.21)	0.40 (0.22, 0.53)	0.00 (0.00, 0.09)	0.60 (0.47, 0.75)	2.54E-03	1.00	1.23E-06	0.77	0.41
Pericalcarine cortex left	0.78 (0.72, 0.84)	0.42 (0.32, 0.50)	0.76 (0.58, 0.85)	0.04 (0.00, 0.22)	0.19 (0.15, 0.25)	3.50E-13	0.86	7.61E-45	0.95	0.10
Pericalcarine cortex right	0.79 (0.72, 0.84)	0.34 (0.24, 0.44)	0.79 (0.66, 0.84)	0.00 (0.00, 0.12)	0.21 (0.16, 0.28)	7.43E-15	1.00	7.56E-38	0.93	0.13
<i>Temporal</i>										
Superior temporal gyrus left	0.37 (0.23, 0.50)	0.23 (0.13, 0.33)	0.46 (0.27, 0.57)	0.00 (0.00, 0.00)	0.54 (0.43, 0.66)	4.34E-04	1.00	2.42E-11		
Superior temporal gyrus right	0.37 (0.23, 0.50)	0.21 (0.11, 0.32)	0.30 (0.00, 0.47)	0.06 (0.00, 0.27)	0.64 (0.53, 0.78)	0.10	0.79	1.11E-08	0.97	0.06
Middle temporal gyrus left	0.45 (0.32, 0.57)	0.16 (0.05, 0.26)	0.43 (0.23, 0.54)	0.00 (0.00, 0.13)	0.57 (0.46, 0.70)	1.39E-03	1.00	3.39E-09	0.96	0.08
Middle temporal gyrus right	0.53 (0.41, 0.64)	0.19 (0.09, 0.29)	0.50 (0.34, 0.60)	0.00 (0.00, 0.10)	0.50 (0.40, 0.62)	3.52E-05	1.00	2.17E-13	0.95	0.09
Inferior temporal gyrus left	0.45 (0.31, 0.57)	0.18 (0.08, 0.27)	0.43 (0.26, 0.54)	0.00 (0.00, 0.11)	0.57 (0.46, 0.69)	6.23E-04	1.00	3.05E-10	0.98	0.04
Inferior temporal gyrus right	0.25 (0.09, 0.39)	0.17 (0.07, 0.26)	0.21 (0.00, 0.40)	0.05 (0.00, 0.25)	0.73 (0.60, 0.88)	0.34	0.86	8.93E-05	0.95	0.09
Banks of the superior temporal sulcus left	0.24 (0.08, 0.38)	0.10 (0.01, 0.20)	0.26 (0.00, 0.38)	0.00 (0.00, 0.19)	0.74 (0.62, 0.89)	0.15	1.00	9.23E-04	0.96	0.08
Banks of the superior temporal sulcus right	0.21 (0.05, 0.36)	0.13 (0.03, 0.22)	0.20 (0.00, 0.37)	0.04 (0.00, 0.23)	0.77 (0.63, 0.91)	0.42	1.00	8.80E-04	0.94	0.11
Fusiform gyrus left	0.19 (0.04, 0.34)	0.19 (0.09, 0.28)	0.00 (0.00, 0.32)	0.18 (0.00, 0.27)	0.81 (0.67, 0.89)	1.00	0.18	5.02E-05	0.96	0.08
Fusiform gyrus right	0.43 (0.29, 0.54)	0.10 (-0.00, 0.20)	0.35 (0.19, 0.47)	0.00 (0.00, 0.10)	0.65 (0.53, 0.77)	2.24E-03	1.00	3.12E-07	0.94	0.12
Transverse temporal cortex left	0.34 (0.19, 0.47)	0.20 (0.10, 0.30)	0.23 (0.00, 0.43)	0.08 (0.00, 0.28)	0.69 (0.57, 0.83)	0.21	0.70	5.56E-07	0.93	0.13
Transverse temporal cortex right	0.40 (0.26, 0.52)	0.18 (0.09, 0.28)	0.41 (0.15, 0.53)	0.00 (0.00, 0.17)	0.59 (0.47, 0.72)	0.01	1.00	1.57E-08	0.89	0.20
Entorhinal cortex left	0.35 (0.20, 0.48)	0.13 (0.04, 0.24)	0.31 (0.07, 0.43)	0.00 (0.00, 0.16)	0.69 (0.57, 0.81)	0.03	1.00	7.54E-06	0.69	0.52
Entorhinal cortex right	0.39 (0.26, 0.52)	0.13 (0.03, 0.23)	0.35 (0.15, 0.47)	0.00 (0.00, 0.14)	0.65 (0.53, 0.77)	0.01	1.00	3.40E-07	0.80	0.37
Temporal pole left	0.27 (0.12, 0.41)	0.12 (0.03, 0.22)	0.26 (0.00, 0.38)	0.00 (0.00, 0.19)	0.74 (0.62, 0.89)	0.15	1.00	5.04E-04	0.80	0.35
Temporal pole right	0.33 (0.18, 0.46)	0.21 (0.11, 0.31)	0.24 (0.00, 0.46)	0.10 (0.00, 0.30)	0.67 (0.54, 0.81)	0.24	0.57	4.68E-08	0.70	0.51
Parahippocampal gyrus left	0.48 (0.36, 0.59)	0.33 (0.24, 0.42)	0.40 (0.12, 0.63)	0.13 (0.00, 0.33)	0.47 (0.36, 0.60)	0.02	0.31	4.90E-19	0.89	0.22
Parahippocampal gyrus right	0.47 (0.34, 0.58)	0.28 (0.18, 0.37)	0.38 (0.11, 0.57)	0.09 (0.00, 0.28)	0.54 (0.43, 0.66)	0.02	0.58	4.30E-14	0.85	0.28
<i>Cingulate</i>										
Rostral anterior cingulate left	0.20 (0.04, 0.34)	0.23 (0.14, 0.32)	0.00 (0.00, 0.26)	0.23 (0.05, 0.32)	0.77 (0.65, 0.85)	1.00	0.03	2.57E-07	0.87	0.24
Rostral anterior cingulate right	0.27 (0.11, 0.41)	-0.01 (-0.10, 0.09)	0.15 (0.00, 0.30)	0.00 (0.00, 0.09)	0.85 (0.70, 0.99)	0.13	1.00	0.18	0.93	0.14
Caudal anterior cingulate left	0.17 (0.01, 0.32)	0.12 (0.03, 0.21)	0.11 (0.00, 0.33)	0.07 (0.00, 0.22)	0.82 (0.67, 0.94)	0.76	0.75	0.01	0.95	0.10
Caudal anterior cingulate right	0.38 (0.23, 0.52)	-0.05 (-0.15, 0.05)	0.21 (0.05, 0.36)	0.00 (0.00, 0.06)	0.79 (0.64, 0.94)	0.03	1.00	0.04	0.95	0.10
Posterior cingulate left	0.30 (0.15, 0.43)	0.11 (0.00, 0.22)	0.27 (0.00, 0.39)	0.00 (0.00, 0.20)	0.73 (0.61, 0.86)	0.11	1.00	9.86E-05	0.95	0.09
Posterior cingulate right	0.45 (0.32, 0.57)	0.08 (-0.03, 0.19)	0.37 (0.22, 0.49)	0.00 (0.00, 0.09)	0.63 (0.51, 0.76)	9.23E-04	1.00	4.24E-07	0.89	0.20
Isthmus cingulate left	0.38 (0.23, 0.51)	0.05 (-0.05, 0.16)	0.29 (0.12, 0.43)	0.00 (0.00, 0.00)	0.71 (0.57, 0.84)	0.01	1.00	3.91E-04	0.89	0.21
Isthmus cingulate right	0.28 (0.12, 0.43)	0.11 (0.01, 0.21)	0.26 (0.00, 0.38)	0.00 (0.00, 0.17)	0.74 (0.62, 0.89)	0.11	1.00	1.83E-03	0.82	0.33
<i>Insular</i>										
Insular cortex left	0.29 (0.14, 0.42)	0.15 (0.06, 0.25)	0.29 (0.00, 0.41)	0.00 (0.00, 0.21)	0.71 (0.59, 0.86)	0.13	1.00	3.84E-05	0.78	0.39
Insular cortex right	0.41 (0.27, 0.53)	0.22 (0.13, 0.32)	0.37 (0.08, 0.52)	0.04 (0.00, 0.25)	0.59 (0.48, 0.72)	0.03	0.94	1.68E-10	0.65	0.58
<u>Cortical Thickness</u>										
<i>Frontal</i>										
Superior frontal gyrus left	0.66 (0.56, 0.74)	0.40 (0.30, 0.49)	0.52 (0.30, 0.72)	0.14 (0.00, 0.32)	0.34 (0.27, 0.43)	3.39E-05	0.25	3.50E-29	0.91	0.17
Superior frontal gyrus right	0.64 (0.54, 0.73)	0.31 (0.21, 0.41)	0.64 (0.42, 0.72)	0.00 (0.00, 0.00)	0.36 (0.28, 0.45)	1.33E-06	1.00	1.33E-24	0.85	0.28
Rostral middle frontal gyrus left	0.53 (0.40, 0.63)	0.35 (0.25, 0.44)	0.37 (0.11, 0.61)	0.15 (0.00, 0.35)	0.48 (0.38, 0.59)	0.01	0.25	7.56E-20	0.88	0.22
Rostral middle frontal gyrus right	0.40 (0.25, 0.52)	0.32 (0.21, 0.42)	0.14 (0.00, 0.42)	0.25 (0.03, 0.42)	0.61 (0.50, 0.74)	0.50	0.05	1.98E-13	0.84	0.29
Caudal middle frontal gyrus left	0.53 (0.41, 0.63)	0.28 (0.17, 0.38)	0.53 (0.25, 0.63)	0.01 (0.00, 0.22)	0.46 (0.37, 0.58)	0.00	1.00	2.64E-16	0.94	0.11
Caudal middle frontal gyrus right	0.31 (0.16, 0.44)	0.15 (0.06, 0.25)	0.31 (0.00, 0.42)	0.00 (0.00, 0.21)	0.69 (0.58, 0.84)	0.10	1.00	8.48E-06	0.84	0.29
Pars opercularis left	0.47 (0.33, 0.58)	0.13 (0.03, 0.23)	0.40 (0.24, 0.51)	0.00 (0.00, 0.10)	0.60 (0.49, 0.72)	5.46E-04	1.00	1.20E-08	0.87	0.25
Pars opercularis right	0.20 (0.05, 0.35)	0.20 (0.10, 0.29)	0.01 (0.00, 0.32)	0.19 (0.00, 0.29)	0.80 (0.66, 0.89)	1.00	0.14	3.39E-05	0.89	0.21
Pars triangularis left	0.38 (0.24, 0.51)	0.06 (-0.04, 0.16)	0.30 (0.14, 0.43)	0.00 (0.00, 0.09)	0.70 (0.57, 0.83)	4.70E-03	1.00	9.99E-05	0.74	0.45
Pars triangularis right	0.36 (0.21, 0.49)	0.17 (0.08, 0.27)	0.36 (0.06, 0.48)	0.00 (0.00, 0.20)	0.64 (0.52, 0.78)	0.04	1.00	9.02E-08	0.90	0.18
Pars orbitalis left	0.26 (0.11, 0.40)	0.14 (0.04, 0.25)	0.21 (0.00, 0.37)	0.03 (0.00, 0.24)	0.76 (0.63, 0.89)	0.29	0.99	3.40E-04	0.84	0.29
Pars orbitalis right	0.27 (0.11, 0.41)	0.05 (-0.04, 0.14)	0.19 (0.01, 0.32)	0.00 (0.00, 0.11)	0.81 (0.68, 0.93)	0.07	1.00	0.02	0.75	0.43
Lateral orbitofrontal cortex left	0.34 (0.19, 0.47)	0.24 (0.14, 0.34)	0.16 (0.00, 0.43)	0.15 (0.00, 0.34)	0.68 (0.56, 0.81)	0.39	0.26	5.98E-09	0.77	0.41

Lateral orbitofrontal cortex right	0.31 (0.16, 0.44)	0.09 (-0.01, 0.19)	0.26 (0.06, 0.39)	0.00 (0.00, 0.00)	0.74 (0.61, 0.86)	0.04	1.00	5.58E-04	0.70	0.51
Medial orbitofrontal cortex left	0.15 (-0.01, 0.29)	0.14 (0.04, 0.24)	0.04 (0.00, 0.31)	0.12 (0.00, 0.24)	0.83 (0.69, 0.93)	1.00	0.44	2.40E-03	0.45	0.79
Medial orbitofrontal cortex right	0.34 (0.19, 0.47)	0.21 (0.10, 0.32)	0.21 (0.00, 0.43)	0.10 (0.00, 0.31)	0.69 (0.57, 0.81)	0.25	0.52	1.52E-07	0.73	0.46
Precentral gyrus left	0.38 (0.23, 0.51)	0.29 (0.18, 0.40)	0.15 (0.00, 0.45)	0.22 (0.00, 0.40)	0.63 (0.51, 0.76)	0.48	0.11	4.01E-11	0.88	0.23
Precentral gyrus right	0.49 (0.36, 0.60)	0.14 (0.03, 0.24)	0.46 (0.30, 0.57)	0.00 (0.00, 0.09)	0.54 (0.43, 0.67)	1.65E-04	1.00	1.70E-09	0.80	0.36
Paracentral lobule left	0.43 (0.29, 0.55)	0.22 (0.12, 0.32)	0.43 (0.12, 0.54)	0.00 (0.00, 0.22)	0.57 (0.46, 0.70)	0.01	1.00	4.21E-11	0.82	0.32
Paracentral lobule right	0.48 (0.35, 0.59)	0.23 (0.13, 0.33)	0.46 (0.20, 0.56)	0.00 (0.00, 0.19)	0.54 (0.44, 0.66)	2.10E-03	1.00	1.65E-12	0.80	0.36
Frontal pole left	0.29 (0.14, 0.43)	0.12 (0.02, 0.22)	0.28 (0.00, 0.40)	0.00 (0.00, 0.19)	0.72 (0.60, 0.86)	0.10	1.00	1.31E-04	0.83	0.30
Frontal pole right	0.29 (0.14, 0.42)	0.18 (0.06, 0.28)	0.21 (0.00, 0.41)	0.07 (0.00, 0.28)	0.72 (0.59, 0.86)	0.34	0.75	8.48E-06	0.70	0.51
<i>Parietal</i>										
Superior parietal cortex left	0.65 (0.56, 0.73)	0.29 (0.19, 0.39)	0.64 (0.47, 0.71)	0.00 (0.00, 0.13)	0.36 (0.29, 0.46)	6.58E-08	1.00	1.33E-24	0.92	0.15
Superior parietal cortex right	0.62 (0.52, 0.70)	0.35 (0.24, 0.44)	0.52 (0.28, 0.68)	0.09 (0.00, 0.27)	0.39 (0.31, 0.49)	7.10E-05	0.56	1.45E-25	0.85	0.28
Inferior parietal cortex left	0.49 (0.36, 0.59)	0.26 (0.16, 0.35)	0.46 (0.18, 0.59)	0.03 (0.00, 0.23)	0.51 (0.41, 0.64)	3.16E-03	1.00	1.24E-14	0.90	0.19
Inferior parietal cortex right	0.49 (0.36, 0.60)	0.18 (0.08, 0.28)	0.47 (0.29, 0.58)	0.00 (0.00, 0.11)	0.53 (0.42, 0.65)	2.40E-04	1.00	2.11E-11	0.81	0.35
Supramarginal cortex left	0.46 (0.32, 0.57)	0.18 (0.09, 0.27)	0.44 (0.24, 0.55)	0.00 (0.00, 0.13)	0.56 (0.45, 0.68)	1.04E-03	1.00	1.20E-10	0.85	0.28
Supramarginal cortex right	0.39 (0.25, 0.52)	0.16 (0.07, 0.25)	0.40 (0.18, 0.51)	0.00 (0.00, 0.13)	0.60 (0.49, 0.73)	4.82E-03	1.00	1.71E-08	0.78	0.39
Postcentral gyrus left	0.55 (0.43, 0.65)	0.34 (0.23, 0.43)	0.42 (0.16, 0.63)	0.12 (0.00, 0.33)	0.45 (0.36, 0.57)	4.64E-03	0.38	3.32E-20	0.88	0.22
Postcentral gyrus right	0.64 (0.54, 0.72)	0.31 (0.20, 0.41)	0.64 (0.43, 0.72)	0.00 (0.00, 0.17)	0.36 (0.28, 0.45)	8.70E-07	1.00	3.38E-25	0.84	0.30
Precuneus cortex left	0.59 (0.48, 0.68)	0.25 (0.14, 0.35)	0.55 (0.37, 0.64)	0.00 (0.00, 0.14)	0.45 (0.36, 0.55)	7.23E-06	1.00	4.54E-18	0.87	0.25
Precuneus cortex right	0.48 (0.35, 0.60)	0.20 (0.09, 0.31)	0.45 (0.22, 0.56)	0.00 (0.00, 0.16)	0.55 (0.44, 0.67)	1.61E-03	1.00	7.19E-11	0.92	0.15
<i>Occipital</i>										
Lateral occipital cortex left	0.51 (0.39, 0.62)	0.35 (0.25, 0.45)	0.32 (0.05, 0.58)	0.19 (0.00, 0.39)	0.49 (0.39, 0.61)	0.04	0.12	5.43E-20	0.94	0.12
Lateral occipital cortex right	0.56 (0.45, 0.66)	0.27 (0.17, 0.37)	0.58 (0.35, 0.67)	0.00 (0.00, 0.18)	0.42 (0.33, 0.53)	4.96E-05	1.00	1.23E-18	0.91	0.18
Lingual gyrus left	0.47 (0.34, 0.58)	0.31 (0.21, 0.41)	0.32 (0.04, 0.57)	0.15 (0.00, 0.35)	0.53 (0.42, 0.66)	0.04	0.25	1.64E-15	0.84	0.30
Lingual gyrus right	0.54 (0.42, 0.64)	0.31 (0.22, 0.40)	0.52 (0.25, 0.67)	0.06 (0.00, 0.26)	0.42 (0.33, 0.54)	6.93E-04	0.73	3.32E-20	0.57	0.67
Cuneus cortex left	0.52 (0.40, 0.62)	0.33 (0.24, 0.43)	0.37 (0.11, 0.61)	0.15 (0.00, 0.34)	0.48 (0.38, 0.60)	0.01	0.25	9.39E-20	0.92	0.15
Cuneus cortex right	0.50 (0.37, 0.61)	0.22 (0.11, 0.32)	0.46 (0.24, 0.56)	0.00 (0.00, 0.16)	0.54 (0.44, 0.65)	6.97E-04	1.00	8.42E-13	0.88	0.22
Pericalcarine cortex left	0.37 (0.23, 0.50)	0.31 (0.22, 0.40)	0.21 (0.00, 0.50)	0.19 (0.00, 0.39)	0.60 (0.47, 0.74)	0.26	0.13	7.64E-13	0.86	0.27
Pericalcarine cortex right	0.55 (0.43, 0.65)	0.31 (0.21, 0.41)	0.54 (0.27, 0.65)	0.02 (0.00, 0.23)	0.44 (0.35, 0.55)	3.35E-04	1.00	1.14E-18	0.78	0.38
<i>Temporal</i>										
Superior temporal gyrus left	0.50 (0.37, 0.61)	0.21 (0.11, 0.31)	0.47 (0.27, 0.57)	0.00 (0.00, 0.13)	0.53 (0.43, 0.65)	3.69E-04	1.00	7.29E-12	0.90	0.20
Superior temporal gyrus right	0.58 (0.47, 0.68)	0.28 (0.17, 0.38)	0.58 (0.34, 0.66)	0.00 (0.00, 0.18)	0.42 (0.34, 0.53)	4.96E-05	1.00	8.22E-19	0.89	0.21
Middle temporal gyrus left	0.33 (0.18, 0.46)	0.20 (0.10, 0.30)	0.30 (0.00, 0.47)	0.05 (0.00, 0.27)	0.65 (0.53, 0.80)	0.12	0.88	2.33E-07	0.88	0.23
Middle temporal gyrus right	0.36 (0.21, 0.49)	0.14 (0.05, 0.24)	0.33 (0.08, 0.45)	0.00 (0.00, 0.16)	0.67 (0.55, 0.80)	0.03	1.00	4.56E-06	0.89	0.20
Inferior temporal gyrus left	0.36 (0.21, 0.49)	0.21 (0.12, 0.31)	0.29 (0.00, 0.48)	0.07 (0.00, 0.28)	0.64 (0.52, 0.79)	0.12	0.73	1.20E-08	0.87	0.24
Inferior temporal gyrus right	0.38 (0.24, 0.51)	0.15 (0.05, 0.26)	0.32 (0.09, 0.43)	0.00 (0.00, 0.18)	0.68 (0.57, 0.79)	0.02	1.00	1.67E-06	0.81	0.34
Banks of the superior temporal sulcus left	0.26 (0.10, 0.40)	0.05 (-0.05, 0.15)	0.21 (0.00, 0.34)	0.00 (0.00, 0.12)	0.79 (0.66, 0.93)	0.09	1.00	0.02	0.89	0.20
Banks of the superior temporal sulcus right	0.20 (0.04, 0.35)	0.04 (-0.04, 0.14)	0.15 (0.00, 0.28)	0.00 (0.00, 0.13)	0.85 (0.72, 0.98)	0.22	1.00	0.10	0.94	0.12
Fusiform gyrus left	0.27 (0.11, 0.41)	0.09 (-0.01, 0.19)	0.22 (0.00, 0.35)	0.00 (0.00, 0.16)	0.78 (0.65, 0.91)	0.12	1.00	3.87E-03	0.85	0.27
Fusiform gyrus right	0.38 (0.24, 0.51)	0.10 (-0.01, 0.21)	0.32 (0.13, 0.44)	0.00 (0.00, 0.13)	0.68 (0.56, 0.80)	0.01	1.00	8.48E-06	0.87	0.24
Transverse temporal cortex left	0.34 (0.19, 0.47)	0.20 (0.10, 0.30)	0.29 (0.00, 0.47)	0.05 (0.00, 0.27)	0.65 (0.53, 0.80)	0.12	0.86	2.42E-07	0.78	0.39
Transverse temporal cortex right	0.33 (0.18, 0.46)	0.21 (0.11, 0.31)	0.23 (0.00, 0.45)	0.09 (0.00, 0.30)	0.68 (0.55, 0.82)	0.22	0.56	1.49E-07	0.67	0.54
Entorhinal cortex left	0.24 (0.08, 0.38)	0.14 (0.04, 0.24)	0.18 (0.00, 0.36)	0.06 (0.00, 0.24)	0.77 (0.64, 0.90)	0.43	0.84	5.07E-04	0.66	0.57
Entorhinal cortex right	0.32 (0.17, 0.45)	0.06 (-0.04, 0.16)	0.24 (0.07, 0.37)	0.00 (0.00, 0.10)	0.76 (0.63, 0.89)	0.03	1.00	2.33E-03	0.76	0.43
Temporal pole left	0.21 (0.05, 0.35)	0.13 (0.03, 0.23)	0.13 (0.00, 0.33)	0.07 (0.00, 0.24)	0.80 (0.67, 0.93)	0.62	0.75	3.13E-03	0.43	0.82
Temporal pole right	0.20 (0.05, 0.35)	0.13 (0.03, 0.23)	0.17 (0.00, 0.34)	0.04 (0.00, 0.22)	0.79 (0.66, 0.93)	0.47	0.98	3.32E-03	0.56	0.69
Parahippocampal gyrus left	0.48 (0.35, 0.59)	0.19 (0.09, 0.30)	0.46 (0.23, 0.56)	0.00 (0.00, 0.16)	0.54 (0.44, 0.66)	1.36E-03	1.00	3.75E-12	0.93	0.14
Parahippocampal gyrus right	0.46 (0.32, 0.57)	0.15 (0.05, 0.25)	0.43 (0.26, 0.55)	0.00 (0.00, 0.10)	0.57 (0.45, 0.70)	6.41E-04	1.00	3.98E-09	0.85	0.28
<i>Cingulate</i>										
Rostral anterior cingulate left	0.30 (0.15, 0.43)	0.20 (0.10, 0.29)	0.24 (0.00, 0.45)	0.08 (0.00, 0.29)	0.68 (0.55, 0.83)	0.26	0.70	5.97E-07	0.71	0.50
Rostral anterior cingulate right	0.30 (0.15, 0.44)	0.11 (0.01, 0.21)	0.27 (0.04, 0.39)	0.00 (0.00, 0.15)	0.73 (0.61, 0.86)	0.05	1.00	5.58E-04	0.76	0.42

Caudal anterior cingulate left	0.41 (0.27, 0.53)	0.18 (0.07, 0.28)	0.38 (0.15, 0.49)	0.00 (0.00, 0.00)	0.62 (0.51, 0.75)	0.01	1.00	4.17E-08	0.69	0.52
Caudal anterior cingulate right	0.44 (0.30, 0.57)	0.16 (0.06, 0.26)	0.40 (0.21, 0.52)	0.00 (0.00, 0.13)	0.60 (0.48, 0.72)	2.51E-03	1.00	3.72E-08	0.85	0.27
Posterior cingulate left	0.36 (0.21, 0.49)	0.16 (0.06, 0.27)	0.35 (0.06, 0.47)	0.00 (0.00, 0.20)	0.65 (0.53, 0.79)	0.04	1.00	1.67E-06	0.87	0.24
Posterior cingulate right	0.40 (0.26, 0.53)	0.17 (0.07, 0.27)	0.38 (0.12, 0.49)	0.00 (0.00, 0.18)	0.62 (0.51, 0.75)	0.01	1.00	1.58E-08	0.92	0.16
Isthmus cingulate left	0.34 (0.18, 0.47)	0.23 (0.12, 0.34)	0.22 (0.00, 0.47)	0.12 (0.00, 0.33)	0.66 (0.53, 0.81)	0.30	0.45	9.02E-08	0.65	0.58
Isthmus cingulate right	0.37 (0.22, 0.51)	0.12 (0.02, 0.23)	0.31 (0.09, 0.43)	0.00 (0.00, 0.15)	0.69 (0.57, 0.81)	0.02	1.00	9.83E-06	0.84	0.30
Insular										
Insular cortex left	0.31 (0.16, 0.45)	0.14 (0.05, 0.24)	0.30 (0.01, 0.42)	0.00 (0.00, 0.19)	0.70 (0.58, 0.84)	0.07	1.00	1.90E-05	0.51	0.74
Insular cortex right	0.41 (0.26, 0.53)	0.11 (0.01, 0.21)	0.35 (0.17, 0.48)	0.00 (0.00, 0.10)	0.65 (0.52, 0.78)	4.08E-03	1.00	3.89E-06	0.37	0.87

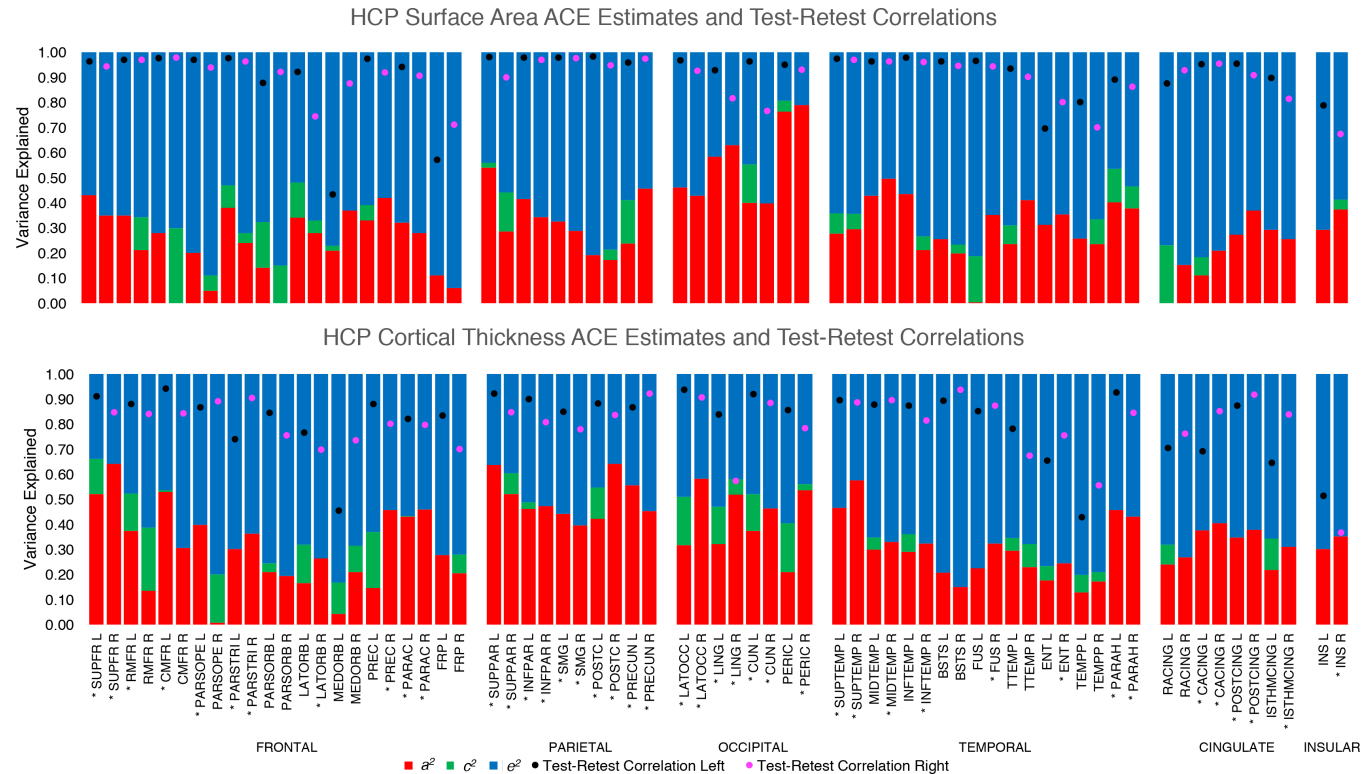
Note. Surface area and cortical thickness of each region is adjusted for total surface area/mean cortical thickness, linear and non-linear age effects, sex, and interactions between age and sex. ROIs are grouped in lobar divisions (Frontal, Parietal, Occipital, Temporal, Cingulate, Insular). a^2 = additive genetic influences; c^2 common or shared environmental influences; e^2 unique or non-shared environmental influences; No A = test of CE model (no additive genetic influence); No C = test of AE model (no common environmental influence); No AC = test of E model (no additive genetic or common environmental influence). Heritability estimates (a^2) significantly different from zero (significant 'No A'; q value < 0.05) appear in bold. Variance explained by measurement error ($1 - r^2$ test-retest correlation) was greater than non-shared environment (e^2) in the following ROIs: surface area – medial orbitofrontal left, insular right, cortical thickness – lingual gyrus right, temporal pole left, insular left and right.

Appendix 16 Twin and Test-Retest Correlations for HCP Surface Area and Cortical Thickness



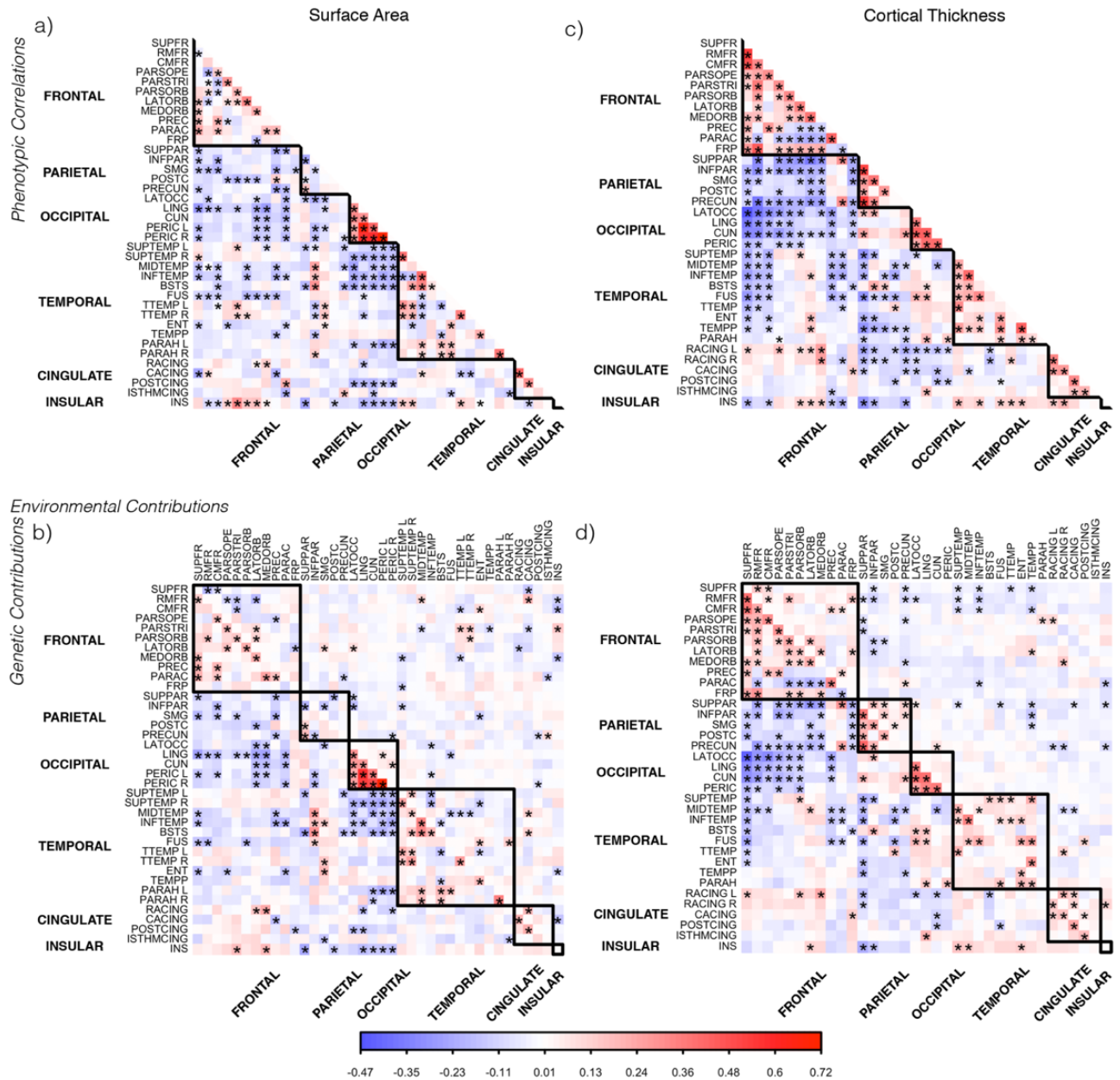
Twin correlations with 95% confidence intervals, and test-retest reliability correlations for surface area (top) and cortical thickness (bottom) for 68 ROIs (34 in each of the left (L) and right (R) hemisphere) in the HCP sample.

Appendix 17 Surface Area and Cortical Thickness ACE Estimates and Test-Retest Correlations in the HCP Dataset



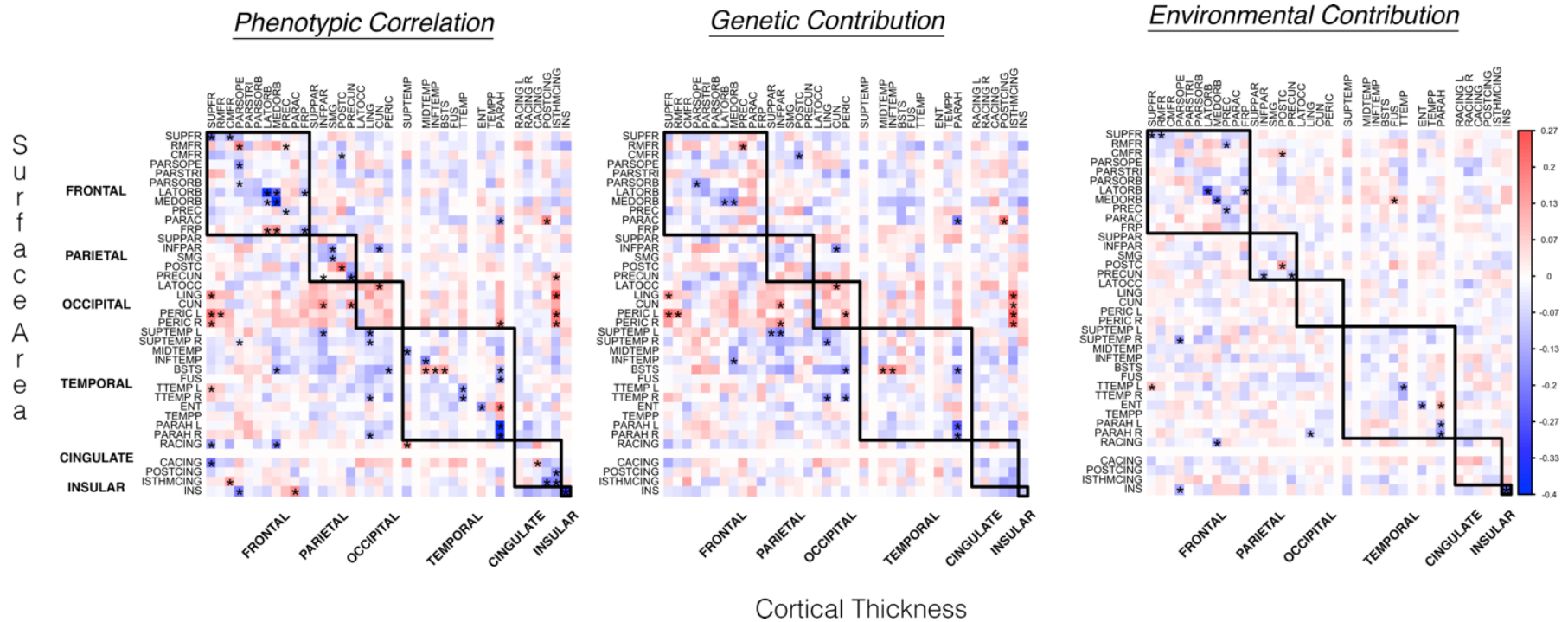
Variance components for surface area (top) and cortical thickness (bottom) for 68 ROIs (34 in each of the left (L) and right (R) hemisphere) in the HCP sample. a^2 = additive genetic (red), c^2 = common environment (green), e^2 = unique environment (blue). * denotes ROIs with heritability estimates (a^2) significantly different from zero. ROIs are grouped in lobar divisions (Frontal, Parietal, Occipital, Temporal, Cingulate, Insular).

Appendix 18 Phenotypic Correlations, with Genetic and Environmental Contributions, for HCP Surface Area and Cortical Thickness



Phenotypic correlations, with genetic and environmental contributions, for surface area and cortical thickness across regions in the HCP sample. Association across regions follow a similar pattern to that observed in the QTIM sample (Figure 4.3). ROI abbreviations listed in Appendix 2. * denotes a significant correlation (q value < 0.05).

Appendix 19 Phenotypic Correlations with Genetic and Environmental Contributions, between HCP Surface Area and Cortical Thickness



Phenotypic correlations (left), with genetic (middle) and environmental (left) contributions, between surface area and cortical thickness across regions in the HCP sample. * denotes a significant correlation (q value < 0.05).

Appendix 20 Means and Variances for Brain Structure Volumes and Body Weight in the QTIM Dataset

Means and raw/non-standardised variance components (additive genetic (V_A), environmental (V_E), and phenotypic (V_P)) for brain structure volumes (mm^3) and body weight (kg) for QTIM (N = 831).

	Mean (SD)	V_A	V_E	V_P	Excluded [†]
<i>Cortical</i>					
<i>Frontal</i>					
Superior frontal	24124 (2587)	5847705	844419	6692123	4
Rostral middle frontal	16622 (2193)	3882586	925251	4807837	6
Caudal middle frontal	6770 (1116)	910359	334591	1244950	5
Pars opercularis	4970 (697)	322936	162657	485593	9
Pars triangularis	4275 (613)	188857	186735	375592	8
Pars orbitalis	2450 (323)	57177	47434	104612	5
Lateral orbitofrontal	6992 (846)	518567	197874	716441	5
Medial orbitofrontal	4988 (602)	200796	161669	362465	4
Precentral	14198 (1630)	2271940	385254	2657194	13
Paracentral lobule	3943 (555)	222637	84875	307513	7
Frontal pole	996 (160)	9322	16362	25684	4
<i>Parietal</i>					
Superior parietal	14147 (1683)	2338020	494232	2832252	4
Inferior parietal	14699 (1952)	2979655	830492	3810147	5
Supramarginal	11550 (1539)	1897186	472249	2369435	19
Postcentral	9952 (1252)	1169480	397965	1567445	13
Precuneus	10733 (1354)	1563091	270710	1833801	4
<i>Occipital</i>					
Lateral occipital	12048 (1430)	1574271	470160	2044431	4
Lingual	7001 (923)	674538	176634	851172	4
Cuneus	3211 (461)	158069	54860	212929	5
Pericalcarine	2359 (379)	123483	20349	143832	4
<i>Temporal</i>					
Superior temporal	11823 (1354)	1306335	528285	1834620	8
Middle temporal	9960 (1376)	1204139	689396	1893534	8
Inferior temporal	8623 (1301)	1120767	573030	1693798	8
Banks of the superior temporal	2552 (400)	100487	59499	159986	4
Fusiform	9164 (1168)	962651	402684	1365335	7
Transverse temporal	1097 (177)	18304	13106	31411	5
Entorhinal	1395 (266)	36560	34248	70808	7
Temporal pole	2023 (365)	58377	75181	133558	9
Parahippocampal	2250 (269)	50340	22041	72381	7
<i>Cingulate</i>					
Rostral anterior cingulate	2620 (433)	110610	76914	187525	5
Caudal anterior cingulate	2159 (370)	63223	73440	136663	6
Posterior cingulate	3449 (466)	138844	78730	217574	5
Isthmus cingulate	2694 (420)	128959	47371	176329	5
<i>Insular</i>					
Insular	6814 (786)	476302	141178	617479	5
<i>Subcortical</i>					
Thalamus	7731 (775)	537833	63492	601325	14
Putamen	6062 (643)	379492	33325	412817	0
Hippocampus	4163 (391)	133426	19349	152775	6
Caudate	4052 (483)	213537	19456	232993	13
Amygdala	1669 (197)	28154	10782	38936	4
Globus Pallidus	1581 (178)	24719	7048	31767	5
Nucleus Accumbens	707 (108)	7885	3681	11566	0
<i>Ventricular</i>					
Lateral Ventricle	6234 (2785)	5083541	2671700	7755241	0
3rd Ventricle	738 (182)	22819	10146	32965	0
4th Ventricle	1647 (498)	186996	60831	247827	0
Choroid Plexus	1256 (263)	53142	15849	68991	0
<i>Global</i>					
Total Brain Volume	1120104 (108283)	11235950382	489341605	11725291987	0
Body Weight	69 (15)	181	45	226	55*

Note. Brain structure volumes (mm^3) not corrected for total brain volume, age or sex. Body weight measured in kilograms. [†]N participants excluded from total sample (N = 831) after quality control. *Body weight not available for 55 participants.

Appendix 21 Mean-Standardised and Relative Variances Estimates, and Test-Retest Correlations for Brain Structure Volume and Body Weight in the QTIM Dataset

Mean-standardised and relative (proportion of total phenotypic variance) variance estimates (with 95% confidence intervals), and test-retest correlations, for cortical, subcortical, and ventricular volumes, as well as total brain volume and body weight, in the QTIM dataset.

	Mean-Standardised Variance Estimates			Relative Variance Estimates		Test Retest Correlation
	Genetic (I_A) (95% CI)	Environmental (I_E) (95% CI)	Phenotypic (I_P) (95% CI)	Genetic (a^2, h^2) (95% CI)	Environmental (e^2) (95% CI)	
<i>Cortical</i>						
<i>Frontal</i>						
Superior frontal	1.00% (0.88, 1.14)	0.15% (0.11, 0.19)	1.15% (1.04, 1.27)	87.38% (83.41, 90.27)	12.62% (9.73, 16.59)	0.97
Rostral middle frontal	1.41% (1.21, 1.62)	0.33% (0.26, 0.43)	1.74% (1.56, 1.92)	80.76% (74.47, 85.30)	19.24% (14.70, 25.53)	0.96
Caudal middle frontal	1.99% (1.67, 2.34)	0.73% (0.58, 0.94)	2.72% (2.46, 3.01)	73.12% (64.93, 79.30)	26.88% (20.70, 35.07)	0.95
Pars opercularis	1.31% (1.06, 1.57)	0.66% (0.52, 0.83)	1.97% (1.77, 2.19)	66.50% (57.01, 73.90)	33.50% (26.10, 42.99)	0.95
Pars triangularis	1.03% (0.74, 1.33)	1.02% (0.82, 1.24)	2.05% (1.86, 2.28)	50.28% (37.46, 60.94)	49.72% (39.06, 62.54)	0.97
Pars orbitalis	0.95% (0.72, 1.19)	0.79% (0.63, 0.95)	1.74% (1.57, 1.94)	54.66% (42.97, 64.22)	45.34% (35.78, 57.03)	0.88
Lateral orbitofrontal	1.06% (0.89, 1.25)	0.40% (0.32, 0.51)	1.47% (1.32, 1.63)	72.38% (64.40, 78.50)	27.62% (21.50, 35.60)	0.84
Medial orbitofrontal	0.81% (0.61, 1.01)	0.65% (0.52, 0.81)	1.46% (1.32, 1.62)	55.40% (43.95, 64.77)	44.60% (35.23, 56.05)	0.85
Precentral	1.13% (0.98, 1.28)	0.19% (0.15, 0.25)	1.32% (1.19, 1.47)	85.50% (80.80, 88.89)	14.50% (11.11, 19.20)	0.98
Paracentral lobule	1.43% (1.22, 1.68)	0.55% (0.44, 0.69)	1.98% (1.78, 2.21)	72.40% (64.63, 78.39)	27.60% (21.61, 35.37)	0.97
Frontal pole	0.94% (0.59, 1.31)	1.65% (1.39, 2.01)	2.59% (2.35, 2.87)	36.30% (23.00, 48.10)	63.70% (51.90, 77.00)	0.69
<i>Parietal</i>						
Superior parietal	1.17% (1.01, 1.34)	0.25% (0.20, 0.32)	1.42% (1.27, 1.58)	82.55% (77.21, 86.50)	17.45% (13.50, 22.79)	0.97
Inferior parietal	1.38% (1.18, 1.47)	0.38% (0.31, 0.49)	1.76% (1.59, 1.95)	78.20% (71.84, 83.01)	21.80% (16.99, 28.16)	0.97
Supramarginal	1.42% (1.22, 1.65)	0.35% (0.28, 0.46)	1.78% (1.60, 1.97)	80.07% (73.74, 84.71)	19.93% (15.29, 26.26)	0.97
Postcentral	1.18% (0.99, 1.38)	0.40% (0.32, 0.51)	1.58% (1.42, 1.77)	74.61% (67.00, 80.35)	25.39% (19.65, 33.00)	0.98
Precuneus	1.36% (1.18, 1.55)	0.23% (0.19, 0.30)	1.59% (1.43, 1.76)	85.24% (80.51, 88.67)	14.76% (11.33, 19.49)	0.98
<i>Occipital</i>						
Lateral occipital	1.08% (0.91, 1.27)	0.32% (0.25, 0.42)	1.41% (1.27, 1.57)	77.00% (69.38, 82.55)	23.00% (17.45, 30.62)	0.94
Lingual	1.38% (1.18, 1.59)	0.36% (0.28, 0.46)	1.74% (1.58, 1.94)	79.25% (72.80, 84.02)	20.75% (15.98, 27.20)	0.96
Cuneus	1.53% (1.29, 1.80)	0.53% (0.42, 0.68)	2.07% (1.86, 2.31)	74.24% (66.40, 80.14)	25.76% (19.86, 33.60)	0.96
Pericalcarine	2.22% (1.94, 2.54)	0.37% (0.29, 0.47)	2.59% (2.32, 2.89)	85.85% (81.27, 89.16)	14.15% (10.84, 18.73)	0.96
<i>Temporal</i>						
Superior temporal	0.93% (0.79, 1.10)	0.38% (0.30, 0.48)	1.31% (1.18, 1.46)	71.20% (62.88, 77.60)	28.80% (22.40, 37.12)	0.88
Middle temporal	1.21% (1.01, 1.46)	0.69% (0.56, 0.87)	1.91% (1.72, 2.12)	63.59% (54.42, 71.02)	36.41% (28.98, 45.58)	0.9
Inferior temporal	1.51% (1.26, 1.80)	0.77% (0.62, 0.97)	2.28% (2.05, 2.54)	66.17% (57.05, 73.39)	33.83% (26.61, 42.95)	0.82
Banks of the superior temporal	1.54% (1.22, 1.85)	0.91% (0.73, 1.16)	2.46% (2.21, 2.74)	62.81% (52.37, 71.06)	37.19% (28.94, 47.63)	0.92

Fusiform	1.15% (0.95, 1.36)	0.48% (0.38, 0.61)	1.63% (1.46, 1.81)	70.51% (61.87, 77.12)	29.49% (22.88, 38.13)	0.82
Transverse temporal	1.52% (1.20, 1.87)	1.09% (0.88, 1.36)	2.61% (2.36, 2.91)	58.27% (47.92, 66.76)	41.73% (33.24, 52.08)	0.92
Entorhinal	1.88% (1.40, 2.38)	1.76% (1.42, 2.11)	3.64% (3.28, 4.05)	51.63% (39.87, 61.51)	48.37% (38.49, 60.13)	0.61
Temporal pole	1.43% (0.99, 1.88)	1.84% (1.50, 2.26)	3.26% (2.95, 3.63)	43.71% (31.15, 54.58)	56.29% (45.42, 68.85)	0.5
Parahippocampal	0.99% (0.84, 1.18)	0.44% (0.34, 0.56)	1.43% (1.29, 1.59)	69.55% (60.43, 76.49)	30.45% (23.51, 39.57)	0.89
<i>Cingulate</i>						
Rostral anterior cingulate	1.61% (1.27, 1.97)	1.12% (0.90, 1.40)	2.73% (2.47, 3.04)	58.98% (48.64, 67.35)	41.02% (32.65, 51.36)	0.89
Caudal anterior cingulate	1.36% (0.96, 1.77)	1.58% (1.28, 1.95)	2.93% (2.65, 3.26)	46.26% (33.65, 56.97)	53.74% (43.03, 66.35)	0.97
Posterior cingulate	1.17% (0.95, 1.39)	0.66% (0.54, 0.82)	1.83% (1.65, 2.04)	63.81% (54.61, 71.19)	36.19% (28.81, 45.39)	0.98
Isthmus cingulate	1.78% (1.48, 2.09)	0.65% (0.51, 0.84)	2.43% (2.18, 2.71)	73.14% (64.88, 79.36)	26.86% (20.64, 35.12)	0.95
<i>Insular</i>						
Insular	1.03% (0.87, 1.18)	0.30% (0.24, 0.39)	1.33% (1.20, 1.48)	77.14% (69.78, 82.55)	22.86% (17.45, 30.22)	0.92
<i>Subcortical</i>						
Thalamus	0.90% (0.79, 1.02)	0.11% (0.08, 0.14)	1.01% (0.91, 1.12)	89.44% (85.88, 91.96)	10.56% (8.04, 14.12)	0.96
Putamen	1.03% (0.92, 1.16)	0.09% (0.07, 0.12)	1.12% (1.02, 1.25)	91.93% (89.38, 93.77)	8.07% (6.23, 10.62)	0.95
Hippocampus	0.77% (0.68, 0.87)	0.11% (0.09, 0.14)	0.88% (0.80, 0.98)	87.33% (83.24, 90.28)	12.67% (9.72, 16.76)	0.92
Caudate	1.30% (1.15, 1.47)	0.12% (0.09, 0.15)	1.42% (1.28, 1.57)	91.65% (88.90, 93.61)	8.35% (6.39, 11.10)	0.99
Amygdala	1.01% (0.86, 1.19)	0.39% (0.31, 0.50)	1.40% (1.26, 1.56)	72.31% (63.91, 78.67)	27.69% (21.33, 36.09)	0.79
Globus Pallidus	0.99% (0.85, 1.14)	0.28% (0.22, 0.37)	1.27% (1.14, 1.42)	77.81% (69.90, 83.41)	22.19% (16.59, 30.10)	0.84
Nucleus Accumbens	1.58% (1.29, 1.88)	0.74% (0.58, 0.94)	2.31% (2.09, 2.58)	68.18% (58.99, 75.31)	31.82% (24.70, 41.01)	0.54
<i>Ventricular</i>						
Lateral Ventricle	13.08% (10.37, 16.00)	6.87% (5.35, 8.89)	19.96% (17.66, 22.70)	65.55% (55.00, 73.63)	34.45% (26.37, 45.00)	1
3rd Ventricle	4.19% (3.45, 5.02)	1.86% (1.46, 2.39)	6.05% (5.42, 6.78)	69.22% (59.88, 76.37)	30.78% (23.89, 40.12)	0.97
4th Ventricle	6.89% (5.84, 8.07)	2.24% (1.79, 2.85)	9.14% (8.23, 10.18)	75.45% (68.51, 80.77)	24.55% (19.23, 31.49)	0.98
Choroid Plexus	3.37% (2.88, 3.91)	1.01% (0.80, 1.27)	4.38% (3.93, 4.89)	77.03% (70.49, 82.03)	22.97% (17.97, 29.51)	0.93
<i>Global</i>						
Total Brain Volume	0.90% (0.80, 1.00)	0.04% (0.03, 0.05)	0.93% (0.85, 1.03)	95.83% (94.52, 96.67)	4.17% (3.33, 5.62)	0.99
Body Weight	3.80% (3.25, 4.42)	0.94% (0.74, 1.23)	4.75% (4.25, 5.33)	80.15% (73.73, 84.84)	19.85% (15.16, 26.27)	NA*

*Test-retest reliability data not available for body weight.

Appendix 22 Associations with Mean-Standardised Variance Estimates in the QTIM Dataset

Correlations between mean-standardised genetic and environmental variance estimates and test-retest correlation, mean structure volume, and spatial direction (medial-lateral, anterior-posterior, superior-inferior) in the QTIM dataset

	Correlation with Test-Retest	<i>p</i> value	Correlation with Mean Volume	<i>p</i> value		
<i>Cortical</i>	<i>34 structures</i>					
Mean-standardised genetic (<i>I_A</i>)	-0.02	0.93	-0.29	0.10		
Mean-standardised environmental (<i>I_E</i>)	-0.71	2.84E-06	-0.65*	2.81E-05		
<i>Subcortical</i>	<i>7 structures</i>					
Mean-standardised genetic (<i>I_A</i>)	-0.66	0.11	-0.49	0.26		
Mean-standardised environmental (<i>I_E</i>)	-0.99	2.16E-05	-0.78	0.04		
<i>Ventricular</i>	<i>4 structures</i>					
Mean-standardised genetic (<i>I_A</i>)	0.83	0.17	0.96	0.04		
Mean-standardised environmental (<i>I_E</i>)	0.80	0.20	0.98	0.02		
	Correlation with Medial-lateral direction	<i>p</i> value	Correlation with Anterior-posterior direction	<i>p</i> value	Correlation with Superior-inferior direction	<i>p</i> value
<i>Cortical</i>	<i>34 structures</i>					
Mean-standardised genetic (<i>I_A</i>)	-0.11	0.55	-0.34	0.05	0.10	0.57
Mean-standardised environmental (<i>I_E</i>)	-0.07	0.69	0.43	0.01	-0.46	0.01

Note. Estimates in bold were significant at a Bonferroni corrected significance level of 0.0028 (0.05/18). Spatial directions (medial-lateral, anterior-posterior, superior-inferior) are illustrated in Figure 5.4a.

*After controlling for test-retest reliability, the correlation between mean-standardised environmental variance and mean structure volume for subcortical and cortical structures remained significant ($r = -0.61$, $p = 1.58E-04$).

Appendix 23 Mean-Standardised and Relative Variances Estimates for HCP Brain Structure Volume

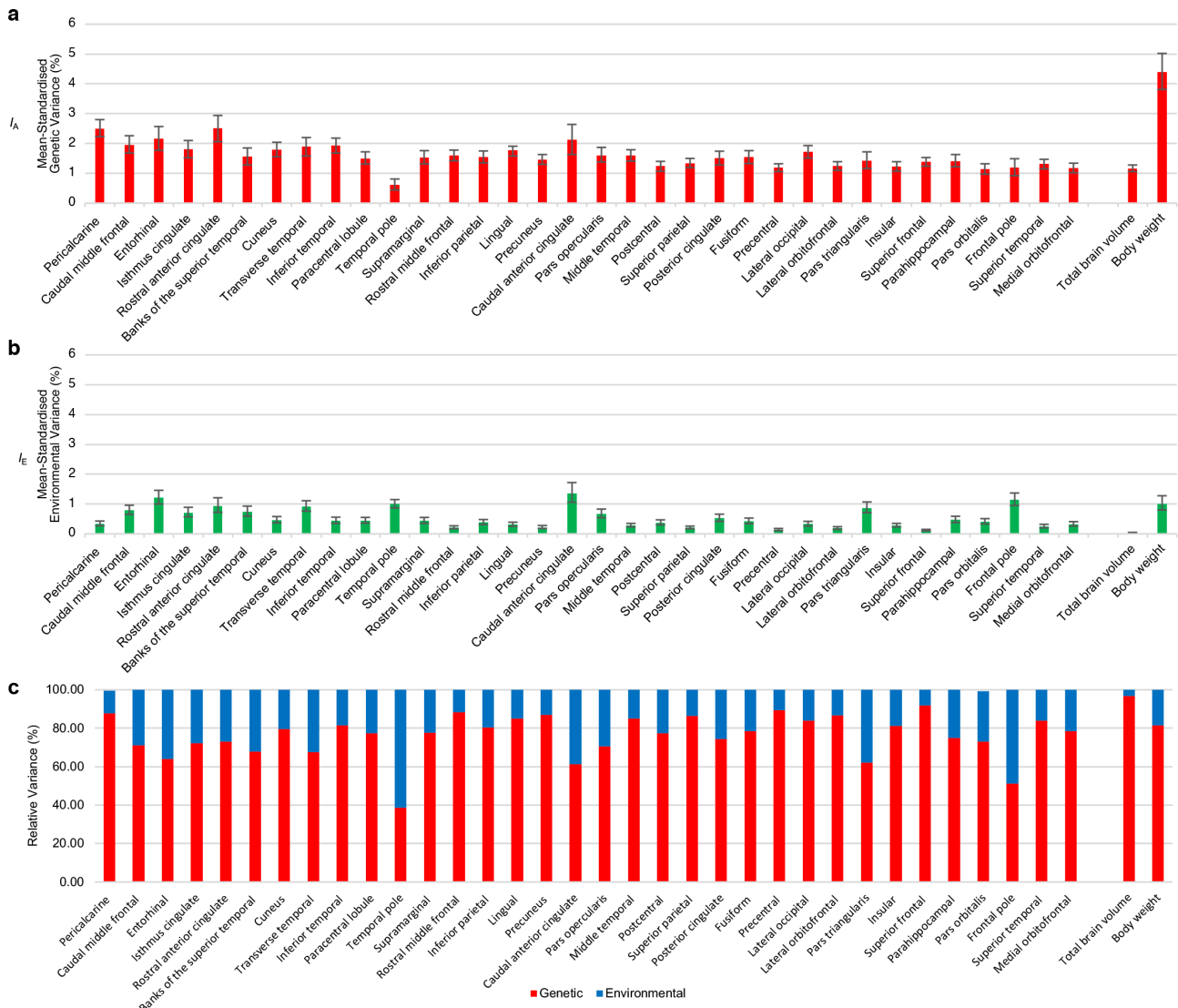
Mean-standardised and relative (proportion of total phenotypic variance) variance estimates (with 95% confidence intervals), and test-retest correlations, for cortical, subcortical, and ventricular volumes, as well as total brain volume and body weight, in the HCP dataset.

	<u>Mean-Standardised Variance Estimates</u>			<u>Relative Variance Estimates</u>		Test Retest Correlation
	Genetic (I_A) (95% CI)	Environmental (I_E) (95% CI)	Phenotypic (I_P) (95% CI)	Genetic (a^2, h^2) (95% CI)	Environmental (e^2) (95% CI)	
<i>Cortical</i>						
<i>Frontal</i>						
Superior frontal	1.38% (1.24, 1.53)	0.12% (0.10, 0.15)	1.50% (1.37, 1.65)	91.91% (89.47, 93.67)	8.09% (6.33, 10.53)	0.99
Rostral middle frontal	1.59% (1.42, 1.78)	0.21% (0.17, 0.26)	1.80% (1.65, 1.98)	88.42% (85.01, 90.93)	11.58% (9.07, 14.99)	0.99
Caudal middle frontal	1.95% (1.69, 2.26)	0.79% (0.65, 0.96)	2.74% (2.50, 3.02)	71.12% (64.39, 76.62)	28.88% (23.38, 35.61)	0.99
Pars opercularis	1.60% (1.38, 1.86)	0.67% (0.55, 0.83)	2.27% (2.09, 2.50)	70.32% (62.73, 76.40)	29.68% (23.60, 37.27)	0.99
Pars triangularis	1.43% (1.15, 1.72)	0.87% (0.71, 1.08)	2.30% (2.10, 2.53)	62.00% (52.58, 69.86)	38.00% (30.14, 47.42)	0.98
Pars orbitalis	1.14% (0.97, 1.33)	0.41% (0.34, 0.51)	1.56% (1.42, 1.71)	73.52% (66.28, 79.18)	26.48% (20.82, 33.72)	0.97
Lateral orbitofrontal	1.24% (1.10, 1.39)	0.19% (0.15, 0.24)	1.43% (1.30, 1.57)	86.81% (82.99, 89.64)	13.19% (10.36, 17.01)	0.98
Medial orbitofrontal	1.17% (1.02, 1.34)	0.32% (0.26, 0.41)	1.49% (1.36, 1.64)	78.45% (72.00, 83.26)	21.55% (16.74, 28.00)	0.93
Precentral	1.19% (1.06, 1.32)	0.14% (0.11, 0.18)	1.33% (1.21, 1.46)	89.23% (86.00, 91.58)	10.77% (8.42, 14.00)	0.99
Paracentral lobule	1.50% (1.31, 1.72)	0.44% (0.35, 0.55)	1.94% (1.77, 2.14)	77.44% (71.29, 82.18)	22.56% (17.82, 28.71)	0.97
Frontal pole	1.20% (0.92, 1.50)	1.14% (0.95, 1.37)	2.34% (2.14, 2.57)	51.35% (41.02, 60.34)	48.65% (39.66, 58.98)	0.88
<i>Parietal</i>						
Superior parietal	1.34% (1.19, 1.50)	0.21% (0.17, 0.26)	1.55% (1.41, 1.70)	86.44% (82.66, 89.28)	13.56% (10.72, 17.34)	0.97
Inferior parietal	1.55% (1.35, 1.75)	0.38% (0.31, 0.48)	1.93% (1.76, 2.13)	80.21% (74.54, 84.48)	19.79% (15.52, 25.46)	0.99

Supramarginal	1.53% (1.32, 1.76)	0.44% (0.35, 0.56)	1.97% (1.81, 2.17)	77.64% (71.17, 82.53)	22.36% (17.47, 28.83)	0.99
Postcentral	1.24% (1.07, 1.40)	0.37% (0.29, 0.46)	1.60% (1.47, 1.77)	77.15% (70.45, 82.21)	22.85% (17.79, 29.55)	0.98
Precuneus	1.46% (1.30, 1.63)	0.22% (0.18, 0.28)	1.68% (1.53, 1.84)	86.85% (83.14, 89.62)	13.15% (10.38, 16.86)	0.99
<i>Occipital</i>						
Lateral occipital	1.72% (1.51, 1.93)	0.33% (0.26, 0.42)	2.05% (1.88, 2.26)	84.01% (79.06, 87.61)	15.99% (12.39, 20.94)	0.99
Lingual	1.78% (1.58, 1.91)	0.31% (0.25, 0.39)	2.09% (1.90, 2.30)	85.06% (80.99, 88.16)	14.94% (11.84, 19.01)	0.98
Cuneus	1.79% (1.56, 2.04)	0.46% (0.37, 0.58)	2.25% (2.05, 2.46)	79.37% (73.59, 83.78)	20.63% (16.22, 26.41)	0.96
Pericalcarine	2.50% (2.24, 2.80)	0.34% (0.28, 0.43)	2.85% (2.60, 3.13)	87.93% (84.61, 90.43)	12.07% (9.57, 15.39)	0.98
<i>Temporal</i>						
Superior temporal	1.31% (1.15, 1.47)	0.25% (0.20, 0.32)	1.56% (1.42, 1.72)	84.10% (79.25, 87.65)	15.90% (12.35, 20.75)	0.99
Middle temporal	1.59% (1.41, 1.79)	0.28% (0.22, 0.35)	1.87% (1.71, 2.06)	85.19% (81.04, 88.31)	14.81% (11.69, 18.96)	0.99
Inferior temporal	1.93% (1.68, 2.18)	0.44% (0.35, 0.56)	2.37% (2.17, 2.62)	81.41% (75.92, 85.49)	18.59% (14.51, 24.08)	0.99
Banks of the superior temporal	1.56% (1.28, 1.85)	0.74% (0.59, 0.93)	2.30% (2.09, 2.53)	67.75% (58.76, 74.87)	32.25% (25.13, 41.24)	0.98
Fusiform	1.54% (1.33, 1.76)	0.42% (0.34, 0.53)	1.96% (1.80, 2.15)	78.36% (72.17, 83.06)	21.64% (16.94, 27.83)	0.99
Transverse temporal	1.89% (1.58, 2.20)	0.91% (0.76, 1.11)	2.80% (2.55, 3.09)	67.56% (59.66, 74.00)	32.44% (26.00, 40.34)	0.97
Entorhinal	2.16% (1.78, 2.57)	1.22% (1.00, 1.46)	3.38% (3.08, 3.73)	63.87% (55.27, 71.00)	36.13% (29.00, 44.73)	0.92
Temporal pole	0.62% (0.44, 0.81)	1.00% (0.87, 1.14)	1.61% (1.48, 1.77)	38.33% (28.11, 47.90)	61.67% (52.10, 71.89)	0.71
Parahippocampal	1.41% (1.22, 1.63)	0.47% (0.38, 0.59)	1.88% (1.73, 2.06)	74.76% (67.78, 80.18)	25.24% (19.82, 32.22)	0.95
<i>Cingulate</i>						
Rostral anterior cingulate	2.51% (2.06, 2.94)	0.93% (0.72, 1.21)	3.44% (3.16, 3.77)	72.94% (63.80, 79.67)	27.06% (20.33, 36.20)	0.98
Caudal anterior cingulate	2.13% (1.63, 2.64)	1.35% (1.05, 1.72)	3.47% (3.15, 3.84)	61.24% (49.31, 70.75)	38.76% (29.25, 50.69)	0.98
Posterior cingulate	1.51% (1.28, 1.74)	0.52% (0.41, 0.65)	2.03% (1.84, 2.24)	74.44% (67.05, 80.10)	25.56% (19.90, 32.95)	0.99
Isthmus cingulate	1.81% (1.51, 2.10)	0.71% (0.56, 0.89)	2.51% (2.28, 2.78)	71.90% (63.94, 78.11)	28.10% (21.89, 36.06)	0.96
<i>Insular</i>						
Insular	1.22% (1.07, 1.39)	0.28% (0.22, 0.35)	1.50% (1.37, 1.65)	81.47% (76.13, 85.48)	18.53% (14.52, 23.87)	0.96
<i>Subcortical</i>						
Thalamus	0.93% (0.82, 1.06)	0.18% (0.14, 0.23)	1.11% (1.02, 1.22)	83.80% (78.88, 87.41)	16.20% (12.59, 21.12)	0.91

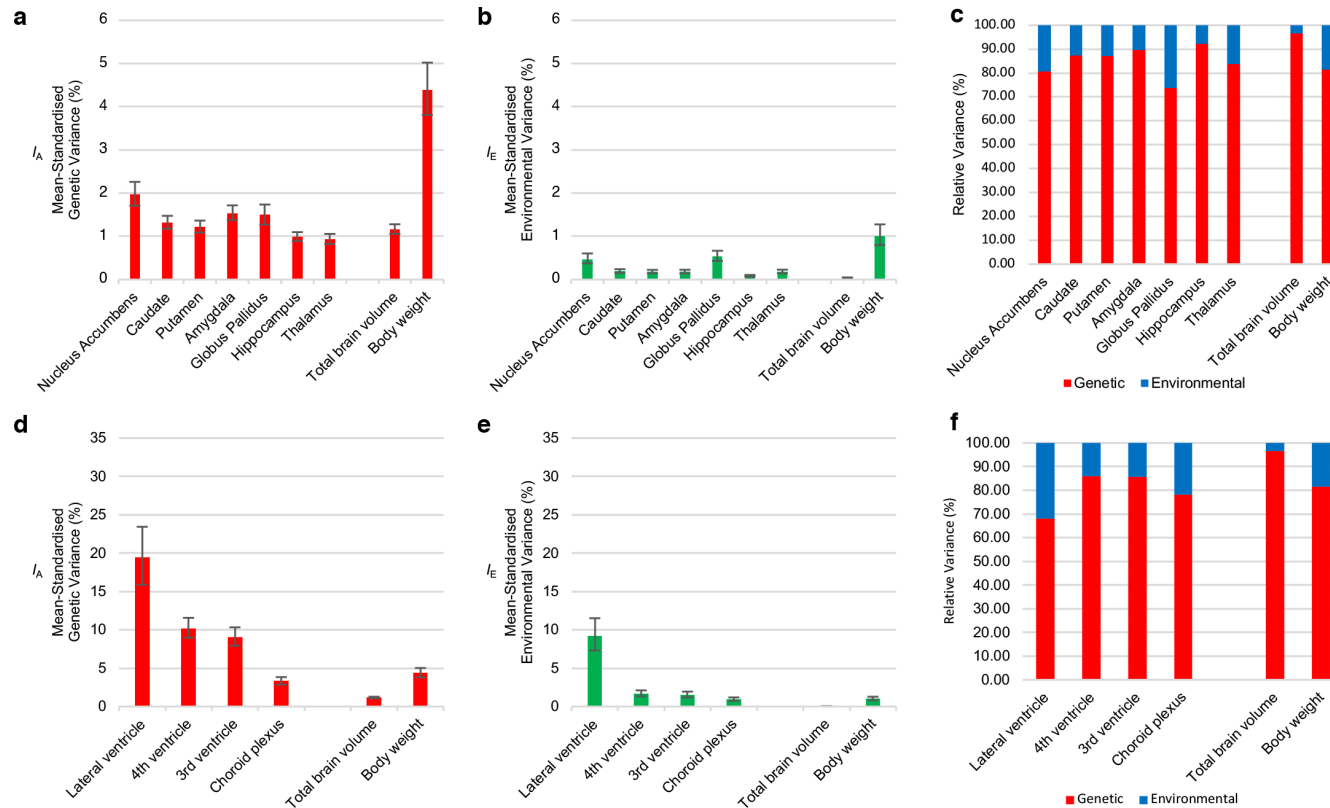
Putamen	1.22% (1.09, 1.36)	0.18% (0.14, 0.23)	1.40% (1.29, 1.53)	87.20% (83.56, 89.92)	12.80% (10.08, 16.44)	0.97
Hippocampus	0.99% (0.89, 1.10)	0.08% (0.07, 0.11)	1.07% (0.98, 1.18)	92.22% (89.80, 93.95)	7.78% (6.05, 10.20)	0.94
Caudate	1.32% (1.18, 1.48)	0.19% (0.15, 0.24)	1.51% (1.39, 1.66)	87.34% (83.77, 90.02)	12.66% (9.98, 16.23)	0.99
Amygdala	1.54% (1.37, 1.72)	0.18% (0.14, 0.23)	1.71% (1.56, 1.89)	89.66% (86.47, 91.97)	10.34% (8.03, 13.53)	0.95
Globus Pallidus	1.50% (1.27, 1.74)	0.53% (0.43, 0.67)	2.03% (1.85, 2.24)	73.70% (66.53, 79.30)	26.30% (20.70, 33.47)	0.87
Nucleus Accumbens	1.98% (1.71, 2.26)	0.47% (0.38, 0.61)	2.45% (2.23, 2.71)	80.69% (74.64, 85.11)	19.31% (14.89, 25.36)	0.90
<i>Ventricular</i>						
Lateral Ventricle	19.43% (15.88, 23.44)	9.17% (7.30, 11.51)	28.60% (25.39, 32.44)	67.94% (59.35, 74.82)	32.06% (25.18, 40.65)	1.00
3rd Ventricle	3.33% (2.85, 3.84)	0.93% (0.74, 1.19)	4.26% (3.86, 4.67)	78.12% (71.42, 83.10)	21.88% (16.90, 28.58)	0.98
4th Ventricle	9.06% (7.93, 10.32)	1.51% (1.19, 1.94)	10.57% (9.55, 11.77)	85.73% (81.17, 89.00)	14.27% (11.00, 18.83)	0.98
Choroid Plexus	10.20% (8.99, 11.56)	1.67% (1.34, 2.11)	11.87% (10.72, 13.22)	85.91% (81.97, 88.87)	14.09% (11.13, 18.03)	0.97
<i>Global</i>						
Total Brain Volume	1.16% (1.06, 1.28)	0.04% (0.03, 0.05)	1.20% (1.11, 1.31)	96.69% (95.80, 97.35)	3.31% (2.60, 4.28)	1.00
Body Weight	4.39% (3.81, 5.02)	1.00% (0.80, 1.28)	5.40% (4.89, 5.98)	81.42% (75.76, 85.60)	18.58% (14.40, 24.24)	0.99

Appendix 24 Mean-Standardised and Relative Genetic and Environmental Variance Estimates for HCP Cortical Structure Volumes



Mean-standardised genetic (a) and environmental (b) variances (with 95% confidence intervals), as well as relative genetic and environmental variance components (c) for cortical structures in the HCP dataset. Estimates are presented in descending order of mean-standardised genetic variance in the QTIM dataset.

Appendix 25 Mean-Standardised and Relative Genetic and Environmental Variance Estimates for HCP Subcortical and Ventricular Structure Volumes



Mean-standardised genetic (a, d) and environmental (b, e) variances (with 95% confidence intervals), as well as relative genetic and environmental variance components (c, f) for subcortical (top row) and ventricular (bottom row) structures in the HCP dataset. Estimates are presented in descending order of mean-standardised genetic variance in the QTIM dataset.

Appendix 26 Associations with Mean-Standardised Variance Estimates in the HCP Dataset

	Correlation with Test-Retest	<i>p</i> value	Correlation with Mean Volume	<i>p</i> value		
<i>Cortical</i>	<i>34 structures</i>					
Mean-standardised genetic (<i>I_A</i>)	0.42	0.01	-0.21	0.23		
Mean-standardised environmental (<i>I_E</i>)	-0.44	0.01	-0.69*	5.20E-06		
<i>Subcortical</i>	<i>7 structures</i>					
Mean-standardised genetic (<i>I_A</i>)	-0.32	0.49	-0.88	0.01		
Mean-standardised environmental (<i>I_E</i>)	-0.76	0.05	-0.65	0.12		
<i>Ventricular</i>	<i>4 structures</i>					
Mean-standardised genetic (<i>I_A</i>)	1.00	4.94E-03	0.90	0.10		
Mean-standardised environmental (<i>I_E</i>)	0.96	0.04	0.99	0.01		
	Correlation with Medial-lateral direction	<i>p</i> value	Correlation with Anterior-posterior direction	<i>p</i> value	Correlation with Superior-inferior direction	<i>p</i> value
<i>Cortical</i>	<i>34 structures</i>					
Mean-standardised genetic (<i>I_A</i>)	-0.22	0.20	-0.26	0.13	0.04	0.83
Mean-standardised environmental (<i>I_E</i>)	-0.12	0.49	0.33	0.06	-0.26	0.14

Note. Estimates in bold were significant at a Bonferroni corrected significance level of 0.0028 (0.05/18). Spatial directions (medial-lateral, anterior-posterior, superior-inferior) are illustrated in Figure 5.4a.

*After controlling for test-retest reliability, the correlation between cortical mean-standardised environmental variance and mean structure volume remained significant ($r = -0.63$, $p = 7.44E-05$).

Appendix 27 Associations Between HCP Cortical Structure and Reading Ability

Heritability of Cortical Structure, Phenotypic Association with Reading Ability (r_{ph}) and Significance Test, Genetic (r_{ph-a}) and Environmental (r_{ph-e}) Contribution to the Phenotypic Correlation in the HCP Dataset.

	Heritability (95% CI)	r_{ph} (95% CI)	p value*	r_{ph-a} (95% CI)	r_{ph-e} (95% CI)
<u>Surface Area</u>					
<i>Frontal</i>					
Pars opercularis left	0.52 (0.41, 0.61)	0.06 (-0.01, 0.13)	0.17		
Pars opercularis right	0.41 (0.30, 0.52)	0.10 (0.04, 0.17)	0.01		
Pars triangularis left	0.52 (0.42, 0.61)	-0.02 (-0.09, 0.05)	0.69		
Pars triangularis right	0.41 (0.29, 0.52)	0.04 (-0.03, 0.10)	0.44		
<i>Parietal</i>					
Inferior parietal cortex left	0.69 (0.61, 0.76)	0.12 (0.05, 0.18)	5.62E-04	0.07 (-0.02, 0.15)	0.05 (0.00, 0.10)
Inferior parietal cortex right	0.65 (0.56, 0.72)	0.11 (0.04, 0.17)	0.01		
Supramarginal cortex left	0.65 (0.55, 0.72)	0.09 (0.02, 0.16)	0.03		
Supramarginal cortex right	0.55 (0.44, 0.65)	0.10 (0.04, 0.17)	2.32E-03	0.05 (-0.04, 0.14)	0.06 (-0.00, 0.12)
<i>Temporal</i>					
Superior temporal gyrus left	0.67 (0.59, 0.74)	0.14 (0.07, 0.20)	2.58E-04	0.12 (0.04, 0.20)	0.01 (-0.04, 0.07)
Superior temporal gyrus right	0.68 (0.59, 0.74)	0.12 (0.05, 0.19)	7.46E-04	0.08 (-0.00, 0.16)	0.04 (-0.01, 0.09)
Fusiform gyrus left	0.62 (0.53, 0.69)	0.12 (0.06, 0.19)	8.42E-04	0.15 (0.07, 0.23)	-0.02 (-0.08, 0.03)
Fusiform gyrus right	0.70 (0.62, 0.77)	0.15 (0.08, 0.21)	7.50E-05	0.17 (0.08, 0.25)	-0.02 (-0.07, 0.03)
<i>Global</i>					
Total Surface Area	0.93 (0.91, 0.94)	0.15 (0.09, 0.22)	2.35E-05	0.13 (0.06, 0.21)	0.02 (-0.01, 0.05)
<u>Cortical Thickness</u>					
<i>Frontal</i>					
Pars opercularis left	0.64 (0.54, 0.72)	-0.01 (-0.08, 0.06)	0.20		
Pars opercularis right	0.54 (0.44, 0.63)	-0.01 (-0.07, 0.06)	0.88		
Pars triangularis left	0.57 (0.46, 0.67)	-0.03 (-0.10, 0.04)	0.29		
Pars triangularis right	0.64 (0.55, 0.71)	-0.02 (-0.08, 0.05)	0.50		
<i>Parietal</i>					
Inferior parietal cortex left	0.71 (0.62, 0.77)	-0.08 (-0.15, -0.01)	0.03		
Inferior parietal cortex right	0.75 (0.69, 0.81)	-0.06 (-0.13, 0.01)	0.20		
Supramarginal cortex left	0.76 (0.69, 0.81)	-0.03 (-0.09, 0.04)	0.42		
Supramarginal cortex right	0.70 (0.63, 0.77)	-0.01 (-0.08, 0.05)	0.52		
<i>Temporal</i>					
Superior temporal gyrus left	0.68 (0.59, 0.74)	-0.00 (-0.07, 0.07)	0.59		
Superior temporal gyrus right	0.68 (0.60, 0.75)	-0.01 (-0.08, 0.06)	0.61		
Fusiform gyrus left	0.56 (0.45, 0.65)	0.04 (-0.02, 0.11)	0.26		
Fusiform gyrus right	0.66 (0.57, 0.73)	0.02 (-0.04, 0.09)	0.79		
<i>Global</i>					
Average Cortical Thickness	0.86 (0.81, 0.89)	-0.02 (-0.09, 0.05)	0.23		

Note. Genetic and environmental contributions estimated for significant phenotypic associations only. Genetic contributions were significant (95% CI did not span zero) for associations between reading score and superior temporal gyrus left surface area, and fusiform gyrus left/right surface area.

* p values in bold are significant at a Bonferroni corrected p value of 0.004 (0.05/13).

Appendix 28 Associations Between QTIM Cortical Structure and Reading Ability

Heritability of Cortical Structure, Phenotypic Association with Reading Ability (r_{ph}) and Significance Test, Genetic (r_{ph-a}) and Environmental (r_{ph-e}) Contribution to the Phenotypic Correlation in the QTIM Dataset.

	Heritability (95% CI)	r_{ph} (95% CI)	p value	r_{ph-a} (95% CI)	r_{ph-e} (95% CI)
<i>Surface Area</i>					
<i>Parietal</i>					
Inferior parietal cortex left	0.56 (0.43, 0.67)	-0.04 (-0.12, 0.04)	0.63	-0.05 (-0.16, 0.06)	0.01 (-0.06, 0.08)
Supramarginal cortex right	0.58 (0.46, 0.68)	0.03 (-0.05, 0.12)	0.66	0.05 (-0.06, 0.16)	-0.02 (-0.09, 0.05)
<i>Temporal</i>					
Superior temporal gyrus left	0.75 (0.64, 0.82)	0.01 (-0.07, 0.10)	0.93	0.01 (-0.11, 0.12)	0.01 (-0.06, 0.08)
Superior temporal gyrus right	0.70 (0.59, 0.78)	-0.02 (-0.11, 0.06)	0.79	-0.01 (-0.12, 0.10)	-0.01 (-0.08, 0.05)
Fusiform gyrus left	0.54 (0.40, 0.65)	-0.05 (-0.13, 0.03)	0.48	-0.06 (-0.17, 0.05)	0.01 (-0.06, 0.09)
Fusiform gyrus right	0.63 (0.49, 0.73)	-0.02 (-0.10, 0.07)	0.90	-0.02 (-0.13, 0.10)	-0.00 (-0.07, 0.07)
<i>Global</i>					
Total Surface Area	0.90 (0.87, 0.93)	-0.00 (-0.08, 0.08)	0.92	0.01 (-0.08, 0.10)	-0.01 (-0.05, 0.03)

Note. Analyses only run for brain/language pairings that were significant in the HCP dataset.